Dissertation

submitted to the

Combined Faculty of Natural Sciences and Mathematics

of the Ruperto Carola University Heidelberg, Germany

for the degree of

Doctor of Natural Sciences

Presented by

M.Sc. Taga Lerner

born in: Be’er Sheva, Israel

Oral examination:

10.12.2021

# Murine Apolipoprotein B mRNA editing enzyme (APOBEC1) regulates transcript fate and macrophage phagocytosis

Referees:

Prof. Dr. Frank Lyko

Prof. Dr. Nina Papavasiliou

# Abstract

From the genome to the proteome, each molecular step is tightly controlled. Advances in RNA-sequencing technologies show that a system of RNA modifiers extensively and dynamically regulates the transcriptome. The posttranscriptional changes alter mRNA stability, localisation, and translational efficiency. However, the effects and dynamics of one of the least studied RNA modifiers, Apolipoprotein B mRNA editing enzyme, catalytic polypeptide 1 (APOBEC1), are unknown. APOBEC1 catalyses cytosine deamination to uracil in a process known as RNA editing. APOBEC1 has a vital role in lipid metabolism, modifies phagocytosis in mouse macrophages, and its activity contributes to the heterogenic nature of macrophages. This work aimed to study how editing modifies macrophage phenotype, transcript-level effects, and dynamics during macrophage activation.

To determine whether APOBEC1 editing is temporally regulated after activation, I analysed RNA-sequencing data from polarised mouse bone-marrow-derived macrophages and the macrophage cell line RAW264.7. I show that global editing levels are altered over time with an early increase followed by a drastic decrease. I report a striking distinction in the pattern of transcript level editing changes after proinflammatory stimulation; transcripts involved in phagosome maturation (processes that acidify phagosomes) have decreased editing while transcripts essential for antigen presentation and processing (processes that increase or require higher pH levels) have increased editing. I find that APOBEC1 increases antigen presentation and processing machinery protein levels and decreases factors involved in acidification and antigen digestion. I demonstrate that the lack of editing decreases the translational efficiency of Cytochrome B-245 Beta Chain (CYBB). CYBB is part of an enzyme complex that produces reactive oxygen species in phagosomes consuming protons during the process, which is critical for preventing antigen over-digestion. The loss of APOBEC1 causes dysfunction in the regulation of phagosomal pH resulting in lower-than-normal pH, which in part is responsible for the previous observations of increased phagocytosis in knockout macrophages. Overall, my work highlights a novel role of APOBEC1 editing in regulating transcript translational efficiency and control of the primary functions of macrophages in phagocytosis and antigen presentation.

# Zusammenfassung

Vom Genom bis zum Proteom wird jeder molekulare Schritt streng kontrolliert. Fortschritte bei RNA-Sequenzierungstechnologien zeigen, dass ein Netzwerk von RNA-Modifizierenden Enzymen das Transkriptom weitgehend und dynamisch reguliert. Die posttranskriptionellen Veränderungen beeinflusst die mRNA-Stabilität, Lokalisierung und Translationseffizienz. Die Wirkung und Dynamik eines der am wenigsten untersuchten RNA-Modifikatoren, Apolipoprotein B mRNA Editing Enzyme, Catalytic Polypeptide 1 (APOBEC1), sind jedoch unbekannt. APOBEC1 katalysiert die Desaminierung von Cytosin zu Uracil in einem Prozess, der als RNA-Editierung bekannt ist. APOBEC1 spielt eine Schlüsselrolle im Fettstoffwechsel, modifiziert die Phagozytose in Mausmakrophagen und trägt durch seine Aktivität zur heterogenen Natur von Makrophagen bei. Diese Arbeit zielte darauf ab, den Einfluss der RNA-Editierung auf den Makrophagen-Phänotyp, Effekte auf Transkriptionsebene und die Dynamik während der Makrophagenaktivierung, zu untersuchen.

Um festzustellen, ob die APOBEC1-Editierung, welche nach der Aktivierung von Makrophagen auftritt, zeitlich reguliert wird, habe ich RNA-Sequenzierungsdaten von polarisierten Makrophagen, die aus dem Maus-Knochenmark gewonnen wurden, sowie der Makrophagen-Zelllinie RAW264.7 analysiert. Ich zeige, dass sich die globale Editierung im Laufe der Zeit ändert, mit einem frühen Anstieg, gefolgt von einem drastischen Rückgang. Ich berichte über einen auffallenden Unterschied im Muster der veränderten Editierung auf Transkriptionsebene nach proinflammatorischer Stimulation; Transkripte, die an der Reifung von Phagosomen beteiligt sind (Prozesse, die Phagosomen ansäuern) weisen eine verringerte Editierung auf, während Transkripte, die für die Antigenpräsentation und -prozessierung (Prozesse, die einen höheren pH-Wert erfordern oder diesen erhöhen) essentiell sind, eine erhöhte Editierung aufweisen. Ich beobachte, dass APOBEC1 die Konzentration von Proteinen, welche in der Antigenpräsentation und der Verarbeitungsmaschinerie involviert sind, erhöht und Faktoren verringert, die an der Ansäuerung und Antigenverdauung beteiligt sind. Ich zeige, dass eine fehlende Bearbeitung durch APOBEC1 die Translationseffizienz der Cytochrome B-245 Beta-Chain (CYBB) verringert. CYBB ist Teil eines Enzymkomplexes, der reaktive Sauerstoffspezies in Phagosomen produziert, die während des Prozesses Protonen verbrauchen. Dies wiederum

ist entscheidend für die Verhinderung einer Überverdauung von Antigenen. Der Verlust von APOBEC1 verursacht eine Dysfunktion bei der Regulation des phagosomalen pH-Wertes. Der reduzierte pH-Wert ist, zumindest teilweise, für die früheren Beobachtungen einer erhöhten Phagozytose bei Knockout-Makrophagen verantwortlich.

Zusammenfassend konnte diese Arbeit eine neuartige Rolle der APOBEC1-Editierung bei der Regulierung der Translationseffizienz und der Kontrolle der primären Funktionen von Makrophagen bei der Phagozytose und Antigenpräsentation aufzeigen.

# Acknowledgements

Throughout my PhD I have been fortunate to be surrounded by wonderful people, from within the lab and from the outside, who always lent their support when needed and helped me grow as a scientist. I extend a special thank you to my supervisor **Prof. Dr Nina Papavasiliou** for being the optimist to my pessimist when it comes to results, for letting me forge my own research path, for listening to my ideas (and sometimes disagreeing with them) and for providing a space to thrive for over four years. Thank you **Riccardo Pecori** for putting up with my constant interruptions to ask questions and to request feedback. A warm thank you to all the members of D150/D160 for making work a fun environment, it has been a pleasure, and I know I have friends for many years to come; **Anastasia, Anna, Annette, Bea, Rafial, Dimitra, Erec, Evi, Gianna, Joey, Monica, Sandra, Tim, Xico, Johan and Monique.** Special mention of **Paulo**, whom I met first from the group at the selection rounds and who had to overcome similar problems as me. Thank you to **Salvatore Di Giorgio** for all your help and support with Bioinformatics, you made things a lot less complicated and together, we made great progress for this work. **Chris Lehmann and Laura Schoppe**, it was a pleasure to teach you, to know you and I am thankful for your help in my work.

Like many PhD students, there were a lot of ups and downs and I want to thank my Faculty supervisor **Prof. Dr. Frank Lyko** and TAC members **Prof. Dr. Michaela Frye** and **Dr, Axel Szabowski** for all their input, suggestions and for taking extra time outside our TAC meetings to help push me forward in the right trajectory.

This work would not have been possible without the help of **Dr. Steffen Schmitt** with S2 sortings and **Dr. Damir Krunic** with assistance on microscopy topics. Special thank you to the members of the **DKFZ biostatistics counselling team** for answering many statistics questions. I am grateful to **Martin Schneider** and **Dr. Dominic Helm** for advice on Mass spectrometry and data analysis.

I would not be where I am today without the help and support of my family from afar. We have lived in different countries from many years but their presence is always with me; my parents **Dalia** and **Jacob,** my grandparents **Miriam** and **Beni,** my brothers Ilay and Rom and my newest family member **Nitzan**, who is making my family grow even more.

Last but very far from least, I want and need to thank **Theresa Schmid** for being a friend when I needed one the most, for supporting and commiserating with me throughout the writing of this thesis. You made the process sometimes even enjoyable, and it would have been far, far more difficult without you.

# List of figures

# List of tables

# Abbreviations

| | |
|---|---|
| A1/APOBEC1 | Apolipoprotein mRNA editing enzyme catalytic polypeptide-like 1 |
| AIM2 | Absent in melanoma 2 |
| APC | antigen presenting cell |
| ARE | AU-rich elements |
| B2M | $\beta_2$ microglobulin |
| BMDM | Bone marrow derived macrophage |
| BSA | bovine serum albumin |
| CD | cluster of differentiation |
| CLP | Common lymphoid prohenitor |
| CYBB | Cytochrome B-245 Beta Chain |
| DAMP | Damage associated molecular pattern |
| DC | Dendritic cell |
| DKFZ | Deutsches Krebsforschungszentrum |
| DMEM | Dulbecco's Modified Eagle Medium |
| DMSO | dimethyl sulfoxide |
| DNA | deoxyribonucleic acid |
| DTT | *dithiothreitol* |
| EDTA | ethylenediaminetetraacetic acid |
| EEA1 | Early endosome antigen 1 |
| EGFR | epidermal growth factor receptor |
| FACS | *fluorescence-activated cell sorting* |
| FCS | fetal calf serum |

| | |
|---|---|
| FcγR | Fcγ-receptors |
| HSC | Heamatopoietic stem cells |
| IFN | interferon |
| IL | interleukin |
| KO | knockout |
| LAMP | lysosomal associated membrane proteins |
| LPS | Lipopolysaccharide |
| LTA | Lipoteichoic acid |
| MDM | Monocyte derived macrophage |
| MHC | major histocompatibility complex |
| MMP | Multipotent progenitors |
| MPLA | monophosphoryl lipid A |
| mRNA | messenger ribonucleic acid |
| MS | mass spectrometry |
| NADPH | Nicotinamide adenine dinucleotide phosphate |
| NGS | next generation sequencing |
| NK | Natural killer |
| NK | natural killer |
| NOD | Nucleotide-binding oligomerisation domain |
| NOX2 | NADPH) oxidase |
| PAMP | Pathogen-asspociated molecular pattern |
| PBS | phosphate buffered saline |
| PCR | polymerase chain reaction |
| PE | phycoerythrin |

| | |
|---|---|
| PRR | Pattern recognition receprot |
| RBP | RNA-binding proteins |
| RIG | Retinoic acid-inducible gene |
| RNA | ribonucleic acid |
| ROS | Reactive oxygen species |
| RT | room temperature |
| SR-A | scavenger receptor A |
| TAP | transporter associated with antigen processing |
| TLR | Toll like receptor |
| TLR | Toll-like receptor |
| TNF | tumor necrosis factor |
| TRIS | Tris(hydroxymethyl)aminomethane |
| UTR | Untranslated region |
| WT | wildtype |

# Table of Contents

# 1 Introduction

## 1.1 The immune system

The human body is constantly exposed to environmental microorganisms and needs to distinguish friend from foe. The immune system evolved to serve this purpose, protect from potential foreign or internal invasion, and maintain homeostasis. It consists of two major parts: The innate and the adaptive immune system. The organs of the immune system include primary lymphoid organs, such as the bone marrow and thymus and the secondary lymphoid organs, such as the spleen, lymph nodes and the lymph system (Murphy *et al.*, 2016). The innate immune system is non-specific because a single cell member can recognise a broad range of targets while the adaptive immune response mounts a defence against a specific antigen. Only the innate immune system will be described further due to its relevance to this thesis.

### 1.1.1 Innate immune system

Anatomical barriers, such as the skin, are the body's first line of defence against a foreign invader. Should these barriers be breached, the innate immune system can sense and respond within minutes to hours without relying on an antigen-specific response (Beutler, 2004). The sensing and response mechanisms, either soluble or cell-associated, are genetically encoded and set at birth.

The soluble sensors or effectors are usually the first to encounter the foreign agent. These include antimicrobial enzymes such as tear lysozyme that digests bacterial cell walls (Ganz, 2004), antimicrobial peptides such as saliva histatins (De Smet and Contreras, 2005), and complement system proteins in blood plasma that either lyse targets or tag them for phagocytosis (Dunkelberger and Song, 2010).

The cellular component of the innate immune system includes cells such as natural killer (NK) cells, macrophages, dendritic cells (DC) and neutrophils. These cells recognise pathogens or sense damage through conserved features shared by many pathogens or general markers of cell integrity. These features or patterns are recognised by pattern

recognition receptors (PRRs) (Wilkins and Gale, 2010). The features on pathogens are called pathogen-associated molecular patterns (PAMPs) (Takeuchi and Akira, 2010), and cell damage features are called damage-associated molecular patterns (DAMPs) (Kono and Rock, 2008). Macrophages are central players in this system, activation of PRRs result in the secretion of inflammatory cytokines and inflammatory cell recruitment. Their role is complex and not limited to inflammation, as they are also crucial in the resolution of inflammation, tissue repair and homeostasis (Gordon, Plüddemann and Martinez Estrada, 2014; Wynn and Vannella, 2016)

### 1.1.2 Origin of macrophages

Macrophages were the first immune cell to be identified by their phagocytic function by Elie Metchnikoff (Nathan, 2008). Elie Metchnikoff is responsible for using the term 'innate immunity' to describe the process he saw, and alongside Paul Ehrlich, the father of adaptive immunity, was awarded a Nobel Prize for his work (Nathan, 2008).

In the 1960s, macrophages were classed under the blanket term 'mononuclear phagocyte system', which included all the different types of monocytes, macrophages and dendritic cells (van Furth and Cohen, 1968). It was initially thought that all macrophages originate from monocyte precursors from the bone marrow. However, current models suggest at least three developmental origins for macrophages from three separate waves during development: Yolk sac derived tissue-resident macrophages, foetal liver-derived tissue-resident macrophages and infiltrating bone marrow-derived macrophages (F. Ginhoux et al. 2010)(Ginhoux and Jung, 2014).

### 1.1.3 Macrophages during embryonic development

In mice on embryonic day (E) 6.5 to E11, haematopoiesis occurs in the extra-embryonic yolk sac, and erytho-myeloid progenitors migrate into and colonise the foetus, developing into macrophages without a monocytic intermediate state (Ginhoux and Guilliams, 2016; van de Laar *et al.*, 2016). Foetal liver-derived tissue-resident

macrophages also derive from the yolk sac. Late yolk sac-derived erytho-myeloid progenitors colonise the liver and form foetal liver monocytes and, in the second wave, from E12.5 seed macrophages in other tissues (Palis and Yoder, 2001; Orkin and Zon, 2008). The final wave of macrophages originates from hematopoietic stem cells (HSC) that colonise the bone marrow and develop into monocytes that continuously repopulate the blood and develop into macrophages throughout life (van de Laar *et al.*, 2016).

The proportion of macrophages originating from precursors from the different sources differs from tissue to tissue. Once tissue-resident macrophages are present, they are self-renewing. However, they can be continuously renewed from circulating monocytes at differing levels. Microglia, tissue-resident macrophages in the brain and spinal cord, seem to originate almost solely from yolk sac progenitors (Ginhoux *et al.*, 2010). The blood-brain barrier under normal conditions prevents the entry of monocytes into the brain. When microglia require replenishing, they are restored from a reservoir of local progenitors without a bone marrow contribution (Ajami *et al.*, 2007; Huang *et al.*, 2018). Kupffer cells and lung alveolar macrophages are primarily composed of foetal liver monocyte precursors (Guilliams *et al.*, 2013; Hoeffel *et al.*, 2015). The intestinal and cardiac macrophages do contain a small population of self-renewing yolk sac derived cells; however, the majority of macrophages are bone marrow monocyte-derived in adults (Molawi *et al.*, 2014; Shaw *et al.*, 2018)

Today we know that macrophages are a highly heterogeneous set of cells from all aspects, including ontogeny, morphology, phenotypes and function (T. A. Wynn, Chawla and Pollard, 2013; Gordon, Plüddemann and Martinez Estrada, 2014; Geissmann and Mass, 2015; Hume, 2015; Gordon and Plüddemann, 2017; Guilliams, Mildner and Yona, 2018).

### 1.1.4 Haematopoiesis: Murine monocyte/macrophage development from the bone marrow

The classical model for the differentiation of monocytes has a hierarchical structure where a set of pluripotent cells differentiate into different branches of

increasingly more restricted progenitors that eventually form all the cells in the blood (Figure 1). With the increase in data from single-cell sequencing experiments, it is clear that the actual structure of haematopoiesis is not so rigid and has multiple intermediate stages, cells primed early on towards a specific branch and progenitors that can develop into additional cell types under the right circumstances (Guilliams, Mildner and Yona, 2018).

At the top of the haematopoiesis hierarchy are haematopoietic stem cells (HSC). Active HSCs differentiate into a pool of multipotent progenitors (MMPs) (Pietras *et al.*, 2015). Although traditionally thought of as one cell type, they are more heterogeneous than that and contain subsets already primed to generate specific cell lineages. Some HSCs can also skip various progressive differentiation steps and directly become unipotent progenitors (Velten *et al.*, 2017). The MMPs can further develop into subsets of common myeloid progenitors (CMP) (Akashi K *et al.*, 2000) or common lymphoid progenitors (CLP) (Kondo, Weissman and Akashi, 1997). CLPs generate T cells, B cells, natural killer (NK) cells (Akashi K *et al.*, 2000), innate lymphoid cells (Juelke and Romagnani, 2016) and a portion of plasmacytoid DC (pDC) cells (Rodrigues *et al.*, 2018).

CMPs are destined to become megakaryocyte and erythrocyte progenitors (MEP) or granulocyte and macrophage progenitors (GMP) (Akashi K *et al.*, 2000). Monocyte/DC progenitors (MDP) differentiate from GMP or directly from a subset of Fms Related Receptor Tyrosine Kinase 3 (Flt3) + CMPs (Yáñez *et al.*, 2017). MDPs branch of into common DC precursors (CDPs) that form classical DCs and a small portion of pDCs and common monocyte progenitors (cMOPs) that then form monocytes(Yáñez *et al.*, 2017).

The commitment of precursors to the monocytic lineage is determined by several haematopoietic growth and transcription factors such as Spi-1 Proto-Oncogene (SPI1 or often known as PU.1), Zinc Finger E-Box Binding Homeobox 2 (ZEB2), Interferon Regulatory Factor 8 (IRF8), GATA Binding Protein 2 (GATA2) and Kruppel Like Factor 4 (KLF4) (McKercher *et al.*, 1996; Alder *et al.*, 2008; Hambleton *et al.*, 2011). Deficiency or absence of these factors results in a reduction in the total number of circulating monocytes. The levels of *Spi1* expression helps determine which cell type progenitors differentiate to: high *Spi1* induces macrophages differentiation, while intermediate *Spi1*

levels induce differentiation into granulocyte-like cell and levels are low in other immune cells(Li, Hao and Hu, 2020). On the opposite side are negative regulatory factors such as BTB Domain And CNC Homolog 2

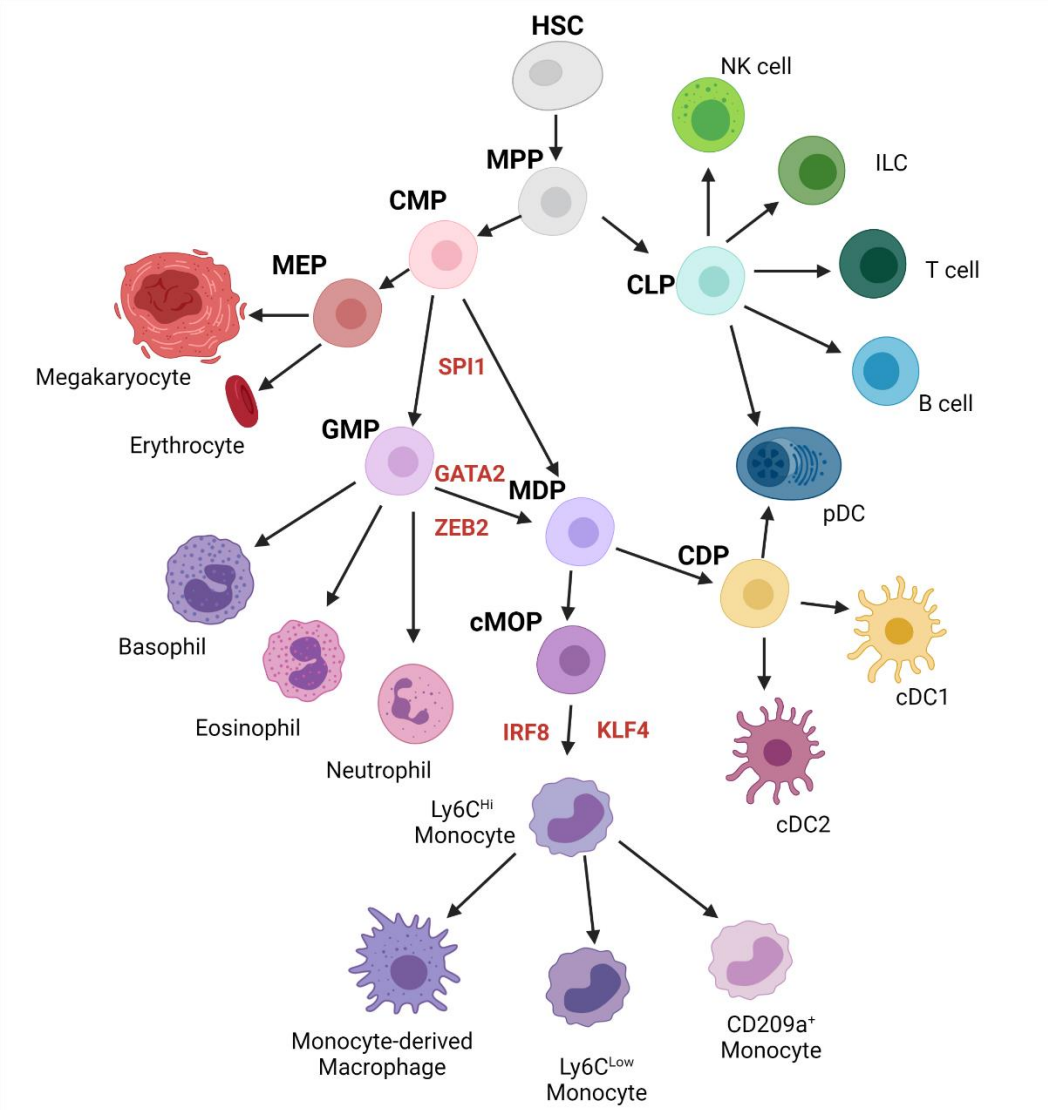


Figure 1 Depiction of haematopoiesis in mice.

Through a series of intermediate precursors, haematopoietic stem cells (HSC) differentiate into all the types of cells found in the blood. Multipotent precursors (MPP) undergo stages where they lose their ability to become certain cell types and are destined to continue on the path of a specific lineage. CMP, common myeloid precursors; GMP, granulocyte-macrophage precursors; MDP, monocyte-macrophage/dendritic cell precursors; CDP, common dendritic cell precursors; cMoP, common monocyte precursors; CLP, common lymphocyte precursors; MEP, megakaryocyte/erythrocyte progenitors; cDC, conventional DC; pDC, plasmacytoid DC. Primary transcription factors involved in monocyte development are indicated in red. Adapted from (Guilliams, Mildner, and Yona 2018). Created with BioRender.com

(BACH2), mice lacking BACH have higher levels of circulating monocytes (Kurotaki et al. 2018).

### 1.1.5 Bone marrow/monocyte-derived macrophages

There are two major types of mouse monocytes in the blood, and they can be distinguished from one another by their expression of lymphocyte antigen 6C (Ly6C). Ly6C$^{Hi}$ monocytes are directly derived from the bone-marrow precursors, while Ly6C$^{Low}$ monocytes originate from the circulating Ly6C$^{Hi}$ population (Yona *et al.*, 2013). A small subset, about 5%, of Ly6C$^{Hi}$ monocytes is defined by the expression Cluster of differentiation 209a (CD209a) (Wolf *et al.*, 2019). These three populations appear to serve different functions; classical Ly6C$^{Hi}$ monocytes leave the circulation and can differentiate into macrophages; CD209a$^{+}$monocytes under inflammatory conditions may differentiate into monocyte-derived DCs; and Ly6C$^{Low}$ cells remain in circulation where they patrol for and remove damaged blood vessel endothelial cells (Carlin *et al.*, 2013; Jakubzick *et al.*, 2013; Wolf *et al.*, 2019).

Under normal physiological conditions, almost all tissues have a minor proportion of extravasated Ly6C$^{Hi}$ monocytes, and therefore monocyte-derived macrophages (MDM) alongside the local tissue-resident pools (Sawai *et al.*, 2016). The adult MDMs can replace embryonic macrophage populations either close to birth (Bain *et al.*, 2014) or gradually over time (Sawai *et al.*, 2016). The MDMs are extraordinarily plastic and undergo transcriptomic modification to resemble tissue-resident macrophages as they adapt to the environment. However, some epigenetic, transcriptional and functional differences persist (Lavin *et al.*, 2014; van de Laar *et al.*, 2016; Cronk *et al.*, 2018). A significant difference in response to inflammation exists between the two different sources of macrophages; tissue macrophages play more significant roles in homeostasis, and the MDMs produce more robust inflammatory responses (Cronk *et al.*, 2018).

When tissue-resident macrophages are challenged with a pathogen, they produce neutrophil chemoattractants such as C-X-C Motif Chemokine Ligand 1(CXCL1), CXCL2, Interleukin (IL)-lα and monocyte chemoattractant protein 1 (MCP-1) (Beck-Schimmer *et al.*, 2005; De Filippo *et al.*, 2008; Barry *et al.*, 2013). Neutrophils are then recruited to the

aggravated site, where they are responsible for recruiting circulating monocytes by secreting additional chemoattractants (Soehnlein *et al.*, 2008), upregulating various adhesion molecules (Lee *et al.*, 2003) and increasing vascular permeability, which promotes monocyte transmigration (Gautam *et al.*, 2001). The inflammatory response recruits circulating monocytes to sites of injury and increases their production and mobilisation from the bone marrow. At the site of inflammation, the monocytes differentiate, and the resultant MDMs produce cytotoxic and proinflammatory mediators, engulf and clear invading microorganisms apoptotic and damaged cells and are also involved in the resolution of inflammation (Gordon, Plüddemann and Martinez Estrada, 2014)

### 1.1.6 Macrophage activation during inflammation

In service to their function as part of the innate immune defence, macrophages can recognise various endogenous and exogenous danger signals through PRRs. There are several different classes of PRRs; Toll-like receptors (TLRs), Retinoic acid-inducible gene (RIG)-I like (RLRs), nucleotide-binding oligomerisation domain (NOD) like receptors (NLRs), Absent in melanoma (AIM) 2 like receptors (ALRs), C-type lectin receptors (CLRs) and intracellular DNA sensors, for instance, cGAS (Kumar, Kawai and Akira, 2009; Kawasaki and Kawai, 2014). TLRs are membrane-bound and localise to the cell surface or other intracellular compartments. Activation of macrophages will be discussed here mainly through specific TLRs. Signalling via activation of other receptor types have many overlapping components, but they vary, and the result is a spectrum of macrophage responses. Once a receptor engages its target, a highly coordinated and orchestrated sequence of transcriptional changes occurs, with genes rapidly turning on or off.

There are ten recognised humans TLRs (TLR1-TLR10) and thirteen in mice (TLR1-13). However, mouse TLR10 is non-functional (Kawasaki and Kawai, 2014). The different cell surface TLRs can recognise a variety of microbial components. TLR4 recognises lipopolysaccharide (LPS) of gram-negative bacteria. Lipoproteins, peptidoglycans,

lipoteichoic acid (LPA), zymosan and mannan are recognised by TLR2, TLR1 or TLR6 and bacterial flagellin is recognised by TLR5 (Kawai and Akira, 2010).

Once a TLR is engaged, adaptor proteins such as myeloid differentiation primary response 88 (MyD88) or Toll-interleukin receptor domain-containing adapter-inducing interferon-β (TRIF) are recruited to initiate signalling transduction pathways (Schroder, Sweet and Hume, 2006). The adapter proteins activate nuclear factor kappa-light-chain-enhancer of activated B cells (NF-κB), IRFs or mitogen-activated protein kinase (MAPK) that are responsible for regulating the expression of cytokines, chemokines, type I interferon (IFN) and pathways that increase the efficiency of macrophage innate immune behaviours (Kawasaki and Kawai, 2014).

The signalling by engagement of PRRs, cytokines and chemokines present in the environment integrate and dictate the behaviour of the macrophages, polarising them in specific directions. A continuum of macrophage polarisation exists and is challenging to study; therefore, and only for ease of study, macrophages are commonly split into the two 'extremes' of the continuum with inflammatory classically activated macrophages (M1) or alternatively activated macrophages (M2). M1 macrophages result from proinflammatory stimuli through Toll-like receptors and the cytokine IFN-γ secreted by T-helper 1 cells. These macrophages are typically associated with a high capacity of pathogen and tumour cell clearance in addition to enhanced antigen presentation efficiency (Lawrence and Natoli, 2011). M2 activation is usually a result of exposure to IL-4 and/or IL13 and is associated with homeostasis, removal of apoptotic cells and debris, tissue repair and remodelling and resolution of inflammation (Galli, Borregaard and Wynn, 2011).

#### *1.1.6.1 Gene and protein regulation during macrophage activation*

The process of macrophage activation is a highly regulated dynamic response that changes over time with genes being turned on and off, changes in translation and protein stability (Gao *et al.*, 2002; Kitamura *et al.*, 2008; Ceppi *et al.*, 2009; Vyas *et al.*, 2009; Hald *et al.*, 2012; Schott *et al.*, 2014; Das *et al.*, 2018). Due to these different regulatory processes, there are genes with early, intermediate or late responses (Gao *et al.*, 2002;

Hald *et al.*, 2012; Das *et al.*, 2018). Control of activation is carried out in a multilevel approach with feedback loops, transcript stability, changes in translation and epigenetic modifications.

The proinflammatory cytokine, tumour necrosis factor-alpha (TNF), induced when TLR4 is activated with LPS, is a well-studied example of this type of multilevel control. The splicing, nuclear export, translation and stability of both human and murine *Tnf* mRNA is regulated post-transcriptionally (Stamou and Kontoyiannis, 2010). AU-rich elements (ARE) are a common feature of the 3' untranslated region (3'UTR) of many inflammatory cytokines and are a hotspot for binding and regulation by RNA-binding proteins (RBP) (Ostareck and Ostareck-Lederer, 2019). Among the RBPs that recognise AREs are T-Cell-Restricted Intracellular Antigen-1 Cytotoxic Granule Associated RNA Binding Protein (TIA1), Fragile X Mental Retardation Autosomal Homolog 1 (FXR1) and Zinc Finger Protein 36 (ZPF36). These RBPs repress *Tnf* mRNA translation (Piecyk *et al.*, 2000; Tiedje *et al.*, 2012) and/or enhance mRNA degradation in the case of ZPF36 (Carballo, Lai and Blackshear, 1998). In the initial stages of TLR induction, the p38 MAPK pathway results in phosphorylation of ZPF36, which reduces its degradation of *Tnf* mRNA, leading to its increased stability and translation (Stoecklin *et al.*, 2004; Tiedje *et al.*, 2012). ZPF36 increases the degradation of approximately 8% of induced mRNAs (Kratochvill *et al.*, 2011). Gene expression after macrophage activation is frequently limited by the mRNA half-lives of the induced genes (Hao and Baltimore, 2009; Rabani *et al.*, 2011). The mRNA half-lives of *Tnf* and other immune-related mRNA are often regulated by microRNAs and constitutive RNA decay elements that suppress their expression (Schott and Stoecklin, 2010; Leppek *et al.*, 2013). Interestingly, TIA1 causes translational silencing and promotes mRNA decay of *Apobec1* (Yamasaki *et al.*, 2007), which is the main focus of this thesis and will be discussed in later chapters.

Negative feedback loops ensure that TLR signalling remains limited. Failure of such systems and excessive activation could play a role in the development of autoimmune diseases. TLR4, for example, induces its own inhibitors preventing signalling from carrying on indefinitely (Renner and Schmitz, 2009). NF-κB becomes activated once its inhibitor NFKBIA (IκBα) is degraded. Degradation of the inhibitor releases NF-κB from the cytoplasm allowing it to enter the nucleus and activate transcription of its targets. Some

of the gene targets of NF-κB are its own inhibitors that re-export NF-κB to the cytoplasm, degrade nuclear NF-κB or prevent its interaction with target promoters (Renner and Schmitz, 2009; Ruland, 2011)

#### *1.1.6.2 Epigenetic/epitranscriptomic regulation of macrophage activation*

Most of the epigenetic landscape that includes DNA methylation, histone modifications and non-coding RNA is already established during macrophage differentiation and is poised for action. These epigenetic mechanisms control chromatin structure and accessibility of DNA to transcription factors or through regulating mRNA stability and have been shown to regulate macrophage polarisation (Park *et al.*, 2017; Piccolo *et al.*, 2017; Davis and Gallagher, 2019).

M1 polarisation is promoted by methylation of the peroxisome proliferator-activated receptor γ (*PPARγ)* promoter by fatty acid-upregulated DNA-methyltransferase-3β (DNMT3b), which results in decreased *PPARγ* transcription (Wang *et al.*, 2016). Acetylation of NF-κB keeps it in an inactive state transcriptionally, allowing M2 polarisation to proceed; histone deacetylase 3 promotes inflammation and puts a break on M2 polarisation by maintaining the deacetylated state of NF-κB (Mullican *et al.*, 2011; Leus, Zwinderman and Dekker, 2016).

N6-methyl-adenosine ($m^6A$) methylation is a common epitranscriptomic RNA modification (Meyer *et al.*, 2012; Yue, Liu and He, 2015). *Stat1* mRNA, a critical transcription factor in M1 polarisation, is methylated and through this $m^6A$ methylation contributes to macrophage polarisation (Liu *et al.*, 2019).

The role of epitranscriptomic modifications and the patterns these modifications follow during macrophage activation are poorly understood. One mRNA modification, RNA deamination and its dynamics during macrophage activation and effect on function will be the primary focus of this thesis and will be discussed further in section 1.2.

### 1.1.7 Macrophage phagocytosis

Phagocytosis is the process of detecting and engulfing particles larger than 0.5µm and in immune cells serves to eliminate threats and recycle cell material. Many cell types are capable of phagocytosis with low efficiency, but professional phagocytes such as macrophages, neutrophils, monocytes, dendritic cells and osteoclast can perform phagocytosis at high efficiency (Uribe-Querol and Rosales, 2020). Phagocytosis is also a key part of the process of exogenous antigen presentation to the Major Histocompatibility Complex (MHC) II compartment and in cross-presentation to the MHC I compartment and through these instructs the adaptive branch of the immune system (Savina *et al.*, 2006; Blum, Wearsch and Cresswell, 2013; den Haan, Arens and van Zelm, 2014; Jakubzick, Randolph and Henson, 2017).

All types of macrophages will carry out phagocytosis. However, different polarisation states have different appropriate targets and ingestion of an inappropriate target can have pathological consequences. M1 macrophages are more critical for pathogen and tumour cell clearance and are more efficient at antigen presentation (Lawrence and Natoli, 2011). M2 macrophages phagocytose more apoptotic cells and debris (Galli, Borregaard and Wynn, 2011). When apoptotic cells trigger the wrong type of macrophage, for example, phagocytosis of apoptotic cells by M1 macrophages, this can lead to the presentation of self-antigens and down the path of autoimmune disease (Uderhardt *et al.*, 2012). M1 and M2 macrophages have differences in expression of phagocytic receptors (Mantovani *et al.*, 2004). The exact process of phagocytosis and the maturation of phagosomes will depend on the receptors present and the environmental stimuli received. Phagocytosis involves four phases: I) Particle recognition, II) Signalling and cellular remodelling, III) Phagosome formation and finally IV) Phagosome maturation.

#### *1.1.7.1 Particle recognition*

PRRs can be involved in the direct initiation of phagocytosis or indirectly involved by activating the phagocytes and increasing phagocytosis efficiency (Kawai and Akira, 2011). Phagocytosis receptors are divided into two groups: I) non-opsonic receptors that

recognise molecular patterns directly on the target particle and II) opsonic receptors that recognise particles bound to host-derived proteins.

#### 1.1.7.1.1 Non-opsonic receptors

PAMP binding receptors that induce phagocytosis include c-type lectin receptors such as Dectin-1, macrophage-inducible C-type lectin (Mincle), macrophage C-type lectin (MCL), and Dendritic Cell-Specific Intercellular adhesion molecule-3-Grabbing Non-integrin (DC-SIGN). These receptors recognise yeast polysaccharides (Herre *et al.*, 2004), trehalose dimycolate, a mycobacterium cell wall component (Ishikawa *et al.*, 2009), α mannans, fucosylated and mannose rich glycans (van Liempt *et al.*, 2006). For many other receptors, it remains unclear if they induce phagocytosis directly or work indirectly and only prime the phagocyte for phagocytosis (Doyle *et al.*, 2004). These include receptors like CD14, scavenger receptor A (SR-A), CD36 and Macrophage receptor with collagenous structure (MARCO). CD14 recognises LPS binding protein (Schiff *et al.*, 1997). CD14 can also recognise the inner membrane components exposed in apoptotic cells (Devitt *et al.*, 1998; Nagata *et al.*, 2016). A signal from the interaction of CD14 and the apoptotic cell marker is dependent on the absence of an inhibitory 'don't eat me' signalling such as from the interaction of CD47- signal regulatory protein alpha (SIRPα) (Tsai and Discher, 2008). SR-A is a polyanionic ligand receptor (binds LPS or LTA) (Peiser *et al.*, 2000) that also binds non LPS related components in bacteria such as *Neisseria meningitis* (Peiser *et al.*, 2006). CD36 recognises a variety of lipoproteins, including LDL (Febbraio, Hajjar and Silverstein, 2001a), parts of apoptotic cells (Greenberg *et al.*, 2006), different forms of LPS (Biedroń, Peruń and Józefowski, 2016a) and *Plasmodium falciparum* infected cells (Patel *et al.*, 2004). MARCO recognises patterns in several bacteria (van der Laan *et al.*, 1999).

#### 1.1.7.1.2 Opsonic receptors

Opsonins are host-derived particles, for example, IgG, IgA and complement proteins, that can label particles for phagocytosis and have specific receptors on phagocytes. Fcγ-receptors (FcγR) bind to the Fc portion of IgG antibodies (Ehrhardt and Cooper, 2010). Once an FcγR and an IgG molecule engage, they can form a large

multivalent complex that clusters on the cell membrane, triggering phagocytosis and downstream cellular responses (Rosales and Uribe-Querol, 2013; Rosales, 2017). There are several different complement receptors, and each one binds to different subsets of complement proteins (Dunkelberger and Song, 2010; Dustin, 2017). Signalling pathways and mechanisms for particle uptake are dependent on the receptor, with those for Fc receptors and complement receptors being the best studied (Uribe-Querol and Rosales, 2020).

#### *1.1.7.2 Remodelling and phagosome formation*

At the site where a particle interacts with a phagocytosis receptor, extensive actin remodelling accompanied by a sequence of changes in the lipid composition occurs, resulting in the formation of a phagosome (Levin, Grinstein and Schlam, 2015; Levin, Grinstein and Canton, 2016)

Phosphatidylinositol-4-5-biphosphate ($PI(4,5)P_2$) rapidly accumulates then declines in the membrane of the phagocytic cup during FcγR mediated phagocytosis (Botelho *et al.*, 2000). The decrease in $PI(4,5)P_2$ likely facilitates actin disassembly playing a role in particle engulfment (Scott *et al.*, 2005)**.** As phagocytosis commences, the membrane-associated cortical cytoskeleton, via the action of coronins (F actin debranching proteins) (Yan *et al.*, 2005), cofilin (Bamburg and Bernstein, 2010) and gelsolin (F-actin severing proteins) (Nag *et al.*, 2013), is modified which allows for the subsequent membrane alterations. $PI(4,5)P_2$ regulates the association and separation of coronins, cofilin and gelsolin from actin filaments (Bravo-Cordero *et al.*, 2013; Nag *et al.*, 2013). These enzymes debranch F-actin and sever the linear fibres enabling the formation of new actin filaments. Further actin polymerisation leads to the extension of membrane protrusions that cover the target particle and invaginate into the cell (Underhill and Goodridge, 2012; Uribe-Querol and Rosales, 2020)

#### *1.1.7.3 Phagosome maturation*

The phagosome maturation process is a sequence of fusions and fissions between early endosomes, late endosomes and lysosomes to the phagosome (Figure 2).

**Early phagosome** (Figure 2 A)

Fusion of the phagosome to early endosomes is regulated by the GTPase, Rab5 (Gutierrez, 2013) through its recruitment of Early endosome antigen 1 (EEA1). EEA1 then mediates the vesicles docking and fusion (Callaghan *et al.*, 1999; Christoforidis *et al.*, 1999). EEA1 promotes the recruitment of proteins such as Rab7, which are necessary for the following steps of phagosome maturation (Vieira *et al.*, 2003). Recycling vesicles bud off the phagosome, so the endosome phagosome size remains approximately the same throughout despite the fusion of endosomes to the phagosomes.

**Late phagosome** (Figure 2 B)

Rab5 is gradually replaced by Rab7 (Vieira *et al.*, 2003). Phagosome and late endosomes fusion is mediated by Rab7 (Rink *et al.*, 2005).Vacuolar (V)-ATPase, a proton ($H^+$) transporter that transfers protons into the phagosome lumen leading to its acidification, also accumulates on the phagosome membranes (Kinchen and Ravichandran, 2008; Marshansky and Futai, 2008). The late endosomes carry lysosomal associated membrane proteins (LAMPs) and proteases such as cathepsins and hydrolases that become part of the phagosome with the fusion of the two (Fairn and Grinstein, 2012; Levin, Grinstein and Canton, 2016).

**Phagolysosome** (Figure 2 C)

In the final stage of phagosome maturation, lysosomes and the late phagosome fuse to become phagolysosomes (Levin, Grinstein and Canton, 2016). The phagolysosome contains many different hydrolytic enzymes that contribute to the degradation of the ingested microorganisms and work at low pHs, such as cathepsins, lysozymes, lipases and cathepsins (Kinchen and Ravichandran, 2008). V-ATPases are found at even greater concentrations on the membranes of phagolysosomes and contribute to significant decreases in pH (as low as 4.5), which is deleterious to many microorganisms (Marshansky and Futai, 2008). Nicotinamide adenine dinucleotide phosphate (NADPH) oxidase (NOX2) complex can also be found on phagolysosome membranes and produces reactive oxygen species (ROS) in particular superoxide (Babior, 2004; Minakami and Sumimoto, 2006). ROS

can result in the formation of hypochlorous acid through the action of myeloperoxidase on $Cl^-$ and $H_2O_2$, which is a potent antimicrobial (Nauseef, 2014).

#### *1.1.7.4 pH regulation in phagolysosomes (Figure 2 C)*

The progressive increase in active V-ATPase is a major contributor to the decrease in phagosome pH. However, it is not the only factor involved in luminal acidification. Other factors that determine pH are phagosome membrane permeability to counterions, luminal buffering capacity, rate of proton leakage, and proton consumption by other enzymes (Canton *et al.*, 2014). The optimal phagosomal pH for the different functions of phagocytes is not uniform. Efficient pathogen killing, antigen presentation and degradation of apoptotic cells and recycling of their components all have different optimal pH.

At early stages of phagocytosis, phagosomes in human M1 macrophages do not acidify but remain at near neutral pH oscillating to alkaline pH due to the intermittent opening of voltage-gated ion channels. In contrast, M2 phagosomes rapidly acidify (Canton *et al.*, 2014). pH remains high in human M1 macrophages as they have a lower proton pumping rate than M2 macrophage; they express higher levels of NOX2 and retain it longer in the phagosome, and produce more ROS (Canton *et al.*, 2014). The sustained NADPH activity in the phagosomes is accompanied by delayed full maturation of the M1 phagosomes and hence delayed acidification. The production of superoxide by NOX2 and its dismutation into hydrogen peroxide consumes protons raising the pH (Jankowski, Scott and Grinstein, 2002; Savina *et al.*, 2006; Mantegazza *et al.*, 2008). Canton *et al.* showed that inhibiting NOX2 in macrophages leads to increased acidification of M1 macrophages.

Unlike their human counterparts, murine M1 macrophages do acidify, likely due to their greater reliance on nitric oxide synthase and production of nitric oxide rather than on superoxide through NOX2 (Mantovani *et al.*, 2004; Schneemann and Schoeden, 2007). Superoxide is still produced in murine macrophages, but it reacts with nitric oxide reducing its capacity to consume luminal protons (Wink *et al.*, 2011).

Sustained ROS production and decrease in acidification has critical functional effects. ROS production enhances antigen cross-presentation in dendritic cells and negatively regulates antigen proteolysis (Minakami and Sumimoto, 2006; Savina *et al.*, 2006; Jancic *et al.*, 2007; Mantegazza *et al.*, 2008). Redox state control of phagosomes also regulates antigen processing and regulates the epitopes loaded onto MHC II for regular antigen presentation (Allan *et al.*, 2014).

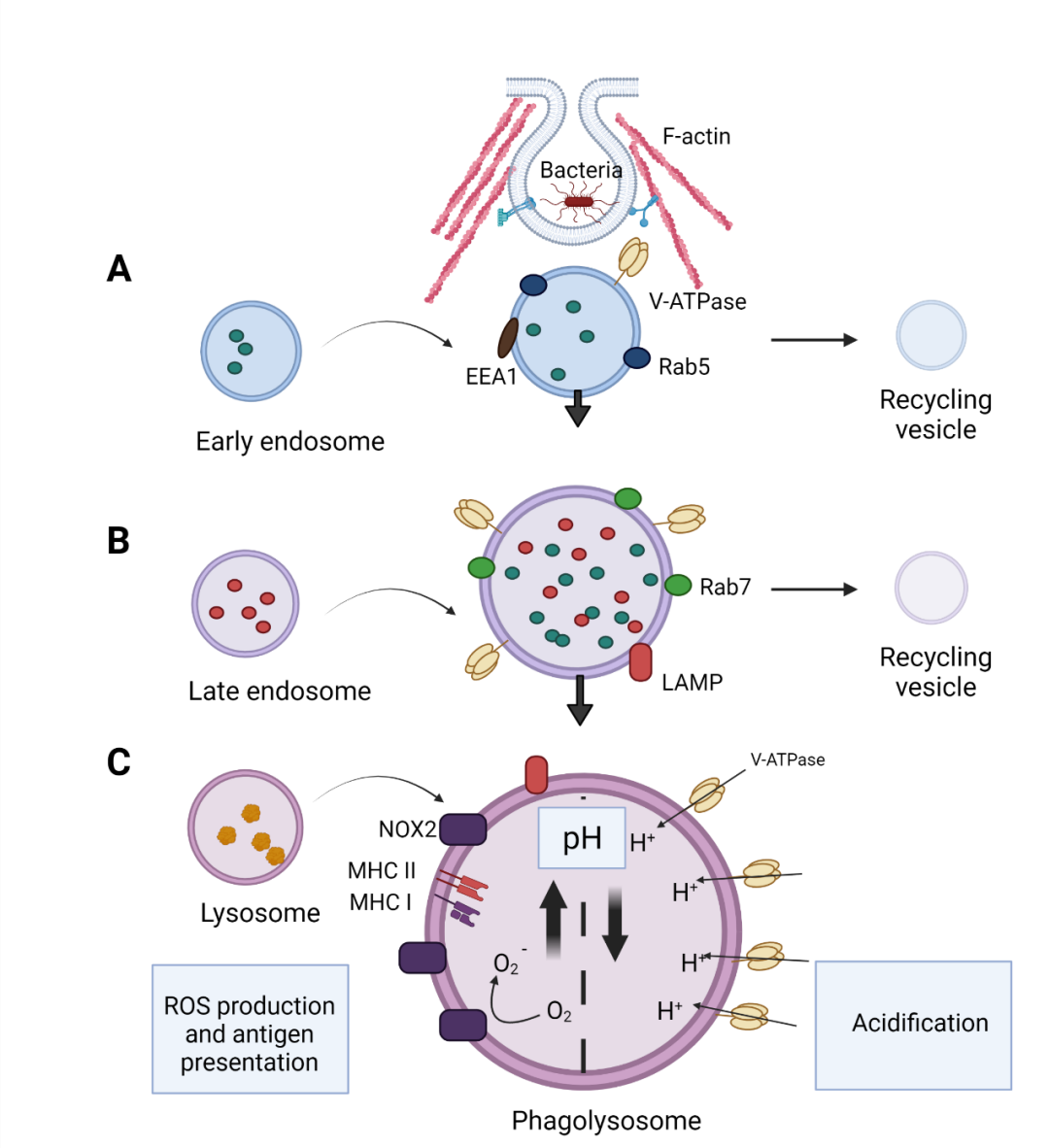


Figure 2. Phagosome maturation.

Sequential fusion events with vesicles from the endocytic pathway result in the incorporation of various microbicidal compounds into the phagosome, finally forming a phagolysosome. There are three major stages of maturation: (**A)** early, **(B)** late, and **(C)**

phagolysosome. Membrane fusion at each stage is controlled by different molecules such as Rab5 and Rab7. Through the proton pumping action of V-ATPase the phagolysosome lumen becomes increasingly acidic. The phagosome acquires more enzymes such as cathepsins, proteases, lipases, and lysozymes that degrade the ingested content with each fusion. EEA1, early endosome antigen 1; NOX2, NADPH oxidase; LAMP, lysosomal-associated membrane protein. (Canton *et al.*, 2014; Uribe-Querol and Rosales, 2020)

## 1.2 RNA modification

RNA has considerable potential for diversity, with over 170 distinct modifications identified (Kadumuri and Janga, 2018; Boo and Kim, 2020; Kumar and Mohapatra, 2021). In comparison, DNA has only six known modifications. All types of RNA experience modification; ribosomal RNAs (rRNA), transfer RNA (tRNAs), messenger RNA (mRNA) to small regulatory RNAs such as small interfering RNAs (siRNA) and enhancer RNAs (eRNA). Most modifications and the best functionally understood are in rRNAs and tRNAs (Jackman and Alfonzo, 2013).

Several post-transcriptional modifications occur in mRNA and have varied consequences on cellular processes like splicing, mRNA export, translation, localisation and degradation (Roundtree *et al.*, 2017; Kumar and Mohapatra, 2021). It is well-established that transcription and thus mRNA levels do not directly correspond to protein levels (Wu *et al.*, 2013), and RNA modifications are believed to be part of the reason for this phenomenon. The term 'epitranscriptomics' was coined to describe these modifications in mRNAs (Saletore *et al.*, 2012).

RNA modifications can be split into two groups 1) Reversible modifications such as methylation by methyltransferases that demethylases can remove, and 2) Irreversible such as deamination of cytidine to uridine and adenosine to inosine. For brevity, I will focus on RNA deamination, which is a critical part of this thesis and provide only an overview of major reversible modifications.

### 1.2.1 Reversible modifications

Among the reversible modifications, $N^6$ -methyladenosine ($m^6A$) is considered the most abundant modification in mRNA (Wu *et al.*, 2016). $m^6A$ modifications can occur along all the mRNA sequence, but high throughput methods have shown that they are enriched in 3'UTRs and at stop codons (Meyer *et al.*, 2012; Liu and Pan, 2016). A variety of writers, methyltransferases (METTL3, METTL14 and WTAP), erasers, demethylases (ALKBH5, FTO) and readers, $m^6A$ binding proteins (YTHDC1, YTHDF1-3) have been identified for $m^6A$ (Niu *et al.*, 2013; Fu *et al.*, 2014; Yue, Liu and He, 2015). It is clear from these discoveries that $m^6A$ is a dynamic process in mRNA regulation, and it is proposed that $m^6A$ influences splicing, mRNA transcription, nuclear export, translation, localisation and stability (Wu *et al.*, 2016).

Additional positions of adenosine and other bases can also be methylated in mRNA. Adenosine, for example, can be methylated in the $N^1$ position to form $m^1A$ or dually methylated in the $C_2$ position of the ribose sugar in addition to $N^6$ to form $m^6Am$ (Hauenschild *et al.*, 2015; Molinie *et al.*, 2016). $m^1A$ at transcription start sites affects mRNA secondary structure that facilitates translation initiation (Hauenschild *et al.*, 2015). The $m^6Am$ modification is found exclusively at transcription initiation sites (Linder *et al.*, 2015).

### 1.2.2 Irreversible modifications

The irreversible modifications with no known eraser enzymes contain the deamination of cytosine, adenosine, and pseudouridine (ψ). Most ψ modifications are observed in rRNA and tRNA; however, they also occur in eukaryote mRNA (Carlile *et al.*, 2014; Schwartz *et al.*, 2014). Deamination effectively results in a change of base as the resultant base is decoded differently, adenosine to inosine (A-to-I) is decoded as guanosine and cytosine to uracil (C-to-U), which lead to these nucleotide changes to be referred to as 'RNA editing'. The term is not to be confused with 'editing' that occurs in trypanosomes kinetoplasts where uridines are inserted or deleted to alter the frame of an RNA (Benne *et al.*, 1986). A-to-I modifications are catalysed by members of the Adenosine Deaminases that act on RNA (ADAR) family and C-to-U modifications by

Activation-Induced Deaminase/Apolipoprotein members B mRNA editing enzyme catalytic polypeptide-like (AID/APOBEC) family.

#### *1.2.2.1 The ADAR family*

There are three members of the ADAR family: ADAR1 and ADAR2 that edited double-stranded(ds)RNA and the catalytically inactive ADAR3 (Wang *et al.*, 2013). ADAR1 has two isoforms: constitutively and ubiquitously expressed, ADAR1p110 and a form induced by interferon ADAR1p150 (Patterson and Samuel, 1995). ADARs bind and edit many dsRNA with a preference for sequences with a pyrimidine before the target A, followed by a guanine (U/CAG) (Quin *et al.*, 2021). As a result of the base change, A-to-I editing is easily detected by RNA sequencing through which millions of sites have been identified in pre-mRNAs, mRNAs and non-coding RNAs (Bazak *et al.*, 2014).

##### 1.2.2.1.1 Functions of A-to-I editing

###### *1.2.2.1.1.1 Editing in coding regions*

Editing in coding regions of mRNA is very rare, with only about 100 low-frequency events accepted in humans and even fewer sites recognised in mice (Ramaswami *et al.*, 2013; Pinto, Cohen and Levanon, 2014). The best-studied specific A-to-I editing event happens to be one of these rare recoding events that occurs in a subunit of a glutamate receptor in the brain, the GluA2 subunit of α-amino-3- hydroxy-5-methyl-4-isoxazolepropionic acid (AMPA) receptor (Sommer *et al.*, 1991). Editing results in codon 586 changing from glutamine to arginine. The AMPA receptor is an ion channel involved in excitatory synaptic signalling. A receptor with glutamine at position 586 allows sodium and calcium to permeate through; however, with arginine in this position, the receptor no longer allows calcium through and has a 10-fold decrease in conductance (Burnashev *et al.*, 1992; Monyer *et al.*, 1992). Editing at this site is almost 100% efficient and is essential for life. ADAR2 is responsible for this editing event in mice. *Adar2*$^{-/-}$ mice die at birth, but lethality can be rescued by introducing the 'edited' version genomically (Higuchi *et al.*, 2000).

A-to-I recoding also affects several other AMPA receptor sites and additional receptors in the brain. AMPA GluA2-4 mRNA can be recoded at position 764, resulting in increased recovery from desensitisation (Lomeli *et al.*, 1994). The Kainite receptors

GluLK1 and Gluk2 (Köhler *et al.*, 1993), voltage-dependent potassium channel $K_v$1.1(Bhalla *et al.*, 2004), calcium channel $Ca_v$1.3(Huang *et al.*, 2012), and the gabra-3 subunit of the GABA-A receptor (Ohlson *et al.*, 2007) are all examples of codon edited brain receptors. RNA editing has significant effects on mammalian neuronal signalling.

#### *1.2.2.1.1.2 Editing in non-coding elements*

*Alu* elements are conserved non-autonomous short interspersed nuclear elements (SINEs) usually found in UTRs and introns of primates (Batzer and Deininger, 2002). SINEs are less common in non-primates such as mice and less evolutionary conserved (Neeman *et al.*, 2006). They are considered an element that generates genetic diversity. These elements have a repetitive nature; sense and antisense repeats are adjacent to one another and form double-stranded structures that are ideal targets for ADAR editing. The A-to-I editing disrupts A-U pair formation in ds areas destabilising and opening the structure (Mannion *et al.*, 2014). It has been postulated that the clustering of editing events at *Alu* repeats may prevent the transposition of these retroelements that could disrupt genes and disrupt the integration of retroviruses (Mannion *et al.*, 2014).

One of the primary functions associated with ADARs is the destabilisation of dsRNA from these SINE elements and other factors in cellular RNA that lead to dsRNA formation. The destabilisation prevents the innate immune system from recognising self RNA as foreign. dsRNA is a PAMP recognised by the cells as foreign by specific TLRs, RLRs and NLRs (Wilkins and Gale, 2010). As part of their life cycle, many viruses have stages with dsRNA; dsRNA viruses, hairpins in viral mRNA, transcription of DNA viruses or dsRNA formed during the transcription of single-stranded(ss)RNA viruses. Cytoplasmatic dsRNA triggers activation of RIG-I and melanoma differentiation-associated gene 5 (MDA5), which recruits mitochondrial antiviral signalling protein (MAVS) (Kang *et al.*, 2002; Yoneyama *et al.*, 2004). MAVS causes the transcription factors IRF3 and NF-κB to translocate into the nucleus inducing IFN type I and proinflammatory cytokines. *Adar1*$^{-/-}$ mice do not survive past embryonic day 12.5; however, lethality is rescued, and mice survive until birth if they are a double knockout also for MAVS (Mannion *et al.*, 2014; Pestal *et al.*, 2015). This suggests that ADAR1 is upstream of MAVS and prevents the sensing of self RNA as foreign

and the triggering of an IFN response. ADAR1 KO cell lines are often characterised by overexpression of IFN response genes and translational shutdown (Chung *et al.*, 2018). It is interesting to note that in our experience, KO of ADAR1 in cells of the immune system both from conditional KOs in primary mouse cells or human and mouse cell lines did not result in upregulation of IFN response genes (B cells, macrophages and natural killer cells, unpublished).

Other processes affected by editing are miRNA processing and miRNA mediated silencing (Ohman, 2007). ADAR1 and ADAR2 have been described to hinder the processing of target miRNAs (Yang *et al.*, 2006), suppressing the formation of mature miRNA (Kawahara *et al.*, 2007) and antagonising miRNA mediated gene silencing (Iizasa *et al.*, 2010). Alternative splicing has also been shown to be influenced by editing where ADAR when editing occurs at splice donor or splice acceptor sites resulting in the formation of a different isoform (Goldberg *et al.*, 2017).

#### *1.2.2.2 The AID/APOBECs family*

There are 12 AID/APOBEC family members in primates; APOBEC 1 (A1), A2, A3A, A3B, A3C, A3D, A3F, A3G, A3H, A4 and AID (Salter, Bennett and Smith, 2016). All family members exhibit C-to-U deaminase activity (except for A2 and A4, considered catalytically inactive and whose function is unknown) on either ssDNA or ssRNA. The first member to appear in the evolutionary history, coinciding with the first appearance of adaptive immunity (Conticello, 2008), was AID that has an essential role in antibody diversification (Muramatsu *et al.*, 2000). Multiple gene duplications through history lead to the appearance of the other family members starting with A1 (Conticello *et al.*, 2005). In rodents, the original duplication of the A3 locus became fused into a single gene, so unlike primates, they have only 5 AID/APOBEC proteins. The family shares many structural similarities and a conserved zinc-dependent deaminase catalytic site, which is also found in ADARs (Salter, Bennett and Smith, 2016). A1, A3A and A3G are the only members currently described as having RNA deamination activity and the others only DNA deamination activity(Lerner, Papavasiliou and Pecori, 2019). However, it is possible that other members also have RNA activity. Studies with the AID/APOBEC family involve

overexpression, resulting in DNA activity that may not actually occur *in vivo,* leading to potential overlooking of an RNA editing ability and only a DNA deaminase activity being described.

#### 1.2.2.2.1 Editing in coding regions

Similarly to A-to-I editing, C-to-U editing is extremely rare in coding regions, and even fewer examples are known than for the former. The founding member of the AID/APOBEC family, A1, was identified for its editing of a coding region of apolipoprotein B *(Apob)* mRNA which is the reason for the name APOBEC. This enzyme catalyses the deamination of cytosine at codon Q2180 of *Apob* pre-mRNA generating a stop codon resulting in a shorter form of the APOB protein called APOB-48 (Navaratnam *et al.*, 1993; Teng, Burant and Davidson, 1993). APOB is a component of chylomicrons and various lipoproteins essential for proper lipid metabolism and transport around the body. Full-length APOB, APOB-100, is found almost exclusively in the liver, while the edited shorter APOB-48 is in the small intestine (Young, 1990; Yao and McLeod, 1994). APOB-100 forms the most prominent low-density lipoproteins (LDL) protein component, and APOB-48 is more frequently found in chylomicrons. APOB-48 containing lipoproteins are more rapidly cleared from the blood and are unlikely to form LDLs. *Apobec1*$^{-/-}$/*LDLR*$^{-/-}$ mice expressing only apoB100 develop spontaneous hypercholesterolemia (Powell-Braxton *et al.*, 1998). It is clear from this evidence that editing plays an important role in proteome diversification that is not directly coded in the genome. The editing or lack of editing in the small intestine vs the liver is governed by the different A1 cofactors and their different levels in each tissue. A1 is expressed in both tissues, but Blanc *et al* showed that A1 targets were governed and differed according to the presence of one of A1 cofactors, A1 complementation factor (A1CF) or RBM47 (Blanc *et al.*, 2018).

In rats, the supramedullary glycine receptor (GlyR) isoform GlyRα3$^{P185L}$ is a result of deamination of cytosine 554. This isoform has increased sensitivity to glycine, promoting chloride conduction that occurs with tonic inhibition (Meier *et al.*, 2005). Interestingly the neurons in which the receptor is present express neither of the known

A1 cofactors, A1CF or RBM47, suggesting that other undiscovered cofactors exist (Zhang *et al.*, 2014).

Other examples of A1 recoding C-to-U events all come from pathologies. Originally it was thought that *Apob* was the only target of A1 and limited to tissues that express APOB (Hirano *et al.*, 1996). When the sequence elements in *Apob* that supported efficient A1 editing were described, additional targets were proposed. A sequence upstream of the edited C and an 11nt downstream element called the mooring sequence affect the efficiency of A1 editing, which is further increased by the presence of an AU rich sequence (Shah *et al.*, 1991; Backus and Smith, 1992). Based on this its hypothesised that these elements create a particular RNA secondary structure suitable for A1 editing (Richardson, Navaratnam and Scott, 1998; Maris *et al.*, 2005). N-acetyltransferase 1 (*Nat1*) mRNA has a sequence homologous to the mooring sequence and was found to be edited in some patients with hepatocellular carcinomas (Yamanaka *et al.*, 1997). A proportion of patients with peripheral nerve sheath tumours have an alternatively spliced form of Neurofibromatosis type (*Nf1*) mRNA that is edited (Skuse *et al.*, 1996; Mukhopadhyay *et al.*, 2002).

In humans, where A1 expression is often limited to the intestines, A3A and A3G can edit RNA (Sharma *et al.*, 2016, 2016). C-to-U editing resulting from A3A was attributed to the formation of a premature stop codon at position 136 of Succinate Dehydrogenase Subunit B (*SDHB*) in peripheral blood mononuclear cells (Baysal, 2007; Sharma *et al.*, 2015). Hypoxia and activation state determined the editing levels, and it was surmised that this might be a hypoxia-adaptive mechanism (Sharma *et al.*, 2015, 2018, 2019). The same group also described identifying an additional 33 editing events that lead to non-synonymous changes to transcripts under these conditions.

#### 1.2.2.2.2 Editing in non-coding regions

Many coding sequences contain motifs and sequences that A1 has been shown to prefer, and yet they are not edited. The vast majority of editing events are limited to 3'UTRs (Rosenberg *et al.*, 2011). It has been suggested that RBPs are responsible for directing the A1 editing to UTRs and not to coding regions. The exact function of many of

these editing events are unknown, but their location in 3'UTR suggests that they have regulatory roles such as those seen for A-to-I editing, namely, stability, localisation and translation (Rosenberg *et al.*, 2011; Blanc *et al.*, 2018). Due to its tendency to occur in AU-rich sequences, the possibility that editing could generate new polyadenylation signals by creating AAUAAA motifs has also been proposed (Lerner, Papavasiliou and Pecori, 2019).

Editing associated with A3A and A3G also seems to be concentrated at 3'UTRs at very select sites. How A3A or A3G are targeted to specific transcripts is not yet known; however, there is a distinct stem-loop structure favoured by both enzymes (Sharma and Baysal, 2017).

### 1.2.3 Editing in macrophages

Murine immune cells express A1 at high levels and human immune cells are the major expressers of A3A and A3G whose expression is also increased with IFN stimulation (Cullen, 2006; Harjanto *et al.*, 2016; Rayon-Estrada *et al.*, 2017). Among immune cells, monocytes and monocyte-derived macrophages have an exceptionally high expression (of A1 in mice and A3A/A3G in human cells) (Sharma *et al.*, 2015, 2018; Rayon-Estrada *et al.*, 2017) (see Figure S 1). Hundreds of transcripts are edited in these cells, with many transcripts showing multiple edited sites.

Editing in murine bone marrow-derived macrophages (BMDM) and microglia is enriched in phagocytosis and transendothelial migration pathways (Cole *et al.*, 2017a; Rayon-Estrada *et al.*, 2017). Knockout cells have a phenotype that differs depending on the cell type; *Apobec1*$^{-/-}$ BMDMs are more phagocytotic and less chemotactic than their wild-type (WT) counterparts, and *Apobec1*$^{-/-}$ microglia are less phagocytotic with aberrant lysosome and autophagosome formation. The exact mechanism for these phenotypes remains unknown; however, both Rayon-Estrada et al. and Cole et al. showed that editing could potentially affect protein abundance by utilising luciferase assays. Most edited transcripts were not differentially expressed between WT and KO macrophages, and the formation and abrogation of miRNA binding sites were studied with only very few editing events affected by miRNA (Rayon-Estrada *et al.*, 2017). This suggests that unlike with A-

to-I editing, most C-to-U editing events do not affect stability leaving the other regulatory options, translation and localisation open for further investigation.

The loss of A1 in mice resulted in a slight increase in the number of circulating Ly6C$^+$ monocytes that are usually more abundant during inflammation (Rayon-Estrada *et al.*, 2017). A3A knockdown in human M1 macrophages decreased the expression of several proinflammatory genes, *IL6, IL23A* and *IL12B,* and the M1 associated surface markers, CD80 and CD86 (Alqassim *et al.*, 2020). On the other hand, inflammatory macrophages are characterised by their metabolic switch to relying almost solely on glycolysis for their needs and knockdown macrophages exhibited increased levels of glycolysis. Editing rates in human macrophages were also dependent on the kind of stimulation and activation state of the cell, with differences observed in resting-state macrophages, M1, M2 and the type of IFN treatment was used (Sharma *et al.*, 2015; Alqassim *et al.*, 2020). So far, the dynamics of editing during macrophage activation and its potential implications to macrophage function has remained unstudied.

# 2 Aims of the Dissertation

The existence of numerous C-to-T editing targets in the 3'UTR of the transcriptome is evident (Rosenberg *et al.*, 2011; Blanc *et al.*, 2014; Harjanto *et al.*, 2016; Cole *et al.*, 2017a; Rayon-Estrada *et al.*, 2017). However, the functional effects of these events and how they are regulated with different stimuli are largely unknown. Mouse macrophages are among the cells with the highest expression of the C-to-T editor APOBEC1 and quickly respond to many environmental cues and are therefore a natural place to begin the study of editing. A better understanding of the role APOBEC1 editing has on macrophage physiology can bring to light new functional mechanisms relevant to their regulation that could have important consequences in pathologies.

## 2.1 Characterise the C-to-T editing landscape during macrophage activation

C-to-T editing has so far only been characterised in resting mouse macrophages and human macrophages only in single time points after activations. Macrophage activation is a tightly regulated process, and indications from human macrophages suggest that editing is affected (Alqassim *et al.*, 2020). Therefore, I aimed to explore the editome by Next-generation-Sequencing over multiple time points of stimulation to capture a picture of editing dynamics.

## 2.2 Determine the effects of editing on protein abundance

Work by Rayon-Estrada *et al*., indicated that editing might cause changes in the translational efficiency of edited transcripts; however, this was not studied in depth. Because the consequences of editing are unknown, I studied in greater detail the effects on protein levels.

## 2.3 Determine how APOBEC1 editing alters macrophage phenotype

APOBEC1 editing is known to alter phagocytosis in mouse macrophages, but how phagocytosis is altered and why are yet unknown. Elucidating the effects on phagocytosis is a large step forward in identifying the functional relevance of APOBEC1.

# 3 Materials and Methods

## 3.1 Materials

### 3.1.1 Reagents

| Name | Specifications | Manufacturer |
|---|---|---|
| Cycloheximide | C1988 | Sigma-Aldrich |
| pHrodo Green S. aureus Bioparticles Conjugate for Phagocytosis (LIFE Technologies) | P35367 | Thermo Fisher Scientific |
| pHrodo Green E. coli Bioparticles Conjugate for Phagocytosis (LIFE Technologies) | P35366 | Thermo Fisher Scientific |
| Cell Line Nucleofector® Kit R | VCA-1001 | Lonza |
| Intracellular pH Calibration Buffer Kit | P35379 | Thermo Fisher Scientific |
| Trizma Base (Tris base) | 93350 | Merck/Sigma-Aldrich |
| Sodium chloride >= 99.5% analytical reagent grade | 10735921 | Thermo Fisher Scientific |
| Magnesium chloride hexahydrate, ≥99 %, p.a., ACS | 2189.1 | Roth |
| Bovine serum albumin, heat shock fraction, pH 7, ≥98% | A7906 | Merck/Sigma-Aldrich |
| TURBO DNA-free kit | AM1907 | Thermo Fisher Scientific/Invitrogen |
| LIVE/DEAD™ Fixable Violet Dead Cell Stain Kit | L34955 | Thermo Fisher Scientific |
| Q5® High-Fidelity DNA Polymerase | M0491L | New England Biolabs |
| Biozym Blue S'Green qPCR Kit Separate ROX | 331416S | Biozym |
| ProtoScript® First Strand cDNA Synthesis Kit | E6300S | New England Biolabs |

| Name | Specifications | Manufacturer |
|---|---|---|
| CloneJET PCR Cloning Kit | K1232 | Thermo Fisher Scientific |
| One Comp eBeads (Invitrogen) | 01-1111-42 | Thermo Fisher Scientific |
| OneStep RT-PCR Kit | 210212 | Qiagen |
| Cell Line Nucleofector Kit V | VCA-1003 | lonza |
| PEQGOLD TRIFAST FL 100 ML | 732-3314 | VWR International |
| Hoechst 33342 | H3570 | Thermo Fisher |
| 2-Mercaptoethanol (50 mM)-20 mL | 31350010 | LIFE Technologies/Thermo Fisher |
| ArC™ Amine Reactive Compensation Bead Kit | A10346 | Thermo Fisher Scientific |
| Sucrose, Molecular Biology grade | S0389-500G | Sigma-Aldrich |
| 100bp DNA Ladder | N3231L | New England Biolabs |
| SYBR Safe DNA Gel Strain | S33102 | Life Technologies |
| TAE - BUFFER (50X) | A1691,1000 | APPLICHEM GMBH |
| Dimethyl sulfoxide | D5879 | Sigma-Aldrich |
| GlycoBlue Coprecipitant (15 mg/mL)-5 x 300 µL | AM9516 | Thermo Fisher Scientific, |

### 3.1.2 Solutions

| Name | Composition/specification | Manufacturer |
|---|---|---|
| Polysome lysis buffer | 20 mM Tris-HCl pH 7.5<br>120mM KCl<br>2mM MgCl2<br>1mM DTT<br>Roche cOmplete protease inhibitor (according to manufacturer recommendation<br>1u/ul Murine RNase inhibitor<br>RNase free water | Self-made |
| 10x Salts solution | 1000 mM NaCl<br>200 mM Tris-HCl (pH 7.5)<br>50 mM MgCl2<br>RNase free water | Self-made |
| Chase solution (60% sucrose) | 40 ml 2.2 M sucrose<br>5 ml H2O<br>5 ml 10x salts solution<br>Small amount of bromophenol blue powder | Self-made |
| RIPA lysis buffer system | sc-24948 | Santa Cruz |
| Invitrogen™ Live Cell Imaging Solution | 12363603 | Fischer scientific |
| HEPES Buffer Solution 1M | 15630-056 | Gibco |
| Sera Pro, South America origin, fetal bovine serum, low endotoxin | | Pan biotech |
| Opti-MEM™ I Reduced Serum Medium | 31985062 | Thermo Fisher Scientific/Gibco |

### 3.1.3 Kits

| | | |
|---|---|---|
| Qubit RNA BR assay kit | Q10211 | Thermo Fisher Scientific/Invitrogen |
| Qubit RNA IQ assay kit | Q33221 | Thermo Fisher Scientific/Invitrogen |
| RNeasy Plus Mini Kit | 74134 | Qiagen |
| KAPA mRNA HyperPrep Kit (KAPABIOSYSTEMS) | KK8580 | Roche |
| KAPA Unique Dual-Indexed Adapter Kit (15 µM) (KAPABIOSYSTEMS) | 08861862001 | Roche |
| NucleoSpin™ Gel and PCR Clean-up Kit | 11992242 | Fisher Scientific |
| Agilent High Sensitivity DNA Kit | 5067-4626 | Agilent |
| PureLink™ HiPure Plasmid Filter Maxiprep Kit | K210017 | Thermo Fisher Scientific |

### 3.1.4 Proteins

| Name | Specifications | Manufacturer |
|---|---|---|
| IFN-gamma, rec. Murine | 315-05-20 | Peprotech |
| Lipopolysaccharide | L2630-10MG | Sigma-Aldrich |

### 3.1.5 Antibodies

| Name | Clone/specification | Dilution | Provider |
|---|---|---|---|
| FITC Rat Anti-Mouse CD86 | Clone GL1 (RUO) | 0.125ug/test | BD biosciences, |
| PE Hamster Anti-Mouse CD80 | Clone 16-10A1 (RUO) | 0.06ug/test | BD biosciences, |
| APC/Fire™ 750 anti-mouse CD40 Antibody | 3/23 | 0.125ug/test | BioLegend |
| APC anti-mouse I-A/I-E Antibody | M5/114.15.2 | 0.125ug/test | BioLegend, |
| Rat IgG2b kappa Isotype Control (eB149/10H5), APC | 17-4031-82 | 0.125ug/test | Thermo Fisher Scientific, |
| Rat IgG2a kappa Isotype Control (eBR2a), FITC | 11-4321-80 | 0.125ug/test | Thermo Fisher Scientific, |
| Hamster IgG2, κ (anti-KLH) PE | 550085 | 0.06ug/test | BD biosciences, |
| APC anti-mouse CD36 | 102611 | 0.125ug/test | Biolegend |
| APC Armenian Hamster IgG Isotype | 400911 | 0.125ug/test | Biolegend |

### 3.1.6 Plastics and consumables

| Name | Specifications | Manufacturer |
|---|---|---|
| Mini Cell Scrapers | PK-CA707-22003 | Promocell |
| Tube, Thinwall, Polyallomer, 4 mL, 11 x 60 mm | 328874 | Beckman coulter |

| Name | Specifications | Manufacturer |
|---|---|---|
| UltraCruz Cell Scrapers | sc-395250 | Santa Cruz |
| 384ST 70ul Tips | 19133-142 | Agilent |
| X25 twin.tec PCR Plate 96 | 10120092 | Thermo Fisher Scientific, |
| Tissue Culture Dish 150 | 93150 | TPP |

### 3.1.7 Laboratory equipment, machines & instruments

| Name | Specifications | Manufacturer |
|---|---|---|
| 2-Gel Tetra and Blotting Module | 1660827EDU | Bio-Rad |
| Centrifuge 5427 R | 5409000010 | Eppendorf |
| Centrifuge 5920 R | 5948000018 | Eppendorf |
| CFX Connect Real-Time PCR Detection System | 1855201 | Bio-Rad |
| Chemidoc | 17001401 | Bio-Rad |
| Eclipse Ts2 Inverted Microscope + DS-Fi3 microscope camera | Ts2-FL + DS-Fi3 | Nikon |
| Mini-PROTEAN Tetra Cell | 1658004EDU | Bio-Rad |
| Multiskan™ FC Microplate Photometer | 51119000 | Thermo Fisher Scientific |
| NanoDrop™ One/OneC Microvolume UV-Vis Spectrophotometer | ND-ONEC-W | Thermo Fisher Scientific |
| Pipetboy acu 2 | 155 019 | Integra Biosciences |

| Name | Specifications | Manufacturer |
|---|---|---|
| PIPETMAN Classic Starter Kit, 4 Pipette Kit, P2, P20, P200, P1000 | F167380 | Gilson |
| Safe 2020 Class II Biological Safety Cabinet | 51026637 | Thermo Fisher Scientific |
| T100 Thermal Cycler | 1861096 | Bio-Rad |
| Thermo Scientific™ Multifuge™ X3R | 75004515 | Thermo Fisher Scientific |
| Bravo Automated Liquid Handling Platform | | Agilent |
| GloMax® Discover Microplate Reader | | promega |

### 3.1.8 Software

| | |
|---|---|
| FACSDIVA v6.1.2 | BD, Franklin Lakes, USA |
| Flowjo 10 | Treestar, Ashland, USA |
| Graph Pad Prism 10 | GraphPad Software Inc., La Jolla, USA |
| Fiji | (Schneider, Rasband and Eliceiri, 2012) |
| Affinity Designer | The Inkscape Team, www.inkscape.org |
| Zotero | https://www.zotero.org/ |
| Microsoft Office 2010 | Microsoft Corporation, Redmond, USA |

## 3.2 Methods

### 3.2.1 Cell culture

#### *3.2.1.1 Cell line maintenance*

RAW 264.7 cells were purchased from the ATCC. Before the start of this work the cell lines were tested for mycoplasma contamination (done by Multiplexion, Immenstaad) and one additional time after 3 years to confirm cells were still not contaminated. Cells were maintained in an incubator at 37 °C, 95 % relative humidity and 5 % $CO_2$. Cell culture was performed in a laminar flow hood. For routine maintenance RAW 264.7 cells were grown in 150 $mm^2$ dishes and were passaged approximately twice a week (or as needed) to maintain a confluence of under 90%. To passage the cells, cells were lifted from plates with a cell scraper and seeded in fresh plates with fresh complete DMEM at the appropriate density (for routine passaging, cells were diluted into two plates by volume, one plate 1:10 and one 1:20). Plates were swirled to distribute the cells evenly.

#### *3.2.1.2 Freezing and thawing of cells*

Cells were harvested for freezing with a cell scraper, transferred to a 50ml falcon tube, and spun down (422 g, 5 min, RT). The supernatant was removed, and the cells were resuspended with freezing medium (90% FCS, 10% DMSO). Cells obtained from one 90% confluent 150$mm^2$ dish and resuspended in freezing medium were aliquoted into five cryovials. The vials were transferred to -80°C for up to one week and then transferred to a liquid nitrogen cryotank for long term storage.

To reconstitute cells, cryovials were collected from the liquid and thawed. The thawed cell mixture was transferred to a 15ml falcon tube with 10ml of complete DMEM and centrifuged at 422g for 5 minutes. After centrifugations supernatant was immediately decanted and replaced with fresh complete DMEM and plated onto 100$mm^2$ dishes.

#### *3.2.1.3 Transfection of RAW 264.7 cells*

RAW 264.7 cells were nucleofected (nuleofection and transfection are used here synonymously) using Amaxa nucleofection device II and Amaxa Cell Line Nucleofector Solution V according to the manufacurers instructions. In brief: One day before transfection cells were passage to achieve 80% confluence. On day of transfection cells

were scraped and collected into a falcon tube. The cells were stained with trypan blue and counted with a hematocytometer and 2 million cells were transferred to a tube and centrifuged at 422 g for 5 minutes at RT, the supernatant was discarded, and cells resuspended in 100 ul RT nucleofector solution mixed with 2ug of DNA to be transfected. The mixture was quickly transferred to a cuvette and nucelofected with program D-032. Immediately after nucleofection 1ml complete DMEM (High Glucose DMEM, 10%Endotoxin low FCS, 1% pen/strep, 1% glutamine) was added to the cuvette and the mixture was aspirated and transferred to a plate with complete media (plate size depends on the application, one cuvette was nucleofected per 3ml final volume of media to be used) and transferred to an incubator.

#### *3.2.1.4 Generation of APOBEC1 knockout RAW 264.7 cells*

Generation of the APOBEC1 Knockout (A1 KO) RAW 264.7 cell line is described in Lerner et al. 2021. Wild-type RAW 264.7 cells were co-nucleofected with Cas9 constructs PX458-APOBEC1 exon 4 and PX458-APOBEC1 exon 5 (1 µg each). PX458 vector (pSpCas9(BB)-2A-GFP (PX458) was a gift from Feng Zhang (Addgene plasmid # 48138 ; http://n2t.net/addgene:48138 ; RRID:Addgene_48138) contains Cas9 under the chicken β actin promoter followed by enhanced green fluorescent protein (EGFP) linked by the self-cleaving peptide T2A and a U6 promoter for the guide RNA in the same backbone (Ran *et al.*, 2013).To ensure enough cells were available for sorting 4 cuvettes with 2 million cells each were transfected and plated together on one 150 $mm^2$ cell culture dish. 48 hours post transfection the cells were scraped, counted as described before and diluted to a concentration of $5\times10^6$ cells per ml in phenol red-free DMEM. EGFP positive cells were single-cell sorted onto five 96 well plates (sorting was carried out by Dr. Stefan Schmitt of the DKFZ flow cytometry core facility using a BDFACsAriaII). Immediately prior to sorting cells were stained with 1ul of propidium iodide. One week after sorting, clonality was confirmed by visual inspection with a microscope.

Screening for successful knockout was performed by extraction of genomic DNA and PCR amplification of the targeted region; exon 4 with the primers TL022_A1_KO1A_fw and TL023_A1_KO1A_rv and exon 5 with the primers TL024_A1_KO2A_fw and TL025_A1_KO2A_rv. After PCR clean-up DNA was sent for sequencing with the forward primer. Clones that showed breaks in the chromatograms at the location of the guide that

indicated an indel and mixed sequenced were subcloned into pJET1.2 from CloneJET PCR cloning Kit (Thermofischer) according to the manufacturer's instructions to determine biallelic loss of APOBEC1 after PCR product was cleaned with Macherey-Nagel™ NucleoSpin™ Gel and PCR Clean-up Kit. Ligation products were transformed into DH5α bacteria, 20 of the resultant colonies were sequenced with pJET1.2 fw using *E coli* Nightseq service (Microsynth). A single knockout clone with a single base pair deletion on one allele and a two base pair deletion on the second allele in exon 5 was identified. At a later date a second clone was generated by the same protocol by Laura Schoppe.

A second confirmation of successful knockout was carried out by extracting DNase treated RNA from the wild-type (WT) parental RAW 264.7 cells and from the potential knockout and performing an RT-PCR of the 3'UTR of *B2m* with the primers RE079_b2m_fw and RE080_b2m_rv. Absence of editing in the knockout was confirmed by calculating editing percentage using MultiEditR (Kluesner *et al.*, 2021). Amplified *B2m* was also subcloned with CloneJET PCR cloning Kit (Thermofischer) to ensure absence of editing had not dropped below detection level of Sanger sequencing.

#### *3.2.1.5 Macrophage activation*

To stimulate WT and A1 KO RAW 264.7 cells into an M1 type proinflammatory phenotype the following was carried out: cells were counted and 2 million cells were plated in 100 $mm^2$ dishes one day before proinflammatory activation (unless different numbers indicated). Media was replaced with complete media containing 100ng/ml LPS and 100 units (U)/ml of IFN-γ or media containing an equal volume of PBS. Plates were incubated for 1, 2, 4 ,12 or 24 hours. Untreated controls were collected at the same time as the last time point of the experiment.

#### *3.2.1.6 Fixing RAW 264.7 cells*

For use of cells on devices outside of S2 conditions they were fixed prior to removal. Media was removed from wells and the cells were washed one time with PBS and scraped with fresh PBS in the well and transferred to a round bottom 96 well plate. Cells were centrifuged for 5 minutes at 500g at 4°C and the supernatant was discarded. Cells were then resuspended in 200ul of 4% paraformaldehyde and kept on ice for 15

minutes in the dark. Cells were recentrifuged as previously and washed 3 times with cold PBS and finally resuspended in 200ul of PBS.

### 3.2.2 General molecular biology

#### *3.2.2.1 Genomic DNA extraction*

Cells were scraped and harvested at 422 g for 5 minutes at RT and then washed one time with PBS before centrifugation and resuspended with 200ul of PBS and extracted with High Pure PCR Template Preparation Kit (Roche) according to the manufacturer's instructions.

#### *3.2.2.2 RNA extraction*

Media was removed from the well and cells were washed one time with PBS. RLT plus buffer (RNeasy plus kit) supplemented with 10 µl β-mercaptoethanol per 1 ml buffer RLT Plus was added directly to the wells. Lysate was scraped and collected into tubes and RNA extraction was performed according to the manufacturer's instructions. At the final stage RNA was eluted with 30ul of RNase free double distilled water and then re-eluted with the same 30ul of water.

To ensure no DNA was left contaminating the RNA samples they were treated with DNase (Turbo DNA-free kit, Invitrogen) according to the instructions with one modification: after 20 minutes of incubation with 1ul of enzyme an additional 1ul was added and the sample was incubated for a further 20 minutes.

According to the instructions, RNA concentration was determined where needed with Qubit 4 Fluorometer and Qubit RNA BR Assay Kit. RNA integrity was measured with Qubit RNA IQ kit.

According to the manufacturer's instructions, RNA extraction after polysome profiling was done using peqGOLD TriFast FL (VWR). 1ul of GlycoBlue was added at the time indicated as an option in the instructions to act as a carrier for the RNA and make the pellet more visible. Due to the high sucrose levels present in the samples, it was impossible to use the columns from the RNeasy plus kit as they became blocked. RNA pellets were resuspended in 20ul RNase free water.

### *3.2.2.3 (Reverse transcriptase) Polymerase Chain Reaction, and agarose gel electrophoresis*

For the amplification from DNA sequences, Q5® High-Fidelity DNA Polymerase (New England Biolabs, NEB) was used according to the manufacturer's recommendations, 1ul of template (templates were diluted so 10ng was used). PCR reactions were carried out in a thermal cycler (Bio-Rad) under the following conditions: 98 °C for 30s (3min for genomic DNA) and 30 cycles of 95 °C for 10 s, 50 – 72 °C annealing for 20 s (annealing temp dependent of primers), 72 °C extension (20s per kb of amplified target), a final extension at 72 °C for 10 minutes. Samples were left on hold at 12 °C till they were removed from the thermal cycler. 5ul of PCR was loaded onto a 1% agarose gel and imaged with a Chemidoc (Bio-rad) to confirm successful amplification.

For RT-PCR QIAGEN® OneStep RT-PCR was step up according to the manufacturer's instructions without optional additives reactions, 1 ul of template RNA was used. RT-PCR was carried out in a thermal cycler under the following conditions: 50°C for 30 min, 95°C for 15min then 30-35 cycles of 94°C for 30s, 50–68°C annealing for 30s.

#### 3.2.2.3.1 Primers

| Primer name | Sequence | Purpose |
|---|---|---|
| TL014_A1KO_11_fw | CACCGAGCAAGATGAGTTCCGAGAC | Cloning guide for A1 KO exon4 into PX458 |
| TL015_A1KO_11_rv | AAACGTCTCGGAACTCATCTTGCTC | Cloning guide for A1 KO exon4 into PX458 |
| TL016_A1KO_39_fw | CACCGTAGCTGTTGATCCCACTCTG | Cloning guide for A1 KO exon5into PX458 |
| TL017_A1KO_39_rv | AAACCAGAGTGGGATCAACAGCTAC | Cloning guide for A1 KO exon5 into PX458 |
| TL022_A1_KO1A_fw | CATTGATGGCTCTGTGGGTGTTC | Amplify A1 exon 4 |
| TL023_A1_KO1A_rv | GCTGAAAAGCACCCAGGGAC | Amplify A1 exon 4 |
| TL024_A1_KO2A_fw | GTACCTCTCAGATCCTTTGAGAAGTC | Amplify A1 exon 5 |
| TL025_A1_KO2A_rv | GCATGCTGTAACCCTGTAGTTC | Amplify A1 exon 5 |
| RE079_b2m_fw | CAAGCATCATGATGCTCTGAAG | RT-PCR primer validate b2m 3'UTR editing |
| RE080_b2m_rv | GTAAAAGTAACAAAAGCAGAAGTAGCC | RT-PCR primer validate b2m 3'UTR editing |
| RE075_Cybb1_fw | CTCCAGCCAAACTTTGAACTG | RT-PCR primer validate Cybb1 3'UTR editing |
| RE076_Cybb1_rv | GCAACACGAAGGTCTGTCTGG | RT-PCR primer validate Cybb1 3'UTR editing |

| | | |
|---|---|---|
| RE077_Cybb2_fw | CAGACTGCAGACTGGCCCCTC | RT-PCR primer validate Cybb2 3'UTR editing |
| RE078_Cybb2_rv | CCGTGATAACAACAGCCAATTCAGTCC | RT-PCR primer validate Cybb2 3'UTR editing |
| TL030_Lamp2_AI_fw | TCAGGCTAAGTCGACAACAAG | RT-PCR primer validate lamp2 3'UTR editing |
| TL031_Lamp2_AI_rv | CTCTTTCAGCCCGATACTTAACA | RT-PCR primer validate lamp2 3'UTR editing |
| RE069_Tmem69_fw | GCCAGAAGACTGTTGAATCCCCTG | RT-PCR primer validate Tmem69 3'UTR editing |
| RE070_Tmem69_rv | GGTTCTTAGTAGTGCCTTAGATTCCC | RT-PCR primer validate Tmem69 3'UTR editing |
| TL53_Sppl2a1_fw | CTGTGTACACATGCTACTAGAC | RT-PCR primer validate Sppl2a 3'UTR editing |
| TL54_Sppl2a1_rv | GCGCTTCTGCGATGACTTG | RT-PCR primer validate Sppl2a 3'UTR editing |
| TL55_Sppl2a2_fw | CTTGCTAACCTAACACCAATAC | RT-PCR primer validate Sppl2a 3'UTR editing |
| TL56_Sppl2a2_rv | CATGAATGCCAGCAGCATATG | RT-PCR primer validate Sppl2a 3'UTR editing |
| TL67_ctnnb1_fw | CCAAGCTGAGTTTCCTATG | RT-PCR primer validate Ctnnb1 3'UTR editing |
| TL68_ctnnb1_rv | GATTACAATTAGCGTGATTATG | RT-PCR primer validate Ctnnb1 3'UTR editing |
| TL69_Rprd1a_fw | GAGACAGGTTAGGTGAATAG | RT-PCR primer validate Rprd1a 3'UTR editing |
| TL70_Rprd1a_rv | CGGCATCCATGTCTAGTG | RT-PCR primer validate Rprd1a 3'UTR editing |
| TL91_bglob_f | CTGGTTGTCTACCCATGGAC | qPCR forward for rabbit βglobin |
| TL92_bglob_rv | TGACTCAGACCCTCACTGAA | qPCR forward for rabbit βglobin |
| TL106_fw2_cybb_591 | CAT GTG CTT GTT GTT TGA GAA C | Fw RT-PCR sequence position chrx 9435591 |
| TL107_rv2_cybb_591 | CAG TAT CTT TGC TAG TTG GAT TC | Rv RT-PCR sequence position chrx 9435591 |
| TL108_CD36_fw | GATGAGCCTACATATACACTGGC | RT-PCR primer validate CD36 3'UTR editing |
| TL109_CD36_rv | GTCATGATAGCAGTTTCCTCCAG | RT-PCR primer validate CD36 3'UTR editing |
| pU6 | GAGGGCCTATTTCCCATGATTCC | Sequencing from human U6 promoter |

#### *3.2.2.4 Quantitative reverse transcriptase PCR*

Before commencing RT-qPCR RNA concentration was determined with Qubit RNA BR Assay Kit and RNA integrity was measured with Qubit RNA IQ kit. The concentration and integrity of RNA from polysome profiles were not calculated, and the same volume (6 ul total) was used for each reaction. Samples not from polysomes were diluted to 2.5ng/ul. cDNA was produced with ProtoScript® First Strand cDNA Synthesis Kit according to the instructions, with one change; 1ul of Random primer and 1 ul of Oligo-dT primer was used instead of 2ul of only one. Final cDNA was diluted to a final volume of 60ul.

qPCR for cDNA not generated from polysome profiles was done using Biozym Blue S'Green qPCR Mix separate ROX according to the instructions on a BioRad CFX Connect Real-Time PCR Detection System in a 96 well plate. Relative expression was determined by the $2^{-\Delta\Delta Ct}$ method (Livak and Schmittgen, 2001).

For qPCRs from polysome profiles 2 master mix 96 plates one containing cDNA and the other mastermix of the same kit described above and appropriate primers (see list below), cDNA and reaction mix were combined into a 384 well plate by a Bravo Automated Liquid Handling Platform. 4 plates were prepared during each session and kept on ice in the dark till placed in the qPCR machine. Ct values were normalized to rabbit βglobin spike in Ct values and relative mRNA distribution was calculated as described in (Panda, Martindale and Gorospe, 2017) in Brief; ΔCt was calculated as Ct (Fraction 1) – Ct(Fraction X), followed by determining the $2^{\Delta Ct}$ and the sum of all values. The % mRNA in each fraction was calculated as $\frac{2^{\Delta Ctx} \times 100}{Sum}$.

All qPCR primers were confirmed primers from Sigma-Aldrich with undisclosed sequences except for:

| | | |
|---|---|---|
| qPCR_18SrRNA_F | agtgttcaaagcaggcccgagc | 18S rRNA, Pol I ref gene |
| qPCR_18SrRNA_R | ccccggccgtccctcttaatca | |

These primers were prepared by Jose Paulo Lorenzo and were used as a housekeeping control. They amplify part of the 18s ribosomal RNA

### *3.2.2.5 Transformation of bacterial cells*

For transformation of bacterial cells, DH5-alpha competent cells (prepared by Monique Van Straaten) kept at -80°C were thawed on ice and up to 2.5 ul of the plasmid to be transformed was added to the bacteria just as they thawed. The mixture was incubated on ice for 30 minutes. Heat shock was carried out at 42 °C for 45 seconds, and then the cells were allowed to recover on ice for 3 minutes before the addition of 900ul Luria-Bertani (LB) medium and a 1-hour incubation with shaking at 37 °C for 45 minutes. The cells were then plated out on agar plates containing either ampicillin or kanamycin depending on the resistance gene of the vector and incubated at 37 °C overnight.

For plasmid cloning, 10 bacterial clones were picked and used to inoculated 5 ml of LB media containing ampicillin/kanamycin. Bacteria were incubated overnight and 2ml were used to extract plasmids with NucleoSpin Plasmid, Mini kit for plasmid DNA (Macherey-Nagel). Plasmid was confirmed by sequencing with the forward primer (Mycrosynth); once plasmid was confirmed a PureLink™ HiPure Plasmid Filter Maxiprep Kit to amplify the amount of available plasmid, kit instructions were followed.

#### *3.2.2.6 Cloning of PX458-APOBEC1 exon 4/5*

pSpCas9(BB)-2A-GFP (PX458) was a gift from Feng Zhang (Addgene plasmid #48138; http://www.addgene.org/48138/;RRID: Addgene_48138) (Ran *et al.*, 2013). 5 µg of the empty plasmid was digested with BbsI at 37°C for one hour then heat-inactivated at 65°C for 20min. The mixture was then dephosphorylated with Rapid DNA Dephos & Ligation kit (Roche). sgRNA targeting exon 4 and exon 5 was designed using the E-CRISP tool (http://www.e-crisp.org/E-CRISP/). The following oligo pairs were ordered 5' phosphorylated TL014_A1KO_11_fw and TL014_A1KO_11_rv for exon 4 and TL016_A1KO_39_fw and TL016_A1KO_39_rv for exon 5. The oligos were annealed to the digested and dephosphorylated PX458 backbone. Succes of cloning was confirmed by Sanger sequencing and Sanger sequencing using a primer pU6.

### 3.2.3 Flow cytometry for M1 polarisation

M1 polarisation of macrophages is characterised by upregulation of certain surface markers, to determine if differences between the activation state of wild-type and knockout RAW 264.7 cells changes in four surface markers (CD80, CD86, MHC-II, CD40) were assessed by flow cytometry. Low passage (passage 3-7) WT and A1 KO were plated at 100,000 cells/ml into 12 well plates and allowed to settle into plates for four hours. Media was replaced with complete DMEM with LPS/IFN-γ or PBS as described previously for 24 hours. After 24 hours the cells were scraped and transferred to round bottom 96 well plates and centrifuged for 5 minutes at 1500 revolutions per minute (rpm) at 4 °C. Supernatant was discarded and the cells were resuspended in 50ul supernatant from an anti-mouse CD16/CD32 hybridoma (kind gift from Prof. Dr. Adelheid Cerwenka) and kept on ice for 5 minutes. 50ul was carefully mixed in of PBS 1% bovine serum albumin (BSA)

with 0.06ug anti-mouse CD80 PE, 0.125ug anti-mouse mouse I-A/I-E (MHC-II) APC, 0.125ug anti-mouse CD86 FITC and a 0.125ug anti-mouse CD40 APC/Fire™ 750 for 30 minutes in the dark on ice. Cells were then washed once with PBS and resuspended in 100ul of live/dead fixable violet (Thermofischer) in PBS for 30 minutes. The cells were then washed twice with PBS before being fixed with 4% paraformaldehyde as previously described. Compensation controls were prepared using OneComp eBeads™ Compensation Beads for all antibodies, ArC™ Amine Reactive Compensation Bead Kit according to the manufacturer's instructions and one sample on unstained RAW 264.7 cells. Flow cytometry was performed with a BD FACS canto II. Cells were gated according to description in Figure S **6.** Flow cytometry data was analysed using FlowJo v10 and Prism10. During first repetition cells were also stained with isotype controls to determine specific binding (see Antibodies 3.1.5).

### 3.2.4 RNA sequencing

#### *3.2.4.1 Library preparation*

Stimulated and unstimulated WT and A1 KO cells were prepared exactly as described in 3.2.1.5 and RNA extracted as described in 3.2.2.2. All time points were done in triplicate and only High quality RNA samples were used which is important for high-quality sequencing data; therefore only RNA IQ values over 8 were used to prepare libraries if a value of a replicate was below 8, a fresh sample was prepared. To prepare libraries for RNA sequencing 1ug of each replicate was used to as input for the KAPA mRNA HyperPrep Kit for Illumina platforms according to the instructions using the following options: Fragmentation was done for 8 minutes at 94°C. KAPA Unique Dual-Indexed Adapter Kit (15 µM) was used for adapters, each adapter was diluted to 7 µM with KAPA adapter dilution buffer. Combinations of adapters were used according to the recommendation for 6 plex sequencing (column 2 9-14 and column 12 89 – 94 were used). The to avoid PCR errors the minimum number of cycles (8) that provided sufficient cDNA for sequencing according to the DKFZ Genomics & Proteomics Core Facility High Throughput Sequencing Unit requirements.

Library concentration was determined with Qubit 1X dsDNA HS Assay Kit and insert size distribution and quality was determined with a Bioanalyzer High Sensitivity DNA

Analysis according to the instructions. Concentration of each library was determined by using the average insert size from the bioanalyzer analysis. One replicate from each time point was mixed into a multiplex in equal molar concentrations to make 3 multiplexes for the WT and 3 for the A1 KO. Each multiplex was sequenced on one lane with HiSeq 4000 Paired-End 100bp

#### *3.2.4.2 Data processing*

##### 3.2.4.2.1 BMDM RNA sequencing

RNA-Seq data with the accession number GSE103958 from Das et al. 2018 was downloaded from the NCBI GEO repository. Downloaded data is in the Sequence Read Archive (SRA) files format, to convert the data to FASTQ files the NCBI SRA Toolkit (Leinonen *et al.*, 2011) was used. Once FASTQ files were available BMDM data and RAW 264.7 data were processed in the same process unless otherwise stated.

##### 3.2.4.2.2 RNA-seq preprocessing and quality assurance.

To ensure maximum reliability of the datasets and prevent ambiguous alignment poor quality reads and remaining adapter sequenced were trimmed with trim-galore (developed at The Babraham Institute by @FelixKrueger) using standard settings for paired-end reads and a stringency of 5.

##### 3.2.4.2.3 Alignment

Trimmed reads were aligned to the latest publicly available mouse reference genome 'mm10' (ENSEMBL https://www.ensembl.org/info/data/ftp/ ) using the STAR package (Dobin *et al.*, 2013). Files were supplied to STAR paired for the paired FASTQ files generated by paired-end sequencing and default options. Bam sorted by coordinate files were outputted after alignment. Before proceeding to the next stages data was deduplicated with Picard tools ("Picard Toolkit." 2019. Broad Institute, GitHub Repository. http://broadinstitute.github.io/picard/; Broad Institute) to reduce variation introduced by technical artifacts and then sorted and indexed with Samtools (Li *et al.*, 2009).

#### 3.2.4.2.4 RNA editing calling

Bam files and indexed files from the previous step were used with REDItools V2 to call edited sites (Picardi and Pesole, 2013; Picardi *et al.*, 2015; Lo Giudice *et al.*, 2020). REDItools scans every genomic coordinate comparing to the reference and noting every base which is different. Output tables created by REDItools include information about all positions, to reduce the size of the output file strict activate mode was engaged so that only edited positions are included in the output file. To increase the confidence positions with the following criteria were excluded: positions with more than 4 identical nucleotides in homopolymeric regions, read quality of below 25 and base quality below 35 and within the first 15 or last 15 base pairs of the read (similarly to Sanger sequencing positions at the beginning and the end of a sequence are less accurate). For regular editing calling positions with less than a read coverage of 10 and 5 variation supporting reads were excluded to remove potential sequencing errors. For comparison of positional editing values, a 50 read coverage threshold was set based on calculations presented in Harjanto et al. 2016 showing that over a coverage of 50 no significant increase in editing percentage accuracy occurs. Finally positions that were present in both the knockout and the wild-type tables were filtered out of the wild-type tables to remove positions that are single nucleotide polymorphism, sequencing errors, or base changes not due to APOBEC1. Tables were annotated by annotation script available with REDItools. Filtering of editing tables was done by Dr. Salvatore Di Giorgio.

One way annova and graphing were done with python SciPy (Virtanen *et al.*, 2020) and figures drawn with Seaborn (Waskom, 2021).

#### 3.2.4.2.5 Differential expression

Differential expression analysis between WT and A1 KO RAW 264.7 cells over the time points was performed by Dr. Salvatore Di Giorgio using the edgeR package (Robinson, McCarthy and Smyth, 2010; McCarthy, Chen and Smyth, 2012) with a False Discovery Rate (FDR) of $< 0.001$ and a Fold Change (FC) $> 2$. Volcano plots were created with ggplot2 package in R (Wickham, 2009).

#### 3.2.4.2.6 Pathway enrichment analysis

Over representation analysis of KEGG pathways was performed using WEB-based GEne SeT AnaLysis Toolkit (WebGestatlt)(Liao *et al.*, 2019). The expressed genes as determined from RNA sequencing were inputted as the background. False discovery rate (FDR) was set to ≤ 0.05 based on a background of genes expressed in the dataset. Over representation analysis determines the probability that a subset of genes in a pathway are selected out of the background by chance or the pathway is enriched.

KEGG pathway Gene Set Enrichment Analysis (GESA) for the differentially expressed genes was performed by Dr. Salvatore Di Giorgio using clusterProfiler (Yu *et al.*, 2012) with an FDR ≤ 0.05. This is a computational method that determines whether a set of genes shows statistically significant differences between the wild type and APOBEC1 Knockout RAW 264.7 cells weighing the significance and fold change of the differences.

### 3.2.5 Mass Spectrometry

$2x10^6$ WT or A1 KO RAW 264.7 cells were plated into $100mm^2$ one day before treatment with LPS/IFN-γ as described earlier in a preliminary experiment in triplicates with stimulation and a second set of samples for 0, 1, 2, 4, 12, 24 hours in 5 replicates each and for 8 and 16 hour in a single replicate. After stimulation cells were washed once with PBS and 0.6 ml complete RIPA lysis buffer (Santa cruz), with 10ul sodium orthovanadate and 20ul protease inhibitor cocktail added fresh to 1 ml of RIPA Lysis Buffer, was added directly to the plate. Cells were scraped and collected into an Eppendorf and agitated at 4°C for 15 minutes. The samples were then centrifuged at 4°C for 15 minutes at 20,000g and the supernatant transferred to new tube. 10ug of each sample was aliquoted into a new tube and submitted to the DKFZ proteomics core facility for further analysis.

Initial analysis of mass spectrometry data was done by Marting Schneider of the proteomics core facility. MSMS identified peptides and proteins based on an FDR cutoff of 0.01 on peptide and protein level by MaxQuant (version 1.6.14.0). Label-free

quantification was done with MaxLFQ algorithm (Cox *et al.*, 2014). Volcano plot was created by me using ggplot2 (Wickham, 2009).

### 3.2.6 Polysome profiling

#### *3.2.6.1 Preparation of sucrose gradient for fractionation*

Sucrose gradients were prepared fresh the day before they were needed by following the dry ice protocol described in (Bajak and Clayton, 2020). 50% and 15% sucrose solutions were prepared in DEPC treated water. The 50% and 15% solutions were mixed to create sucrose solutions of 41.25%, 32.5%, 23.75%. 790ul of each sucrose solution was added to a Beckman Centrifuge tube (11x 60mm), starting with the most concentrated sucrose solution (50%) to the least concentrated (15%). Before adding the next diluted sucrose solution, the tube was placed in dry ice to freeze the solution quickly and the following solution was added on top of the frozen sucrose. The frozen gradients were kept on dry ice to prevent agitation of the gradient during transfer to 4°C cold room for overnight thawing so the gradient could equilibrate.

A chase solution consisting of 60% sucrose in DEPC treated water was also prepared to be used during the fractionation and kept at 4°C.

#### *3.2.6.2 Lysate preparation*

Day before fractionation RAW 264.7 cells were split so that they would be 80% confluent in the morning of the following day, they cells must not be overly confluent as overly dense cells slow down translation levels however too few cells decrease peak heights (Panda, Martindale and Gorospe, 2017). On morning of fractionation 1 x $10^7$ cells were plated into 150 $mm^2$ plates in triplicate and were activated or left untreated with LPS and IFN-γ for 2 hours. After the 2 hours 100ug/ml cycloheximide (CHX) was added to media and incubated for 10 mins at 37°C. CHX arrests ribosomes and blocks translation by inhibiting eEF2 mediated translocation (Schneider-Poetsch *et al.*, 2010). Media was removed and the cells were washed twice with ice cold PBS with 100ug/ml CHX. The PBS was removed carefully so that as little as possible was left behind so it would not dilute the lysis buffer. Right before 350ul polysome extraction buffer was added directly to the

plate it was supplemented with 1 x complete protease inhibitor and 1:1000 murine RNase inhibitor. The cells were then scrapped off, transferred to an Eppendorf tube and tumbled for 10 minutes in the cold room. To remove nuclei and debris the lysate was centrifuged at 12,000g for 10 minutes at 4°C. The supernatant was transferred to a fresh tube. 300ul of lysate was carefully loaded onto gradients being careful not to disturb them. Where necessary extra polysome extraction buffer was added to balance centrifuged tubes. The tubes were centrifuged for 2 hours at 40,000 rpm at 4°C in in an SW60 rotor (Acceleration:7, Deceleration 1 – deceleration much be slow to avoid disruption of the gradients). During centrifugation, RNA distributes according to weight across the gradient with heaviest portions at the bottom where sucrose levels are high, and RNA is associated with polysomes to free RNA at the Top.

#### *3.2.6.3 Polysome fractionation*

Before the end of the ultracentrifugation a Teledyne Isco Foxy Jr. fractionator was assembled as described in Bajak and Clayton 2020 where the same device was used. The tubes for peristaltic pump were cleaned with RNase free water and chase solution was pumped into the tubing and one gradient was set up in the device. Pumping speed was set to 50% and sensitivity to 1, chase solution was pumped into the centrifuge tube whose contents were displaced into the fractionator. Once a signal was detected with the UV/VIS detector fraction collection started. 15 fractions with a volume of approximately 250 µl in Eppendorf tubes were collected while following the absorption with Peak Trak. RNA was extracted as described in 3.2.2.2 with peqGOLD TriFast FL.

### 3.2.7 Phagocytosis assays

#### *3.2.7.1 pHrodo green phagocytosis assay*

In order to determine phagocytosis ability of WT and A1 KO RAW cells the same assay as perform in Rayon-Estrada et al. was repeated. 100,000 WT or A1 KO RAW cells were collected spun down and media was replaced with Optimem, plated in flat bottomed 96 well plates and allowed to settle and attach for at least one hour. pHrodo green *Staphylococcus aureus* or *Escherichia coli* bioparticles were prepared according to the manufacturer's instructions. Optimem was replaced with 100ul of prepared bioparticles at Multiplicity of infection (MOI) 300 or diluted to an MOI of 100 or with PBS control for

unstained cells each triplicate for four hours or one hour respectively. At the end of the incubation period supernatant were removed and the wells were washed twice before the cells were fixed as described before. Cells were maintained in the dark to avoid photobleaching of the dye. Fluorescence was determined by flow cytometry with a Guava® easyCyte™ Flow Cytometer or with a BD FACSCanto™ II. Example of similar gating strategy can be seen in Figure S **6**. Each phagocytosis assay had at least 3 independent repetitions. Flow cytometry was analysed with FlowJo v10 to determine geometric mean of fluorescence intensity (MFI) of each sample and the percentage of pHrodo Green positive cells, base line fluorescence was set according to fluorescence intensity of unstained cells. Relative phagocytosis index was determined as the increase in MFI between treated and untreated as a ratio of the increase in MFI of the WT cells

#### *3.2.7.2 Phagosome pH measurement*

Determining phagosomal pH is based on the same phagocytosis assay described above with a few differences. Assay was carried out in clear bottomed black walled 96 well plates and fluorescence was determined with GloMax fluorescence plate reader with live cells. WT and A1 KO RAW 264.7 cells were plated in triplicate for the following conditions: 3 wells to be left untreated, 3 wells treated with an MOI of 100 of *S. aureus* or *E. coli* bioparticles or 3 wells also treated with bioparticles and after 1 hour buffers at pH 4.5, 5.5, 6.5 or 7.5 from the pHrodo Intracellular pH Calibration Buffer Kit. pH buffers were supplemented with 10 mM each of Valinomycin and Nigericin. Valinomycin and Nigericin are pore forming antibiotics that allow the buffers to equilibrate across the cell membranes, so the pH is consistent throughout the well. Before addition of the buffers of known pH wells were washed twice with live cell imagining solution (thermofischer) and the wells without the calibration buffers were left with 100ul of live cell imaging solution. The pH calibration buffers were left on for 5 minutes at 37°C before all samples were imaged with the plate reader. Protocol followed was according to the buffer calibration kit recommendations. pH was determined by comparing values to standard curve generation with calibration buffers. The WT cells and the A1 KO cells were each determined according to their own calibration curve. Figures and statistics were calculated with Prism10, p values and statistical tests indicated in figure legend.

#### *3.2.7.3 Measuring number of ingested bacteria*

Phagocytosis assay was repeated in clear bottomed black walled 96 well plates with decreased cell numbers of 50, 000 cells per well. To count the number of ingested bacteria with microscopy a lower number of cells ensures that each cell can be more easily separated from its neighbours with a microscope. After one hour of incubation with the bioparticles the wells were washed twice with live cell imaging solution and stained with 1ug/ml Hoechst 33342 for 5 minutes before another wash and were left with 100ul live cell imaging solution. The live cells were imaged with Zeiss cell observer with a x40 air objective, 6 images from WT and A1KO from each bacteria type were taken. Images were analysed with Fiji using a macro to count particles in each cell. The macro was provided by Dr. Damir Krunic from the DKFZ light microscopy facility.

### 3.2.8 Statistics

For calculation of statistical significance, GraphPad Prism 10 software was used for non-RNA-sequency data. For bioinformatics data analysed the statistical packages used are indicated in their respective sections above. The statistical tests are indicated in the figure legends for the respective figures.

# 4 Results

## 4.1 Temporal dynamics of C-to-T editing in stimulated BMDMs

RNA editing levels in specific positions resulting from A3A and A3G have been observed to change under different conditions such as hypoxia or LPS stimulation (Sharma *et al.*, 2015, 2019; Alqassim *et al.*, 2020). However, at each instance, only a snapshot of a single time point was obtained. The question remains how and if editing changes temporally under these conditions. Macrophages express high levels of C-to-T editing enzymes (referred to in the introduction as C-to-U, however, the uracil (U) in RNA sequencing is read as a Thymidine (T), and from this point, the deamination events are referred to as CT events), and bone marrow-derived macrophages are among the highest expressing macrophages (Figure S 1). Therefore, they are a potential model for studying editing. In mice, A1 and not the single mouse A3 is responsible for most RNA CT editing events, and its dynamic changes with stimuli as a model for human macrophages has not been studied.

A publicly available dataset of stimulated BMDMs over a time course was used to study the temporal dynamics of editing (Das *et al.*, 2018). The bone marrow precursors were extracted and stimulated *ex-vivo* with M-CSF to differentiate them into macrophages. The cells were left untreated or primed and stimulated with 100ng/ml LPS and 100U/ml simultaneously for 1-, 4- ,12- or 24 hours to represent macrophages with M1 polarisation or treated with 12 hours of IL13 or IL4, which are associated with M2 polarisation. They then performed stranded RNA-seq after rRNA depletion in triplicates.

### 4.1.1 Global C-to-T levels change with stimulation

Putative CT events in the BMDMs were ascertained using the REDItools2 suite after the Das et al. dataset was aligned with STAR. REDItools 2 produces an output table with all positions where the read base differs from the reference genome (mm10). The total CT changes identified can originate from polymorphisms, sequencing errors, A1 editing, and other biological processes. To eliminate these other sources of CT changes in RNA-

seq and knockout (KO) is used as a reference. BMDMs from *Apobec1*$^{-/-}$ mice from the same genetic background (C57BL/6J) were previously sequenced and were used as a reference (Rayon-Estrada et al. 2017). To validate the accuracy of the detected editing events, specific known positions, such as in the 3'UTR of *B2m* (Figure 3), were investigated with the integrated genome browser (IGV). When an editing event occurs, reads with a T in the edited position can only be found in WT samples. CT changes do not occur in every single transcript at a specific position therefore editing is reported as a percentage reflecting the proportion of reads carrying the editing event.

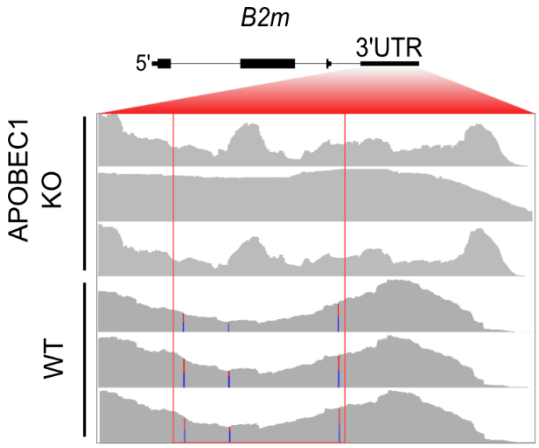


Figure 3 Integrated genome browser view of *B2m* 3'UTR.

B2m is known to be edited; three edited positions can be seen in the wild-type control BMDM reads as red and blue bars that give an indication of the percentage of edited reads in each position. In the absence of the editor APOBEC1, no CT events occur at these positions.

A coverage threshold of ten reads is commonly used when calling editing to decrease the likelihood that a random sequencing error is included as an editing event. At a 10 read coverage threshold, 103022 positions with CT events attributed to A1 could be identified, with over 99.9% of the positions having an editing rate of less than 10%, which corresponds to previously published data (Rosenberg *et al.*, 2011; Cole *et al.*, 2017b; Rayon-Estrada *et al.*, 2017). However, the lower the coverage, the lower the probability that this fraction represents the true editing rate of the population, or the events are real in lower quality and coverage RNA-sequencing. The RNA sequencing data had an average

sequencing depth of 15 million reads per replicate which is lower than the typical 100 million reads that we routinely use for RNA editing calling. Therefore, a stricter coverage threshold was necessary. Based on Bayesian modelling of editing performed by Harjanto *et al*., a threshold coverage cut-off of 50 was selected. A coverage threshold of 10, while sufficient to call whether a position is edited was shown not to provide a sufficiently accurate measure of rate and above coverage of 50 no significant increase in accuracy occurs(Harjanto *et al.*, 2016). Positions were additionally filtered so a minimum of 5 editing supporting reads were present to ensure only true editing events and not sequencing errors or false percentages were included in the analysis. Due to these necessary strict filtering parameters, the loss of many positions must be accepted. Filtering positions by these parameters results in a list of 395 edited positions

The number of CT changes were calculated for each time point and normalised to library size to obtain an overview of any potential change in the number of events over time (this was performed by Dr. Salvatore Di Giorgio). A significant increase in the number of events was observed after 1 hour of stimulation, followed by a decrease (Figure 4). No significant changes in levels of other base changes were observed (Figure S 3). The number of CT events detected were small but the increase in levels after one hour were significant suggesting that editing is temporally regulated during stimulation.

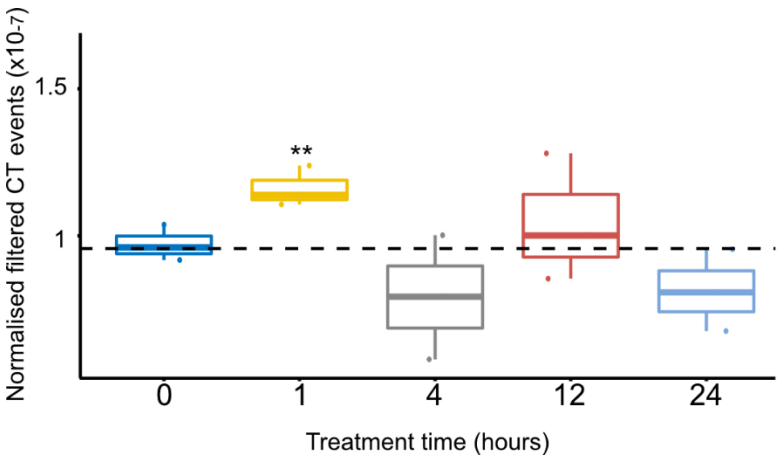


Figure 4. Dynamics of CT levels in BMDM.

CT counts filtered against A1 KO BMDMs with a coverage cut-off of 50 reads from REDItools tables are normalised to total reads per replicate. N=3 for each sample. Dashed line represents mean of CT numbers. Treatment time indicates hours stimulated with 100ng/ml LPS and 100U/ml IFN-γ. Box show mean and interquartile range. Data analysed by one-way ANOVA p value = 0.035. ** p <0.01

### 4.1.2 Editing levels change in a transcript, time and stimuli dependent manner

After looking at the global changes in editing, I zoomed in at the positional level to identify specific groups of transcripts with differential editing levels. To identify these transcripts I performed one-way ANOVA with a Benjamini-Hochberg correction (Benjamini and Hochberg, 1995) and set false discovery rate (FDR) at ≤ 0.05. 67 positions were identified with statistically significant changes over the treatments (Table S **1**). All 67 positions are in 3'UTRs and with some transcripts having multiple edited positions such as 20 positions in the 3UTR of Cytochrome b (also known as NADPH oxidase 2, NOX2, *Cybb*), 5 in Secreted Phosphoprotein 1 (*Spp1*) and 4 in Beta 2 microglobulin (*B2m*). In total, 29 unique transcripts had positions with differential editing.

The 9 positions with the most significant changes in positional editing are shown in Figure 5. The changes in editing are both determined by the stimulus, the transcript or the position. While the dynamics of editing in different positions of the same transcripts are similar, they are not identical. *Spp1* positions show an initial decrease after 4 hours of LPS and IFN-γ (20% to 9.3%, 6.3% to 3.3% and 5.3% to 3.7%) with a subsequent increase to levels higher than unstimulated control (33.7%, 11% and 11.7%) (Figure 5 a-c respectively). The levels of editing during IL13 or IL4 stimulation decreased in positions *Spp1* Chr5:104440840 and Chr5:104440953 (Figure 5 a & c). In *Spp1* Chr5:104440908, levels increased with IL 13 and decreased with IL4; however, these changes were not statistically significant. *Cybb* exhibited a similar pattern with an LPS mediated editing drop after 4 hours (37.7% to 12.7%, 2.7% to 1% and 9.7% to 4.3%), followed by an increase that did not reach levels before stimulation at the 24 hour time point (13%, 2% and 5.7 %) (Figure 5 g-i respectively). At ChrX:9435719, *Cybb* showed only minor insignificant changes in editing during LPS stimulation but did show a comparatively large increase with IL4 stimulation (2.7% to 6%) (Figure 5 h), which was not seen in the other two positions shown in Figure 5 (g & i). Both *B2m* Chr2:12215902 and *Lcp1* (Lymphocyte Cytosolic Protein 1) Chr14:75230678 show a decrease in editing with LPS that reaches a minimum after 4 hours (47% to 34.7% and 6.7% to 1.3% respectively) and only *B2m* showing an increase after 12 hours (40.3% after 24 hours) which does not return to the same level as before stimulation (Figure 5 d & e). *B2m* and *Lcp 1* have a drop in editing in both IL13 and IL4 (35.7% and 34.7% ,3.3% and 4% respectively) (Figure 5d & e). C5a anaphylatoxin

chemotactic receptor 1 (*C5ar1*) shows an oscillating pattern of changes with LPS stimulation, a decrease at 1 hr (2% to 0.7%) followed by an increase above unstimulated levels (4.3%) and another round of decrease (0%) and increase (2.7%) (Figure 5 f). The same *C5ar1* position editing had higher editing after IL13 treatment (4.3%) and lower after IL 4 treatment (0.7%). The changes in editing levels did appear to directly correlate to transcription levels determined from the RNA-sequencing, suggesting that the activity of A1 at these positions is regulated temporally.

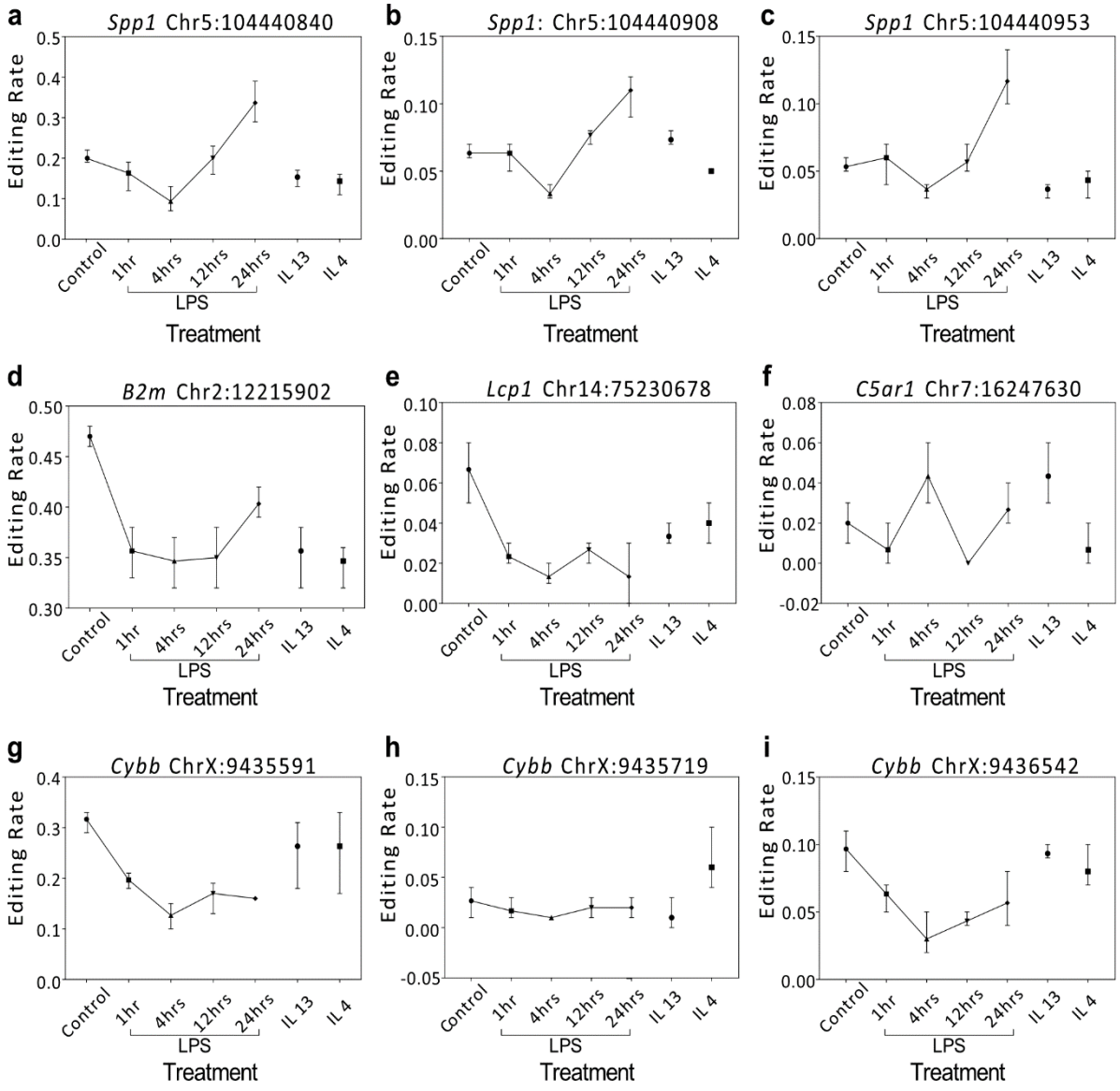


Figure 5. Positional editing frequency changes with macrophage stimulation.

The topmost significantly changing edited positions from the 67 identified in the 3'UTRs of a-c. Secreted Phosphoprotein 1 (*Spp1*). d. Beta 2 microglobulin (*B2m*). e. Lymphocyte

Cytosolic Protein 1 (*Lcp1*). f. C5a anaphylatoxin chemotactic receptor 1 (*C5ar1*). g-i. Cytochrome b (*Cybb*). Data shown is mean of 3 replicates and range.

### 4.1.3 Differentially edited transcripts are enriched in phagocytosis related processes

Multiple transcripts described in the previous section have a role in phagocytosis or associated macrophage functions. For example, CYBB forms part of the NADPH oxidase complex that generates reactive oxygen species (Minakami and Sumimoto, 2006), LCP1 is involved in the formation of the phagocytic cup (Morley, 2012) and C5ar1 is part of a phagocytosis receptor (Haggadone *et al.*, 2016) to name a few. To establish whether a connection between these dynamically edited transcripts and a functional pathway exists, I surveyed the 29 differentially edited transcripts for categorical enrichment of KEGG pathways using an over-representation analysis with a Benjamini-Hochberg correction (Benjamini and Hochberg, 1995), false discovery rate (FDR) of ≤ 0.05 based on a background of genes expressed in the dataset. WEB-based GEne SeT AnaLysis Toolkit (WebGestatlt) was used to perform the analysis (Liao *et al.*, 2019).

One pathway, Lysosome, was identified as significantly enriched by over-representation analysis (Figure 6). However, based on the algorithm used for this analysis, only 4 genes out of the 29 were described as belonging to the lysosomal pathway, Lysosomal-associated membrane protein 1 (*Lamp1*), Cation-dependent mannose-6-phosphate receptor (*M6pr)*, Lipase A, Lysosomal Acid Type (*Lipa*) and Cathepsin B (*Ctsb*). Multiple other lysosomal genes are present in the differentially edited list and should also fall in this category such as Lysozyme C-2 *(Lyz2*) (Markart *et al.*, 2004) and Cellular repressor of E1A stimulated genes (*Creg1*) (Liu *et al.*, 2021). This highlights the one of the limitations of these pathway analyses, they are dependent on which genes are currently annotated as belonging in that pathway and it also fails to highlight pathways that intersect with one another, such as

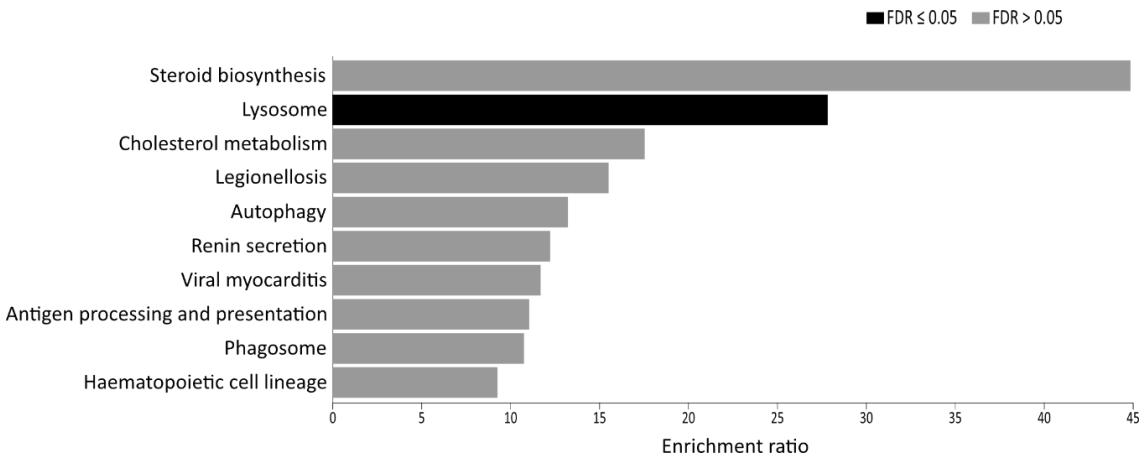


Figure 6 Over-representation KEGG pathway analysis.

Enrichment of pathways with transcripts with changes in editing levels per position in LPS and IFNγ or IL4 or IL 13 stimulated BMDMs shows enrichment for lysosomal pathways. FDR < 0.05

phagosomes and lysosomes. Therefore, I conducted a systematic analysis of currently available literature in search of the functions of these genes in the context of macrophages. Many of these genes have multiple functions and roles in other cells, which are not described here. This analysis revealed that 25 of 29 genes play some role in the phagosome-endosome-lysosome pathway (Table 1). 11 of the 29 genes were also involved in macrophage motility. The majority of the genes involved in macrophage migration have a dual function and are also involved in phagocytosis by virtue of being involved in membrane and cytoskeletal remodelling and formation of the phagocytotic cup and transport of endosomal, lysosomal and phagosomal vesicles within the cell (Hugo *et al.*, 1996; Erwig *et al.*, 2006; Patel *et al.*, 2011; Morley, 2012; Edwards *et al.*, 2014). It is not unexpected to find that genes involved in the phagosome-endosome-lysosome pathway are enriched for editing changes as these pathways are enriched for editing (Cole *et al.*, 2017b; Rayon-Estrada *et al.*, 2017).

| Gene | Function | Category | |
|---|---|---|---|
| Spp1 | Cell-matrix interaction, inflammatory cytokine, phagocytosis | 1&2 | (Blom *et al.*, 2003; Kourepini *et al.*, 2014; Zhang *et al.*, 2017) |
| Cybb | Generates superoxide | 1 | (Kinchen and Ravichandran, 2008; Kotsias *et al.*, 2013) |
| B2m | Antigen presentation, anti-bacterial | 1 | (Strominger *et al.*, 1987; Kim *et al.*, 2012; Holch *et al.*, 2020) |
| Lcp1 | Podosome and phagocytic cup formation | 1&2 | (Morley, 2012) |
| C5ar1 | Complement receptor, stimulates activation, phagocytosis and migration | 1&2 | (Haggadone *et al.*, 2016; Skjeflo *et al.*, 2019) |
| Nptn | Cell Adhesion? | 2? | (Owczarek and Berezin, 2012) |
| Creg1 | Cell proliferation, lysosome biogenesis | 1 | (Liu *et al.*, 2021) |
| Eef1b2 | Translation elongation | other | (McLachlan, Sires and Abbott, 2019) |
| Unc93b1 | Trafficking of TLRs to endolysosomes | 1 | (Pelka *et al.*, 2018) |
| Selenof | $Ca2^{+}$ signalling, redox state homeostasis | 1 | (Narayan *et al.*, 2015; Pitts and Hoffmann, 2018) |
| Adgre1 | Unknown, involved in induction of $CD8^{+}$ T reg cells | other | (Lin *et al.*, 2005) |
| Lipa | uptake and digestion of lipoproteins | 1 | (Maxfield, Barbosa-Lorenzi and Singh, 2020) |
| Itm2b | unknown – located in endosomes/lysosomes | 1? | (Schröder and Saftig, 2016) |
| Lyz2 | Anti-microbial | 1 | (Markart *et al.*, 2004) |
| Rtn4 | Mediates transendothelial migration, proper TLR9 localisation to endolysosomes, formation and stabilisation of endoplasmic reticulum (ER) tubules | 1 | (Yu *et al.*, 2009; Kimura *et al.*, 2015) |
| Mpeg1 | Antibacterial. Essential for antibacterial activity of ROS and NO | 1 | (Fields *et al.*, 2013; McCormack *et al.*, 2015; Strbo *et al.*, 2019) |
| Sdcbp | Exosome biogenesis, positive regulation of TGFB1-induced cell migration, vesicle trafficking | 1&2 | (Zimmermann *et al.*, 2001; Baietti *et al.*, 2012; Hwangbo *et al.*, 2016; Philley, Kannan and Dasgupta, 2016) |
| Ctsb | lysosomal cysteine protease | 1&2 | (He *et al.*, 2008; Sendler *et al.*, 2018) |
| Arf1 | Vesicle trafficking, phagosome formation | 1 | (Beemiller, Hoppe and Swanson, 2006; Zhang *et al.*, 2018; Tanguy *et al.*, 2019)( |
| Selenop | Ca2+ signalling, redox state homeostasis | 1 | (Narayan *et al.*, 2015; Pitts and Hoffmann, 2018) |
| Anxa1 | Promotes migration and phagocytic cup formation via actin rearrangement | 1&2 | (Ernst *et al.*, 2004; Yona *et al.*, 2006; Patel *et al.*, 2011) |
| Anxa5 | Stabilises membranes, induces exosome uptake | 1 | (Rosenbaum *et al.*, 2011; Tontanahal, Arvidsson and Karpman, 2021)( |
| M6pr | P-type lectin receptor, mediates efferocytosis and targeting proteins to lysosomes | 1 | (Dhami and Schuchman, 2004; Lackman *et al.*, 2007) |
| Lamp1 | Mediates phagosome-lysosome fusion | 1 | (Huynh *et al.*, 2007; Gray *et al.*, 2016) |
| Msn | Modulation of actin rearrangement, phagosome formation, maturation and cell migration | 1&2 | (Hugo *et al.*, 1996; Erwig *et al.*, 2006; Zawawi *et al.*, 2010; Mu *et al.*, 2018) |
| Mtpn | Regulates actin rearrangement in phagocytic cup formation and lamellipodia/ filopodia | 1&2 | (Edwards *et al.*, 2014) |
| Ahnak | Likely role in cell migration and potentially in phagocytosis | 1&2? | (Han *et al.*, 2013; Davis, Loos and Engelbrecht, 2014; Sudo *et al.*, 2014) |
| Cd9 | Function unclear Potentially involved in migration, prevention of giant cell formation, phagocytosis co-receptor | 1&2? | (Kaji *et al.*, 2001; Takeda *et al.*, 2003; Huang, Febbraio and Silverstein, 2011; Brosseau *et al.*, 2018) |
| Eif4g2 | Translation initiation | other | (Smirnova *et al.*, 2019) |

Table 1. Manual gene functional association based on current published literature.

Category 1 denotes functions falling in the phagosome-endosome-lysosome pathway and Category 2 denotes function associated with cell migration and adhesion. Category other suggests that transcript does not have a function related to category 1 or 2 with the current scientific understanding. A question mark indicates that a clear function has not yet been established, but evidence suggests it.

## 4.2 APOBEC1 RNA editing in RAW 264.7 cells

The number of mapped reads required from an RNA-sequencing experiment is dependent on the experimental aims. For differential expression analysis, as few as five million mapped reads can be considered sufficient to quantify medium to highly expressed genes. Up to one hundred million reads are sometimes sequenced to quantify genes with low expression levels and for alternative splicing analysis (Conesa *et al.*, 2016). In most cases, coverage falls between these two values, such as BMDM Das *et al.,* data with approximately fifteen million reads per replicate. Accurately calling editing requires greater coverage than expression analysis, and we typically aim for a minimum of one hundred million reads. As a result of the comparatively low coverage in the BMDM dataset, a relatively low number of editing events could be detected after filtering steps.

Additionally, every time BMDMs are produced by culturing myeloid progenitor cells from the bone marrow, they can vary from production to production as they are acutely sensitive to minor changes in the environment (Bailey *et al.*, 2020) that can lead to increased heterogeneity in editing, making the analysis more complex. Cell lines tend to be more homogenous than primary cells, so a mouse macrophage cell line was selected for further analysis to generate high-quality, high depth sequencing libraries. Furthermore, sequencing data was only available for unstimulated KO BMDMs; this increases that editing events will both be missed or false events included due to all the gene expression changes that occur during activation. Repetition of RNA sequencing with greater depth, less heterogeneity and better KO controls were necessary.

RAW 264.7 cells (referred to as RAW cells) are a mouse macrophage-like cell line with a high A1 expression (Figure S 2) and are relatively easy to manipulate genetically. An initial query of the RAW 264.7 cells was made to determine if changes occur in editing with LPS and IFN-γ stimulation similarly to the BMDMs (In my hands, RAW cells failed to respond IL13 or IL4 as determined by flow cytometry analysis of classical M2 markers (not

shown) and therefore were not included in subsequent experiments). RNA was extracted from stimulated cells and the 3'UTR regions of *B2m,* and *Cybb* that contain edited positions ( Chr2:1221590 and ChrX:9435591 respectively) in multiple cell types and tissues (Cole *et al.*, 2017b; Rayon-Estrada *et al.*, 2017; Blanc *et al.*, 2018) were amplified and sequenced. RNA editing percentage at each position was calculated with MultiEditR (Kluesner *et al.*, 2021) (Figure 7).

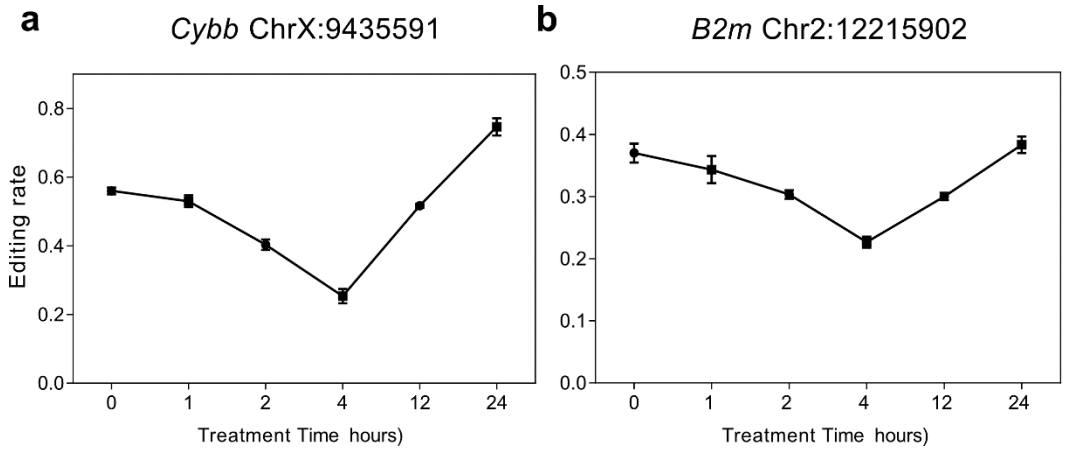


Figure 7 Editing changes in RAW 264.7 macrophages with LPS stimulation.

Editing of **a**. Cybb at position ChrX:9435591 and **b**. B2m position Chr2:12215902 was determined from RT-PCR of RAW cells co-stimulated with 100ng/ml LPS and 100units/ml IFN-γ over a time period, then sanger sequenced and calculating editing ratewith MultieditR using genomic DNA as a reference

The editing rate pattern of *Cybb* ChrX:9435591 (Figure 7 a) and *B2m* Chr2:12215902 (Figure 7 b) during LPS stimulation follows a similar pattern to BMDM transcripts (Figure 5 g & d). *B2m* shows minimum editing levels after 4 hours, while in the BMDMs, this point was reached after the first hour and is followed by a steeper increase in editing in the RAW cells (Figure 7 a and Figure g respectively). Overall editing frequency at *Cybb* ChrX:9435591 is higher in the RAW cells than in BMDMs, starting at rest at 56% vs 31.6%. After 24 hours *Cybb* editing levels in RAW cells increase above the initial levels to 74.7%, whereas in the BMDMs they remained below the initial levels, at 16 %.

These data suggest that RAW 264.7 cells also show dynamic editing. In addition to this, their high expression of A1, their transfectability and higher homogeneity than primary cells make them a valuable model for studying A1 driven editing in a macrophage context.

### 4.2.1 Generation of APOBEC1 knockout RAW 264.7 cells

To accurately determine the CT editome of RAW 264.7 cells, a KO is required as a reference to distinguish editing events from single nucleotide polymorphisms (SNPs), sequencing errors or changes not due to A1. CRISPR-Cas9 guides targeting the first coding exon of APOBEC1, exon 5 were designed for creating the KO (Figure 8 a). Exon 5 is a short coding-exon located upstream of the A1 activate site. The sequence of exon 5 is suitable for CRISPR-Cas9 targeting as it includes a protospacer adjacent motif, which is necessary for the cleavage activity of Cas9 (Shah *et al.*, 2013). A guide for exon 4 was also created, however successful KO was generated against the region in exon5.

RAW 264.7 cells were nucleofected with PX458_A1KO, which contains an RNA expression system for the guide RNA (Figure 8 b, guide sequence is marked in grey) and Cas9-2A-GFP (Ran *et al.*, 2013). 48 hours post-transfection, the cells were single-cell sorted into 96 well plates based on their GFP expression. Transfection efficiency was low at approximately 1%, which necessitated cell sorting to increase the likelihood of a successful KO clone. Six clones grew from this sort.

No suitable antibody is currently available against A1; therefore, the KO was confirmed by two methods 1) by amplifying the targeted region from genomic DNA and sequencing and 2) testing for the absence of editing at the known editing site in *B2m* Chr2:12215902. The amplified genomic DNA of all six clones were effectively targeted by Cas9, as was evident by the appearance of overlapping peaks at the guide site in sanger sequencing (example from clone 4 Figure 8 b middle).

To validate that a clone is a true KO and to identify the mutation that occurred, the amplified region was subcloned into a Pjet 2.1 vector, transformed to bacteria, and for each clone 20 bacterial subclones were sequenced. Only one DNA copy is inserted into the vector allowing for separation of the two A1 alleles. The probability that the two alleles experienced the same mutation is low, giving rise to the typical sanger sequence double peace break seen in Figure 8b as the two alleles diverge and no longer have the same sequence. All clones apart from clone four contained either in-frame mutations or were heterozygotes for the wild-type allele. Clone four had one allele with a single base

pair deletion and one with a two-base pair deletion, resulting in a frame shift (Figure 8 bottom).

An additional round of nucleofection, sorting and screening was performed by Laura Schoppe to produce more clones. Two 96 well plates were plated with single-cell sorted GFP positive cells from the nucleofection. Approximately 80% of the wells grew a single cell clone, unlike in the first round, where only very few cells grew. It is possible a difference in the sorting conditions contributed to this. Cas9 successfully hit all screened clones; however, only one clone had frameshift deletions. The deletions occurred in the same position as the original clone. The first clone generated by me is from this point was named clone 1, and the clone generated by Laura Schoppe was named clone 2. All figures henceforth with the description Al KO without a description of the clone refer to clone 1.

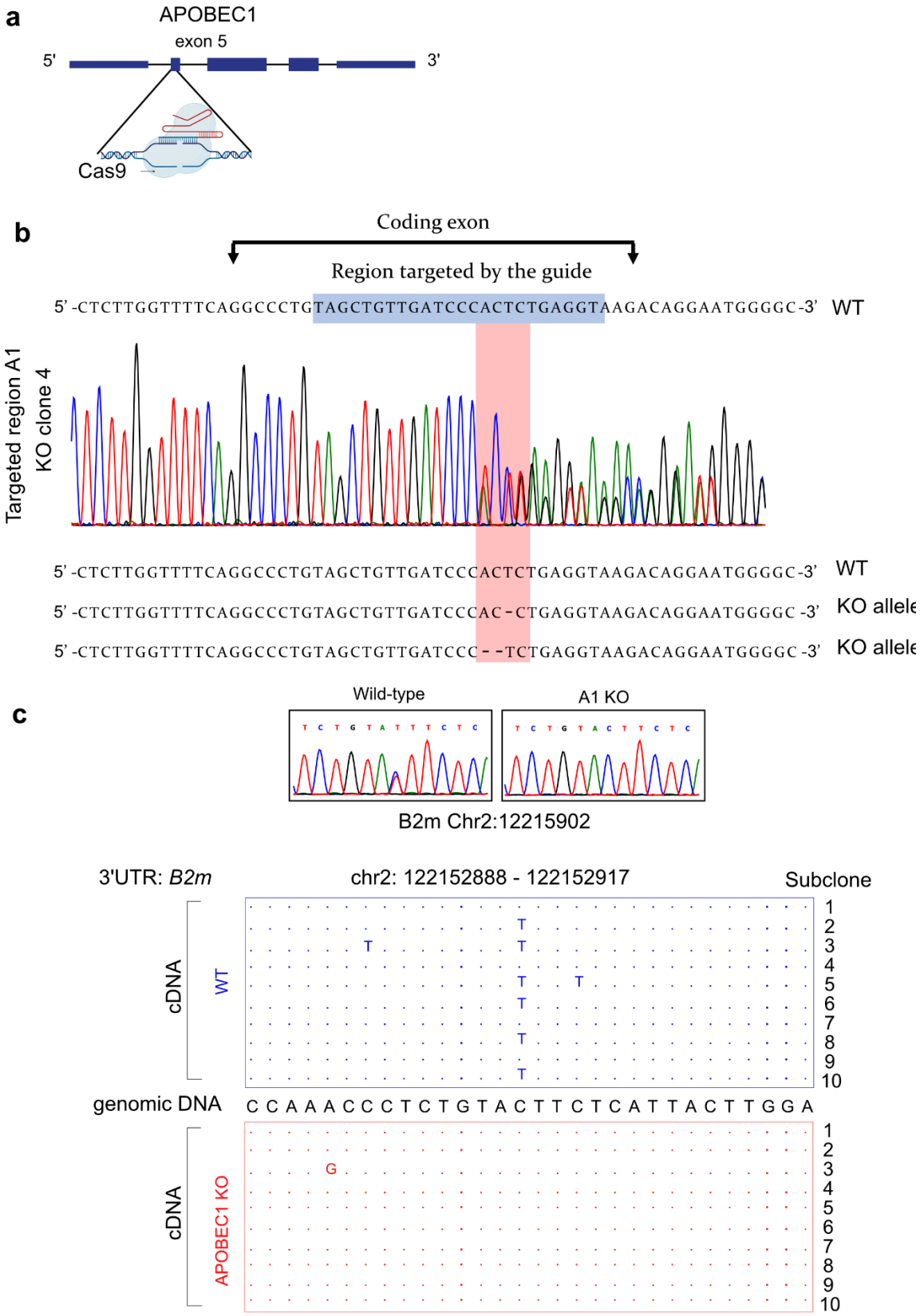
a
APOBEC1
exon 5
5'
3'
Cas9
b
Coding exon
Region targeted by the guide
5' -CTCTTGGTTTTCAGGCCCTGTAGCTGTTGATCCCACTCTGAGGTAAGACAGGAATGGGGC-3' WT
Targeted region A1
KO clone 4
5' -CTCTTGGTTTTCAGGCCCTGTAGCTGTTGATCCCACTCTGAGGTAAGACAGGAATGGGGC-3' WT
5' -CTCTTGGTTTTCAGGCCCTGTAGCTGTTGATCCCAC-CTGAGGTAAGACAGGAATGGGGC -3' KO allele
5' -CTCTTGGTTTTCAGGCCCTGTAGCTGTTGATCCC--TCTGAGGTAAGACAGGAATGGGGC -3' KO allele
c
Wild-type
A1 KO
B2m Chr2:12215902
3'UTR: B2m
chr2: 122152888 - 122152917
Subclone
cDNA
WT
genomic DNA
C C A A A C C C T C T G T A C T T C T C A T T A C T T G G A
cDNA
APOBEC1 KO

Figure 8 Generation of RAW 264.7 cell APOBEC1 KO.

Guides targeting exon 5 with CRISPR-Cas9 were used to knock out A1. a. Schematic representation of the A1 gene and the relative location of exon 5 targeted for CRISPR-CAS9 KO. **b**. Top: Sequence of APOBEC1 exon 5 coding regions with the sequence of the targeting guide. Middle: Sanger sequencing of amplified targeted APOBEC1 region in clone 4 showing point in the sequence where successful targeting of APOBEC1 occurred and two sequences overlap from this point on. Bottom: Subcloning of extracted genomic DNA to determine CRISPR effects on the region in clone 4. Two alleles were detected with frame shit mutations, one with a single base pair deletion and one with a two-base pair deletions. **c**. Validation of APOBEC1 KO by screening for absence of editing in known editing site Chr2: 12215902. Top: Extract of Sanger sequencing of edited and unedited 3'UTR of B2m left in WT and right in KO. Bottom: Subcloning of the sequence shown in the top

### 4.2.2 C-to T levels dynamically change in stimulated RAW cells

A1 KO and WT RAW 264.7 cells were incubated with 100ng/ml LPS and 100U/ml IFN-γ for 0, 1, 2, 4, 12 and 24 hours in triplicate. RNA was extracted, and RNA-seq libraries were prepared with the aim of achieving a sequencing depth of at least 100 million reads. Similarly to the BMDM datasets, CT events were determined from aligned RNA-seq using REDItools 2, and the resultant WT tables were filtered by events in KO, a minimum coverage of 50 and 5 mutation supporting reads. After the filtering steps, the average number of CT events detected at each time point were; 2048, 2109, 2118, 2062, 1906 and 1760 at 0, 1, 2, 4, 12 and 24 hours of activation, respectively. Due to the more comprehensive RNA-sequencing coverage, about 6 times more events after filtering could be identified in this dataset than the BMDM dataset. CT events were normalised to total reads and their numbers were plotted over time (done by Dr. Salvatore Di Giorgio). A significant editing increase occurs after 1 hour of simulation with a gradual decline over the remaining time points (Figure 9 a). The CT pattern is specific to this base pair and observed for other base pairs (Figure S 3). The changes in editing levels were not directly correlated to the levels of A1. A1 expression determined from the RNA-seq using the trimmed mean of M values to compare levels between samples (Robinson and Oshlack, 2010) shows only very minor statistically insignificant changes through the stimulation

time course (Figure 9). A1 levels start to decrease after the first hour of stimulation and reach a minimum after four hours.

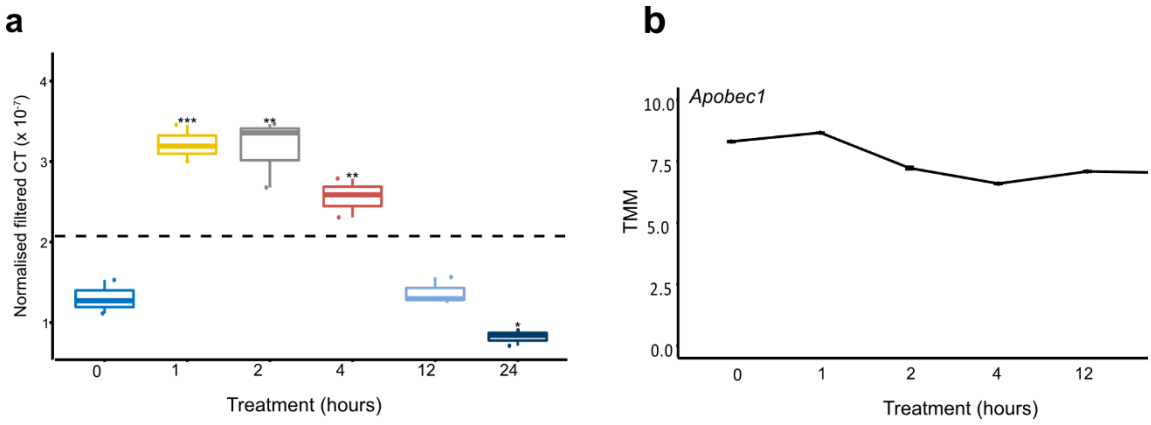


Figure 9 Dynamics of C-to-T levels in RAW264.7 cells with LPS stimulation.

**a**. CT counts with a coverage of 50 reads from REDItools tables normalized to total reads per replicate. Dashed line represents mean C-to-T levels. Box show mean and interquartile range and whiskers indicate range. **b**. Trimmed mean of M values (TMM) of APOBEC1. Data analysed by one-way ANNOVA $p < 0.0000001$. * = p value ≤ 0.05, ** = p value ≤ 0.01, * = p value ≤ 0.001 relative to control untreated 0 hours. N=3 for each time point

### 4.2.3 Editing levels in RAW 264.7 cells are temporally regulated and transcript dependent

As described previously, a one-way ANOVA with an FDR <0.05 was used to characterise positions with temporal editing changes. 85 positions could be identified with significant changes in editing percentage per position during the time course (Table S **2**). In accordance with the BMDM data, all the positions were in 3'UTRs. There were no overlapping positions between the BMDMs and the RAW cells. However, five transcripts were on both lists: *Selenof*, *Nptn*, *Msn*, *Lcp1* and *B2m*. It is clear positions in other transcripts that were edited in the BMDMs are also edited in the RAW 264.7 cells and that editing rates change, for example, in *Cybb* and *Spp1,* but they failed one of the filtering steps and were excluded from the list. Therefore, identified positions are only representative of the changes that occur in the population and not all the changes that do occur.

Most of the genes with changes in proportions of editing in the RAW 264.7 cells are also in the endosome -lysosome-phagosome pathway. Lysosome-associated membrane protein 2, which is essential for the maturation and development of phagolysosomes (Huynh *et al.*, 2007), has four positions that change. Several transcripts that all contain multiple edited positions include components that form part of the lysosomal proton transporting vacuolar ATPase (v-ATPase): *Atpapl, Atpap2, Atpb6v1a* and *Atp6v1c1*, which are crucial for the acidification of vesicles of the endolysosomal /phagosomal system (Strasser *et al.*, 1999; Xia *et al.*, 2019) show editing that responds to stimulation (Figure 10 a & g.) Most positions had an initial increase in editing peaking at one hour (Figure 10 b, f, & i) or after 4 hours (Figure 10 a). The position in Chr:126890834 in signal peptide peptidase like 2A (*Sppl2a*) (Figure 10 c) and the positions Chr3:31144597438 and 144597442 in *Selenof* (Figure 10 d & e) maintain editing levels within the first four hours followed by a drop in editing. The patterns are similar to the overall changes in CT levels observed.

Expression changes in activated macrophages fall into early, middle and late categories, with affected transcripts being downregulated or upregulated at different time points (Nilsson *et al.*, 2006; Sharif *et al.*, 2007; Medzhitov and Horng, 2009; Eichelbaum and Krijgsveld, 2014; Smale and Natoli, 2014; Das *et al.*, 2018). Editing percentage dynamics also appear to fall into different groups depending on time, and this is exemplified by the positions shown in Figure 10 and Figure 7. *Sdcbp* and *Msn* are early responders that quickly increase editing after one hour, followed by a gradual decrease (Figure 10 b & f). *Atp6v1a*, *Trfc* and *Fkp1a* respond quickly, maintain higher editing levels in the middle time points, and drop at later time points (Figure 10 a, h & i). *Cybb* and *B2m* follow a different response pattern, with a decrease in the first 4 hours followed by an increase (Figure 7). Late responders maintain editing levels in the first 2-4 hours, followed by a decrease in editing (Figure 10 c, d, e & g).

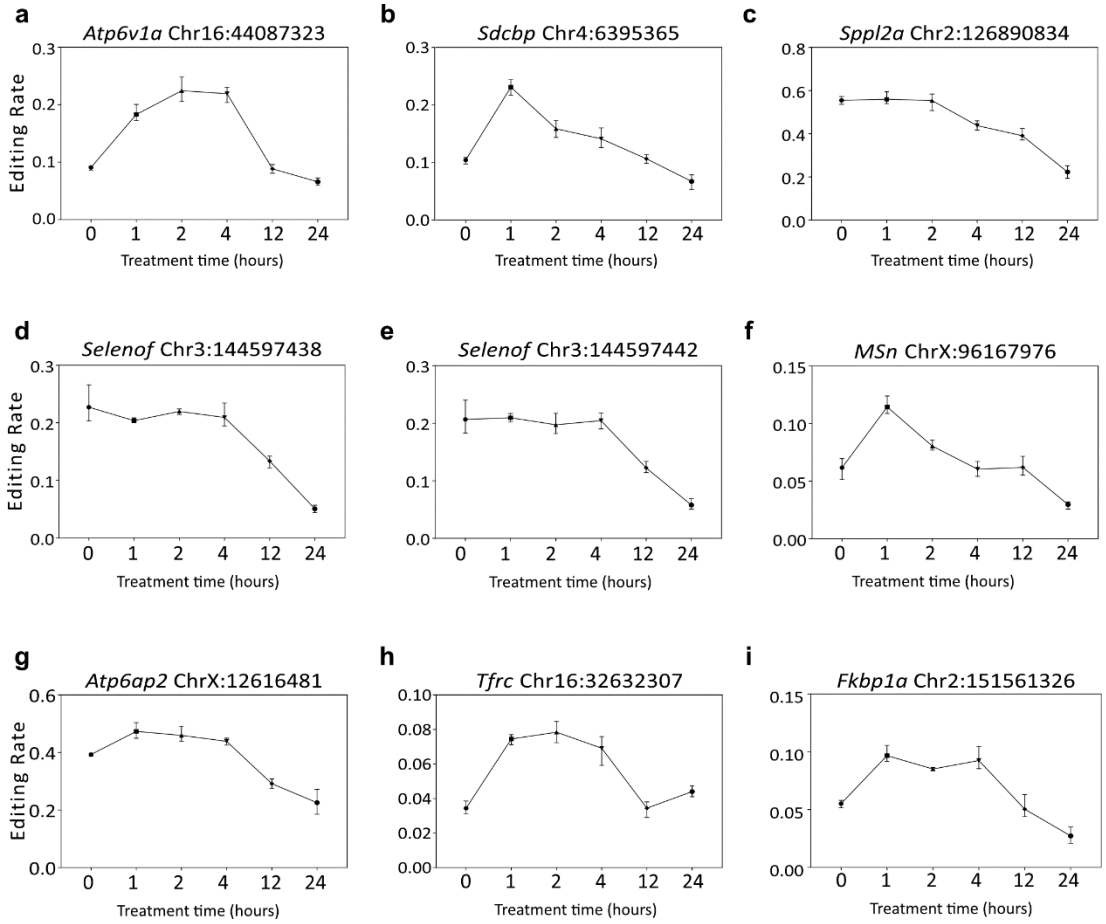


Figure 10. editing frequency changes during RAW 264.7 cell stimulation.

RAW 264.7 were stimulated and primed with 100ng/ml LPS and 100U/ml IFN-γ for 1, 2 4, 12, 24 hours or left untreated. Editing rates are calculated by REDItools2. Shown are the 9 most significantly changing edited positions by one-way ANOVA with FDR ≤ 0.05. Each time points is from RNA-sequencing in triplicates. Values shown are mean with range. **a** ATPase H+ Transporting V1 Subunit A (*Atp6v1a*). **b** Syndecan Binding Protein (*Sdcbp*). **c** Signal peptide peptidase like 2A (*Sppl2a*). **d** & **e** Selenoprotein F (*Selenof*). f Moesin (*Msn*). **g** ATPase H+ Transporting Accessory Protein 2 (*Atp6ap2*). **f** Transferrin Receptor (*Tfrc*). i FKBP Prolyl Isomerase 1A (*Fkbp1a*).

### 4.2.4 Changes in the number of editing events per transcript with stimulation

From studying the 85 positions with significant editing changes, it is possible to see that some positions have editing rates that drop to 0%, which brings about the question of if there are apparent differences in the number of editing events per transcript. While the effects of RNA editing on transcript fate are not entirely known, one can presume that

the number of events could significantly impact a transcript. A1 tends to target AU-rich regions (Blanc and Davidson, 2010), which are hotspots for RNA binding proteins and transcript regulation (Plass, Rasmussen and Krogh, 2017; Otsuka *et al.*, 2019). RNA binding proteins (RBP) can regulate the fate of a transcript by affecting stability, translation and localisation(Plass, Rasmussen and Krogh, 2017; Otsuka *et al.*, 2019) and editing, by altering sequence, can lead to changes in the binding of RBPs and RNA secondary structure which also influences stability and RBP binding.

The number of editing events is easier to determine from REDItools tables than RNA editing percentages as only a yes or no editing question needs to be answered. The number of editing events per transcript were determined by Dr. Salvatore Di Giorgio. Statistical analysis and generation of graphs was performed by both Dr. Salvatore Di Giorgio and myself independently as a cross-validation step with guidance from the DKFZ biostatistics consulting team.

A one-way ANOVA with an FDR ≤ 0.05 identified 149 genes with significantly altered number of editing events over the time course of LPS stimulation (Figure 11 a &Table S 3). These genes are separated into four pools that differ in their overall trends of editing number change. Cluster 1 and 4 are highly alike and have an early increase in the editing frequency in the first 1-2 hours followed by a decrease (Figure 11 b & e). These two clusters differ in the overall number of editing events, with the members of cluster 4 starting and ending the time course with a higher editing level. Cluster 2 also resembles clusters 1 and 4 but shows a lower increase in editing at early time points with a sharper decrease which reaches the mean low after 12 hours of stimulation (Figure 11 c).

Cluster 3 contains only 6 genes: *H2-L, H2-D1, Lilr4b, Ifi207, Cybb* and *Ms4a6c*. H2-L and H2-D1 are major histocompatibility class I (MHC I) molecules and are important for cellular antigen presentation to CD8+ T cells, activation of adaptive immune responses and NK cells (Neefjes *et al.*, 2011). Leukocyte Immunoglobulin Like Receptor B4 (LILR4B), commonly referred to as ILT3, is an inhibitory MHC I receptor that downregulates immune responses and affects the antigen presentation phenotype of antigen-presenting cells (APCs) (Cella *et al.*, 1997; Chang *et al.*, 2002; Brown *et al.*, 2009; Singh *et al.*, 2021; Xu *et al.*, 2021). The exact function of Interferon-activated gene 207 (IFI207) is unknown;

however, it belongs to the Pryin and HIN domain family that contains multiple members such as AIM2 and IFI16, which bind to foreign DNA and form inflammasomes or drive type I IFN gene transcription (Schattgen and Fitzgerald, 2011; Cridland *et al.*, 2012; Connolly and Bowie, 2014). CYBB forms part of the NADPH oxidase complex that generates ROS essential for macrophage activity (Minakami and Sumimoto, 2006). Generation of ROS also plays a role in regulating antigens for presentation on MHC-II and cross-presentation on MHC-I (Savina *et al.*, 2006; Underhill and Goodridge, 2012; Kotsias *et al.*, 2013; Dingjan *et al.*, 2017). Membrane-spanning 4-domains subfamily A member 6C (MS4A6C) also has an unknown function; however, it belongs to the MS4A gene family that have been determined in human microglia to interact with triggering receptor expressed on myeloid cells 2 (TREM2) and is important for activation, survival, and phagocytosis of microglia (Deming *et al.*, 2019). Cluster 3 is the most distinctly different group among the differential editing groups as it demonstrates an increase in the number of events over the course of LPS stimulation as opposed to the decrease seen in other groups. The few transcripts that fall in this group all appear to be associated with antigen presentation and processing.

The two opposing forces during the maturation of phagosomes have opposite changes in editing levels. On the one hand, with increased editing, the members of cluster 3 are primarily involved in antigen processing and presentation; for this purpose, regulation of phagosomal pH and lysis of peptides is critical(Kotsias et al. 2013(Kotsias *et al.*, 2013). Production of ROS by enzymes such as NOX2 (*Cybb* in cluster 3) consumes protons and is essential for proper antigen processing and presentation on MHC molecules such as H2-L and H2-D1 (also in cluster 3). A decrease in editing numbers is seen in multiple transcripts involved in the maturation and acidification of phagosomes that increase peptide digestion, for example, *Lamp2*, *Atp6ap2* and *Rab7* in cluster 4.

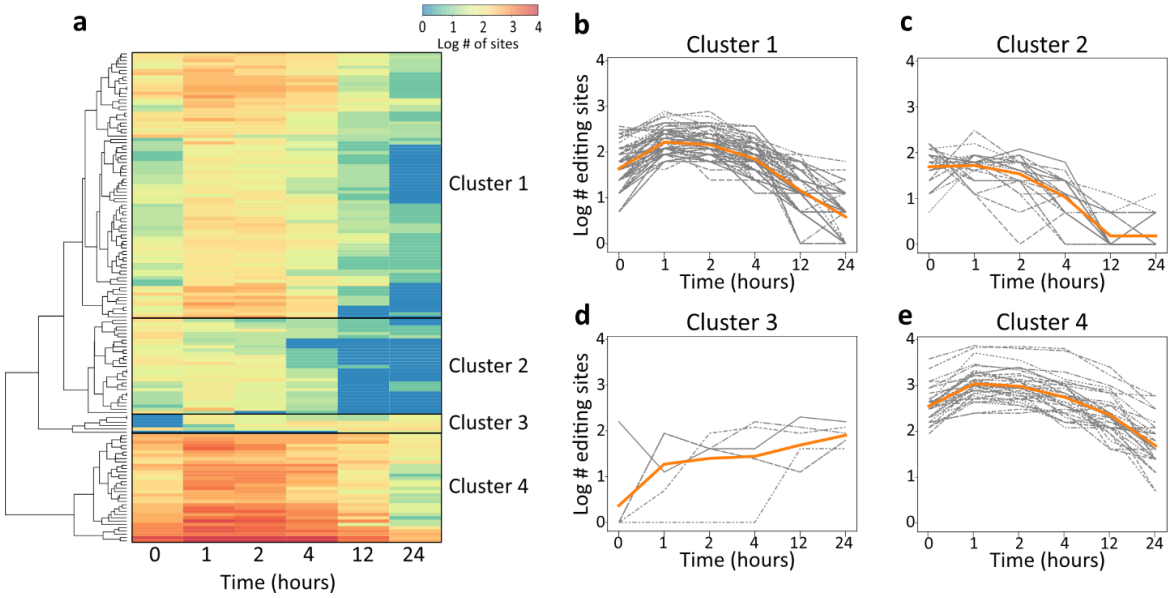


Figure 11 Number of editing events per transcript are dynamic.

Time series of interferon-g (IFN-γ)-primed lipopolysaccharide (LPS)-induced changes in the number of APOBEC1 editing evens. **a** Heat map representation depicting the log change in the number of editing events in transcripts in RAW 264.7 after IFN-γ-primed LPS stimulation ($P \leq 0.05$). **b-e** line graphs showing the log change in the number of edited sites over time of each cluster from **a**. Orange line shows mean editing in the group.

### 4.2.5 C-to-T editing affects multiple transcripts in the phagocytosis pathway

To better understand the pathways involved in editing in RAW cells and differential editing, a KEGG pathway over-representation analysis was performed as previously discussed. To establish whether transcripts that are differentially edited (from Figure 11) were involved in different pathways when compared to all other edited genes, they were split into two groups, edited but no significant differential number of editing occurrences (Figure 12 a) and genes with differential number of editing events (Figure 12 b). In concordance with previous pathway analysis in BMDMs (Figure 6, (Rayon-Estrada *et al.*, 2017), the endo-lysosomal-phagosomal pathways are significantly enriched in RAW cells (Figure 12) with a more significant fold enrichment of the phagosome compartment in genes with changes in editing numbers (Figure 12 b).

Terms such as 'Citrate cycle', 'Carbon metabolism' and 'Pentose phosphate pathways' can also be associated with the endo-lysosomal-phagosomal pathways and

effector activities of macrophages stimulated towards a proinflammatory phenotype. A switch from relying on oxidative phosphorylation (citrate cycle) to primarily relying on glycolysis and the pentose phosphate pathway for their energy demands characterises the metabolic signature of inflammatory macrophages (Ryan and O'Neill, 2017; Hayek *et al.*, 2019; Viola *et al.*, 2019). These processes generate both ATP and the NADPH, which is used by enzymes such NOX2 to generate ROS, which is crucial for their activity (Iles and Forman, 2002).

All over-representation analyses performed were done considering the background genes expressed specifically in the RAW 264.7 cells to decrease the effect of natural enrichment of phagocytosis associated genes in a cell whose primary function arguably is phagocytosis. Performing the analyses in this context suggests that the phagocytosis associated pathways are truly enriched for editing by A1. To further rule out the possibility that these pathways are over-represented due to their natural over-representation, a comparison was made with genes edited with another editing enzyme ADAR1. ADAR1 edits adenosines to inosines in RNA, primarily in 3'UTRs (Yang *et al.*, 2017; Chung *et al.*, 2018), which appear as guanosines in sequencing data and targets double-stranded RNA. In general, ADAR1 is less specific in its targets selection and is associated with preventing intracellular mechanisms from sensing endogenous double-stranded RNA regions as foreign (Mannion *et al.*, 2014; Chung *et al.*, 2018). At the same time that the A1 KO was created, CRISPR-Cas 9 KO guides targeting a region common to the two ADAR1 isoforms p110 and the inducible form p150 were designed and used for creating a RAW 264.7 KO. RNA was extracted from the KO cells and sent for sequencing and the RNA ADAR1 editome was determined using REDItools 2. KEGG pathway over-representation analysis with the same parameters as used previously revealed no pathway that was significantly enriched for A-to-I editing (Table S 4). This further points to phagocytosis being a major target for regulation by APOBEC 1 editing.

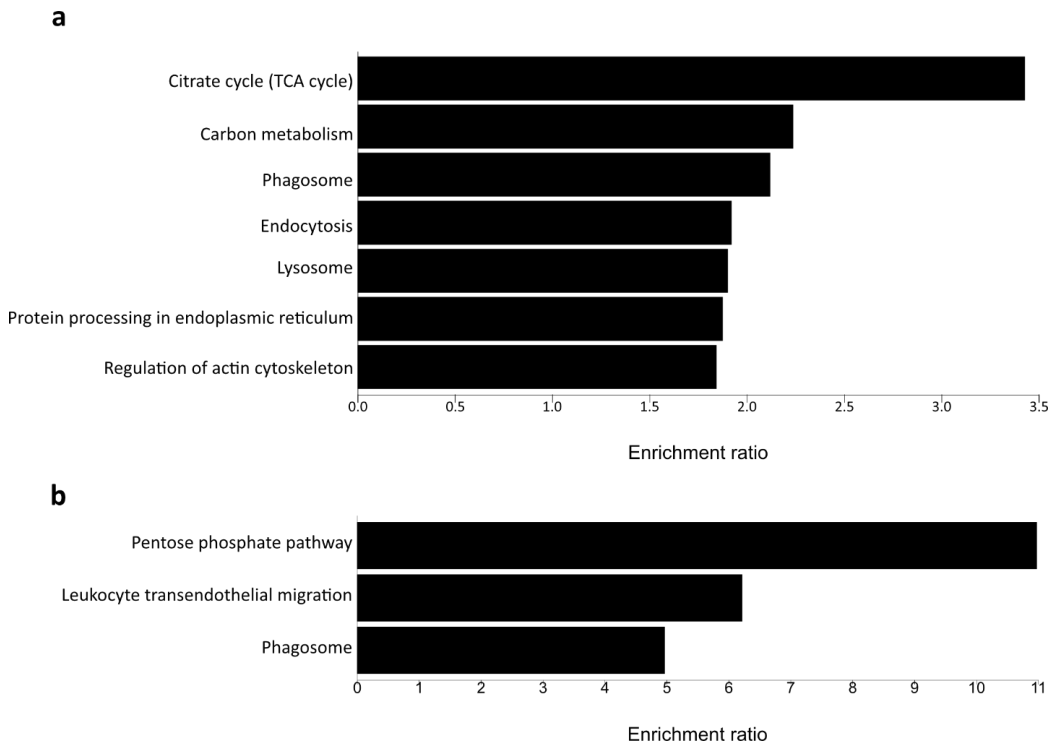


Figure 12 Endo-lysosome-phagosome pathways are enriched for editing.

Over-representation KEGG pathway analysis of genes edited in stimulated RAW264.7 macrophages a. Enrichment of pathways for all edited genes minus genes that show significant changes in the number of editing events. b. pathway enrichment for genes that exhibited modifications in the number of editing events.

### 4.2.6 Editing does not affect transcript expression

The data thus far indicates that A1 editing is regulated in a time-dependent manner. Nevertheless, what effects does this editing have on the transcripts or the cells as a whole? A-to-I editing is known to affect the stability of transcript and can therefore lead to the appearance of differences in expression (Rosenberg *et al.*, 2011; Blanc *et al.*, 2018). Previous studies with A1 suggest no direct link between editing and transcript expression/stability(Blanc *et al.*, 2014; Rayon-Estrada *et al.*, 2017). If editing affects the expression, one could expect to observe a correlation with the increase and decrease in the number of editing events during stimulation. A DEseq2 differential expression analysis compared the WT and A1 KO RAW 264.7 cells from the previously described activation experiment to identify any connection between editing and expression.

269, 347, 337, 70, 385, and 1101 differentially expressed genes were identified after 0, 1, 2, 4, 12 and 24 hours of LPS and IFN-γ (Figure 13). After 24 hours of stimulation, the WT and A1 KO macrophages are the most divergent from one another. Most edited transcripts did not exhibit a significant expression difference between WT and the KO (Figure 13 labelled in yellow). These transcripts showed no significant changes in expression irrespective of whether editing increased or decreased, which suggests that there is no direct link between editing and expression. Only one edited transcript, Insulin Growth Factor like 2 receptor (*Igf2r*), was consistently upregulated in the KO cells at all time points. IGF2R mediates the transport of mannose 6-phosphate tagged lysosomal enzymes such as cathepsin between the Goli and the lysosomes (McCormick *et al.*, 2008). It is also involved in T cell coactivation (Ikushima *et al.*, 2000).

Differential expression of non-edited genes could be a direct result of A1 binding or indirect through the action of A1 on its edited targets. It is unclear which one of these leads to the changes in expression seen between the WT and the KO. There are claims that A1 can bind to some transcripts and stabilise them without editing, although the evidence is not entirely clear (Anant and Davidson, 2000; Anant *et al.*, 2004).

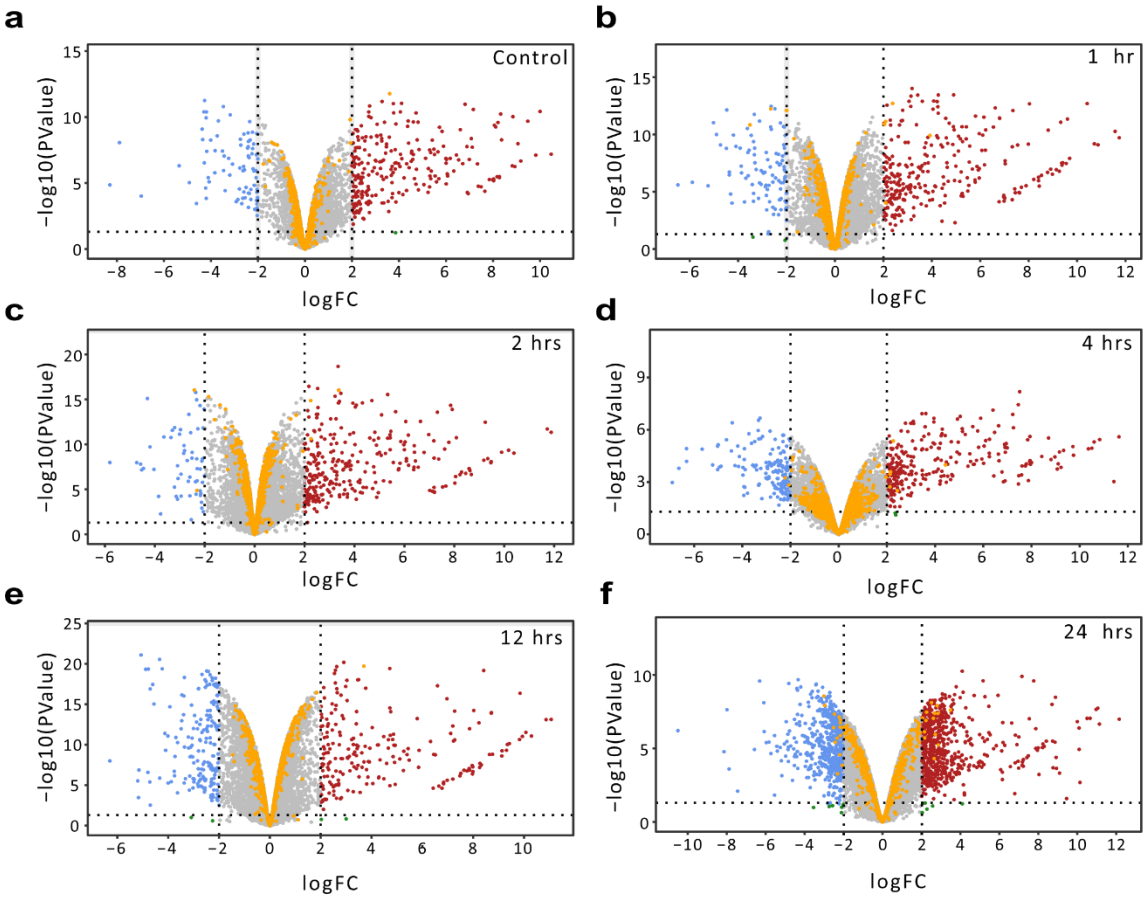


Figure 13 CT RNA editing does not correlate with expression.

Differential gene expression analysis of WT vs A1 KO RAW 264.7 cells during time course with 100ng/ml LPS and 100U/ml IFN-γ. **a.** No treatment control **b.** 4 hours and **c**. 24 hours. The x-axis represents the log2 fold change in expression (WT vs A1 KO) for each transcript. The y-axis represents negative log10 of the adjusted p-value of Fisher's exact test. Dotted vertical lines represent the biological cut off of a 3-fold change in expression between the WT and A1 KO cells. Dotted horizontal lines represent the adjusted p-value cut off of < 0.0001. Red data points represent transcripts upregulated for expression, blue circles for down-regulated. Yellow circles are for edited genes and grey for non-significantly changing genes.

### 4.2.7 Pathways affected by A1 KO in macrophages

There is minimal overlap between the edited genes and the differentially expressed genes. A KEGG pathway Gene Set Enrichment Analysis (GESA) analysis was performed, using clusterProfiler package in R (Yu *et al.*, 2012), to better understand the

pathways affected by differential expression (analysis performed by Dr. Salvatore Di Giorgio). This method differs from the overrepresentation analysis used with the edited genes; edited transcripts all have equal whereas with GESA genes with more significant, and higher fold change are assigned a greater weight in the analysis (Subramanian *et al.*, 2005).

Early time points are characterised by downregulation of PAMP and DAMP signalling as signified by terms such as TNF signalling, Toll-like receptor signalling, NOD-Like receptor signalling pathway, and cytosolic DNA -sensing pathway (Figure 14 b & Figure S 7). After 12 hours, antigen presentation and processing pathways are downregulated (Figure 14 c & Figure S 7). Notably, transcripts associated with this pathway show an increase in editing levels (Figure 11 a cluster 3). Production of ROS, which is also affected by editing, is also affected by differential expression. There are overlaps between edited pathways and differential expression affected pathways. M1 activated macrophages are more reliant on glycolysis for their energy demands and downregulate oxidative phosphorylation (Ryan and O'Neill, 2017). The A1 KO macrophages appear to be more reliant on glycolysis as oxidative phosphorylation is further downregulated in the KO cels.

The changes in gene expression pathways with loss of A1 are very similar to the patterns observed for its human counterpart, A3A, in human macrophages (Alqassim *et al.*, 2020). Human macrophages where A3A is knocked-down show downregulated Antigen processing and presentation, changes in inflammatory signalling pathways and upregulation of glycolysis. This further supports the notion that A3A performs a similar function in human macrophages as A1 in mouse macrophages.

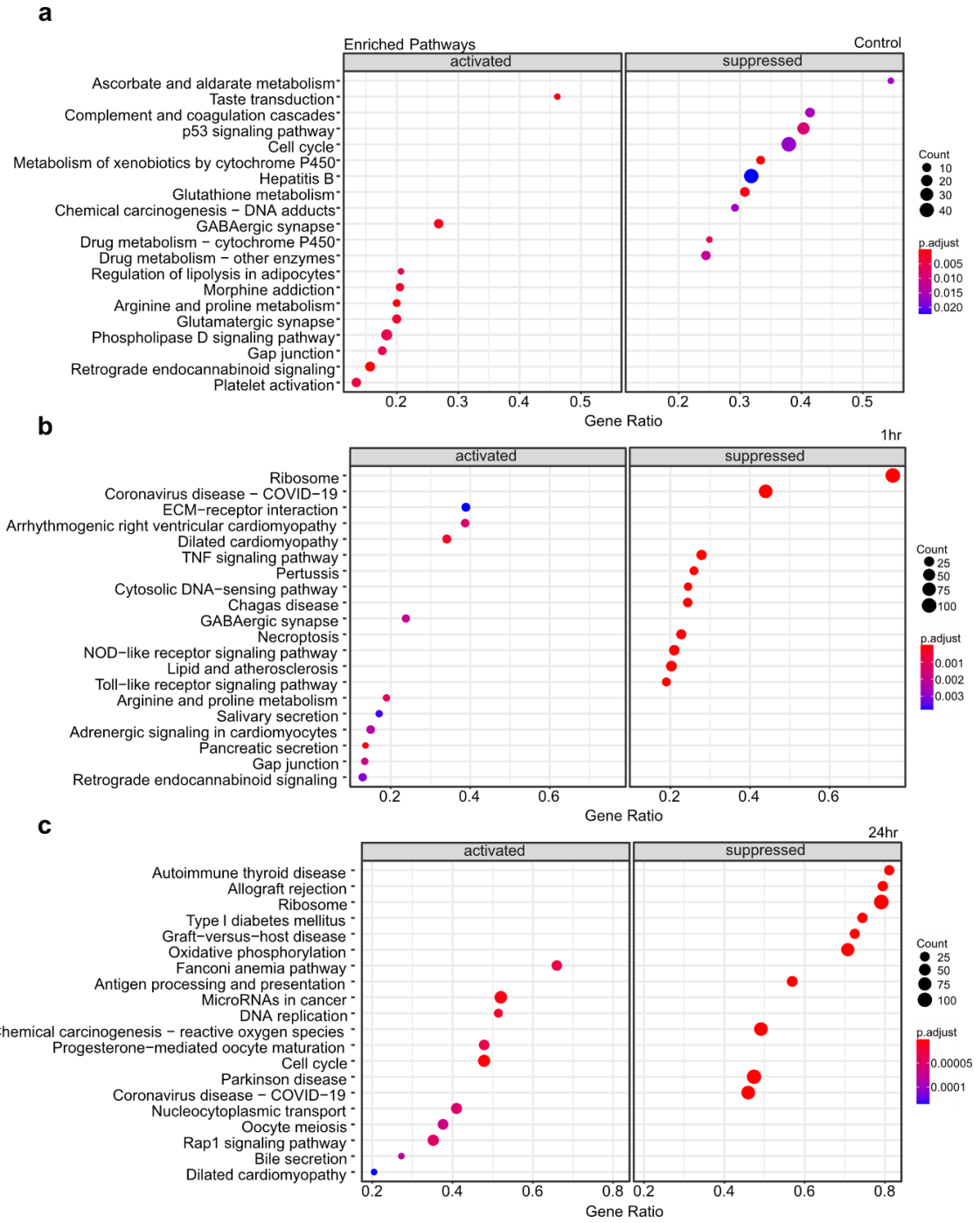


Figure 14 Differential expression in A1 KO RAW cells during stimulation

KEGG pathway Gene Set Enrichment analysis of WT vs A1 KO raw 264.7 cells after incubation with 100ng/ml LPS and 100U/ml IFN-γ. Representative time points form a. 0 hours control b. 1hr c. 24hrs are shown, other time points are similar. P values corrected with Benjamini-Hochberg correction. FDR < 0.0001 FC > 3.

## 4.3 Effects of editing on protein abundance

The effects of editing on transcripts and the relevance of its dynamic regulation is unknown. Previous studies on the function of editing have suggested that protein abundance is affected (Cole *et al.*, 2017b; Rayon-Estrada *et al.*, 2017). Luciferase assays showed editing reduces the protein levels of CD36, B2M, APP and LAMP1 (Rayon-Estrada *et al.*, 2017) and increases LAMP2 (Cole *et al.*, 2017b). The luciferase assays are a valuable tool for studying the edited 3'UTR; however, they are artificial. In order to investigate editing in a more native context, RAW 264.7 WT and KO cell lysates in triplicates were prepared for label-free LC-MSMS-based comparative proteomics. Mass spectrometry was done by the DKFZ MS-based Protein Analysis Core Facility. Initial data analysis was performed by Martin Schneider of the protein analysis core facility. 3 replicates of untreated WT and KO cell lysates were sent for mass spectrometry in a preliminary experiment. A total of 59257 peptides and 4866 proteins were identified based on an FDR cutoff of 0.01 on peptide level and protein level. Label-free quantification was done by MaxLFQ algorithm (Cox *et al.*, 2014), and 3167 proteins were possible to quantify in all samples.

A total of 39 proteins showed differential abundance between the WT and the KO at an FDR < 0.05 and a fold change > 1.5 (Figure 15Figure 15). 16 proteins had lower levels in the WT, and 23 have higher protein levels. A subset of edited transcripts results in different protein abundances. From these 39 proteins, 12 have edited transcripts in macrophages. Among the proteins with edited transcripts, Collectin Subfamily Member 12 (COLEC12), Cyclin Y (CCNY), Catalase (CAT), Guanine Deaminase (GDA) and Cathepsin S (CTSS) are in lower concentrations in the WT cells. At the same time, Integrin Subunit Alpha 4 (ITGA4), histocompatibility 2, D region locus L (H2-L), Cybb, Lipoprotein Lipase (LPL), CD36, CD44 and Transporter 2, ATP Binding Cassette Subfamily B Member (TAP2) are more abundant. COLEC12, CYBB, H2-L and LPL all have transcripts that show differential editing numbers (Figure 11). Both H2-L and TAP2 are part of the antigen processing and presentation system, and their higher levels in WT cells is consistent with the observation that other members of this pathway show expression downregulation in the absence of A1 (Figure 14).

A second mass spectrometry experiment was also submitted for label-free LC-MSMS-based comparative proteomics in 5 replicates of both the WT and the KO with a time course of 100ng/ml of LPS and 100 units/ml IFNγ at 0, 1, 2, 4, 12, and 24 hours with additional single replicates after 8 hours and 16 hours. At the time this thesis was written, this dataset was not yet thoroughly analysed. Processing of the data proved more challenging than in the preliminary experiment. Quantification with the MaxLFQ algorithm assumes that only a small number of proteins between the two comparisons are different (Cox *et al.*, 2014)t. When RAW 264.7 cells are treated with LPS a large number of changes occur, many genes are activated, and over the 24 hours, the cells change from a monocyte like appearance (small and round) to a macrophage-like appearance (large, flattened and with many pseudopodia), therefore the assumption that most proteins do not change is false. A different method of data normalisation and quantification was necessary. A proteomic ruler which utilises the combined histone intensities for sample normalisation was used (Wiśniewski *et al.*, 2014).

Validation of successful KO of A1 was done as described in section 4.2.1 without an antibody as none is available. Although failure to detect a peptide by mass spectrometry does not indicate that a protein is absent, it is of note that in almost all the WT samples, both from the preliminary and second larger mass spectrometry experiment (35 samples in total) A1 was detected, but not a single peptide was detected in any KO sample. A1 mRNA is still produced in the KO cells; however, the mutations as a result of Cas9 targeted activity causes a frameshift which the mass spectrometry data suggests a protein is not produced.

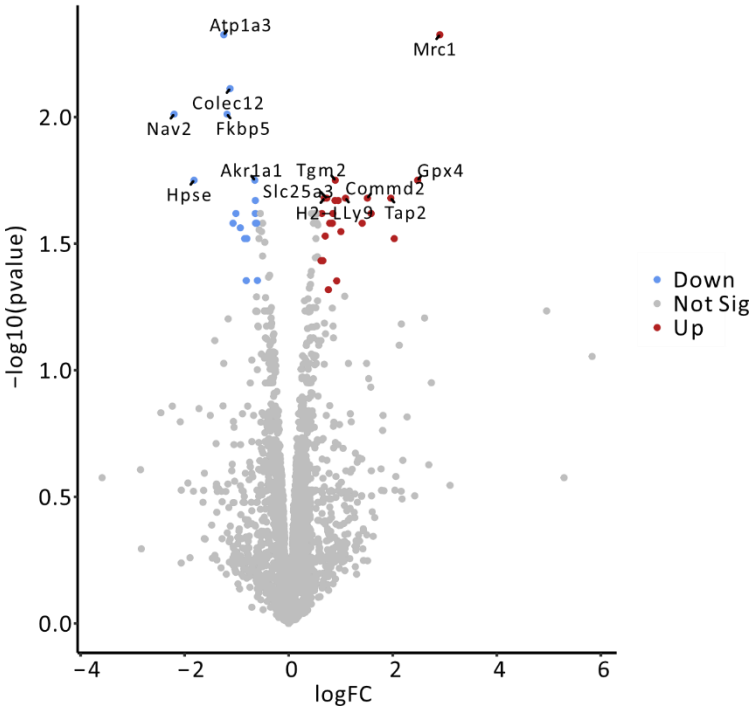


Figure 15 Editing causes differential protein abundance in a subset of targets.

Volcano plot generated from MaxLFQ quantified mass spectrometry comparison of wild-type compared to A1 KO RAW 264.7 cells. Coloured labels indicated values with an FDR <0.05 and a fold change >1.5. Red coloured dots show upregulated proteins, blue shows downregulated proteins, and grey shows not significant proteins. The top 10 most significant proteins are labelled.

### 4.3.1 Editing affects protein levels of CD36 and CYBB without affecting transcript levels

Among the transcripts that exhibit differences in protein abundance CD36 and CYBB have the highest levels of editing, and CYBB also shows significant changes in editing events with LPS stimulation (Figure 11). CD36 protein levels were also found to be different in WT and APOBEC 1 KO BMDMs (Rayon-Estrada *et al.*, 2017). However, unlike in the RAW 264.7 cells, CD36 levels were higher in the KO cell. CD36 and CYBB were selected for further analysis.

CD36 is a surface scavenger receptor that binds to various lipid moieties, including LPS (Febbraio, Hajjar and Silverstein, 2001b; Biedroń, Peruń and Józefowski, 2016b;

Grajchen *et al.*, 2020). Good antibodies exist, so flow cytometry can easily confirm protein levels (Figure 16 a & b). CD36 was lower in the A1 KO cells, as expected, and remained lower after 24 hours of LPS activation. RNA seq data did not reveal significant differences in the transcriptional levels of CD36 or CYBB between the WT and KO, and this was corroborated by RT-qPCR (Figure 16 c & d). 12 hours after stimulation, A1 KO cells appeared to have higher transcription levels than in their WT counterparts, but considerable inter-experimental variability was observed (Figure 16 d).

The changes in CD36 and CYBB protein levels are not connected to the transcriptional levels, which remained similar between the WT and A1 KO cells. One hypothesis to explain this difference is that editing is causing changes in translational efficiency; this idea was previously proposed by Rayon-Estrada *et al*.

Interestingly, the case of CD36 is a clear example of transcription and translation not always being coordinated. After 24 hours of LPS stimulation, transcription levels of CD36 fall below the unstimulated levels, but at the same time protein levels are higher in the stimulated cells than the unstimulated cells (Figure 16).

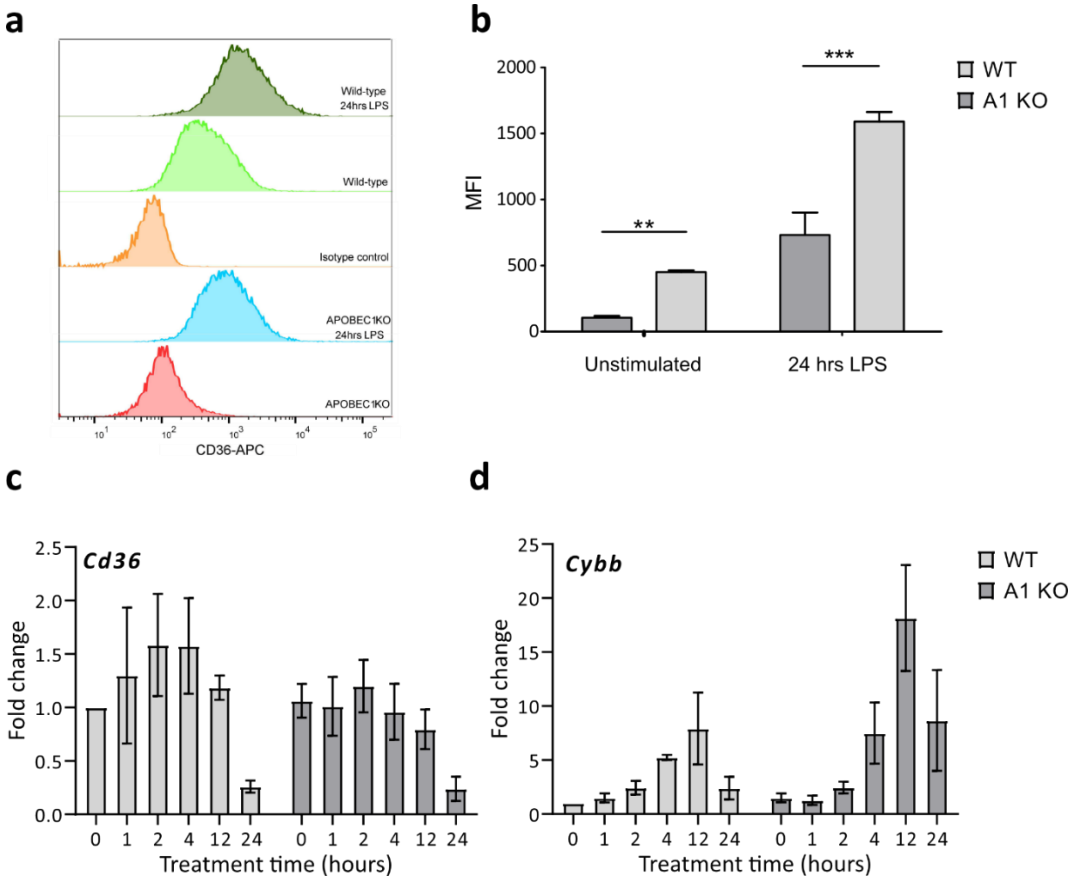


Figure 16 Editing of *Cd36* and *Cybb* changes protein abundance but not transcript levels.

WT and A1 KO RAW 264.7 cells were either unstimulated or treated with 100ng/ml LPS and 100U/ml IFN-γ for 24 hours and/or 1, 2, 4, and 12 hours. Levels of Cd36 were measured by flow cytometry **a**. representative plot of flow cytometry histograms of stimulated or unstimulated WT and A1 KO cells with anti-CD36 antibody or isotype control **b** mean fluorescence intensity (MFI) of CD36 N=3. RT-qPCR of c. *Cd36* and d. *Cybb*. ** p <0.01, *** p<0.001, Welch's T-test.

### 4.3.2 APOBEC1 influences the translational efficiency of CD36 and CYBB

Standard ribosomal profiling experiments used to assess translation have the disadvantage of not being suitable to query the 3'UTRs due to 3'UTR digestion during the production of libraries (O'Connor, Andreev and Baranov, 2016). Polysome fractionation analysis is a powerful method to assess ribosome - mRNA association by fractionating mRNA with a sucrose gradient according to the number of bound ribosomes (Panda,

Martindale and Gorospe, 2017). At the same time, the entire mRNA, including the 3'UTRs, are maintained so editing can also be assessed. More ribosomes attached to mRNA are usually believed to indicate more translation, and untranslated mRNAs are found more frequently not associated with the polysomes.

In order to determine the translational efficiency of edited and unedited transcripts, polysome fractions of WT and A1 KO RAW 264.7 cells without stimulation and after 2 hours of 100ng/ml LPS and 100units/ml of IFNγ in triplicate were prepared by fractionating cell lysates on a sucrose gradient and collecting the separate fractions. Before RNA was extracted from each fraction, a spike in of 10 pM of rabbit β globin RNA, as a control for the efficiency of RNA extraction (construct for in-vitro transcription, preparation of RNA and design of primers for qPCR rabbit β globin was performed by Kathrin Bajak) was added. RT-qPCR was performed to determine the distribution of mRNA across the fractions (Panda, Martindale and Gorospe, 2017).

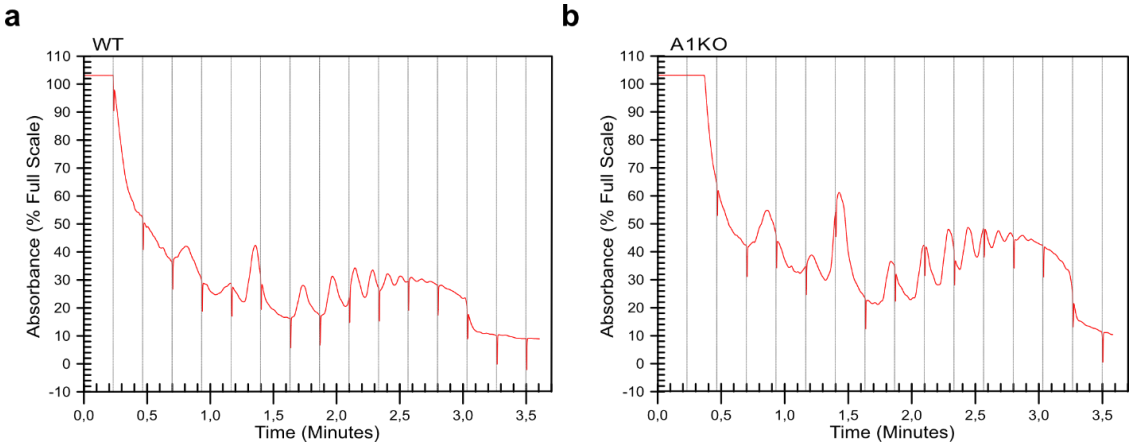


Figure 17 Polysome profiles

Profiles of unstimulated a. WT and b. A1 KO RAW 264.7 cells from spectral absorption during fractionation.The experiment was performed with 5 replicates from 2 independent experiments; one representative profile is shown

Global translation levels can be assessed by the profiles generated by the density gradient fractionation system (Figure 17 & Figure S 4). The amplitude and the number of peaks provides an overview of translation (Chassé *et al.*, 2016). When translational shutdown occurs, such as with ADAR1 KO (Chung *et al.*, 2018) or when cells slow down and stop dividing (Mazor *et al.*, 2018) fewer peaks are seen. Translation appears normal

in both WT and KO RAW 264.7 cells with clear peaks for the 40s, 60s and 80s ribosomes and clear polysomes (Figure 17 & Figure S 4). Input protein levels were not calibrated; therefor peak heights can not be compared between the samples.

RT-qPCR was performed on RNA extracted from polysome fractions described above from WT and KO cells treated and untreated. CT values from the RT- qPCR of *Cd36*, *Cybb* and the house keeping gene Hypoxanthine phosphoribosyltransferas (*Hprt*) were normalised to spike in control and the relative distribution of the percentage mRNA from total was determined across the 15 fractions in each replicate from two independent experiments (Figure 18). The housekeeping control, *Hprt,* showed no differences in mRNA distribution between the WT and the KO (Figure 18 a). Both *Cd36* and *Cybb* in unstimulated cells unexpectedly showed a minor shift in distribution to the high molecular weight fraction with a greater proportion of RNA in fraction 14 in the KO cells compared to the WT (Figure 18 b & c left). *Cd36* and *Cybb* would be expected to be shifted towards the higher polysomes in the WT samples, not the KO samples because the WT cells have higher protein levels. One theory to explain this observation is that the rate of translation has decreased, and ribosomes are stalled, taking longer to detach from the mRNA, which may increase the likelihood that more ribosomes are found on a transcript in one snapshot. After 2 hours of LPS, there are no observable differences between the WT and KO with *Cybb,* while the same shift towards the higher polysomes is still seen in the KO with *Cd36* (Figure 18 b & c right). Interestingly, this appears to correlate with the editing levels of both transcripts. *Cybb* shows differential editing at the positional level (Figure 7) and the number of events (Figure 11); the overall trend in both is a decrease during the first four hours and then an increase. After 2 hours of LPS stimulation, editing decreases, and this coincides with the disappearance of the RNA shift observed in the unstimulated cells (Figure 18 b). On the other hand, editing of *Cd36* does not experience the same significant changes either in position or number, and the shift of the KO cells towards the higher polysomes seems even more apparent after 2 hours (Figure 18 c).

Lack of editing does not cause an mRNA distribution shift in all transcripts. *Rprd1a*, *Sppl2a, Tmem55a* are highly edited and/or differentially edited; they did not show significant changes in protein levels in unstimulated cells, nor do they show any shift in mRNA distributions across the polysomes (Figure S 5). However, *B2m,* another highly

edited transcript that was unfortunately not detected in the mass spectrometry, showed a shift .

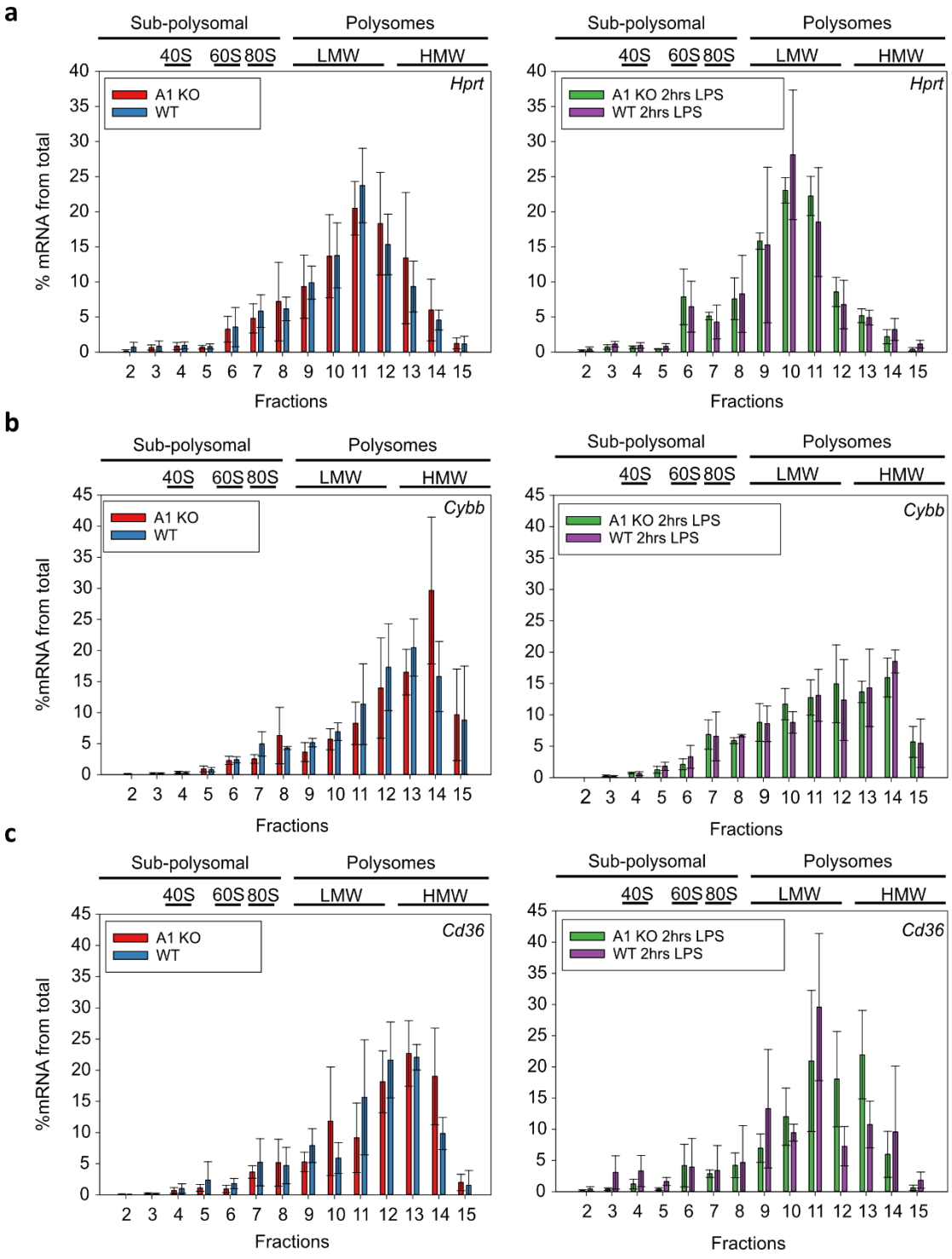


Figure 18 Editing increases translational efficiency in a subset of targets.

mRNA distributions of **a**. housekeeping control *Hprt*. **b**. *Cybb* and **c**. *Cd36* as determined by RT-qPCR from RNA extracted from polysome fractionations from Figure 17.Data shows percentage calculated from 5 replicates, RT-qPCR of each done in triplicates. Error bars show standard deviation.

## 4.4 APOBEC1 regulates phagocytosis

The RNA sequencing and proteomics shown thus far all point to editing having a role in phagocytosis and that the protein abundance of particular transcripts is modulated by editing. The question remains what effect editing and these changes in protein levels have on the physiology of macrophages. The phagocytosis performance of wild type and A1 KO BMDMs and microglia was assessed in previous studies (Cole *et al.*, 2017b; Rayon-Estrada *et al.*, 2017). Both the A1 KO BMDM and microglia exhibited differences in phagocytotic ingestion of bacteria compared to wild-type cells. The change in phagocytosis depended on the context, with A1 KO BMDMs being more phagocytotic than their wild type counterparts and KO microglia being less phagocytotic.

The phagocytosis assay used to study BMDMs was replicated with the RAW 264.7 cells to determine their phagocytosis phenotype. Serum starved RAW cells were incubated with pHrodo green *Staphylococcus aureus* (*S.aureus*) particles at a multiplicity of infection (MOI) of 300, as recommended by the manufacturer, for four hours. pHrodo green is a pH-sensitive fluorophore that exhibits very low fluorescence levels at a pH of approximately 7, such as the pH of the cell culture media, and high fluorescence at low pH, for example, the pH found in phagosomes (Ogawa *et al.*, 2010). The Fluorescence intensity acts as a marker for the uptake of the bacteria particles and can be easily gauged by flow cytometry. The A1 KO RAW cells have the same phagocytotic phenotype as the KO BMDMs; they have an increase of approximately 20% in phagocytosis relative to wild type cells (Figure 19).

Two factors determine the signal obtained from this type of phagocytosis assay; 1) luminal pH of the compartment the bacteria are in and 2) the number of bacteria bioparticles ingested. After 4 hours of phagocytosis and at an MOI of 300 the process has reached a steady-state where 100% of the macrophages have ingested bacteria, likely ingesting the maximum possible number of bacteria. Therefore, it is not possible to separate the two components responsible for the increase in the phagocytotic index.

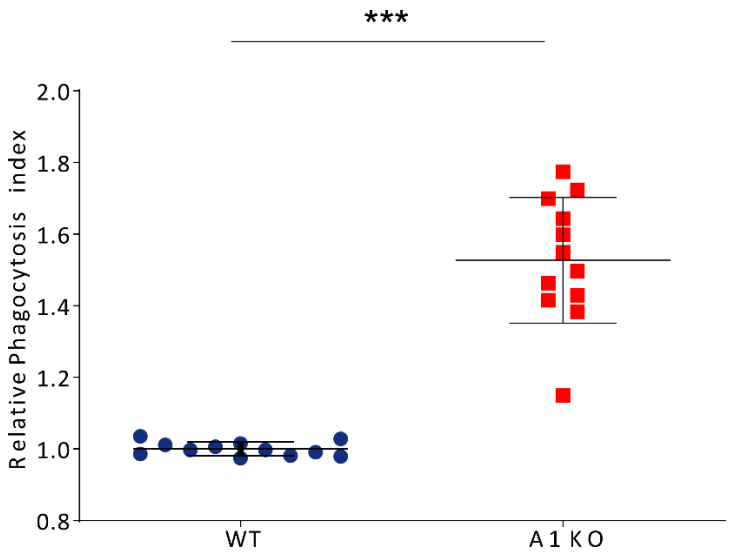


Figure 19 APOBEC1 is involved in macrophage phagocytosis.

WT and A1 KO RAW 264.7 cells were incubated with an MOI of 300 if pHrodo green Staph. Aureus bioparticles for 4 hours. n = 12, from four independent experiments in triplicates. Relative phagocytosis index calculated as increase relative to WT mean fluorescence intensity from the same experiment. P ≤ 0.001 calculated as T test with Welch's correction

### 4.4.1 APOBEC1 regulates the number of ingested bacteria and phagosomal pH

To better understand which factor is contributing to the increased phagocytosis, the analysis time was decreased to 1 hour, and the MOI was decreased to 100 particles so that phagocytosis is in the linear range (Figure 20). In addition, the phagocytosis of *Escherichia coli* (*E.coli*) bioparticles was also studied (Figure 21). This thesis's temporal dynamics of editing study was conducted under LPS stimulation; LPS originates from gram-negative bacteria such as *E. coli*. The original phagocytosis experiments were carried out with S*. aureus* bioparticles which are gram-positive bacteria and have no LPS but have a similar component that is recognised by the immune system, Lipoteichoic acid (LTA). Similar signalling pathways are activated in macrophages when LPS or LTA stimulates them; however, there are differences (Nilsen *et al.*, 2008). Editing was shown to differ between LPS, IL 13 or IL 4 stimulation; therefore, it is possible that editing and its dynamics may differ with LTA stimulation, so the phenotype with *E. coli* is also essential to consider.

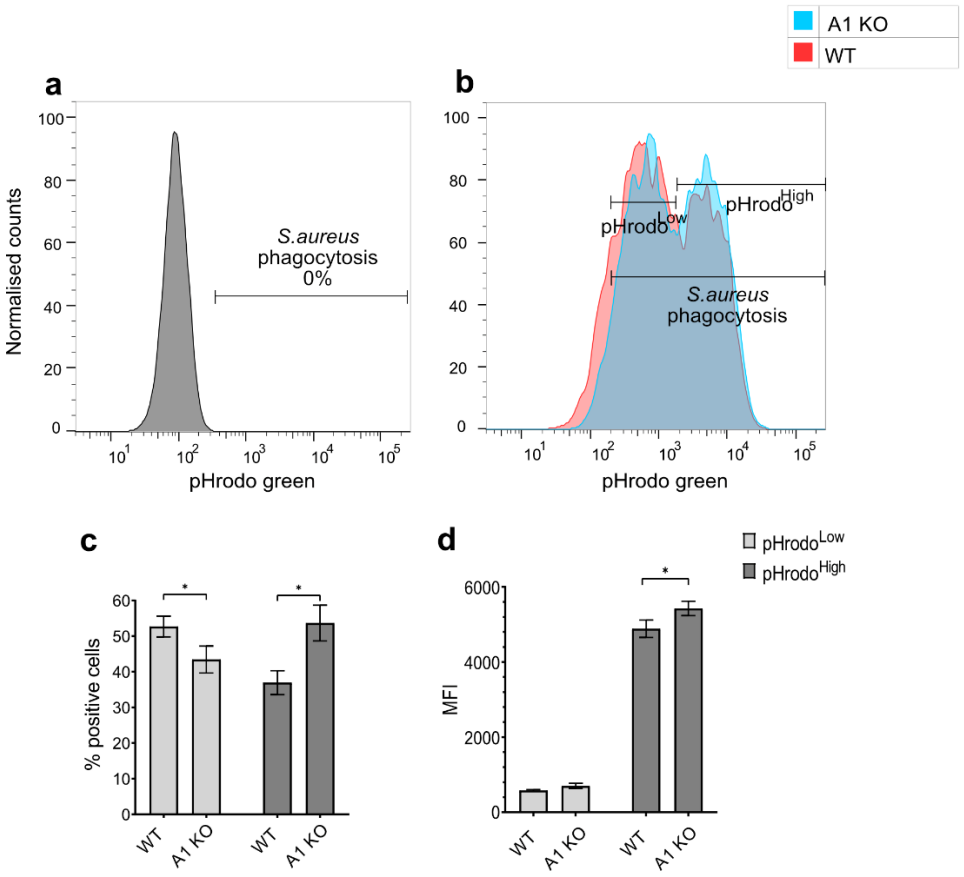


Figure 20 APOBEC1 loss increases *S.aureus* ingestion and decreases phagosomal pH.

**a**. Control untreated WT RAW 264.7 fluorescence histogram; one representative replicate shown, A1 KO cells have the same background fluorescence. **b**. Representative fluorescence histogram of WT cells in red and A1 KO cells with pHrodo green labelled *S. Aureus* particles (n=3) **c**. Percentage of cells positive for high or low pHrodo green signal. **d**. Mean fluorescence intensity (MFI) of pHrodo$^{Low}$ and pHrodo$^{High}$ fractions indicated in b in WT and A1 KO RAW cells (n=3). Error bars represent standard deviation; statistical significance was obtained with an unpaired t test with Welch's correction. * = $p \leq 0.05$

After a one-hour *S.aureus* bioparticles incubation, phagocytosis differences between WT and A1 Ko cell is maintained (Figure 20). The fluorescence histograms obtained by flow cytometry show more than one peak of positive cells (Figure 20 b) instead of the single peak visible after four hours of incubation (Figure 19). The two separate peaks are most likely indicators of populations of cells that have ingested a different number of bacteria. They were split into two groups according to their fluorescence intensity where pHrodo$^{Low}$ denotes cells that have ingested few bacteria and pHrodo$^{High}$ for cells that ingested higher amounts of bacteria. The percentage of

pHrodo$^{High}$ A1 KO cells (53.7%) is significantly higher than WT cells (36.9%). The fluorescence intensity of the pHrodo$^{High}$ A1 KO fraction is also significantly higher (MFI 5427) that the wild type (MFI of 4886). These data indicate that the A1 KO macrophages are ingesting more bacteria particles, and their phagosomal pH is lower.

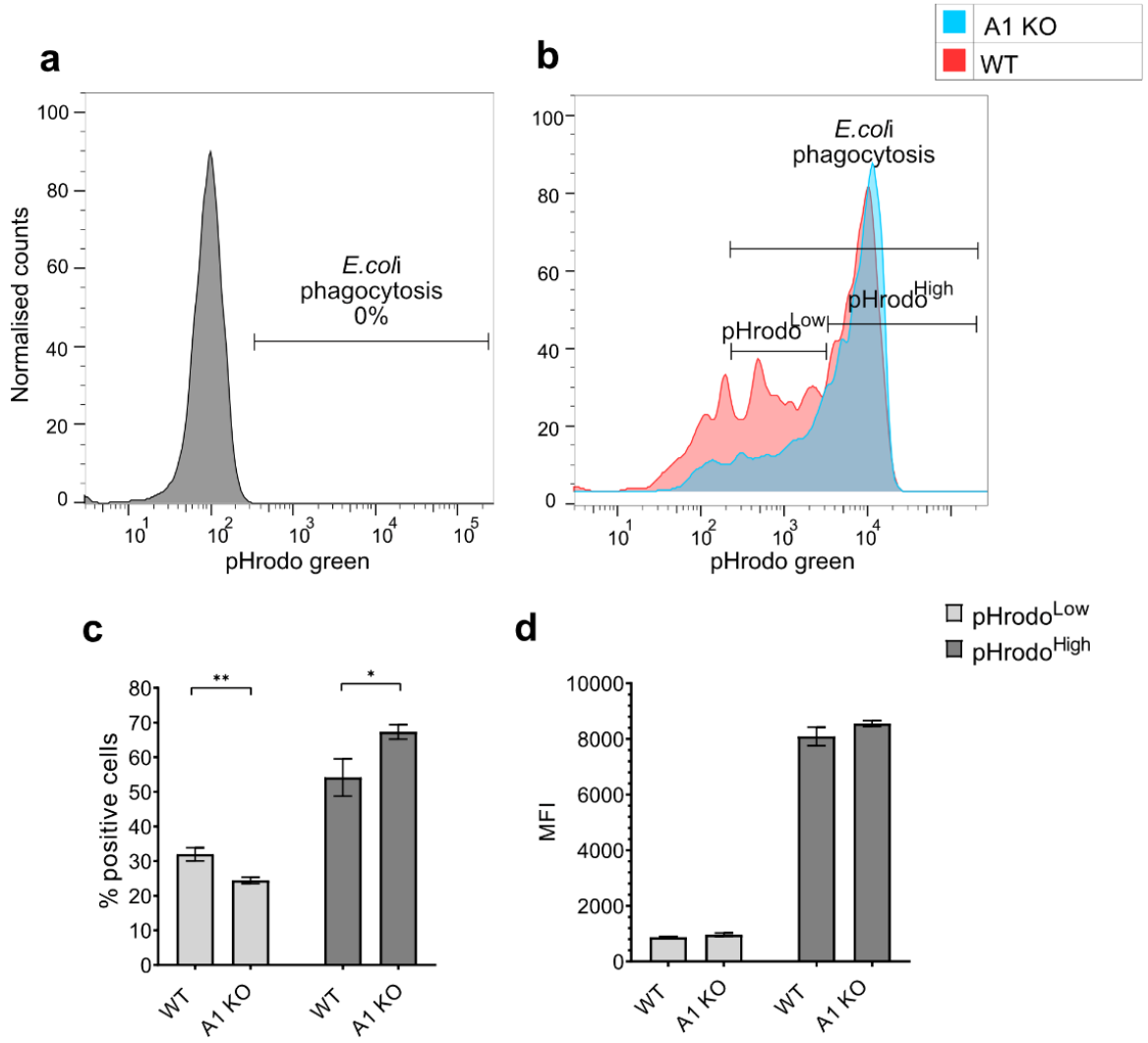


Figure 21. APOBEC 1 regulates phagocytosis of the gram-negative bacteria E.coli.

**a**. Control untreated WT RAW 264.7 fluorescence histogram; one representative replicate shown. **b**. Representative fluorescence intensity after phagocytosis of WT cells in red and A1 KO cells with pHrodo green labelled E. coli particles (n=3) **c**. Percentage of cells positive for high or low pHrodo green signal. **d**. Mean fluorescence intensity (MFI) of pHrodo$^{Low}$ and pHrodo$^{High}$ fractions in WT and A1 KO RAW cells (n=3). Error bars represent standard deviation; statistical significance was obtained with an unpaired t-test with Welch's correction. * = $p \leq 0.05$

A1 KO cells also have an increased phagocytosis index with *E.coli* bioparticles (Figure 21). The WT cells can be seen to have distinct populations that ingest varying numbers of bacteria, as seen by the number of smaller peaks in Figure 21 b. The A1 KO cells have a clear tendency to phagocytose more *E.coli* particles than the WT cells (67.3%) (Figure 21 c). The A1 KO cells do not show the distinct peaks associated with different number of bacteria in the pHrodo$^{Low}$ range (Figure 21 b). In the pHrodo$^{High}$ range A1 KO cells have a slight not statistically significant increase in the MFI, (Figure 21 d).

Taken together the data indicates that the phagocytosis phenotype in A1 KO macrophages stems both from an impact on phagosomal pH and the uptake on the number of particles and is independent of the gram-negative or positive status of the bacteria. The decreased protein levels of *Cybb* could help to account for the decrease in pH levels as during its enzymatic activity, CYBB consumes protons in the phagosome lumen (Savina *et al.*, 2006). Mass spectrometry data has shown that the protein levels of the scavenger receptor, COLEC12, whose transcripts are edited, is upregulated in KO cells (Figure 15). COLEC12 promotes binding and phagocytosis of bacteria and yeast (Cheng *et al.*, 2021) and could contribute to the increased bacterial uptake observed.

### 4.4.2 Validation of phagosomal pH

pHrodo fluorophore fluorescence intensity is proportional to the pH of the surroundings, increasing in fluorescence with decreasing pH. This quality can help quantify intracellular pH when the fluorescence intensity is calibrated to cells exposed to buffers of known pH. To validate that pH is a factor in the differences in phagocytosis seen in the previous section, this pH property was used and compared to standard curves generated for WT and A1 KO cells phagocytosing either *E.coli* or *S.aureus* bioparticles. Cells were incubated for 1 hour with the bioparticles, then washed thoroughly and incubated with buffers of pH 4.5, 5.5, 6.5 and 7.5 with 10 µM of Valinomycin and 10 µM of Nigericin (which form membrane pores allowing the buffer to equilibrate across the membranes) before measuring fluorescence with a plate reader. The generated standard curves were used to determine the luminal pH of phagocytosis assays performed in parallel to the pH calibration. While similar approaches to this have been used in the past to measure

luminal pH (Savina *et al.*, 2006; Canton *et al.*, 2014), in my hands, this process has one caveat that renders the measurements only an indication of relative pH and not absolute pH. Namely, bacteria bioparticles could be seen attached to the outside of the macrophages or remain attached to the cell surface or well even after extensive washing (Figure S **8**). As a result, pH values obtained from the standard curves represent overestimations of the true pH, which is likely lower than what is recorded. Nevertheless, relative differences in pH levels can be determined. Both *E.coli* and *S.aureus* A1 KO RAW cells exhibited lower phagosomal pH than the WT cells ( Figure 22). Luminal pH was 0.44 pH units lower in A1 KO cells than WT cells (Figure 22 left). There was a more significant difference in pH in cells that phagocytosed *S.aureus* bioparticles, with the A1 KO having a pH of 1.56 units lower (Figure 22 right). These data match the observations seen with the flow cytometry assay where the shift in peaks with *E.coli* between WT and A1 KO was minimal (Figure 21 b) in comparison to the shift in fluorescence peaks with *S.aureus* (Figure 20 b).

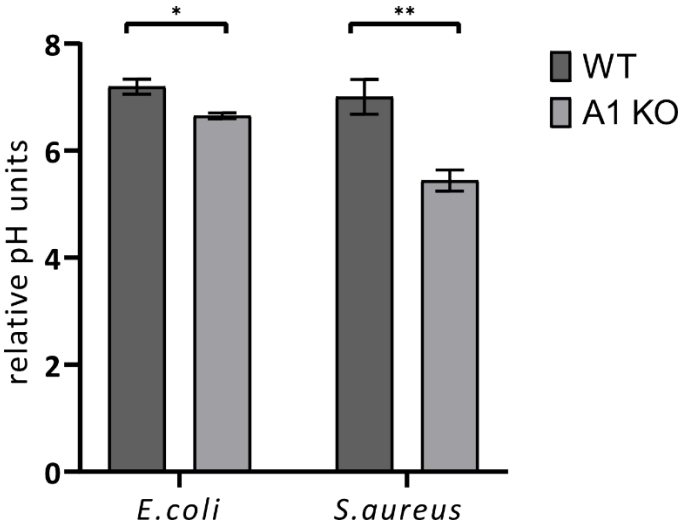


Figure 22 APOBEC1 regulates phagosomal pH.

Relative pH was determined by comparing fluorescence intensity during phagocytosis assay to a standard curve generated by replacing supernatant with buffers of known pH. n=3. Statistic derived from unpaired T test with Welch's correction. * $p \leq 0.05$ ** $p \leq 0.01$

### 4.4.3 Validation of differences in the number of bacteria ingested

To verify that different numbers of bacteria were ingested by WT and A1 KO macrophages, cells were incubated with an MOI of 100 of either *E. coli* or *S. auerus* for an hour, then stained with DAPI and images were taken with a Zeiss cell observer. The number of bacteria per cell was counted in 6 images from 3 well replicates with Fiji with the help of a macro kindly provided by Dr. Damir Krunic. Bacteria that were not ingested could be seen in the phase-contrast images and were also stained at low intensity by DAPI (Figure 23 a). A1 KO ingested on an average more significant number of particles per cell both of *S. aureus* (14.9 vs 28.2) (Figure 23 b top) and *E. coli* (13.9 vs 18.8?) (Figure 23 b bottom).

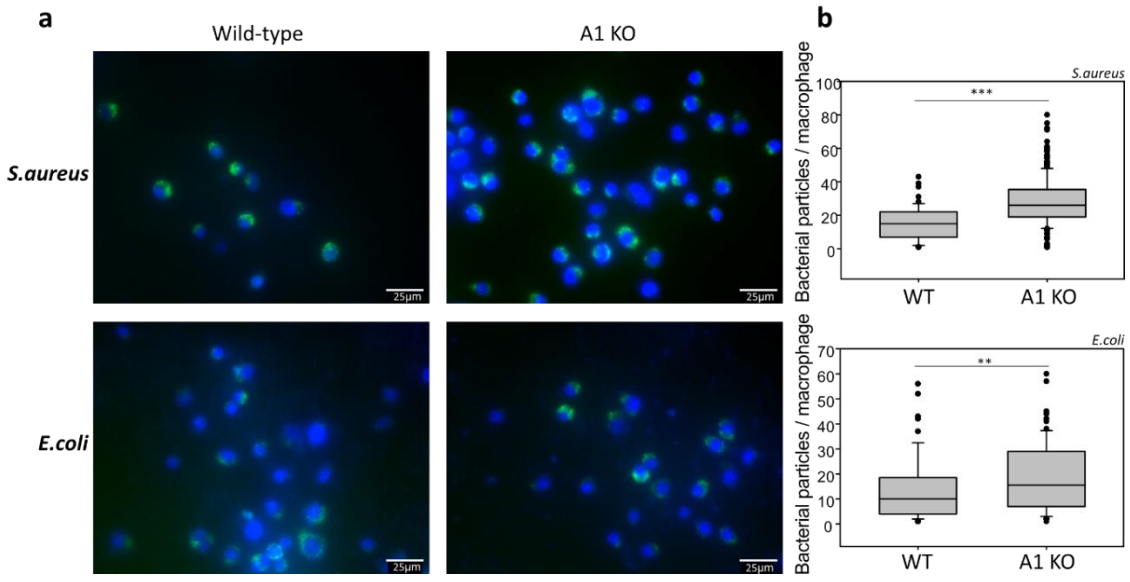


Figure 23. APOBEC1 regulates the number of bacterial particles phagocytosed.

WT and A1 KO macrophages were incubated with an MOI of 100 of *S.aureus* **a**. top and *E.coil* **a**. bottom and imaged with a cell observer. 6 snapshots were taken of each condition, and images were analysed with Fiji, and fluorescent bacterial particles were counted **b**. Box plots of the number of bacteria per macrophage. Shows median and percentile range. P values calculated with Mann-Whitney rank-sum test. ** p <0.01, *** p <0.001

## 4.5 APOBEC1 and macrophage activation markers

When macrophages receive a proinflammatory stimulus, such as exposure to bacterial PAMPs, various activation associated surface markers are upregulated. The pathways that become activated when such a stimulus is received have multiple edited targets, which may change the activity of macrophages and their surface markers. Knockdown of A3A in human macrophages is associated with the downregulation of surface markers such as CD80 and CD86 (Alqassim *et al.*, 2020). The activation markers, CD80, CD86, CD40 and MHC II, in stimulated ( 24 hours of 100ng/ml of LPS and 100units/ml IFNγ) and unstimulated WT and KO RAW cells were assessed by flow cytometry. All four of these surface markers are either T cell co-stimulatory molecules or play a role in antigen presentation to T cells (Van Gool *et al.*, 1997; Slavik, Hutchcroft and Bierer, 1999; Klein *et al.*, 2014).

CD86, CD40 and MHC II showed no significant differences between treated and untreated cells (Figure 24 b, c & d). CD80 showed considerable variability in relative increase after stimulation between experiments, but in each WT, cells showed a significant increase from mock-treated cells, whereas the A1 KO showed only a very slight increase, which was significantly lower than the WT cells (Figure 24 a). Downregulation of CD80 was also observed in human cells with the absence of A3A. A1 is affecting signalling pathways of macrophages that lead to changes in upregulation of T cell co-stimulatory molecules upon activation.

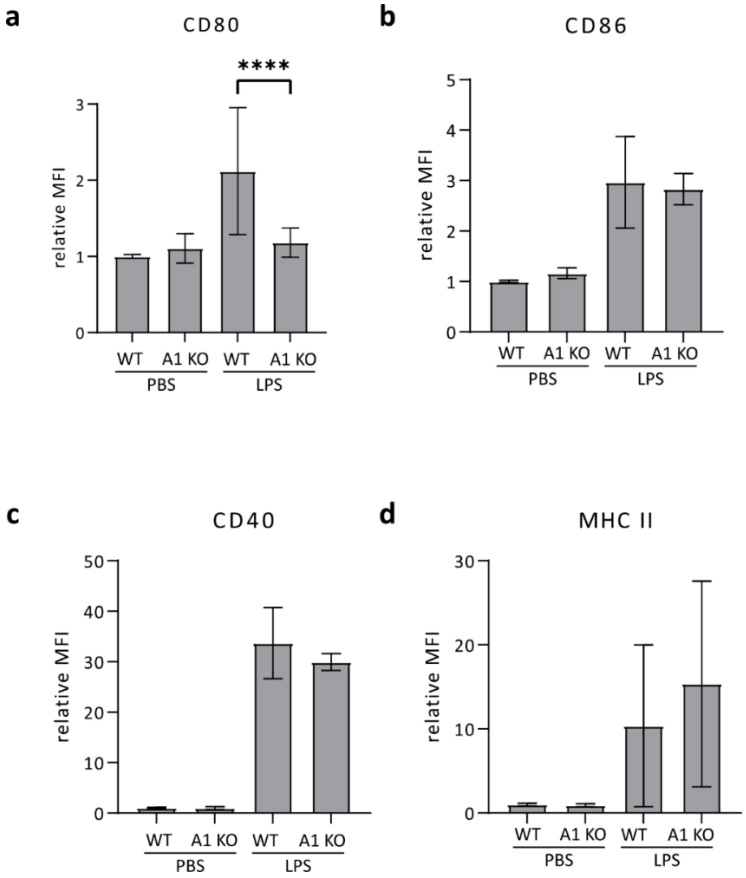


Figure 24 CD80 is not upregulated in activated A1 KO RAW cells.

Summary bar graphs of the relative mean fluorescence intensity (MFI) of inflammatory molecules CD80 **a**, CD86 **b**, CD40 **c**, and MHC-II **d** after twenty-four hours of LPS-stimulated or control PBS treated WT and A1 KO RAW 264.7 The results are illustrated as the mean ± standard deviation of the MFI relative to PBS treated WT cells from respective independent experiment; CD80 and CD86 data come from 4 independent experiments n = 12. CD40 and MHC II from 2 independent experiments n =6. MFI relative to WT PBS treated from same experiment. Analysis done with Mann-Whitney test ****$p < 0.0001$

# 5 Discussion

Macrophages are terminally differentiated cells originating from self-renewing populations in the tissues and present from early embryonic development or develop from bone marrow monocytes (Gessain, Blériot and Ginhoux, 2020). In the tissues, macrophages have immune and non-immune functions, including protecting tissue integrity by eliminating pathogens and damaged cells, maintaining homeostasis, and activating the adaptive immune system (Fujiwara and Kobayashi, 2005; Murray and Wynn, 2011; T. a. Wynn, Chawla and Pollard, 2013). Macrophages polarise and occupy a spectrum of activation states by integrating multiple environmental cues (Xue *et al.*, 2014; Glass and Natoli, 2016). The different polarisation states affect the phenotypes and functions of the macrophages, and their plasticity is truly remarkable. The genetic background, location, tissue and inflammatory state all shape identity and diversity of macrophages. RNA editing is a potential mechanism that generates some of the cellular heterogeneity.

The level of RNA editing in a specific position is not 100%, meaning that a mixture of both edited and unedited transcripts exists in the same cell. The level of editing in a specific cell can differ from the level of editing in its neighbours (Harjanto *et al.*, 2016). Therefore, it is possible that RNA editing can generate heterogeneity within the same population and contribute to the plasticity of macrophages. These differences could increase the probability that the immune system will have a cell in the same population best suited to handle an environmental variability or pathogen; this is the same concept as the benefit of genetic diversity for the long-term survival of a species. Why the same cells differ in editing levels within the same cell population in the same location is unknown. The spatial orientation of a cell, the identity of its neighbours and gradients of signalling molecules the cell is exposed to could all be factors in the observed differences.

The question that needs to be answered is what functional relevance does heterogeneity of C-to-T editing have to macrophages, and how are these phenotypic changes achieved? Most editing events occur in 3'UTRs of transcripts suggesting that they affect stability, translation, or localisation (Kumar and Mohapatra, 2021). This thesis has

focused on the functional consequences of editing on the transcript and the dynamics of editing during mouse macrophages responses to activation.

## 5.1 Temporal dynamics of C-to-U RNA editing

Macrophage activation is a process regulated both in time and space and on multiple levels; feedback loops, changes in translation, epigenetic modifications and the timely turning on and off of transcription (Gao *et al.*, 2002; Kitamura *et al.*, 2008; Ceppi *et al.*, 2009; Vyas *et al.*, 2009; Hald *et al.*, 2012; Schott *et al.*, 2014; Das *et al.*, 2018). Phagocytosis and trans-endothelial migration are affected by A1 in BMDMs ( the first increasing the second decreasing in the A1 KO) (Rayon-Estrada *et al.*, 2017), which are processes determined by the activation state of macrophages (Cui *et al.*, 2018; Yunna *et al.*, 2020). This connection first led me to suspect that C-to-T editing, like everything else during activation, would be regulated by or be itself a regulator of activation. We often monitor editing through Sanger sequencing of known sites and frequently use *B2m* as an editing marker because it is commonly edited in many cell types (Rosenberg *et al.*, 2011; Blanc *et al.*, 2014; Rayon-Estrada *et al.*, 2017). During a routine experiment looking at *B2m* in stimulated and unstimulated macrophages, I observed a consistent phenomenon: a small but reproducible drop in the percentage of editing at Chr2:12215902 from approximately 48% to 39%.

With this impetus, due to the plethora of publicly available data on stimulated macrophages, one dataset with LPS, IL 14 and IL3 stimulated BMDMs was selected to help address the question of whether editing remained constant or if it changed, as this would be suggestive of the regulation (Das *et al.*, 2018). This specific dataset was chosen due to the availability of RNA -sequencing from A1 KO BMDMs from the same genetic background (necessary for the accurate filtering out of SNPs). The data also contained at least three replicates (to reduce the probability of false-positive edited sites), multiple stimulation time points, and a sufficient sequencing depth.

### 5.1.1 Dynamics in BMDMs

The BMDM dataset was aligned, editing was determined by REDItools2, filtered based on the A1 KO BMDMs and normalised and global C-to-T events plotted. This revealed that after an hour of stimulation, there was a significant spike in C-to-T levels followed by a drop back to levels not significantly different from the unstimulated controls (Figure 4). Unfortunately, the available A1 KO BMDM RNA-seq originated only from resting macrophages. As a result, transcriptional changes in the stimulated macrophages are absent in the A1 KO reference. Consequently, some editing sites were missed, and false-positive C-to-T changes could not be removed due to the lack of an appropriate reference. The low sequencing depth of the dataset, the extreme filtering requirements, and the errors introduced by lack of stimulated KO BMDMs as a reference contributed to the low numbers of C-to-T events detected and could mask changes that occur at the global level. Nevertheless, the data suggest editing is temporally regulated.

Zooming in from a global editing view to specific edited positions revealed that editing percentages in 67 positions of 29 transcripts were statistically significantly fluctuating (Table S 1). The changes in editing levels were dependent on the stimulus type; percentages were different with proinflammatory stimulation by LPS or with anti-inflammatory cytokines IL 4 or IL 13 (Figure 5). Most positions showed a decrease in editing over time, and different positions from the same transcript displayed the same trend. The most prominent member of this list was *Cybb* (also called gp91phox or gp91 and is a subunit of NADPH oxidase, NOX2) with 20 positions. *Cybb* and *Spp1* (Secreted phosphoprotein 1 or known as osteopontin), belong to a small cluster of transcripts whose trend in editing over time involves an increase in percentage after the first four hours of stimulation rather than the decrease displayed by most other transcripts (Figure 5 a-c & g-i).

NOX2 is an important enzyme in the production of ROS. ROS supports the antimicrobial function of phagosomes (Winterbourn and Kettle, 2013), promotes the preservation of antigens for presentation (Mantegazza *et al.*, 2008; Kotsias *et al.*, 2013; Allan *et al.*, 2014) and acts as a signalling molecule within the cell (Iles and Forman, 2002). SPP1 is a complex protein with a long list of associated functions dependent on the

expressed splice variant, phosphorylation state and the cellular and environmental context (Rittling, 2011). These functions include cell-matrix interaction promoting migration and extravasation, induction of inflammatory cytokine production and phagocytosis (Blom *et al.*, 2003; Kourepini *et al.*, 2014; Zhang *et al.*, 2017). NOX2 also affects *Spp1* through its superoxide production, which is eventually converted into hydrogen peroxide, which regulates both the transcription and translation of *Spp1* (Lyle *et al.*, 2014).

An over-representation analysis and systematic search of the literature revealed that most of the 29 transcripts are either involved in the endo-lysosome-phagosome pathways or actin cytoskeleton rearrangements for migration, phagocytic cup formation or vesicle transport (Figure 6 & Table 1). Finding these pathways enriched is not a surprise, given that editing targets these pathways in BMDMs (Rayon-Estrada *et al.*, 2017). However, significance and enrichment levels are higher for transcripts with dynamic editing changes.

Due to the changes in editing at a global and positional level, it was hypothesised that some transcripts would show changes in the number of C-to-T events per 3'UTR. However, this data processing was not fruitful in the BMDM dataset, likely due to the limitations already discussed concerning the dataset; sequencing depth, filtering and the lack of a proper stimulated knockout control.

### 5.1.2 Dynamics in RAW 264.7 cells

RNA-sequencing with better coverage and appropriate stimulated knockout controls was necessary to obtain a more in-depth look at editing dynamics. The switch was made to RAW264.7 cells, a mouse macrophage-like cell line, because of their high A1 levels, their greater homogeneity in comparison to primary cells, which would help maintain more consistent results and their relative ease of genetic manipulation can. Two A1 KO RAW cell clones were generated by targeting exon 5 with CRISPR-Cas9 (

Figure 8). KO and WT cells were untreated or treated with LPS and IFN-γ, replicating work done with the BMDMs but with an additional time point of 2 hours. The cells were sequenced, editing was called, and the same type of comparisons were made as were described for the BMDM dataset.

A more distinct picture of global editing changes was obtained in the RAW cells, likely due to the far greater number of detected C-to-T events (Figure 9). A jump in the number of events occurs in the first hours, followed by a gradual decrease over the remaining time points (Figure 9 a). A1 expression also decreased; however, the change was minor and not statistically significant (Figure 9 b). The change in A1 levels based on trimmed mean of M values (Robinson and Oshlack, 2010) was not statistically significant, and the difference between the 4 hour time point and 24-hour time point appears to be a slight increase in levels whereas, the C-to-T levels drop between the 4 hours and 24-hour time point. This data should be corroborated by RT-qPCR, which was not done at the time this work was written.

Looking at editing level variation at specific positions showed 85 significantly changing positions (Table S 2). Although the transcripts are in similar pathways, there was a minor overlap between the RAW cell and BMDM positions. The filtering steps to eliminate false edited positions are strict and if a position is included in the analysis depends on how well covered they are in a specific library set. Therefore, it is to be expected that positions included when comparing one dataset to another will vary. A minimum coverage threshold of at least 50 in two out of three replicates was necessary in order to be able to compare the percentage of editing between the time points (Harjanto *et al.*, 2016). The overall trend in these changing positions is similar to the global change in C-to-T levels, an initial increase followed by a steep decrease.

The positions with editing changes were once more in transcripts in the endo-lysosome-phagosome axis. Of note is the presence of multiple subunits of the large protein complex that forms the vacuolar ATPase (*Atp6ap1*, *Atp6ap2*, *Atp6v1a*, *Atp6v1c1*), an H+ transporter responsible for the acidification of vesicles (Marshansky and Futai, 2008). There are multiple editing sites in many of these subunits, and additional subunits are edited but do not have statistically significant fluctuating editing.

With the increase in depth of the RAW cell RNA-seq and KO control, it was possible to obtain a picture of the number of editing events per transcript (Figure 11). Transcripts that had a differential number of editing sites fell into one of four groups. Cluster 1 and Cluster 4 have the same pattern that follows the global C-to-T levels, increasing the number of editing sites in early time points followed by a decrease (Figure 11 b & e). Cluster 2 exhibited less of an increase at early time points and a decrease to almost no editing at a late time point (Figure 11 c). Cluster 3 stands out as it shows the opposite effect to all the others; editing increases over the time course.

Editing targets and transcripts that show an increase and decrease in editing levels are summarised in Figure 25. Pathway analysis once more pointed to strong enrichment of editing in phagocytosis processes, enriched to an even greater extent in transcripts with differential editing (Figure 12). Enrichment in these pathways was not seen in the ADAR1 catalysed A-to-I editome in RAW cells (Table S 4), which indicates that the enrichment is not due to the cells simply being macrophages whose primary function is phagocytosis.

An attempt was also made to determine editing changes in the RAW cell also by M2 polaristion. However, treatment of RAW 264.7 cells with IL-4 yielded no increase in markers of M2 activation. Therefore, IL-4 activation was no longer pursued and is hence not shown here. IL-4 has been used to stimulate RAW cells by others successfully (He *et al.*, 2011; Sheldon *et al.*, 2013), which suggests a fault existed with the IL-4 preparation used.

## 5.2 Regulation of phagocytosis and antigen presentation by APOBEC1

Phagocytosis is an essential macrophage function, which is essential for clearance of pathogens, tumour cells, apoptotic cells and debris and at the same time process relevant antigens and presents them to activate the adaptive immune system (Arandjelovic and Ravichandran 2015; Hirayama, Iida, and Nakase 2018). Since phagocytosis related pathways are enriched for editing, for transcripts that show differential editing and a phenotype in BMDMs from KO mice was previously observed, this function of macrophages was further studied to elucidate the roles of editing.

Maturation of phagosomes and antigen processing are carefully regulated and timed. The phagosome maturation involves decreasing pH levels and the introduction of different lysosomal enzymes that function at their optimum at these low pH (Levin, Grinstein and Canton, 2016). However, the decreasing pH and proteolysis can be detrimental for antigen processing as the antigen becomes over digested or can change how an antigen is processed and alongside which enzymes are present in the lumen determines which epitopes will be presented (Lennon-Duménil *et al.*, 2002; Delamarre *et al.*, 2005; Mantegazza *et al.*, 2008; Allan *et al.*, 2014). Therefore, depending on the location, genetic background and polarisation state of a macrophage, the timing and level of acidification is highly regulated (R. A. Russell *et al.*, 2009).

### 5.2.1 pH and antigen presentation

The two parts of phagocytosis, mechanisms that acidify phagosomes and antigen processing, are edited oppositely. Editing in antigen processing and presentation pathway machinery increases over time with M1 polarisation with LPS (Figure 11 cluster 3 & Figure 25) and decreases in phagosome maturation and acidification components (Figure 25 red and blue boxes, respectively).

*Cybb*, the gp91 subunit of the NOX2 (Figure 25), is differentially edited both at the level of the number of edited sites (Figure 11 cluster 3) and on the positional level (Figure 10). Signalling through TLRs by PAMPs results in activation of NOX2 and the formation of an active enzymatic complex (Panday *et al.*, 2015). NOX2 assembles on membranes that will become the phagosome already at the phagocytic cup stage. Phagosomes interact with vesicles from the endocytic and lysosomal pathways, the MHC I and MHC II compartments (multi-vesicular bodies), and the endoplasmic reticulum (D. G. Russell *et al.*, 2009). Superoxide is introduced into the vesicle lumen by the enzymatic activity of the activated NOX2 complex (Panday *et al.*, 2015). The generation of superoxide and its conversion in the phagosome luminal space into hydrogen peroxide consumes protons, increasing the pH and is characteristic of early stages of M1 type macrophages (Canton et al. 2014). In humans, mutations in NOX2 subunits can result in Chronic granulomatous disease (CGD) which is characterised by frequent and life-threatening bacterial and fungal infections and inflammation (Singel and Segal, 2016). The excessive inflammation and the

increased susceptibility to various autoimmune diseases are due to increased proinflammatory activity and deregulation of inflammation resolution (Nauseef, 2019).

NOX2 negatively regulates proteolysis within phagosomes by both pH and pH-independent mechanisms. Lysosomal enzymes have optimal low pH values in which they function, and by using up protons, NOX2 can reduce their activity (Kotsias *et al.*, 2013). ROS can inactivate some enzymes by causing irreversible oxidation of cysteines, for example, on cathepsins (Rybicka *et al.*, 2010). The phagosomal redox state induced by NOX2 also reduces the phagosome ability to reduce disulphides. It is well established that decreased proteolysis in phagosomes is vital for antigen processing and presentation (Lennon-Duménil *et al.*, 2002; Savina *et al.*, 2006; Savina and Amigorena, 2007; Rybicka *et al.*, 2010). Both pH and proteolysis are essential for antigen presentation (Savina *et al.*, 2006; Mantegazza *et al.*, 2008; Kotsias *et al.*, 2013; Allan *et al.*, 2014).

The absence of A1 induced editing of Cybb resulted in a slight reduction in the protein levels of CYBB without affecting transcript levels (Figure 15 & Figure 16). In addition, the expression of other factors involved in the generation of ROS are suppressed in A1 KO RAW cells (Figure 13). Increased phagocytosis was previously observed in A1 KO BMDMs (Rayon-Estrada *et al.*, 2017), which led me to suspect that the increase in phagocytosis was due to a decrease in pH due to the lower levels of ROS production and CYBB. The A1 KO RAW cells also showed increased phagocytosis (Figure 19). In both cases, the phagocytosis assays were based on ingestion of pHrodo green labelled *S. aureus* bioparticles. pHrodo dyes are pH sensitive, and a lower pH would cause an appearance of increased phagocytosis. Decreasing the time and MOI of the phagocytosis assays and calibrating pHrodo fluorescence levels to a standard curve revealed that knockout cells had phagosomes with lower pH (Figure 20and Figure 21). This occurred with gram-positive *S. aureus*, 1.56 pH units lower and gram-negative *E. coli* , 0.44 pH units lower (Figure 22). The lower pH levels in the A1 KO cells are probably contributed to by the decrease in CYBB, leading to a lower enzymatic level of ROS production and fewer protons consumed in the process.

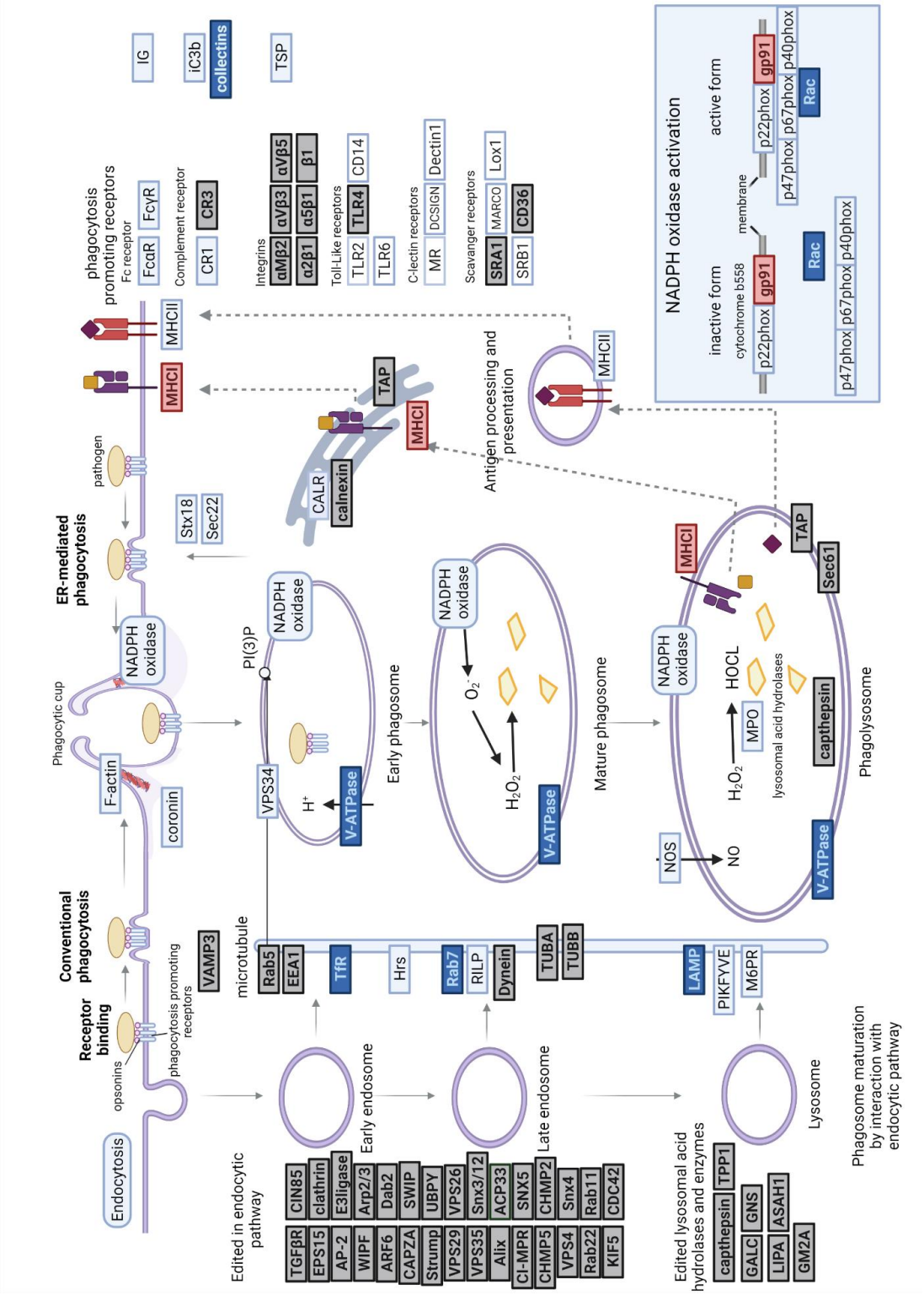
Endocytosis
Receptor binding
opsonins
phagocytosis promoting receptors
Conventional phagocytosis
VAMP3
F-actin
coronin
Phagocytic cup
NADPH oxidase
ER-mediated phagocytosis
pathogen
Stx18
Sec22
phagocytosis promoting receptors
Fc receptor
FcαR
FcγR
Complement receptor
CR1
CR3
IG
iC3b
collectins
TSP
Integrins
αMβ2
αVβ3
αVβ5
α2β1
α5β1
β1
Toll-Like receptors
TLR2
TLR4
CD14
TLR6
C-lectin receptors
MR
DCSIGN
Dectin1
Scavanger receptors
SRA1
MARCO
Lox1
SRB1
CD36
MHCII
MHCI
TAP
CALR
calnexin
Antigen processing and presentation
NADPH oxidase activation
inactive form
cytochrome b558
p22phox
gp91
membrane
active form
p47phox
p67phox
p40phox
Rac
microtubule
Rab5
EEA1
TfR
Hrs
Rab7
RILP
Dynein
TUBA
TUBB
LAMP
PIKFYVE
M6PR
PI(3)P
VPS34
H+
V-ATPase
Early phagosome
Mature phagosome
Phagolysosome
O2-
H2O2
HOCL
MPO
lysosomal acid hydrolases
capthepsin
Sec61
NOS
NO
Edited in endocytic pathway
Early endosome
Late endosome
Lysosome
Edited lysosomal acid hydrolases and enzymes
TGFβR
CIN85
clathrin
EPS15
E3ligase
AP-2
Arp2/3
WIPF
Dab2
ARF6
SWIP
CAPZA
UBPY
Strump
VPS26
VPS29
Snx3/12
VPS35
ACP33
Alix
SNX5
CI-MPR
CHMP2
CHMP5
Snx4
VPS4
Rab11
Rab22
CDC42
KIF5
TPP1
capthepsin
GNS
GALC
ASAH1
LIPA
GM2A
Phagosome maturation by interaction with endocytic pathway

Figure 25 Phagosome and endo-lysosomal pathways are enriched for editing by APOBEC1.

Phagocytosis begins with direct pathogen recognition or opsonin receptors such as complement receptor 3 (CR3). Recognition initiates signalling cascades that cause membrane F-actin modifications in the cell membrane-associated cytoskeleton and actin associated with vesicles of the endosome pathway. The membrane invaginates around the pathogen forming a phagosome. Fusions with vesicles from the endocytic pathway in coordinated stages introduce V-ATPase that acidifies phagosomes, NADPH oxidase that generates reactive oxygen species and hydrolytic enzymes. All these three processes can be deleterious and break down the pathogen. Exogenous proteins are cleaved, and the phagosome vesicles interact with the major histocompatibility complex I and II (MHC-I and MHC-II) compartments for loading and shuttling to the cell membrane for antigen presentation. Multiple transcripts for proteins involved in the acidification of phagosomes show a decrease in editing with macrophage stimulation (in blue).In contrast, transcripts involved in the production of ROS and antigen presentation, which raise pH and increase the efficiency of antigen presentation (respectively), show an increase in editing over time with LPS and IFN-γ stimulation (red). Proteins marked in grey are edited transcripts not determined to show differences in the number of editing events over time, although the percentage of editing per position may still be changing. Names do not indicate specific transcripts but represent all transcripts that form the specific complex or fall in the same group. A list of full protein names for the abbreviations can be found in section X. Figure I based on the KEGG phagosome pathway and generated with Biorender.com

It is more than likely that the observed change in pH is not due solely to the editing actions on *Cybb*. Multiple subunits of V-ATPase, which pumps protons into the lumen, are edited or differentially edited (Figure 10 & Figure 11 & Figure 25). There is also a significant increase in protein levels of the subunit ATP1A3 in the A1 KO cells (Figure 15). The V-ATPases are introduced to phagosomes through fusion with endocytic and lysosmal vesicles through docking enzymes (Kinchen and Ravichandran, 2008), which are also edited (e.g. Lamp1, Rab7, Rab5 see Figure 25). How editing affects these transcripts has not been investigated yet in this work. Fusion kinetics between the phagosomes and these vesicles could be enhanced by the absence of editing leading to faster and more prominent acidification. One method of investigating the kinetics of phagosome/endosome/lysosome fusion would be to use a Förster /fluorescence

resonance energy transfer (FRET) based assay (D. G. Russell *et al.*, 2009). The macrophages can be labelled with a hydrophilic acceptor fluorophore that will be endocytosed into the cells and become part of lysosomes. Then, the macrophages would be cultured with the bioparticles/beads labelled with a donor fluorophore that will be phagocytosed. FRET will occur once the compartments containing the two fluorophores fuse and are close enough to one another.

The actual phagosomal pH in this work was not measured, while others have previously used similar approaches to measure phagosomal pH by utilising a pH-sensitive dye; this was not successful here. These studies showed a swift drop in pH that was considerably lower than detected here (Figure 22, (Yates, Hermetter and Russell, 2005; Canton *et al.*, 2014)). The reason for the higher pH detected in this work was abundantly clear when visualising the cells (Figure S 8). Despite thorough washing of the assay plates, many bacterial particles remained attached to the well bottom and the surface of the macrophages. These non-internalised bioparticles have very low fluorescence in the neutral pH of the media and do not otherwise interfere with the phagocytosis assay. However, once a solution of known pH, with antibiotics that form membrane pores allowing the buffer to equilibrate the internal cell pH to the solution's pH, is added, all the bioparticles in the well will have the same fluorescence. Since the fluorescent value includes both internalised and non-internalised particles, this results in an overestimation of pH in the test wells. Naturally, as only internalised particles that have experienced pH drops in the lumen of phagosomes will give a signal in the test well, the signal from these wells will be lower. Published data involving similar assays did not indicate that this was an issue (Yates, Hermetter and Russell, 2005; Canton *et al.*, 2014). In my hands, this method only allows me to determine relative differences in pH between the WT and the KO rather than a more accurate absolute pH value.

It is possible that switching to different plate types would be sufficient to reduce the number of non-engulfed particles (3 different plate types were tested without a change in outcome) or to use the same components as other studies which were based on a similar concept but were not identical. One method involved IgG coupled carboxylated silica beads and labelled with pH-sensitive indicator fluoro-chrome carboxyfluorescein succinimidyl ester (SE) (Yates, Hermetter and Russell, 2005). Yates et

al mixed these beads with BMDMs in cuvettes and continuously measured changes in pH. pH was determined by comparison to a standard curve. pH values dropped from 7.5 to a minimum of 5 within the first 10 minutes of the experiment and then remained at this level – this is an expected result based on current literature. The beads are possibly not as 'sticky' as the bacterial bioparticles, so they did not attach to the vessel walls. I suspect that some number of beads would be bound to the macrophage cell membrane through FcRγ receptors to some degree, so the pH drop may also be underestimated in this system. Beads, however, are not bacteria, and the receptors and signalling engaged when the bacteria are directly phagocytosed versus through FcRγ receptors will differ. It is clear from Figure 20 and Figure 21that the pH and phagocytosis dynamics with different types of bacteria are different. Canton et al had another similar approach with pH-sensitive fluorescently labelled zymosan (Canton *et al.*, 2014).

Exogenous proteins are proteolytically cleaved into oligopeptides of 15-24 amino acids for loading onto MHC-II and presentation to CD4+ (Allan *et al.*, 2014). Exogenous peptides can also be directed towards the MHC-I compartment and be cross-presented to CD8+ T cells (Neefjes *et al.*, 2011). Peptide proteolysis is controlled in the endo-phagosome vesicles, and too much proteolysis can lead to over-digestion of the oligopeptides, decreasing presentation efficiency. Control of proteolysis is critical for correct APC activity and is regulated by the phagosomal pH (Delamarre *et al.*, 2005, 2006). Antigen cross-presentation is the forte of DCs and macrophages are less efficient APCs; nevertheless, they can productively present or cross-present and activate T cells (Muntjewerff, Meesters and van den Bogaart, 2020). A potential reason for the decreased efficiency of macrophages as APCs compared to DCs is that they have a twenty-to-sixty-fold higher level of proteolysis in phagolysosomes (Steinman and Swanson, 1995; Lennon-Duménil *et al.*, 2002; Delamarre *et al.*, 2005).

The data shown in this thesis suggests that APOBEC1 exerts control on antigen processing and presentation in multiple ways:

1) APOBEC1 increases CYBB that increases the pH, and at the same time decreases the V-ATPase protein levels preventing excessive acidification regulating proteolysis (Figure 15).

2) APOBEC 1 targets transcripts involved in the docking and fusion of endosomes and lysosomes and potentially delays maturation and excessive pH decrease and introduction of lysosomal enzymes (Figure 25).
3) APOBEC1 targets the lysosomal enzymes directly. Lack of editing of cathepsin S results in reduced protein levels (Figure 15). The regulation of which enzyme is present where and how much and how active it is affects what epitopes are generated (Delamarre *et al.*, 2005).
4) APOBEC1 also edits and reduces the expression of many proteins that are responsible for the loading of antigens and presenting them. Editing has also affected protein levels; H2-L and TAP2 are decreased in A1 KO (Figure 15). TAP2 forms part of a transporter associated with antigen processing delivering antigens to the MHC-I loading compartment, where they are assembled onto MHC-I by proteins such as calreticulin and calnexin (which is also edited see Figure 25) (Diedrich *et al.*, 2001; Blum, Wearsch and Cresswell, 2013).

I suggest that A1 via editing and indirect means is a previously undescribed layer of spatiotemporal control of the local phagosomal redox state and components of antigen presentation with functional consequences. The changes of pH were studied in this work, but the effects on antigen presentation remain to be studied. It is highly likely that due to the decreased levels of MHC-I that A1 KO macrophages would have a decreased ability to stimulate T cells which co-culture experiments can determine. Another avenue for further research of both presentation through MHC-I and MHC-II is the potential regulation that A1 can elicit on the presented peptide repertoires. Superoxide generated by NOX2 regulates hydrolytic enzymes in the lumen, affecting antigen processing and which peptides are generated for T cell presentation (Allan *et al.*, 2014). Editing could influence the enzymes through NOX2, and by directly targeting them. The regulation of which enzyme is present where and how much also affects what epitopes are generated (Delamarre *et al.*, 2005). It would be interesting to study the peptide repertoires that A1 KO macrophages can produce compared to WT cells. Although the study of the peptides onto MHC molecules is not trivial, it is possible to pull down MHC molecules and determine the loaded peptides through mass spectrometry (Caron *et al.*, 2015).

B2m is one of the subunits that makes the MHC-I receptor present on the membrane of nearly all cells (Strominger *et al.*, 1987). *B2m* shows the opposite tendency in the number of editing events, a decrease in editing, compared to the increase of *H2-L* and *H2-D*. This observed inconsistency could result from two factors; 1) the effect of editing on the B2m transcript is different 2) The other functions of *B2m* dictate how it is regulated. B2m also has antibacterial activity against *Listeria monocytogenes, S. aureus, Proteus vulgaris*, and *E. coli* (Kim *et al.*, 2012). A fragment of B2M is shed from cells and acts as a monocyte chemoattractant that enhances *S. aureus* phagocytosis (Chiou *et al.*, 2016). The antimicrobial activity is pH-dependent and is enhanced by low pH, making editing changes similar to other antimicrobial factors rather than MHC-I. Early time points in phagocytosis show low levels of editing in transcripts involved in ROS production and antigen processing which require higher levels of pH (Savina *et al.*, 2006; Canton *et al.*, 2014).

pH was not the only factor contributing to the increased phagocytosis in the A1 KO RAW cells; flow cytometry and visualisation by microscopy indicated that the number of internalised bacteria in the KO was higher (Figure 20 & Figure 21). Among the edited transcripts are actin remodelling proteins and phagocytosis receptors that could play a part in the increased bacterial digestion (Figure 25). *Colec12* is a differentially edited class A scavenger receptor that binds to and promotes the phagocytosis of gram-positive and gram-negative bacteria (Thomas *et al.*, 2000; Amie *et al.*, 2007; Whelan *et al.*, 2012) and has higher protein levels in A1 KO cells (Figure 15). However, other scavenger receptors are found in higher protein levels in the WT, such as CD36 and MCR1 . The final activity is a result of more than one factor within the cells. Further study of the reason for the increased number of particles ingested is needed to elucidate more details; high-resolution imaging would assist in determining if there are changes in the attachment of bacteria and phagocytic cup formation in the KO cells.

CD36 is an excellent example of how editing in the same transcript has different consequences dependent on context and cell type(Blanc *et al.*, 2014; Rayon-Estrada *et al.*, 2017). In this work, protein levels of CD36 in the absence of A1 were lower with the same level of transcription (Figure 16). In BMDMs surface CD36 was higher in the absence of A1; however, in this study, CD36 showed the exact opposite effect and protein abundance

was greater in WT cells. CD36 is edited in the intestine and the liver and has decreased mRNA expression (Blanc *et al.*, 2014). The decreased levels did not correlate with a miRNA as CD36 editing destroyed a miRNA seed in the liver. Rayon-Estrada et al. also did not find a global connection between C-to-U editing and miRNA, although it is possible that in specific instances, it may be the case. CD36 has many different functions, including acting as a PRR or a fatty acid translocase in the intestinal tract (Febbraio, Hajjar and Silverstein, 2001b; Baranova *et al.*, 2008). CD36's many functions likely contribute to the differences in protein abundance and whether the expression is altered due to A1 as it would be regulated differently depending on the context; genes expressed in the particular cell and the environmental cues.

### 5.2.2 Inflammatory markers

M1 macrophages depend almost exclusively on glycolysis for energy demands and forgo oxidative phosphorylation (O'Neill and Pearce, 2016). Oxidate phosphorylation is more characteristic of M2 macrophages, and inducing oxidative phosphorylation in M1 macrophages tends to push them towards an M2 phenotype (Vats *et al.*, 2006; Rodríguez-Prados *et al.*, 2010). A glycolysis assay was not performed during this work; however, the glycolic state of the macrophages could be assessed by assays such as the SeaHorse Glycolytic Stress assay, which was done with a knockdown of A3A in human macrophages. Human macrophages do not express A1, but they do express RNA editors that are not expressed in mouse cells, A3A and A3G.

Knockdown (KD) of A3A increased glycolysis and RNA sequencing showed enhanced pyruvate metabolism and glycolysis-gluconeogenesis(Alqassim *et al.*, 2020). In the A1 KO macrophages, a greater reliance on glycolysis also seems to be apparent in M1 macrophages as oxidative phosphorylation is suppressed (Figure 14 c). The similarities between the pathways affected by the loss of A1 and the knockdown of A3A do not end there. The A3A knockdown also causes downregulation of antigen processing and presentation machinery, including MHC-II and MHC-I. There is overlap between some of the editing targets of A1 and A3A, and editing changes have been observed in both between resting and activated macrophages. Many parallels indicate that A1 and A3A perform related functions, one in mice the other in humans. Although, not everything is

identical, and one must consider that in the case of the human cells, they were knockdowns and not knockouts, and some editing still occurred, possibly also due to other A3s. KD of A3A resulted in decreased proinflammatory markers CD86 and CD80 and upregulation of CD206, a marker for M2 macrophage (levels were higher in M2 macrophages) (Alqassim *et al.*, 2020). Flow cytometry of macrophage activation markers in RAW cells showed decreased levels of CD80 after activation but not CD86 in the A1 KO cells (Figure 24a & b). Interestingly higher levels of CD206, also known as MRC1, were found in WT RAW cells at rest by mass spectrometry (Figure 15).

Expression of other proinflammatory markers was tested (such as of *Tnfa* and *Inos*), but they were not shown in this work. No differences were observed between WT and KO RAW cells. However, the housekeeping genes used for normalisation were later discovered to change between WT and the KO cells. Different, more stable housekeeping genes were used for all other RT-qPCR normalisation.

### 5.2.3 Are A1 KO macrophages proinflammatory?

Whether or not A1 KO macrophages have a more inflammatory phenotype remains unclear; on the one hand, there is the increased phagocytosis, increased reliance on glycolysis, downregulation of markers classically associated with anti-inflammatory macrophages and on the other hand, decrease in co-stimulatory proteins and potentially reduced production of reactive oxygen species. Nevertheless, the macrophages do not function normally, and what consequences this has *in vivo* have yet to be studied.

*Apobec1*$^{-/-}$ mice have increased levels of demyelination at old age in the central nervous system, potentially as a result of aberrant microglia activity and failure to clear myelin debris which is critical for neuronal health (Cole *et al.*, 2017a). Otherwise, *Apobec1*$^{-/-}$ mice appear to be normal. However, A1 KO macrophages at rest without a challenge also appear similar to WT macrophages at the surface level; to my knowledge, no inflammatory challenge given to these mice has been published. How they respond and recover from an infection will reveal potential consequences of the actions of A1 on the cells of the immune system.

## 5.3 Effects of editing on transcripts

The work presented in this thesis and data published by others (Blanc *et al.*, 2014; Rayon-Estrada *et al.*, 2017) suggests that editing for most transcripts does not affect transcript stability leaving changes on translation and intracellular localisation as possibilities. Rayon-Estrada et al. suggested that translational efficiency of specific transcripts was affected, while Blanc et al. claimed there was little overlap between protein abundance and editing. Each group studied editing in different cells, so differences can be expected to occur between them and that editing changes the translational efficiency of only a subset of transcripts. Armed with the potential that editing may change translational efficiency of some transcripts, polysome profiles of transcripts identified as edited and with differential protein abundance were performed (Figure 18).

### 5.3.1 Editing and translational efficiency

mRNA is often depicted in illustrations as a naked straight sequence; however, this is greatly misleading as they are usually covered by RBPs and have areas of secondary structure. The RBPs dictate a large part of what the mRNA life cycle will look like from its transcription to degradation (Glisovic *et al.*, 2008). These RBPs bind specific sequences all along the mRNA but are more abundant on 5' and 3' UTRs (Gebauer, Preiss and Hentze, 2012). 3'UTR contain regulatory elements that dictate stability, intracellular localisation and translation (Szostak and Gebauer, 2013). Regulation of translation contributes to the disparity commonly observed between the transcriptome and the proteome (Vogel *et al.*, 2010; Schwanhäusser *et al.*, 2011).

Translation initiation factors form a ribosome recruiting complex at the 5'UTR to begin translation at an initiator AUG codon. One of the scaffolding proteins, eIF4G, that forms this complex also binds to poly(A)-binding protein (PABP), which is bound to the poly(A) tail at the other end of the transcript (Wells *et al.*, 1998). The binding of eIF4G to PABP results in mRNA pseudo-circularisation. This loop is thought to increase the recycling of ribosomes back for additional rounds of translation (Szostak and Gebauer, 2013). It also allows RBPs bound to the 3'UTR to act on ribosomes on the other end of the transcript. Many RBPs target translation initiation but have also been shown to affect peptide elongation. Pumilio and FBF (PUF) proteins complexed with Argonaute (Ago) on 3'UTRs

can interact with the translation elongation factor eEF1A (Friend *et al.*, 2012). This interaction can inhibit the GTPase activity of eEF1A, which slows down translation elongation. Editing through changing the sequence and structure of 3'UTRs can therefore affect the binding of specific RBPs with different functions.

After mass spectrometry of macrophages at rest, 12 edited transcripts were found to have differential protein abundance between the WT and the KO. From these 12 options, two *Cd36* and *Cybb*, were selected for further analysis. These two transcripts were edited in RAW cells, BMDMs and the gastrointestinal system (Rosenberg *et al.*, 2011; Blanc *et al.*, 2014; Rayon-Estrada *et al.*, 2017); they have positions with high levels of editing, multiple edited positions, and in untreated macrophages, transcription levels are the same between WT and the KO (Figure 16), all factors in their selection.

Polysome profiling was carried out with *Cd36, Cybb* and a housekeeping gene control *Hprt* (Figure 17). From the lower protein abundance found in the mass spectrometry experiments, one would expect, if translation was affected, that mRNA from WT cells would be found at a greater frequency associated with more ribosomes. mRNA associated with the heavy polysome fractions is typically considered better translated. However, the opposite was observed; the unedited transcripts in the KO shifted towards the high polysomal fractions (Figure 17 left). After 2 hours of LPS stimulation, the shift was absent with the *Cybb* transcript but still present for *Cd36*. This was consistent with the levels of editing; *Cybb* experiences a decrease in editing rate at the positional level and a decrease in the number of events at 2 hours (Figure 7 & Figure 11). Editing in *Cd36* remains at the same level after 2 hours, the same as the polysome shift. Not all edited transcripts showed such a shift; transcripts that did not show differential protein abundance by mass spectrometry also exhibited no difference between the WT and KO mRNA distributions. Other edited transcripts that showed differential protein expression at the time of writing have not yet been tested but should be explored for changes in translational efficiency or effects on expression.

Lack of editing is not preventing translation or sequestering the mRNA as the differences in protein levels while they exist are minor. Editing in the 3'UTR could affect the binding of an RBP; either a translation enhancing RBP binds to the sequence or an

inhibitory RBP is removed, increasing the efficiency of translation. The binding to and scanning of 3'UTRs by A1 could also lead to the displacement of RBP that could alter translation. Without editing, elongation could be slower to a ribosome spending more time on the transcripts, increasing the probability of finding transcripts with a larger number of associated stalled ribosomes and the shift that I see in the polysomes that are not indicative of increased translation.

To better understand the translational dynamics of these two transcripts, additional experiments should be carried out. Treatment of samples with puromycin and then performing polysome profiles can help distinguish actively translating ribosomes from non-translating ribosomes (Chassé *et al.*, 2016). Puromycin disrupts the elongation phase of translation only in actively translating ribosomes and would cause mRNA that is being translated to shift to fractions that contain the monosomes. It was initially planned to perform the polysome profiles also with puromycin treatment; however, unexpected events prevented this from occurring before the writing of this thesis.

Several mass spectrometry-based methods can be used to determine the rate of formation of nascent polypeptides that usually involve short bursts of pulse labelling (Dermit, Dodel and Mardakheh, 2017). One of the most used methods is pulse Stable Isotope Labelling by/with Amino acids in Cell culture (p-SILAC), where cell culture media containing different weight amino acids isotopes is added for short periods before creating samples for mass spectrometry.

#### 1.1.1.1 *Mass spectrometry and polysome profiles after LPS treatment*

The relation between protein abundance and editing has so far been described here for resting macrophages and only for CD36 and CYBB. The other 12 edited proteins remain open to investigation and what happens to protein abundance after LPS stimulation. Do the differences in RNA editing levels observed at different time points result in changes to protein abundance? As indicated, a larger mass spectrometry experiment with the same LPS time points was also carried out but was not yet analysed during the writing of this thesis.

Data normalisation proved a challenge due to the extensive physiological and genetic changes that occur when RAW cells are activated. The assumptions of

quantification by MaxLFQ algorithm (Cox *et al.*, 2014) do not hold under the conditions of macrophage activation. While leading to better results, the alternative method using a proteomic ruler (Wiśniewski et al. 2014) had limitations, chiefly that the significance of proteins with small changes in abundance can be lost. Examples of this include CYBB and CD36, which have been shown by other methods to have differential abundance.

### 5.3.2 Editing and mRNA localisation

The work presented in this thesis showed that editing causes changes in translation in a subset of edited transcripts. This subset is small, and others have described the small overlap between editing and protein abundance in the liver and intestine (Blanc *et al.*, 2014). That leaves open the question of what editing does in all the other transcripts whose expression levels are not majorly affected? The potential answer to that is that it could regulate mRNA intracellular localisation.

The transport of mRNA around the cell is a highly regulated process. Changes in the localisation of mRNA could have serious effects on the function of a cell if a transcript is produced, but it is not translated at the right time and place in the cell. Restricting mRNAs and protein production to subcellular compartments or areas permits the cell to quickly respond to environmental stimuli as they do not have to be mobilised from distant cell locations(Xing and Bassell, 2013). This is particularly important in cells with distinct polarity, such as intestinal epithelial cells, neurons, or macrophages with leading and lagging edges when migrating (Moor *et al.*, 2017; Mofatteh, 2020).

RNA localisation was not discussed in this thesis, but during the work done here, a Master's student under my supervision, Laura Schoppe, was developing a method for single-molecule RNA visualisation where a difference in one base pair in the target could be distinguished. This would allow monitoring of transcripts and distinguishing edited and unedited transcripts even within the same cell.

Laura Schoppe produced protein and guide RNA for staining of RAW cells by a protocol similar to single molecule- fluorescence in-situ-hybridisation. The method is based on the RNA guided RNA targeting Cas13a (Shmakov et al., 2015) bound to GFP. Previous work with catalytically active Cas13a showed that target RNA sequences with

single-base differences could be distinguished from one another with the correct guide design (Gootenberg et al., 2017). While the method is promising, optimisation of the protocol is necessary as there is a considerable background signal. Other options for studying RNA moieties with single-base differences can also be pursued should it prove impossible to eliminate background noise sufficiently, for example, clampFISH (Rouhanifard *et al.*, 2018). clampFISH has an advantage over Cas13a-GFP in that there are rounds of amplification that increase the signal to noise ratio. Using Cas13a bound to GFP relies on a single molecule of GFP per transcript being sufficiently bright to give a signal; this may work for abundant transcripts for low abundant transcripts, the signal might be too weak.

# 6 Summary

In this thesis, I have used RNA-sequencing, ribosome profiling and quantitive proteomics to characterise the dynamics and consequences of A1 catalysed C-to-T editing in the mouse macrophage cell line RAW 264.7. A1 leads to changes in protein abundance of critical components that regulate phagosomal pH and antigen processing and presentation. This work identifies RNA editing as a novel mechanism of affecting protein levels and altering the behaviour of macrophages.

# 7 References


Ajami, B. *et al.* (2007) 'Local self-renewal can sustain CNS microglia maintenance and function throughout adult life', *Nature Neuroscience*, 10(12), pp. 1538–1543. doi:10.1038/nn2014.

Akashi K *et al.* (2000) 'A clonogenic common myeloid progenitor that gives rise to all myeloid lineages', *Nature*, 404(6774), pp. 193–197.

Alder, J.K. *et al.* (2008) 'Kruppel-Like Factor 4 Is Essential for Inflammatory Monocyte Differentiation In Vivo', *The Journal of Immunology*, 180(8), pp. 5645–5652. doi:10.4049/jimmunol.180.8.5645.

Allan, E.R.O. *et al.* (2014) 'NADPH Oxidase Modifies Patterns of MHC Class II–Restricted Epitopic Repertoires through Redox Control of Antigen Processing', *The Journal of Immunology*, 192(11), pp. 4989–5001. doi:10.4049/jimmunol.1302896.

Alqassim, E. *et al.* (2020) 'RNA editing enzyme APOBEC3A promotes pro-inflammatory (M1) macrophage polarization', *Biorxiv* [Preprint]. doi:10.1101/2020.03.20.988980.

Amie, E. *et al.* (2007) 'Scavenger Receptor-A Functions in Phagocytosis of E. Coli by Bone Marrow Dendritic Cells', *Experimental cell research*, 313(7), pp. 1438–1448. doi:10.1016/j.yexcr.2007.02.011.

Anant, S. *et al.* (2004) 'Apobec-1 protects intestine from radiation injury through posttranscriptional regulation of cyclooxygenase-2 expression', *Gastroenterology*, 127(4), pp. 1139–1149. doi:10.1053/j.gastro.2004.06.022.

Anant, S. and Davidson, N.O. (2000) 'An AU-Rich Sequence Element (UUUN[A/U]U) Downstream of the Edited C in Apolipoprotein B mRNA Is a High-Affinity Binding Site for Apobec-1: Binding of Apobec-1 to This Motif in the 3' Untranslated Region of c- *myc* Increases mRNA Stability', *Molecular and Cellular Biology*, 20(6), pp. 1982–1992. doi:10.1128/MCB.20.6.1982-1992.2000.

Babior, B.M. (2004) 'NADPH oxidase', *Current Opinion in Immunology*, 16(1), pp. 42–47. doi:10.1016/j.coi.2003.12.001.

Backus, J.W. and Smith, H.C. (1992) 'Three distinct RNA sequence elements are required for efficient apolipoprotein B (apoB) RNA editing in vitro.', *Nucleic Acids Research*, 20(22), pp. 6007–6014.

Baietti, M.F. *et al.* (2012) 'Syndecan–syntenin–ALIX regulates the biogenesis of exosomes', *Nature Cell Biology*, 14(7), pp. 677–685. doi:10.1038/ncb2502.

Bailey, J.D. *et al.* (2020) 'Isolation and culture of murine bone marrow-derived macrophages for nitric oxide and redox biology', *Nitric Oxide*, 100–101, pp. 17–29. doi:10.1016/j.niox.2020.04.005.

Bain, C.C. *et al.* (2014) 'Constant replenishment from circulating monocytes maintains the macrophage pool in the intestine of adult mice', *Nature Immunology*, 15(10), pp. 929–937. doi:10.1038/ni.2967.

Bajak, K. and Clayton, C. (2020) 'Polysome Profiling and Metabolic Labeling Methods to Measure Translation in Trypanosoma brucei', in Michels, P.A.M., Ginger, M.L., and Zilberstein, D. (eds) *Trypanosomatids*. New York, NY: Springer US (Methods in Molecular Biology), pp. 99–108. doi:10.1007/978-1-0716-0294-2_7.

Bamburg, J.R. and Bernstein, B.W. (2010) 'Roles of ADF/cofilin in actin polymerization and beyond', *F1000 Biology Reports*, 2. doi:10.3410/B2-62.

Baranova, I.N. *et al.* (2008) 'Role of Human CD36 in Bacterial Recognition, Phagocytosis, and Pathogen-Induced JNK-Mediated Signaling', *The Journal of Immunology*, 181(10), pp. 7147–7156. doi:10.4049/jimmunol.181.10.7147.

Barry, K.C. *et al.* (2013) 'IL-1α Signaling Initiates the Inflammatory Response to Virulent Legionella pneumophila In Vivo', *The Journal of Immunology*, 190(12), pp. 6329–6339. doi:10.4049/jimmunol.1300100.

Batzer, M.A. and Deininger, P.L. (2002) 'Alu repeats and human genomic diversity', *Nature Reviews Genetics*, 3(5), pp. 370–379. doi:10.1038/nrg798.

# References


Baysal, B.E. (2007) 'A Recurrent Stop-Codon Mutation in Succinate Dehydrogenase Subunit B Gene in Normal Peripheral Blood and Childhood T-Cell Acute Leukemia', *PLoS ONE*, 2(5), p. e436. doi:10.1371/journal.pone.0000436.

Bazak, L. *et al.* (2014) 'A-to-I RNA editing occurs at over a hundred million genomic sites, located in a majority of human genes', *Genome Research*, 24(3), pp. 365–376. doi:10.1101/gr.164749.113.

Beck-Schimmer, B. *et al.* (2005) 'Alveolar macrophages regulate neutrophil recruitment in endotoxin-induced lung injury', *Respiratory Research*, 6, pp. 1–14. doi:10.1186/1465-9921-6-61.

Beemiller, P., Hoppe, A.D. and Swanson, J.A. (2006) 'A Phosphatidylinositol-3-Kinase-Dependent Signal Transition Regulates ARF1 and ARF6 during Fcγ Receptor-Mediated Phagocytosis', *PLoS Biology*. Edited by E. Brown, 4(6), pp. e162–e162. doi:10.1371/journal.pbio.0040162.

Benjamini, Y. and Hochberg, Y. (1995) 'Controlling the False Discovery Rate: A Practical and Powerful Approach to Multiple Testing', *Journal of the Royal Statistical Society: Series B (Methodological)*, 57(1), pp. 289–300. doi:10.1111/j.2517-6161.1995.tb02031.x.

Benne, R. *et al.* (1986) 'Major transcript of the frameshifted coxll gene from trypanosome mitochondria contains four nucleotides that are not encoded in the DNA', *Cell*, 46(6), pp. 819–826. doi:10.1016/0092-8674(86)90063-2.

Beutler, B. (2004) 'Innate immunity: an overview', *Molecular Immunology*, 40(12), pp. 845–859. doi:10.1016/j.molimm.2003.10.005.

Bhalla, T. *et al.* (2004) 'Control of human potassium channel inactivation by editing of a small mRNA hairpin', *Nature Structural & Molecular Biology*, 11(10), pp. 950–956. doi:10.1038/nsmb825.

Biedroń, R., Peruń, A. and Józefowski, S. (2016a) 'CD36 differently regulates macrophage responses to smooth and rough lipopolysaccharide', *PLoS ONE*, 11(4), pp. 2012–2017. doi:10.1371/journal.pone.0153558.

Biedroń, R., Peruń, A. and Józefowski, S. (2016b) 'CD36 differently regulates macrophage responses to smooth and rough lipopolysaccharide', *PLoS ONE*, 11(4), pp. 2012–2017. doi:10.1371/journal.pone.0153558.

Blanc, V. *et al.* (2014) 'Genome-wide identification and functional analysis of Apobec-1-mediated C-to-U RNA editing in mouse small intestine and liver', *Genome Biology*, 15(6), p. R79. doi:10.1186/gb-2014-15-6-r79.

Blanc, V. *et al.* (2018) 'APOBEC1 complementation factor (A1CF) and RBM47 interact in tissue-specific regulation of C to U RNA editing in mouse intestine and liver', *RNA*, p. rna.068395.118-rna.068395.118. doi:10.1261/rna.068395.118.

Blanc, V. and Davidson, N.O. (2010) 'APOBEC-1-mediated RNA editing', *Wiley Interdisciplinary Reviews: Systems Biology and Medicine*, 2(5), pp. 594–602. doi:10.1002/wsbm.82.

Blom, T. *et al.* (2003) 'Comment on "The influence of the proinflammatory cytokine, osteopontin, on autoimmune demyelinating disease".', *Science*, 299(5614), pp. 1731–1736. doi:10.1126/science.1078985.

Blum, J.S., Wearsch, P.A. and Cresswell, P. (2013) 'Pathways of Antigen Processing', *Annual Review of Immunology*, 31(1), pp. 443–473. doi:10.1146/annurev-immunol-032712-095910.

Boo, S.H. and Kim, Y.K. (2020) 'The emerging role of RNA modifications in the regulation of mRNA stability', *Experimental & Molecular Medicine*, 52(3), pp. 400–408. doi:10.1038/s12276-020-0407-z.

Botelho, R.J. *et al.* (2000) 'Localized Biphasic Changes in Phosphatidylinositol-4,5-Bisphosphate at Sites of Phagocytosis', *Journal of Cell Biology*, 151(7), pp. 1353–1368. doi:10.1083/jcb.151.7.1353.

Bravo-Cordero, J.J. *et al.* (2013) 'Functions of cofilin in cell locomotion and invasion', *Nature Reviews Molecular Cell Biology*, 14(7), pp. 405–415. doi:10.1038/nrm3609.

Brosseau, C. *et al.* (2018) 'CD9 Tetraspanin: A New Pathway for the Regulation of Inflammation?', *Frontiers in Immunology*, 9(OCT), pp. 1–12. doi:10.3389/fimmu.2018.02316.

# References


Brown, D.P. *et al.* (2009) 'The inhibitory receptor LILRB4 (ILT3) modulates antigen presenting cell phenotype and, along with LILRB2 (ILT4), is upregulated in response to Salmonella infection', *BMC Immunology*, 10(1), pp. 56–56. doi:10.1186/1471-2172-10-56.

Burnashev, N. *et al.* (1992) 'Divalent Ion Permeability of AMPA Receptor Channels Is Dominated bv, the Edited Form of a Single Subunit', *Neuron*, 8, pp. 189–198.

Callaghan, J. *et al.* (1999) 'Direct interaction of EEA1 with Rab5b', *European Journal of Biochemistry*, 265(1), pp. 361–366. doi:10.1046/j.1432-1327.1999.00743.x.

Canton, J. *et al.* (2014) 'Contrasting phagosome pH regulation and maturation in human M1 and M2 macrophages', *Molecular Biology of the Cell*, 25(21), pp. 3330–3341. doi:10.1091/mbc.E14-05-0967.

Carballo, E., Lai, W.S. and Blackshear, P.J. (1998) 'Feedback Inhibition of Macrophage Tumor Necrosis Factor-α Production by Tristetraprolin', *Science*, 281(5379), pp. 1001–1005. doi:10.1126/science.281.5379.1001.

Carlile, T.M. *et al.* (2014) 'Pseudouridine profiling reveals regulated mRNA pseudouridylation in yeast and human cells.', *Nature*, 515(7525), pp. 143–6. doi:10.1038/nature13802.

Carlin, L.M. *et al.* (2013) 'Nr4a1-dependent Ly6Clow monocytes monitor endothelial cells and orchestrate their disposal', *Cell*, 153(2), pp. 362–375. doi:10.1016/j.cell.2013.03.010.

Caron, E. *et al.* (2015) 'Analysis of Major Histocompatibility Complex (MHC) Immunopeptidomes Using Mass Spectrometry*', *Molecular & Cellular Proteomics*, 14(12), pp. 3105–3117. doi:10.1074/mcp.O115.052431.

Cella, M. *et al.* (1997) 'A Novel Inhibitory Receptor (ILT3) Expressed on Monocytes, Macrophages, and Dendritic Cells Involved in Antigen Processing', *Journal of Experimental Medicine*, 185(10), pp. 1743–1751. doi:10.1084/jem.185.10.1743.

Ceppi, M. *et al.* (2009) 'Ribosomal protein mRNAs are translationally-regulated during human dendritic cells activation by LPS', *Immunome Research*, 5, p. 5. doi:10.1186/1745-7580-5-5.

Chang, C.C. *et al.* (2002) 'Tolerization of dendritic cells by Ts cells: The crucial role of inhibitory receptors ILT3 and ILT4', *Nature Immunology*, 3(3), pp. 237–243. doi:10.1038/ni760.

Chassé, H. *et al.* (2016) 'Analysis of translation using polysome profiling', *Nucleic Acids Research*, p. gkw907. doi:10.1093/nar/gkw907.

Cheng, C. *et al.* (2021) 'Recognition of lipoproteins by scavenger receptor class A members', *Journal of Biological Chemistry*, 297(2), p. 100948. doi:10.1016/j.jbc.2021.100948.

Chiou, S.-J. *et al.* (2016) 'A novel role for β2-microglobulin: a precursor of antibacterial chemokine in respiratory epithelial cells', *Scientific Reports*, 6(1), p. 31035. doi:10.1038/srep31035.

Christoforidis, S. *et al.* (1999) 'The Rab5 effector EEA1 is a core component of endosome docking', *Nature*, 397(6720), pp. 621–625. doi:10.1038/17618.

Chung, H. *et al.* (2018) 'Human ADAR1 Prevents Endogenous RNA from Triggering Translational Shutdown', *Cell*, 172(4), pp. 811-824.e14. doi:10.1016/j.cell.2017.12.038.

Cole, D.C. *et al.* (2017a) 'Loss of APOBEC1 RNA-editing function in microglia exacerbates age-related CNS pathophysiology.', *Proceedings of the National Academy of Sciences of the United States of America*, 114(50), pp. 13272–13277. doi:10.1073/pnas.1710493114.

Cole, D.C. *et al.* (2017b) 'Loss of APOBEC1 RNA-editing function in microglia exacerbates age-related CNS pathophysiology.', *Proceedings of the National Academy of Sciences of the United States of America*, 114(50), pp. 13272–13277. doi:10.1073/pnas.1710493114.

Conesa, A. *et al.* (2016) 'A survey of best practices for RNA-seq data analysis', *Genome Biology*, 17(1), p. 13. doi:10.1186/s13059-016-0881-8.

Connolly, D.J. and Bowie, A.G. (2014) 'The emerging role of human PYHIN proteins in innate immunity: Implications for health and disease', *Biochemical Pharmacology*, 92(3), pp. 405–414. doi:10.1016/j.bcp.2014.08.031.

Conticello, S.G. *et al.* (2005) 'Evolution of the AID/APOBEC family of polynucleotide (deoxy)cytidine deaminases', *Molecular biology and evolution*, 22(2), pp. 367–377. doi:10.1093/molbev/msi026.

Conticello, S.G. (2008) 'The AID/APOBEC family of nucleic acid mutators.', *Genome biology*, 9(6), pp. 229–229. doi:10.1186/gb-2008-9-6-229.

Cox, J. *et al.* (2014) 'Accurate Proteome-wide Label-free Quantification by Delayed Normalization and Maximal Peptide Ratio Extraction, Termed MaxLFQ', *Molecular & Cellular Proteomics : MCP*, 13(9), pp. 2513–2526. doi:10.1074/mcp.M113.031591.

Cridland, J.A. *et al.* (2012) 'The mammalian PYHIN gene family: Phylogeny, evolution and expression', *BMC Evolutionary Biology*, 12(1), pp. 140–140. doi:10.1186/1471-2148-12-140.

Cronk, J.C. *et al.* (2018) 'Peripherally derived macrophages can engraft the brain independent of irradiation and maintain an identity distinct from microglia', *Journal of Experimental Medicine*, 215(6), pp. 1627–1647. doi:10.1084/jem.20180247.

Cui, K. *et al.* (2018) 'Distinct Migratory Properties of M1, M2, and Resident Macrophages Are Regulated by αDβ2 and αMβ2 Integrin-Mediated Adhesion', *Frontiers in Immunology*, 9, p. 2650. doi:10.3389/fimmu.2018.02650.

Cullen, B.R. (2006) 'Role and mechanism of action of the APOBEC3 family of antiretroviral resistance factors.', *J Virol*, 80(3), pp. 1067–1076. doi:10.1128/JVI.80.3.1067.

Das, A. *et al.* (2018) 'High-resolution mapping and dynamics of the transcriptome, transcription factors, and transcription co-factor networks in classically and alternatively activated macrophages', *Frontiers in Immunology*, 9(JAN). doi:10.3389/fimmu.2018.00022.

Davis, F.M. and Gallagher, K.A. (2019) 'Epigenetic Mechanisms in Monocytes/Macrophages Regulate Inflammation in Cardiometabolic and Vascular Disease', *Arteriosclerosis, thrombosis, and vascular biology*, 39(4), pp. 623–634. doi:10.1161/ATVBAHA.118.312135.

Davis, T.A., Loos, B. and Engelbrecht, A.-M. (2014) 'AHNAK: The giant jack of all trades', *Cellular Signalling*, 26(12), pp. 2683–2693. doi:10.1016/j.cellsig.2014.08.017.

De Smet, K. and Contreras, R. (2005) 'Human Antimicrobial Peptides: Defensins, Cathelicidins and Histatins', *Biotechnology Letters*, 27(18), pp. 1337–1347. doi:10.1007/s10529-005-0936-5.

Delamarre, L. *et al.* (2005) 'Differential Lysosomal Proteolysis in Antigen-Presenting Cells Determines Antigen Fate', *Science*, 307(5715), pp. 1630–1634. doi:10.1126/science.1108003.

Delamarre, L. *et al.* (2006) 'Enhancing immunogenicity by limiting susceptibility to lysosomal proteolysis', *The Journal of Experimental Medicine*, 203(9), pp. 2049–2055. doi:10.1084/jem.20052442.

Deming, Y. *et al.* (2019) 'The MS4A gene cluster is a key modulator of soluble TREM2 and Alzheimer's disease risk', *Science Translational Medicine*, 11(505), pp. eaau2291–eaau2291. doi:10.1126/scitranslmed.aau2291.

Dennis, G.J. *et al.* (2003) 'DAVID: Database for Annotation, Visualization, and Integrated Discovery', *Genome Biology*, p. 11.

Dermit, M., Dodel, M. and Mardakheh, F.K. (2017) 'Methods for monitoring and measurement of protein translation in time and space', *Molecular BioSystems*, 13(12), pp. 2477–2488. doi:10.1039/C7MB00476A.

Devitt, A. *et al.* (1998) 'Human CD14 mediates recognition and phagocytosis of apoptotic cells', *Nature*, 392(6675), pp. 505–509. doi:10.1038/33169.

Dhami, R. and Schuchman, E.H. (2004) 'Mannose 6-phosphate receptor-mediated uptake is defective in acid sphingomyelinase-deficient macrophages: Implications for Niemann-Pick disease enzyme replacement therapy', *Journal of Biological Chemistry*, 279(2), pp. 1526–1532. doi:10.1074/jbc.M309465200.

Diedrich, G. *et al.* (2001) 'A Role for Calnexin in the Assembly of the MHC Class I Loading Complex in the Endoplasmic Reticulum', *The Journal of Immunology*, 166(3), pp. 1703–1709. doi:10.4049/jimmunol.166.3.1703.

Dingjan, I. *et al.* (2017) 'VAMP8-mediated NOX2 recruitment to endosomes is necessary for antigen release', *European Journal of Cell Biology*, 96(7), pp. 705–714. doi:10.1016/j.ejcb.2017.06.007.

Dobin, A. *et al.* (2013) 'STAR: ultrafast universal RNA-seq aligner', *Bioinformatics*, 29(1), pp. 15–21. doi:10.1093/bioinformatics/bts635.

Doyle, S.E. *et al.* (2004) 'Toll-like Receptors Induce a Phagocytic Gene Program through p38', *Journal of Experimental Medicine*, 199(1), pp. 81–90. doi:10.1084/jem.20031237.

Dunkelberger, J.R. and Song, W.-C. (2010) 'Complement and its role in innate and adaptive immune responses', *Cell Research*, 20(1), pp. 34–50. doi:10.1038/cr.2009.139.

Dustin, M.L. (2017) 'Complement receptors in myeloid cell adhesion and phagocytosis', *Myeloid Cells in Health and Disease: A Synthesis*, pp. 429–445. doi:10.1128/9781555819194.ch23.

Edwards, M. *et al.* (2014) 'Capping protein regulators fine-tune actin assembly dynamics', *Nature Reviews Molecular Cell Biology*, 15(10), pp. 677–689. doi:10.1038/nrm3869.

Ehrhardt, G.R.A. and Cooper, M.D. (2010) *Immunoregulatory roles for fc receptor-like molecules*, *Current Topics in Microbiology and Immunology*. doi:10.1007/82-2010-88.

Eichelbaum, K. and Krijgsveld, J. (2014) 'Rapid temporal dynamics of transcription, protein synthesis, and secretion during macrophage activation', *Molecular and Cellular Proteomics*, 13(3), pp. 792–810. doi:10.1074/mcp.M113.030916.

Ernst, S. *et al.* (2004) 'An Annexin 1 N-Terminal Peptide Activates Leukocytes by Triggering Different Members of the Formyl Peptide Receptor Family', *The Journal of Immunology*, 172(12), pp. 7669–7676. doi:10.4049/jimmunol.172.12.7669.

Erwig, L.-P. *et al.* (2006) 'Differential regulation of phagosome maturation in macrophages and dendritic cells mediated by Rho GTPases and ezrin-radixin-moesin (ERM) proteins', *Proceedings of the National Academy of Sciences*, 103(34), pp. 12825–12830. doi:10.1073/pnas.0605331103.

Fairn, G.D. and Grinstein, S. (2012) 'How nascent phagosomes mature to become phagolysosomes', *Trends in Immunology*, 33(8), pp. 397–405. doi:10.1016/j.it.2012.03.003.

Febbraio, M., Hajjar, D.P. and Silverstein, R.L. (2001a) 'CD36: A class B scavenger receptor involved in angiogenesis, atherosclerosis, inflammation, and lipid metabolism', *Journal of Clinical Investigation*, 108(6), pp. 785–791. doi:10.1172/JCI14006.

Febbraio, M., Hajjar, D.P. and Silverstein, R.L. (2001b) 'CD36: A class B scavenger receptor involved in angiogenesis, atherosclerosis, inflammation, and lipid metabolism', *Journal of Clinical Investigation*, 108(6), pp. 785–791. doi:10.1172/JCI14006.

Fields, K.A. *et al.* (2013) 'Perforin-2 Restricts Growth of Chlamydia trachomatis in Macrophages', *Infection and Immunity*. Edited by R.P. Morrison, 81(8), pp. 3045–3054. doi:10.1128/IAI.00497-13.

De Filippo, K. *et al.* (2008) 'Neutrophil Chemokines KC and Macrophage-Inflammatory Protein-2 Are Newly Synthesized by Tissue Macrophages Using Distinct TLR Signaling Pathways', *The Journal of Immunology*, 180(6), pp. 4308–4315. doi:10.4049/jimmunol.180.6.4308.

Friend, K. *et al.* (2012) 'A conserved PUF/Ago/eEF1A complex attenuates translation elongation', *Nature structural & molecular biology*, 19(2), pp. 176–183. doi:10.1038/nsmb.2214.

Fu, Y. *et al.* (2014) 'Gene expression regulation mediated through reversible m6A RNA methylation', *Nature Reviews Genetics*, 15(5), pp. 293–306. doi:10.1038/nrg3724.

Fujiwara, N. and Kobayashi, K. (2005) 'Macrophages in inflammation', *Current Drug Targets: Inflammation and Allergy*, 4(3), pp. 281–286. doi:10.2174/1568010054022024.

van Furth, R. and Cohen, Z.A. (1968) 'Origin and Kinetics of Mononuclear Phagocytes', *J Exp Med*, 128(3), pp. 415–435. doi:10.1084/jem.128.3.415.

Galli, S.J., Borregaard, N. and Wynn, T.A. (2011) 'Phenotypic and functional plasticity of cells of innate immunity: Macrophages, mast cells and neutrophils', *Nature Immunology*, 12(11), pp. 1035–1044. doi:10.1038/ni.2109.

Ganz, T. (2004) 'Antimicrobial polypeptides', *Journal of Leukocyte Biology*, 75(1), pp. 34–38. doi:10.1189/jlb.0403150.

Gao, J.J. *et al.* (2002) 'Regulation of gene expression in mouse macrophages stimulated with bacterial CpG-DNA and lipopolysaccharide', *Journal of Leukocyte Biology*, 72(6), pp. 1234–1245. doi:10.1189/jlb.72.6.1234.

Gautam, N. *et al.* (2001) 'Heparin-binding protein (HBP/CAP37): A missing link in neutrophil-evoked alteration of vascular permeability', *Nature Medicine*, 7(10), pp. 1123–1127. doi:10.1038/nm1001-1123.

Gebauer, F., Preiss, T. and Hentze, M.W. (2012) 'From Cis-Regulatory Elements to Complex RNPs and Back', *Cold Spring Harbor Perspectives in Biology*, 4(7), p. a012245. doi:10.1101/cshperspect.a012245.

Geissmann, F. and Mass, E. (2015) 'A stratified myeloid system, the challenge of understanding macrophage diversity', *Seminars in Immunology*, 27(6), pp. 353–356. doi:10.1016/j.smim.2016.03.016.

Gessain, G., Blériot, C. and Ginhoux, F. (2020) 'Non-genetic Heterogeneity of Macrophages in Diseases—A Medical Perspective', *Frontiers in Cell and Developmental Biology*, 8, p. 1459. doi:10.3389/fcell.2020.613116.

Ginhoux *et al.* (2010) 'Fate Mapping Analysis Reveals That Adult Microglia Derive from Primitive Macrophages', *Science*, 330(6005), pp. 841–845. doi:10.1126/science.1194637.

Ginhoux, F. and Guilliams, M. (2016) 'Tissue-Resident Macrophage Ontogeny and Homeostasis', *Immunity*, 44(3), pp. 439–449. doi:10.1016/j.immuni.2016.02.024.

Ginhoux, F. and Jung, S. (2014) 'Monocytes and macrophages: Developmental pathways and tissue homeostasis', *Nature Reviews Immunology*, 14(6), pp. 392–404. doi:10.1038/nri3671.

Glass, C.K. and Natoli, G. (2016) 'Molecular control of activation and priming in macrophages.', *Nature immunology*, 17(1), pp. 26–33. doi:10.1038/ni.3306.

Glisovic, T. *et al.* (2008) 'RNA-binding proteins and post-transcriptional gene regulation', *FEBS letters*, 582(14), pp. 1977–1986. doi:10.1016/j.febslet.2008.03.004.

Goldberg, L. *et al.* (2017) 'Alternative Splicing of STAT3 Is Affected by RNA Editing.', *DNA and cell biology*, 36(5), pp. 367–376. doi:10.1089/dna.2016.3575.

Gootenberg, J.S. *et al.* (2017) 'Nucleic acid detection with CRISPR-Cas13a/C2c2.', *Science (New York, N.Y.)*, 356(6336), pp. 438–442. doi:10.1126/science.aam9321.

Gordon, S. and Plüddemann, A. (2017) 'Tissue macrophages: Heterogeneity and functions', *BMC Biology*, 15(1), pp. 1–18. doi:10.1186/s12915-017-0392-4.

Gordon, S., Plüddemann, A. and Martinez Estrada, F. (2014) 'Macrophage heterogeneity in tissues: Phenotypic diversity and functions', *Immunological Reviews*, 262(1), pp. 36–55. doi:10.1111/imr.12223.

Grajchen, E. *et al.* (2020) 'CD36-mediated uptake of myelin debris by macrophages and microglia reduces neuroinflammation', *Journal of Neuroinflammation*, 17(1), pp. 1–14. doi:10.1186/s12974-020-01899-x.

Gray, M.A. *et al.* (2016) 'Phagocytosis Enhances Lysosomal and Bactericidal Properties by Activating the Transcription Factor TFEB', *Current Biology*, 26(15), pp. 1955–1964. doi:10.1016/j.cub.2016.05.070.

Greenberg, M.E. *et al.* (2006) 'Oxidized phosphatidylserine-CD36 interactions play an essential role in macrophage-dependent phagocytosis of apoptotic cells', *Journal of Experimental Medicine*, 203(12), pp. 2613–2625. doi:10.1084/jem.20060370.

Guilliams, M. *et al.* (2013) 'Alveolar macrophages develop from fetal monocytes that differentiate into long-lived cells in the first week of life via GM-CSF', *Journal of Experimental Medicine*, 210(10), pp. 1977–1992. doi:10.1084/jem.20131199.

Guilliams, M., Mildner, A. and Yona, S. (2018) 'Developmental and Functional Heterogeneity of Monocytes', *Immunity*, 49(4), pp. 595–613. doi:10.1016/j.immuni.2018.10.005.

Gutierrez, M.G. (2013) 'Functional role(s) of phagosomal Rab GTPases', *Small GTPases*, 4(3), pp. 148–158. doi:10.4161/sgtp.25604.

den Haan, J.M.M., Arens, R. and van Zelm, M.C. (2014) 'The activation of the adaptive immune system: Cross-talk between antigen-presenting cells, T cells and B cells', *Immunology Letters*, 162(2), pp. 103–112. doi:10.1016/j.imlet.2014.10.011.

Haggadone, M.D. *et al.* (2016) 'Bidirectional crosstalk between C5a receptors and the NLRP3 inflammasome in macrophages and monocytes', *Mediators of Inflammation*, 2016. doi:10.1155/2016/1340156.

Hald, A. *et al.* (2012) 'LPS counter regulates RNA expression of extracellular proteases and their inhibitors in murine macrophages', *Mediators of Inflammation*, 2012. doi:10.1155/2012/157894.

Hambleton, S. *et al.* (2011) 'IRF8 Mutations and Human Dendritic-Cell Immunodeficiency', *New England Journal of Medicine*, 365(2), pp. 127–138. doi:10.1056/NEJMoa1100066.

Han, Y. *et al.* (2013) 'Proteomic investigation of the interactome of FMNL1 in hematopoietic cells unveils a role in calcium-dependent membrane plasticity', *Journal of Proteomics*, 78, pp. 72–82. doi:10.1016/j.jprot.2012.11.015.

Hao, S. and Baltimore, D. (2009) 'The stability of mRNA influences the temporal order of the induction of genes encoding inflammatory molecules', *Nature Immunology*, 10(3), pp. 281–288. doi:10.1038/ni.1699.

Harjanto, D. *et al.* (2016) 'RNA editing generates cellular subsets with diverse sequence within populations.', *Nature communications*, 7, pp. 12145–12145. doi:10.1038/ncomms12145.

Hauenschild, R. *et al.* (2015) 'The reverse transcription signature of N-1-methyladenosine in RNA-Seq is sequence dependent', *Nucleic Acids Research*, p. gkv895. doi:10.1093/nar/gkv895.

Hayek, I. *et al.* (2019) 'Limitation of TCA Cycle Intermediates Represents an Oxygen-Independent Nutritional Antibacterial Effector Mechanism of Macrophages', *Cell Reports*, 26(13), pp. 3502-3510.e6. doi:10.1016/j.celrep.2019.02.103.

He, Z. *et al.* (2008) 'Characterization of conserved motifs in HIV-1 Vif required for APOBEC3G and APOBEC3F interaction.', *Journal of molecular biology*, 381(4), pp. 1000–11. doi:10.1016/j.jmb.2008.06.061.

He, Z. *et al.* (2011) 'The interaction between different types of activated RAW 264.7 cells and macrophage inflammatory protein-1 alpha', *Radiation Oncology (London, England)*, 6, p. 86. doi:10.1186/1748-717X-6-86.

Herre, J. *et al.* (2004) 'Dectin-1 uses novel mechanisms for yeast phagocytosis in macrophages', *Blood*, 104(13), pp. 4038–4045. doi:10.1182/blood-2004-03-1140.

Higuchi, M. *et al.* (2000) 'Point mutation in an AMPA receptor gene rescues lethality in mice de®cient in the RNA-editing enzyme ADAR2', 406, p. 4.

Hirano, K.-I. *et al.* (1996) 'Targeted Disruption of the Mouse apobec-1 Gene Abolishes Apolipoprotein B mRNA Editing and Eliminates Apolipoprotein B48', *Journal of Biological Chemistry*, 271(17), pp. 9887–9890. doi:10.1074/jbc.271.17.9887.

Hoeffel, G. *et al.* (2015) 'C-Myb+ Erythro-Myeloid Progenitor-Derived Fetal Monocytes Give Rise to Adult Tissue-Resident Macrophages', *Immunity*, 42(4), pp. 665–678. doi:10.1016/j.immuni.2015.03.011.

Holch, A. *et al.* (2020) 'Respiratory ß-2-Microglobulin exerts pH dependent antimicrobial activity', *Virulence*, 11(1), pp. 1402–1414. doi:10.1080/21505594.2020.1831367.

Huang, H. *et al.* (2012) 'RNA Editing of the IQ Domain in Cav1.3 Channels Modulates Their Ca2+-Dependent Inactivation', *Neuron*, 73(2), pp. 304–316. doi:10.1016/j.neuron.2011.11.022.

Huang, W., Febbraio, M. and Silverstein, R.L. (2011) 'CD9 Tetraspanin Interacts with CD36 on the Surface of Macrophages: A Possible Regulatory Influence on Uptake of Oxidized Low Density Lipoprotein', *PLoS ONE*. Edited by A. Zernecke, 6(12), pp. e29092–e29092. doi:10.1371/journal.pone.0029092.

Huang, Y. *et al.* (2018) 'Repopulated microglia are solely derived from the proliferation of residual microglia after acute depletion', *Nature Neuroscience*, 21(4), pp. 530–540. doi:10.1038/s41593-018-0090-8.

Hugo, C. *et al.* (1996) 'The cytoskeletal linking proteins, moesin and radixin, are upregulated by platelet-derived growth factor, but not basic fibroblast growth factor in experimental mesangial proliferative glomerulonephritis.', *Journal of Clinical Investigation*, 97(11), pp. 2499–2508. doi:10.1172/JCI118697.

Hume, D.A. (2015) 'The many alternative faces of macrophage activation', *Frontiers in Immunology*, 6(JUL), pp. 1–10. doi:10.3389/fimmu.2015.00370.

Huynh, K.K. *et al.* (2007) 'LAMP proteins are required for fusion of lysosomes with phagosomes', *The EMBO Journal*, 26(2), pp. 313–324. doi:10.1038/sj.emboj.7601511.

Hwangbo, C. *et al.* (2016) 'Syntenin regulates TGF-β1-induced Smad activation and the epithelial-to-mesenchymal transition by inhibiting caveolin-mediated TGF-β type I receptor internalization', *Oncogene*, 35(3), pp. 389–401. doi:10.1038/onc.2015.100.

Iizasa, H. *et al.* (2010) 'Editing of Epstein-Barr Virus-encoded BART6 MicroRNAs Controls Their Dicer Targeting and Consequently Affects Viral Latency', *The Journal of Biological Chemistry*, 285(43), pp. 33358–33370. doi:10.1074/jbc.M110.138362.

Ikushima, H. *et al.* (2000) 'Internalization of CD26 by mannose 6-phosphate/insulin-like growth factor II receptor contributes to T cell activation', *Proceedings of the National Academy of Sciences of the United States of America*, 97(15), pp. 8439–8444.

Iles, K.E. and Forman, H.J. (2002) 'Macrophage signaling and respiratory burst', *Immunologic Research*, 26(1–3), pp. 95–105. doi:10.1385/ir:26:1-3:095.

Ishikawa, E. *et al.* (2009) 'Direct recognition of the mycobacterial glycolipid, trehalose dimycolate, by C-type lectin Mincle', *Journal of Experimental Medicine*, 206(13), pp. 2879–2888. doi:10.1084/jem.20091750.

Jackman, J.E. and Alfonzo, J.D. (2013) 'Transfer RNA modifications: nature's combinatorial chemistry playground', *WIREs RNA*, 4(1), pp. 35–48. doi:10.1002/wrna.1144.

Jakubzick, C. *et al.* (2013) 'Minimal differentiation of classical monocytes as they survey steady-state tissues and transport antigen to lymph nodes', *Immunity*, 39(3), pp. 599–610. doi:10.1016/j.immuni.2013.08.007.

Jakubzick, C. V., Randolph, G.J. and Henson, P.M. (2017) 'Monocyte differentiation and antigen-presenting functions', *Nature Reviews Immunology*, 17(6), pp. 349–362. doi:10.1038/nri.2017.28.

Jancic, C. *et al.* (2007) 'Rab27a regulates phagosomal pH and NADPH oxidase recruitment to dendritic cell phagosomes', *Nature Cell Biology*, 9(4), pp. 367–378. doi:10.1038/ncb1552.

Jankowski, A., Scott, C.C. and Grinstein, S. (2002) 'Determinants of the Phagosomal pH in Neutrophils', *Journal of Biological Chemistry*, 277(8), pp. 6059–6066. doi:10.1074/jbc.M110059200.

Juelke, K. and Romagnani, C. (2016) 'Differentiation of human innate lymphoid cells (ILCs)', *Current Opinion in Immunology*, 38, pp. 75–85. doi:10.1016/j.coi.2015.11.005.

Kadumuri, R.V. and Janga, S.C. (2018) 'Epitranscriptomic Code and Its Alterations in Human Disease', *Trends in Molecular Medicine*, 24(10), pp. 886–903. doi:10.1016/j.molmed.2018.07.010.

Kaji, K. *et al.* (2001) 'Functional Association of CD9 with the Fcγ Receptors in Macrophages', *The Journal of Immunology*, 166(5), pp. 3256–3265. doi:10.4049/jimmunol.166.5.3256.

Kang, D. *et al.* (2002) 'mda-5: An interferon-inducible putative RNA helicase with double-stranded RNA-dependent ATPase activity and melanoma growth-suppressive properties', *Proceedings of the National Academy of Sciences of the United States of America*, 99(2), pp. 637–642. doi:10.1073/pnas.022637199.

Kawahara, Y. *et al.* (2007) 'RNA editing of the microRNA-151 precursor blocks cleavage by the Dicer–TRBP complex', *EMBO Reports*, 8(8), pp. 763–769. doi:10.1038/sj.embor.7401011.

Kawai, T. and Akira, S. (2010) 'The role of pattern-recognition receptors in innate immunity: update on Toll-like receptors', *Nature Immunology*, 11(5), pp. 373–384. doi:10.1038/ni.1863.

Kawai, T. and Akira, S. (2011) 'Toll-like Receptors and Their Crosstalk with Other Innate Receptors in Infection and Immunity', *Immunity*, 34(5), pp. 637–650. doi:10.1016/j.immuni.2011.05.006.

Kawasaki, T. and Kawai, T. (2014) 'Toll-like receptor signaling pathways', *Frontiers in Immunology*, p. 8. doi:10.3389/fimmu.2014.00461.

Kim, J.Y. *et al.* (2012) 'Novel Antibacterial Activity of β2-Microglobulin in Human Amniotic Fluid', *PLoS ONE*, 7(11), pp. 3–8. doi:10.1371/journal.pone.0047642.

Kimura, T. *et al.* (2015) 'Endoplasmic Protein Nogo-B (RTN4-B) Interacts with GRAMD4 and Regulates TLR9-Mediated Innate Immune Responses', *The Journal of Immunology*, 194(11), pp. 5426–5436. doi:10.4049/jimmunol.1402006.

Kinchen, J.M. and Ravichandran, K.S. (2008) 'Phagosome maturation: Going through the acid test', *Nature Reviews Molecular Cell Biology*, 9(10), pp. 781–795. doi:10.1038/nrm2515.

Kitamura, H. *et al.* (2008) 'Genome-wide identification and characterization of transcripts translationally regulated by bacterial lipopolysaccharide in macrophage-like J774.1 cells', *Physiological Genomics*, 33(1), pp. 121–132. doi:10.1152/physiolgenomics.00095.2007.

Klein, L. *et al.* (2014) 'Positive and negative selection of the T cell repertoire: What thymocytes see (and don't see)', *Nature Reviews Immunology*, 14(6), pp. 377–391. doi:10.1038/nri3667.

Kluesner, M. *et al.* (2021) 'MultiEditR: The first tool for detection and quantification of multiple RNA editing sites from 3 Sanger sequencing demonstrates comparable fidelity to RNA-seq', *Molecular Therapy: Nucleic Acid* [Preprint]. doi:10.1016/j.omtn.2021.07.008.

Köhler, M. *et al.* (1993) 'Determinants of ca2+ permeability in both TM1 and TM2 of high affinity kainate receptor channels: Diversity by RNA editing', *Neuron*, 10(3), pp. 491–500. doi:10.1016/0896-6273(93)90336-P.

Kondo, M., Weissman, I.L. and Akashi, K. (1997) 'Identification of clonogenic common lymphoid progenitors in mouse bone marrow', *Cell*, 91(5), pp. 661–672. doi:10.1016/S0092-8674(00)80453-5.

Kono, H. and Rock, K.L. (2008) 'How dying cells alert the immune system to danger', *Nature Reviews Immunology*, 8(4), pp. 279–289. doi:10.1038/nri2215.

Kotsias, F. *et al.* (2013) 'Reactive oxygen species production in the phagosome: Impact on antigen presentation in dendritic cells', *Antioxidants and Redox Signaling*, 18(6), pp. 714–729. doi:10.1089/ars.2012.4557.

Kourepini, E. *et al.* (2014) 'Osteopontin expression by CD103 dendritic cells drives intestinal inflammation', *Proceedings of the National Academy of Sciences of the United States of America*, 111(9). doi:10.1073/pnas.1316447111.

Kratochvill, F. *et al.* (2011) 'Tristetraprolin-driven regulatory circuit controls quality and timing of mRNA decay in inflammation', *Molecular Systems Biology*, 7, p. 560. doi:10.1038/msb.2011.93.

Kumar, H., Kawai, T. and Akira, S. (2009) 'Toll-like receptors and innate immunity', *Biochemical and Biophysical Research Communications*, 388(4), pp. 621–625. doi:10.1016/j.bbrc.2009.08.062.

Kumar, S. and Mohapatra, T. (2021) 'Deciphering Epitranscriptome: Modification of mRNA Bases Provides a New Perspective for Post-transcriptional Regulation of Gene Expression', *Frontiers in Cell and Developmental Biology*, 9, p. 550. doi:10.3389/fcell.2021.628415.

van der Laan, L.J. *et al.* (1999) 'Regulation and functional involvement of macrophage scavenger receptor MARCO in clearance of bacteria in vivo.', *Journal of immunology (Baltimore, Md. : 1950)*, 162(2), pp. 939–47.

van de Laar, L. *et al.* (2016) 'Yolk Sac Macrophages, Fetal Liver, and Adult Monocytes Can Colonize an Empty Niche and Develop into Functional Tissue-Resident Macrophages', *Immunity*, 44(4), pp. 755–768. doi:10.1016/j.immuni.2016.02.017.

Lackman, R.L. *et al.* (2007) 'Innate Immune Recognition Triggers Secretion of Lysosomal Enzymes by Macrophages', *Traffic*, 8(9), pp. 1179–1189. doi:10.1111/j.1600-0854.2007.00600.x.

Lavin, Y. *et al.* (2014) 'Tissue-resident macrophage enhancer landscapes are shaped by the local microenvironment', *Cell*, 159(6), pp. 1312–1326. doi:10.1016/j.cell.2014.11.018.

Lawrence, T. and Natoli, G. (2011) 'Transcriptional regulation of macrophage polarization: Enabling diversity with identity', *Nature Reviews Immunology*, 11(11), pp. 750–761. doi:10.1038/nri3088.

Lee, T.D. *et al.* (2003) 'CAP37, a neutrophil-derived inflammatory mediator, augments leukocyte adhesion to endothelial monolayers', *Microvascular Research*, 66(1), pp. 38–48. doi:10.1016/S0026-2862(03)00010-4.

Leinonen, R. *et al.* (2011) 'The Sequence Read Archive', *Nucleic Acids Research*, 39(Database), pp. D19–D21. doi:10.1093/nar/gkq1019.

Lennon-Duménil, A.-M. *et al.* (2002) 'Analysis of Protease Activity in Live Antigen-presenting Cells Shows Regulation of the Phagosomal Proteolytic Contents During Dendritic Cell Activation', *The Journal of Experimental Medicine*, 196(4), pp. 529–540. doi:10.1084/jem.20020327.

Leppek, K. *et al.* (2013) 'Roquin Promotes Constitutive mRNA Decay via a Conserved Class of Stem-Loop Recognition Motifs', *Cell*, 153(4), pp. 869–881. doi:10.1016/j.cell.2013.04.016.

Lerner, T., Papavasiliou, F.N. and Pecori, R. (2019) 'RNA editors, cofactors, and mRNA targets: An overview of the c-to-U RNA editing machinery and its implication in human disease', *Genes*, 10(1), pp. 1–19. doi:10.3390/genes10010013.

Leus, N.G., Zwinderman, M.R. and Dekker, F.J. (2016) 'Histone deacetylase 3 (HDAC 3) as emerging drug target in NF-κB-mediated inflammation', *Current Opinion in Chemical Biology*, 33, pp. 160–168. doi:10.1016/j.cbpa.2016.06.019.

Levin, R., Grinstein, S. and Canton, J. (2016) 'The life cycle of phagosomes: formation, maturation, and resolution', *Immunological Reviews*, 273(1), pp. 156–179. doi:10.1111/imr.12439.

Levin, R., Grinstein, S. and Schlam, D. (2015) 'Phosphoinositides in phagocytosis and macropinocytosis', *Biochimica et Biophysica Acta (BBA) - Molecular and Cell Biology of Lipids*, 1851(6), pp. 805–823. doi:10.1016/j.bbalip.2014.09.005.

Li, G., Hao, W. and Hu, W. (2020) 'Transcription factor PU.1 and immune cell differentiation (Review)', *International Journal of Molecular Medicine*, 46(6), pp. 1943–1950. doi:10.3892/ijmm.2020.4763.

Li, H. *et al.* (2009) 'The Sequence Alignment/Map format and SAMtools', *Bioinformatics*, 25(16), pp. 2078–2079. doi:10.1093/bioinformatics/btp352.

Liao, Y. *et al.* (2019) 'WebGestalt 2019: gene set analysis toolkit with revamped UIs and APIs', *Nucleic Acids Research*, 47(W1), pp. W199–W205. doi:10.1093/nar/gkz401.

van Liempt, E. *et al.* (2006) 'Specificity of DC-SIGN for mannose- and fucose-containing glycans', *FEBS Letters*, 580(26), pp. 6123–6131. doi:10.1016/j.febslet.2006.10.009.

Lin, H.H. *et al.* (2005) 'The macrophage F4/80 receptor is required for the induction of antigen-specific efferent regulatory T cells in peripheral tolerance', *Journal of Experimental Medicine*, 201(10), pp. 1615–1625. doi:10.1084/jem.20042307.

Linder, B. *et al.* (2015) 'Single-nucleotide-resolution mapping of m6A and m6Am throughout the transcriptome', *Nature Methods*, 12(8), pp. 767–772. doi:10.1038/nmeth.3453.

Liu, J. *et al.* (2021) 'CREG1 promotes lysosomal biogenesis and function', *Autophagy*, pp. 1–17. doi:10.1080/15548627.2021.1909997.

Liu, N. and Pan, T. (2016) 'Probing N 6-methyladenosine (m6A) RNA Modification in Total RNA with SCARLET', in Dassi, E. (ed.) *Post-Transcriptional Gene Regulation*. New York, NY: Springer (Methods in Molecular Biology), pp. 285–292. doi:10.1007/978-1-4939-3067-8_17.

Liu, Y. *et al.* (2019) 'The N6-methyladenosine (m6A)-forming enzyme METTL3 facilitates M1 macrophage polarization through the methylation of STAT1 mRNA', *American Journal of Physiology - Cell Physiology*, 317(4), pp. C762–C775. doi:10.1152/ajpcell.00212.2019.

Livak, K.J. and Schmittgen, T.D. (2001) 'Analysis of Relative Gene Expression Data Using Real-Time Quantitative PCR and the 2−ΔΔCT Method', *Methods*, 25(4), pp. 402–408. doi:10.1006/meth.2001.1262.

Lo Giudice, C. *et al.* (2020) 'Quantifying RNA Editing in Deep Transcriptome Datasets', *Frontiers in Genetics*, 11, p. 194. doi:10.3389/fgene.2020.00194.

Lomeli, H. *et al.* (1994) 'Control of kinetic properties of AMPA receptor channels by nuclear RNA editing', *Science*, 266(5191), pp. 1709–1713. doi:10.1126/science.7992055.

Lyle, A.N. *et al.* (2014) 'Hydrogen Peroxide Regulates Osteopontin Expression through Activation of Transcriptional and Translational Pathways', *Journal of Biological Chemistry*, 289(1), pp. 275–285. doi:10.1074/jbc.M113.489641.

Mannion, N.M. *et al.* (2014) 'The RNA-Editing Enzyme ADAR1 Controls Innate Immune Responses to RNA', *Cell Reports*, 9(4), pp. 1482–1494. doi:10.1016/j.celrep.2014.10.041.

Mantegazza, A.R. *et al.* (2008) 'NADPH oxidase controls phagosomal pH and antigen cross-presentation in human dendritic cells', *Blood*, 112(12), pp. 4712–4722. doi:10.1182/blood-2008-01-134791.

Mantovani, A. *et al.* (2004) 'The chemokine system in diverse forms of macrophage activation and polarization', *Trends in Immunology*, 25(12), pp. 677–686. doi:10.1016/j.it.2004.09.015.

Maris, C. *et al.* (2005) 'NMR structure of the apoB mRNA stem–loop and its interaction with the C to U editing APOBEC1 complementary factor', *RNA*, 11(2), p. 173. doi:10.1261/rna.7190705.

Markart, P. *et al.* (2004) 'Comparison of the microbicidal and muramidase activities of mouse lysozyme M and P', *Biochemical Journal*, 380(2), pp. 385–392. doi:10.1042/bj20031810.

Marshansky, V. and Futai, M. (2008) 'The V-type H+-ATPase in vesicular trafficking: targeting, regulation and function', *Current Opinion in Cell Biology*, 20(4), pp. 415–426. doi:10.1016/j.ceb.2008.03.015.

Maxfield, F.R., Barbosa-Lorenzi, V.C. and Singh, R.K. (2020) 'Digestive exophagy: Phagocyte digestion of objects too large for phagocytosis', *Traffic*, 21(1), pp. 6–12. doi:10.1111/tra.12712.

Mazor, K.M. *et al.* (2018) 'Effects of single amino acid deficiency on mRNA translation are markedly different for methionine versus leucine', *Scientific Reports*, 8(1), p. 8076. doi:10.1038/s41598-018-26254-2.

McCarthy, D.J., Chen, Y. and Smyth, G.K. (2012) 'Differential expression analysis of multifactor RNA-Seq experiments with respect to biological variation', *Nucleic Acids Research*, 40(10), pp. 4288–4297. doi:10.1093/nar/gks042.

McCormack, R.M. *et al.* (2015) 'Perforin-2 is essential for intracellular defense of parenchymal cells and phagocytes against pathogenic bacteria', *eLife*, 4(September2015), pp. 1–29. doi:10.7554/eLife.06508.

McCormick, P.J. *et al.* (2008) 'Palmitoylation Controls Recycling in Lysosomal Sorting and Trafficking', *Traffic (Copenhagen, Denmark)*, 9(11), pp. 1984–1997. doi:10.1111/j.1600-0854.2008.00814.x.

McKercher, S.R. *et al.* (1996) 'Targeted disruption of the PU.1 gene results in multiple hematopoietic abnormalities', *EMBO Journal*, 15(20), pp. 5647–5658. doi:10.1002/j.1460-2075.1996.tb00949.x.

McLachlan, F., Sires, A.M. and Abbott, C.M. (2019) 'The role of translation elongation factor eEF1 subunits in neurodevelopmental disorders', *Human Mutation*, 40(2), pp. 131–141. doi:10.1002/humu.23677.

Medzhitov, R. and Horng, T. (2009) 'Transcriptional control of the inflammatory response', *Nature Reviews Immunology*, 9(10), pp. 692–703. doi:10.1038/nri2634.

Meier, J.C. *et al.* (2005) 'RNA editing produces glycine receptor α3P185L, resulting in high agonist potency', *Nature Neuroscience*, 8(6), pp. 736–744. doi:10.1038/nn1467.

Meyer, K.D. *et al.* (2012) 'Comprehensive Analysis of mRNA Methylation Reveals Enrichment in 3' UTRs and near Stop Codons', *Cell*, 149(7), pp. 1635–1646. doi:10.1016/j.cell.2012.05.003.

Minakami, R. and Sumimoto, H. (2006) 'Phagocytosis-coupled activation of the superoxide-producing phagocyte oxidase, a member of the NADPH oxidase (Nox) family', *International Journal of Hematology*, 84(3), pp. 193–198. doi:10.1532/IJH97.06133.

Mofatteh, M. (2020) 'mRNA localization and local translation in neurons', *AIMS Neuroscience*, 7(3), pp. 299–310. doi:10.3934/Neuroscience.2020016.

Molawi, K. *et al.* (2014) 'Progressive replacement of embryo-derived cardiac macrophages with age', *Journal of Experimental Medicine*, 211(11), pp. 2151–2158. doi:10.1084/jem.20140639.

Molinie, B. *et al.* (2016) 'm6A-LAIC-seq reveals the census and complexity of the m6A epitranscriptome', *Nature Methods*, 13(8), pp. 692–698. doi:10.1038/nmeth.3898.

Monyer, H. *et al.* (1992) 'Heteromeric NMDA Receptors: Molecular and Functional Distinction of Subtypes', *Science*, 256(5060), pp. 1217–1221. doi:10.1126/science.256.5060.1217.

Moor, A.E. *et al.* (2017) 'Global mRNA polarization regulates translation efficiency in the intestinal epithelium', *Science*, 357(6357), pp. 1299–1303. doi:10.1126/science.aan2399.

Morley, S.C. (2012) 'The actin-bundling protein L-plastin: A critical regulator of immune cell function', *International Journal of Cell Biology*, 2012. doi:10.1155/2012/935173.

Mu, L. *et al.* (2018) 'A phosphatidylinositol 4,5-bisphosphate redistribution-based sensing mechanism initiates a phagocytosis programing', *Nature Communications*, 9(1), pp. 4259–4259. doi:10.1038/s41467-018-06744-7.

Mukhopadhyay, D. *et al.* (2002) 'C→U Editing of Neurofibromatosis 1 mRNA Occurs in Tumors That Express Both the Type II Transcript and apobec-1, the Catalytic Subunit of the Apolipoprotein B mRNA–Editing Enzyme', *The American Journal of Human Genetics*, 70(1), pp. 38–50. doi:10.1086/337952.

Mullican, S.E. *et al.* (2011) 'Histone deacetylase 3 is an epigenomic brake in macrophage alternative activation', *Genes & Development*, 25(23), pp. 2480–2488. doi:10.1101/gad.175950.111.

Muntjewerff, E.M., Meesters, L.D. and van den Bogaart, G. (2020) 'Antigen Cross-Presentation by Macrophages', *Frontiers in Immunology*, 11, p. 1276. doi:10.3389/fimmu.2020.01276.

Muramatsu, M. *et al.* (2000) 'Class switch recombination and hypermutation require activation-induced cytidine deaminase (AID), a potential RNA editing enzyme', *Cell* [Preprint]. doi:10.1016/S0092-8674(00)00078-7.

Murphy, K. *et al.* (2016) *Janeway's immunobiology, 9th ed.* New York: Garland Science.

Murray, P.J. and Wynn, T.A. (2011) 'Protective and pathogenic functions of macrophage subsets.', *Nature reviews. Immunology*, 11(11), pp. 723–37. doi:10.1038/nri3073.

Nag, S. *et al.* (2013) 'Gelsolin: The tail of a molecular gymnast', *Cytoskeleton*, 70(7), pp. 360–384. doi:10.1002/cm.21117.

Nagata, S. *et al.* (2016) 'Exposure of phosphatidylserine on the cell surface', *Cell Death and Differentiation*, 23(6), pp. 952–961. doi:10.1038/cdd.2016.7.

Narayan, V. *et al.* (2015) 'Epigenetic regulation of inflammatory gene expression in macrophages by selenium', *The Journal of Nutritional Biochemistry*, 26(2), pp. 138–145. doi:10.1016/j.jnutbio.2014.09.009.

Nathan, C. (2008) 'Metchnikoff's Legacy in 2008', *Nature Immunology*, 9(7), pp. 695–698. doi:10.1038/ni0708-695.

Nauseef, W.M. (2014) 'Myeloperoxidase in human neutrophil host defence', *Cellular Microbiology*, 16(8), pp. 1146–1155. doi:10.1111/cmi.12312.

Nauseef, W.M. (2019) 'The phagocyte NOX2 NADPH oxidase in microbial killing and cell signaling', *Current Opinion in Immunology*, 60, pp. 130–140. doi:10.1016/j.coi.2019.05.006.

Navaratnam, N. *et al.* (1993) 'The p27 catalytic subunit of the apolipoprotein B mRNA editing enzyme is a cytidine deaminase', *Journal of Biological Chemistry*, 268(28), pp. 20709–20712.

Neefjes, J. *et al.* (2011) 'Towards a systems understanding of MHC class I and MHC class II antigen presentation', *Nature Reviews Immunology*, 11(12), pp. 823–836. doi:10.1038/nri3084.

Neeman, Y. *et al.* (2006) 'RNA editing level in the mouse is determined by the genomic repeat repertoire', *RNA*, 12(10), pp. 1802–1809. doi:10.1261/rna.165106.

Nilsen, N.J. *et al.* (2008) 'Cellular trafficking of lipoteichoic acid and Toll-like receptor 2 in relation to signaling; role of CD14 and CD36', *Journal of Leukocyte Biology*, 84(1), pp. 280–291. doi:10.1189/jlb.0907656.

Nilsson, R. *et al.* (2006) 'Transcriptional network dynamics in macrophage activation', *Genomics*, 88(2), pp. 133–142. doi:10.1016/j.ygeno.2006.03.022.

Niu, Y. *et al.* (2013) 'N6-methyl-adenosine (m6A) in RNA: An Old Modification with A Novel Epigenetic Function', *Genomics, Proteomics & Bioinformatics*, 11(1), pp. 8–17. doi:10.1016/j.gpb.2012.12.002.

O'Connor, P.B.F., Andreev, D.E. and Baranov, P.V. (2016) 'Comparative survey of the relative impact of mRNA features on local ribosome profiling read density', *Nature Communications*, 7(1), p. 12915. doi:10.1038/ncomms12915.

Ogawa, M. *et al.* (2010) 'High sensitivity detection of cancer in vivo using a dual-controlled activation fluorescent imaging probe based on H-dimer formation and pH activation', *Molecular BioSystems*, 6(5), p. 888. doi:10.1039/b917876g.

Ohlson, J. *et al.* (2007) 'Editing modifies the GABAA receptor subunit α3', *RNA*, 13(5), pp. 698–703. doi:10.1261/rna.349107.

Ohman, M. (2007) 'A-to-I editing challenger or ally to the microRNA process', *Biochimie*, 89(10), pp. 1171–1176. doi:10.1016/j.biochi.2007.06.002.

O'Neill, L.A.J. and Pearce, E.J. (2016) 'Immunometabolism governs dendritic cell and macrophage function', *Journal of Experimental Medicine*, 213(1), pp. 15–23. doi:10.1084/jem.20151570.

Orkin, S.H. and Zon, L.I. (2008) 'Hematopoiesis: An Evolving Paradigm for Stem Cell Biology', *Cell*, 132(4), pp. 631–644. doi:10.1016/j.cell.2008.01.025.

Ostareck, D.H. and Ostareck-Lederer, A. (2019) 'RNA-binding proteins in the control of LPS-induced macrophage response', *Frontiers in Genetics*, 10(FEB), pp. 1–10. doi:10.3389/fgene.2019.00031.

Otsuka, H. *et al.* (2019) 'Emerging Evidence of Translational Control by AU-Rich Element-Binding Proteins', *Frontiers in Genetics*, 10(MAY), pp. 1–10. doi:10.3389/fgene.2019.00332.

Owczarek, S. and Berezin, V. (2012) 'Neuroplastin: Cell adhesion molecule and signaling receptor', *The International Journal of Biochemistry & Cell Biology*, 44(1), pp. 1–5. doi:10.1016/j.biocel.2011.10.006.

Palis, J. and Yoder, M.C. (2001) 'Yolk-sac hematopoiesis: The first blood cells of mouse and man', *Experimental Hematology*, 29(8), pp. 927–936. doi:10.1016/S0301-472X(01)00669-5.

Panda, A., Martindale, J. and Gorospe, M. (2017) 'Polysome Fractionation to Analyze mRNA Distribution Profiles', *BIO-PROTOCOL*, 7(3). doi:10.21769/BioProtoc.2126.

Panday, A. *et al.* (2015) 'NADPH oxidases: an overview from structure to innate immunity-associated pathologies', *Cellular & Molecular Immunology*, 12(1), pp. 5–23. doi:10.1038/cmi.2014.89.

Park, S.H. *et al.* (2017) 'Type I interferons and the cytokine TNF cooperatively reprogram the macrophage epigenome to promote inflammatory activation', *Nature Immunology*, 18(10), pp. 1104–1116. doi:10.1038/ni.3818.

Patel, D.M. *et al.* (2011) 'Annexin A1 is a new functional linker between actin filaments and phagosomes during phagocytosis', *Journal of Cell Science*, 124(4), pp. 578–588. doi:10.1242/jcs.076208.

Patel, S.N. *et al.* (2004) 'CD36 Mediates the Phagocytosis of Plasmodium falciparum-Infected Erythrocytes by Rodent Macrophages', *Journal of Infectious Diseases*, 189(2), pp. 204–213. doi:10.1086/380764.

Patterson, J.B. and Samuel, C.E. (1995) 'Expression and regulation by interferon of a double-stranded-RNA-specific adenosine deaminase from human cells: evidence for two forms of the deaminase.', *Molecular and Cellular Biology*, 15(10), pp. 5376–5388.

Peiser, L. *et al.* (2000) 'Macrophage class A scavenger receptor-mediated phagocytosis of Escherichia coli: Role of cell heterogeneity, microbial strain, and culture conditions in vitro', *Infection and Immunity*, 68(4), pp. 1953–1963. doi:10.1128/IAI.68.4.1953-1963.2000.

Peiser, L. *et al.* (2006) 'Identification of Neisseria meningitidis nonlipopolysaccharide ligands for class A macrophage scavenger receptor by using a novel assay', *Infection and Immunity*, 74(9), pp. 5191–5199. doi:10.1128/IAI.00124-06.

Pelka, K. *et al.* (2018) 'The Chaperone UNC93B1 Regulates Toll-like Receptor Stability Independently of Endosomal TLR Transport', *Immunity*, 48(5), pp. 911-922.e7. doi:10.1016/j.immuni.2018.04.011.

Pestal, K. *et al.* (2015) 'Isoforms of RNA-Editing Enzyme ADAR1 Independently Control Nucleic Acid Sensor MDA5-Driven Autoimmunity and Multi-organ Development.', *Immunity*, 43(5), pp. 933–44. doi:10.1016/j.immuni.2015.11.001.

Philley, J.V., Kannan, A. and Dasgupta, S. (2016) 'MDA-9/Syntenin Control', *Journal of Cellular Physiology*, 231(3), pp. 545–550. doi:10.1002/jcp.25136.

Picardi, E. *et al.* (2015) 'Profiling RNA editing in human tissues: towards the inosinome Atlas.', *Scientific reports*, 5, pp. 14941–14941. doi:10.1038/srep14941.

Picardi, E. and Pesole, G. (2013) 'REDItools: High-throughput RNA editing detection made easy', *Bioinformatics*, 29(14), pp. 1813–1814. doi:10.1093/bioinformatics/btt287.

Piccolo, V. *et al.* (2017) 'Opposing macrophage polarization programs show extensive epigenomic and transcriptional cross-talk', *Nature Immunology*, 18(5), pp. 530–540. doi:10.1038/ni.3710.

Piecyk, M. *et al.* (2000) 'TIA-1 is a translational silencer that selectively regulates the expression of TNF-α', *The EMBO Journal*, 19(15), pp. 4154–4163. doi:10.1093/emboj/19.15.4154.

Pietras, E.M. *et al.* (2015) 'Functionally Distinct Subsets of Lineage-Biased Multipotent Progenitors Control Blood Production in Normal and Regenerative Conditions', *Cell Stem Cell*, 17(1), pp. 35–46. doi:10.1016/j.stem.2015.05.003.

Pinto, Y., Cohen, H.Y. and Levanon, E.Y. (2014) 'Mammalian conserved ADAR targets comprise only a small fragment of the human editosome', *Genome Biology*, 15(1), p. R5. doi:10.1186/gb-2014-15-1-r5.

Pitts, M.W. and Hoffmann, P.R. (2018) 'Endoplasmic reticulum-resident selenoproteins as regulators of calcium signaling and homeostasis', *Cell Calcium*, 70, pp. 76–86. doi:10.1016/j.ceca.2017.05.001.

Plass, M., Rasmussen, S.H. and Krogh, A. (2017) 'Highly accessible AU-rich regions in 3' untranslated regions are hotspots for binding of regulatory factors', *PLOS Computational Biology*. Edited by R. Guigo, 13(4), pp. e1005460–e1005460. doi:10.1371/journal.pcbi.1005460.

Powell-Braxton, L. *et al.* (1998) 'A mouse model of human familial hypercholesterolemia: Markedly elevated low density lipoprotein cholesterol levels and severe atherosclerosis on a low-fat chow diet', *Nature Medicine*, 4(8), pp. 934–938. doi:10.1038/nm0898-934.

Quin, J. *et al.* (2021) 'ADAR RNA Modifications, the Epitranscriptome and Innate Immunity', *Trends in Biochemical Sciences*, 46(9), pp. 758–771. doi:10.1016/j.tibs.2021.02.002.

Rabani, M. *et al.* (2011) 'Metabolic labeling of RNA uncovers principles of RNA production and degradation dynamics in mammalian cells', *Nature Biotechnology*, 29(5), pp. 436–442. doi:10.1038/nbt.1861.

Ramaswami, G. *et al.* (2013) 'Identifying RNA editing sites using RNA sequencing data alone', *Nature Methods*, 10(2), pp. 128–132. doi:10.1038/nmeth.2330.

Ran, F.A. *et al.* (2013) 'Genome engineering using the CRISPR-Cas9 system.', *Nature protocols*, 8(11), pp. 2281–2308. doi:10.1038/nprot.2013.143.

Rayon-Estrada, V. *et al.* (2017) 'Epitranscriptomic profiling across cell types reveals associations between APOBEC1-mediated RNA editing, gene expression outcomes, and cellular function', *Proceedings of the National Academy of Sciences*, 114(50), pp. 13296–13301. doi:10.1073/pnas.1714227114.

Renner, F. and Schmitz, M.L. (2009) 'Autoregulatory feedback loops terminating the NF-κB response', *Trends in Biochemical Sciences*, 34(3), pp. 128–135. doi:10.1016/j.tibs.2008.12.003.

Richardson, N., Navaratnam, N. and Scott, J. (1998) 'Secondary Structure for the Apolipoprotein B mRNA Editing Site', *Journal of Biological Chemistry*, 273(48), pp. 31707–31717. doi:10.1074/jbc.273.48.31707.

Rink, J. *et al.* (2005) 'Rab conversion as a mechanism of progression from early to late endosomes', *Cell*, 122(5), pp. 735–749. doi:10.1016/j.cell.2005.06.043.

Rittling, S.R. (2011) 'Osteopontin in macrophage function', *Expert Reviews in Molecular Medicine*, 13, p. e15. doi:10.1017/S1462399411001839.

Robinson, M.D., McCarthy, D.J. and Smyth, G.K. (2010) 'edgeR: a Bioconductor package for differential expression analysis of digital gene expression data', *Bioinformatics*, 26(1), pp. 139–140. doi:10.1093/bioinformatics/btp616.

Robinson, M.D. and Oshlack, A. (2010) 'A scaling normalization method for differential expression analysis of RNA-seq data', *Genome Biology*, 11(3), p. R25. doi:10.1186/gb-2010-11-3-r25.

Rodrigues, P.F. *et al.* (2018) 'Distinct progenitor lineages contribute to the heterogeneity of plasmacytoid dendritic cells', *Nature Immunology*, 19(7), pp. 711–722. doi:10.1038/s41590-018-0136-9.

Rodríguez-Prados, J.-C. *et al.* (2010) 'Substrate Fate in Activated Macrophages: A Comparison between Innate, Classic, and Alternative Activation', *The Journal of Immunology*, 185(1), pp. 605–614. doi:10.4049/jimmunol.0901698.

Rosales, C. (2017) 'Fcγ Receptor Heterogeneity in Leukocyte Functional Responses', *Frontiers in Immunology*, 8, p. 280. doi:10.3389/fimmu.2017.00280.

Rosales, C. and Uribe-Querol, E. (2013) 'Fc receptors: Cell activators of antibody functions', *Advances in Bioscience and Biotechnology*, 04(04), pp. 21–33. doi:10.4236/abb.2013.44A004.

Rosenbaum, S. *et al.* (2011) 'Identification of Novel Binding Partners (Annexins) for the Cell Death Signal Phosphatidylserine and Definition of Their Recognition Motif', *Journal of Biological Chemistry*, 286(7), pp. 5708–5716. doi:10.1074/jbc.M110.193086.

Rosenberg, B.R. *et al.* (2011) 'Transcriptome-wide sequencing reveals numerous APOBEC1 mRNA-editing targets in transcript 3' UTRs.', *Nature structural & molecular biology*, 18(2), pp. 230–6. doi:10.1038/nsmb.1975.

Rouhanifard, S.H. *et al.* (2018) 'ClampFISH detects individual nucleic-acid molecules using click chemistry based amplification', *Nature biotechnology*, p. 10.1038/nbt.4286. doi:10.1038/nbt.4286.

Roundtree, I.A. *et al.* (2017) 'Dynamic RNA Modifications in Gene Expression Regulation.', *Cell*, 169(7), pp. 1187–1200. doi:10.1016/j.cell.2017.05.045.

Ruland, J. (2011) 'Return to homeostasis: downregulation of NF-κB responses', *Nature Immunology*, 12(8), pp. 709–714. doi:10.1038/ni.2055.

Russell, D.G. *et al.* (2009) 'The macrophage marches on its phagosome: dynamic assays of phagosome function', *Nature Reviews Immunology*, 9(8), pp. 594–600. doi:10.1038/nri2591.

Russell, R.A. *et al.* (2009) 'Distinct Domains within APOBEC3G and APOBEC3F Interact with Separate Regions of Human Immunodeficiency Virus Type 1 Vif', *Journal of Virology*, 83(4), pp. 1992–2003. doi:10.1128/JVI.01621-08.

Ryan, D.G. and O'Neill, L.A.J. (2017) 'Krebs cycle rewired for macrophage and dendritic cell effector functions', *FEBS Letters*, 591(19), pp. 2992–3006. doi:10.1002/1873-3468.12744.

Rybicka, J.M. *et al.* (2010) 'NADPH oxidase activity controls phagosomal proteolysis in macrophages through modulation of the lumenal redox environment of phagosomes', *Proceedings of the National Academy of Sciences of the United States of America*, 107(23), pp. 10496–10501. doi:10.1073/pnas.0914867107.

Saletore, Y. *et al.* (2012) 'The birth of the Epitranscriptome: deciphering the function of RNA modifications', *Genome Biology*, 13(10), p. 175. doi:10.1186/gb-2012-13-10-175.

Salter, J.D., Bennett, R.P. and Smith, H.C. (2016) 'The APOBEC Protein Family: United by Structure, Divergent in Function', *Trends in Biochemical Sciences*, 41(7), pp. 578–594. doi:10.1016/j.tibs.2016.05.001.

Savina, A. *et al.* (2006) 'NOX2 Controls Phagosomal pH to Regulate Antigen Processing during Crosspresentation by Dendritic Cells', *Cell*, 126(1), pp. 205–218. doi:10.1016/j.cell.2006.05.035.

Savina, A. and Amigorena, S. (2007) 'Phagocytosis and antigen presentation in dendritic cells', *Immunological Reviews*, 219(1), pp. 143–156. doi:10.1111/j.1600-065X.2007.00552.x.

Sawai, C.M. *et al.* (2016) 'Hematopoietic Stem Cells Are the Major Source of Multilineage Hematopoiesis in Adult Animals', *Immunity*, 45(3), pp. 597–609. doi:10.1016/j.immuni.2016.08.007.

Schattgen, S.A. and Fitzgerald, K.A. (2011) 'The PYHIN protein family as mediators of host defenses', *Immunological Reviews*, 243(1), pp. 109–118. doi:10.1111/j.1600-065X.2011.01053.x.

Schiff, D.E. *et al.* (1997) 'Phagocytosis of Gram-negative bacteria by a unique CD14-dependent mechanism', *Journal of Leukocyte Biology*, 62(6), pp. 786–794. doi:10.1002/jlb.62.6.786.

Schneemann, M. and Schoeden, G. (2007) 'Macrophage biology and immunology: man is not a mouse', *Journal of Leukocyte Biology*, 81(3), pp. 579–579. doi:10.1189/jlb.1106702.

Schneider-Poetsch, T. *et al.* (2010) 'Inhibition of eukaryotic translation elongation by cycloheximide and lactimidomycin', *Nature Chemical Biology*, 6(3), pp. 209–217. doi:10.1038/nchembio.304.

Schott, J. *et al.* (2014) 'Translational Regulation of Specific mRNAs Controls Feedback Inhibition and Survival during Macrophage Activation', *PLoS Genetics*, 10(6). doi:10.1371/journal.pgen.1004368.

Schott, J. and Stoecklin, G. (2010) 'Networks controlling mRNA decay in the immune system', *WIREs RNA*, 1(3), pp. 432–456. doi:10.1002/wrna.13.

Schröder, B. and Saftig, P. (2016) 'Intramembrane Proteolysis within lysosomes', *Ageing Research Reviews* [Preprint]. doi:10.1016/j.arr.2016.04.012.

Schroder, K., Sweet, M.J. and Hume, D.A. (2006) 'Signal integration between IFNγ and TLR signalling pathways in macrophages', *Immunobiology*, 211(6–8), pp. 511–524. doi:10.1016/j.imbio.2006.05.007.

Schwanhäusser, B. *et al.* (2011) 'Global quantification of mammalian gene expression control', *Nature*, 473(7347), pp. 337–342. doi:10.1038/nature10098.

Schwartz, S. *et al.* (2014) 'Transcriptome-wide mapping reveals widespread dynamic-regulated pseudouridylation of ncRNA and mRNA.', *Cell*, 159(1), pp. 148–162. doi:10.1016/j.cell.2014.08.028.

Scott, C.C. *et al.* (2005) 'Phosphatidylinositol-4,5-bisphosphate hydrolysis directs actin remodeling during phagocytosis', *Journal of Cell Biology*, 169(1), pp. 139–149. doi:10.1083/jcb.200412162.

Sendler, M. *et al.* (2018) 'Cathepsin B-Mediated Activation of Trypsinogen in Endocytosing Macrophages Increases Severity of Pancreatitis in Mice', *Gastroenterology*, 154(3), pp. 704-718.e10. doi:10.1053/j.gastro.2017.10.018.

Shah, R.R. *et al.* (1991) 'Sequence requirements for the editing of apolipoprotein B mRNA.', *Journal of Biological Chemistry*, 266(25), pp. 16301–16304. doi:10.1016/S0021-9258(18)55296-0.

Shah, S.A. *et al.* (2013) 'Protospacer recognition motifs: Mixed identities and functional diversity', *RNA Biology*, 10(5), pp. 891–899. doi:10.4161/rna.23764.

Sharif, O. *et al.* (2007) 'Transcriptional profiling of the LPS induced NF-κB response in macrophages', *BMC Immunology*, 8, pp. 1–17. doi:10.1186/1471-2172-8-1.

Sharma, S. *et al.* (2015) 'APOBEC3A cytidine deaminase induces RNA editing in monocytes and macrophages', *Nature Communications*, 6, pp. 1–15. doi:10.1038/ncomms7881.

Sharma, S. *et al.* (2016) 'The double-domain cytidine deaminase APOBEC3G is a cellular site-specific RNA editing enzyme', *Scientific Reports*, 6(December), pp. 1–12. doi:10.1038/srep39100.

Sharma, S. *et al.* (2018) 'Mitochondrial hypoxic stress induces widespread RNA editing by APOBEC3G in lymphocytes', *BioRxiv 389791*, [preprint](August 10th). doi:10.1101/389791.

Sharma, S. *et al.* (2019) 'Mitochondrial hypoxic stress induces widespread RNA editing by APOBEC3G in natural killer cells', *Genome Biology*, 20(1), p. 37. doi:10.1186/s13059-019-1651-1.

Sharma, S. and Baysal, B.E. (2017) 'Stem-loop structure preference for site-specific RNA editing by APOBEC3A and APOBEC3G.', *PeerJ*, 5, pp. e4136–e4136. doi:10.7717/peerj.4136.

Shaw, T.N. *et al.* (2018) 'Tissue-resident macrophages in the intestine are long lived and defined by Tim-4 and CD4 expression', *Journal of Experimental Medicine*, 215(6), pp. 1507–1518. doi:10.1084/jem.20180019.

Sheldon, K.E. *et al.* (2013) 'Shaping the Murine Macrophage Phenotype: IL-4 and cAMP Synergistically Activate the Arginase I Promoter', *Journal of immunology (Baltimore, Md.: 1950)*, 191(5), p. 10.4049/jimmunol.1202102. doi:10.4049/jimmunol.1202102.

Shmakov, S. *et al.* (2015) 'Discovery and Functional Characterization of Diverse Class 2 CRISPR-Cas Systems.', *Molecular cell*, 60(3), pp. 385–97. doi:10.1016/j.molcel.2015.10.008.

Singel, K.L. and Segal, B.H. (2016) 'NOX2-dependent regulation of inflammation', *Clinical science (London, England : 1979)*, 130(7), pp. 479–490. doi:10.1042/CS20150660.

Singh, L. *et al.* (2021) 'ILT3 (LILRB4) Promotes the Immunosuppressive Function of Tumor-Educated Human Monocytic Myeloid-Derived Suppressor Cells', *Molecular Cancer Research*, 19(4), pp. 702–716. doi:10.1158/1541-7786.MCR-20-0622.

Skjeflo, E.W. *et al.* (2019) 'Phagocytosis of live and dead Escherichia coli and Staphylococcus aureus in human whole blood is markedly reduced by combined inhibition of C5aR1 and CD14', *Molecular Immunology*, 112(May), pp. 131–139. doi:10.1016/j.molimm.2019.03.014.

Skuse, G.R. *et al.* (1996) 'The neurofibromatosis type I messenger RNA undergoes base-modification RNA editing.', *Nucleic Acids Research*, 24(3), pp. 478–485.

Slavik, J.M., Hutchcroft, J.E. and Bierer, B.E. (1999) 'CD28/CTLA-4 and CD80/CD86 families: Signaling and function', *Immunologic Research*, 19(1), pp. 1–24. doi:10.1007/BF02786473.

Smale, S.T. and Natoli, G. (2014) 'Transcriptional Control of Inflammatory Responses', *Cold Spring Harbor Perspectives in Biology*, 6(11). doi:10.1101/cshperspect.a016261.

Smirnova, V.V. *et al.* (2019) 'eIF4G2 balances its own mRNA translation via a PCBP2-based feedback loop', *RNA*, 25(7), pp. 757–767. doi:10.1261/rna.065623.118.

Soehnlein, O. *et al.* (2008) 'Neutrophil secretion products pave the way for inflammatory monocytes', *Blood*, 112(4), pp. 1461–1471. doi:10.1182/blood-2008-02-139634.

Sommer, B. *et al.* (1991) 'RNA editing in brain controls a determinant of ion flow in glutamate-gated channels', *Cell*, 67(1), pp. 11–19. doi:10.1016/0092-8674(91)90568-J.

Stamou, P. and Kontoyiannis, D.L. (2010) 'Posttranscriptional Regulation of TNF mRNA: A Paradigm of Signal-Dependent mRNA Utilization and Its Relevance to Pathology', in Kollias, G. and Sfikakis, P.P. (eds) *Current Directions in Autoimmunity*. Basel: KARGER, pp. 61–79. doi:10.1159/000289197.

Steinman, R.M. and Swanson, J.A. (1995) 'The endocytic activity of dendritic cells', *The Journal of Experimental Medicine*, 182(2), pp. 283–288.

Stoecklin, G. *et al.* (2004) 'MK2-induced tristetraprolin:14-3-3 complexes prevent stress granule association and ARE-mRNA decay', *The EMBO Journal*, 23(6), pp. 1313–1324. doi:10.1038/sj.emboj.7600163.

Strasser, J.E. *et al.* (1999) 'Regulation of the macrophage vacuolar ATPase and phagosome-lysosome fusion by Histoplasma capsulatum.', *Journal of immunology (Baltimore, Md. : 1950)*, 162(10), pp. 6148–54.

Strbo, N. *et al.* (2019) 'Single cell analyses reveal specific distribution of anti-bacterial molecule Perforin-2 in human skin and its modulation by wounding and Staphylococcus aureus infection', *Experimental Dermatology*, 28(3), pp. 225–232. doi:10.1111/exd.13870.

Strominger, L. *et al.* (1987) 'Structure of the human class I histocompatibility antigen, HLA-A2', *Nature*, 329(8), pp. 506–512.

Subramanian, A. *et al.* (2005) 'Gene set enrichment analysis: A knowledge-based approach for interpreting genome-wide expression profiles', *Proceedings of the National Academy of Sciences*, 102(43), pp. 15545–15550. doi:10.1073/pnas.0506580102.

Sudo, H. *et al.* (2014) 'AHNAK is highly expressed and plays a key role in cell migration and invasion in mesothelioma', *International Journal of Oncology*, 44(2), pp. 530–538. doi:10.3892/ijo.2013.2183.

Szostak, E. and Gebauer, F. (2013) 'Translational control by 3'-UTR-binding proteins', *Briefings in Functional Genomics*, 12(1), pp. 58–65. doi:10.1093/bfgp/els056.

Takeda, Y. *et al.* (2003) 'Tetraspanins CD9 and CD81 function to prevent the fusion of mononuclear phagocytes', *Journal of Cell Biology*, 161(5), pp. 945–956. doi:10.1083/jcb.200212031.

Takeuchi, O. and Akira, S. (2010) 'Pattern Recognition Receptors and Inflammation', *Cell*, 140(6), pp. 805–820. doi:10.1016/j.cell.2010.01.022.

Tanguy, E. *et al.* (2019) 'Regulation of Phospholipase D by Arf6 during FcγR-Mediated Phagocytosis', *The Journal of Immunology*, 202(10), pp. 2971–2981. doi:10.4049/jimmunol.1801019.

Teng, B.B., Burant, C.F. and Davidson, N.O. (1993) 'Molecular cloning of an apolipoprotein B messenger RNA editing protein', *Science*, 260(5115), pp. 1816–1819. doi:10.1126/science.8511591.

Thomas, C.A. *et al.* (2000) 'Protection from Lethal Gram-Positive Infection by Macrophage Scavenger Receptor–Dependent Phagocytosis', *The Journal of Experimental Medicine*, 191(1), pp. 147–156.

Tiedje, C. *et al.* (2012) 'The p38/MK2-Driven Exchange between Tristetraprolin and HuR Regulates AU–Rich Element–Dependent Translation', *PLoS Genetics*. Edited by P. Anderson, 8(9), p. e1002977. doi:10.1371/journal.pgen.1002977.

Tontanahal, A., Arvidsson, I. and Karpman, D. (2021) 'Annexin Induces Cellular Uptake of Extracellular Vesicles and Delays Disease in Escherichia coli O157:H7 Infection', *Microorganisms*, 9(6), pp. 1143–1143. doi:10.3390/microorganisms9061143.

Tsai, R.K. and Discher, D.E. (2008) 'Inhibition of "self" engulfment through deactivation of myosin-II at the phagocytic synapse between human cells', *Journal of Cell Biology*, 180(5), pp. 989–1003. doi:10.1083/jcb.200708043.

Uderhardt, S. *et al.* (2012) '12/15-Lipoxygenase Orchestrates the Clearance of Apoptotic Cells and Maintains Immunologic Tolerance', *Immunity*, 36(5), pp. 834–846. doi:10.1016/j.immuni.2012.03.010.

Underhill, D.M. and Goodridge, H.S. (2012) 'Information processing during phagocytosis', *Nature Reviews Immunology*, 12(7), pp. 492–502. doi:10.1038/nri3244.

Uribe-Querol, E. and Rosales, C. (2020) 'Phagocytosis: Our Current Understanding of a Universal Biological Process', *Frontiers in Immunology*, 11(June), pp. 1–13. doi:10.3389/fimmu.2020.01066.

Van Gool, S. *et al.* (1997) 'CD80, CD86 and CD40 provide accessory signals in a multiple-step T-cell activation model', *Immunological reviews.*, 153(1), pp. 47–83. doi:10.1111/j.1600-065x.1996.tb00920.x.

Vats, D. *et al.* (2006) 'Oxidative metabolism and PGC-1β attenuate macrophage-mediated inflammation', *Cell metabolism*, 4(1), pp. 13–24. doi:10.1016/j.cmet.2006.05.011.

Velten, L. *et al.* (2017) 'Human haematopoietic stem cell lineage commitment is a continuous process', *Nature Cell Biology*, 19(4), pp. 271–281. doi:10.1038/ncb3493.

Vieira, O.V. *et al.* (2003) 'Modulation of Rab5 and Rab7 Recruitment to Phagosomes by Phosphatidylinositol 3-Kinase', *Molecular and Cellular Biology*, 23(7), pp. 2501–2514. doi:10.1128/mcb.23.7.2501-2514.2003.

Viola, A. *et al.* (2019) 'The Metabolic Signature of Macrophage Responses', *Frontiers in Immunology*, 10(JULY), pp. 1–16. doi:10.3389/fimmu.2019.01462.

Virtanen, P. *et al.* (2020) 'SciPy 1.0: fundamental algorithms for scientific computing in Python', *Nature Methods*, 17(3), pp. 261–272. doi:10.1038/s41592-019-0686-2.

Vogel, C. *et al.* (2010) 'Sequence signatures and mRNA concentration can explain two-thirds of protein abundance variation in a human cell line', *Molecular Systems Biology*, 6, p. 400. doi:10.1038/msb.2010.59.

Vyas, K. *et al.* (2009) 'Genome-Wide Polysome Profiling Reveals an Inflammation-Responsive Posttranscriptional Operon in Gamma Interferon-Activated Monocytes', *Molecular and Cellular Biology*, 29(2), pp. 458–470. doi:10.1128/MCB.00824-08.

Wang, I.X. *et al.* (2013) 'ADAR Regulates RNA Editing, Transcript Stability, and Gene Expression', *Cell Reports*, 5(3), pp. 849–860. doi:10.1016/j.celrep.2013.10.002.

Wang, X. *et al.* (2016) *Epigenetic regulation of macrophage polarization and inflammation by DNA methylation in obesity*. American Society for Clinical Investigation. doi:10.1172/jci.insight.87748.

Waskom, M.L. (2021) 'seaborn: statistical data visualization', *Journal of Open Source Software*, 6(60), p. 3021. doi:10.21105/joss.03021.

Wells, S.E. *et al.* (1998) 'Circularization of mRNA by Eukaryotic Translation Initiation Factors', *Molecular Cell*, 2(1), pp. 135–140. doi:10.1016/S1097-2765(00)80122-7.

Whelan, F.J. *et al.* (2012) 'The evolution of the class A scavenger receptors', *BMC Evolutionary Biology*, 12, p. 227. doi:10.1186/1471-2148-12-227.

Wickham, H. (2009) *ggplot2: Elegant Graphics for Data Analysis*. New York: Springer-Verlag (Use R!). doi:10.1007/978-0-387-98141-3.

Wilkins, C. and Gale, M. (2010) 'Recognition of viruses by cytoplasmic sensors', *Current Opinion in Immunology*, 22(1), pp. 41–47. doi:10.1016/j.coi.2009.12.003.

Wink, D.A. *et al.* (2011) 'Nitric oxide and redox mechanisms in the immune response', *Journal of Leukocyte Biology*, 89(6), pp. 873–891. doi:10.1189/jlb.1010550.

Winterbourn, C.C. and Kettle, A.J. (2013) 'Redox reactions and microbial killing in the neutrophil phagosome', *Antioxidants and Redox Signaling*, 18(6), pp. 642–660. doi:10.1089/ars.2012.4827.

Wiśniewski, J.R. *et al.* (2014) 'A "Proteomic Ruler" for Protein Copy Number and Concentration Estimation without Spike-in Standards', *Molecular & Cellular Proteomics : MCP*, 13(12), pp. 3497–3506. doi:10.1074/mcp.M113.037309.

Wolf, A.A. *et al.* (2019) 'The Ontogeny of Monocyte Subsets', *Frontiers in Immunology*, 10, p. 1642. doi:10.3389/fimmu.2019.01642.

Wu, L. *et al.* (2013) 'Variation and genetic control of protein abundance in humans', *Nature*, 499(7456), pp. 79–82. doi:10.1038/nature12223.

Wu, R. *et al.* (2016) 'N 6-Methyladenosine (m6A) Methylation in mRNA with A Dynamic and Reversible Epigenetic Modification', *Molecular Biotechnology*, 58(7), pp. 450–459. doi:10.1007/s12033-016-9947-9.

Wynn, T. a., Chawla, A. and Pollard, J.W. (2013) 'Origins and Hallmarks of Macrophages: Development, Homeostasis, and Disease', *Nature*, 496(7446), pp. 445–455. doi:10.1038/nature12034.Origins.

Wynn, T.A., Chawla, A. and Pollard, J.W. (2013) 'Macrophage biology in development, homeostasis and disease', *Nature*, 496(7446), pp. 445–455. doi:10.1038/nature12034.

Wynn, T.A. and Vannella, K.M. (2016) 'Macrophages in Tissue Repair, Regeneration, and Fibrosis', *Immunity*, 44(3), pp. 450–462. doi:10.1016/j.immuni.2016.02.015.

Xia, Y. *et al.* (2019) 'The macrophage-specific V-ATPase subunit ATP6V0D2 restricts inflammasome activation and bacterial infection by facilitating autophagosome-lysosome fusion', *Autophagy*, 15(6), pp. 960–975. doi:10.1080/15548627.2019.1569916.

Xing, L. and Bassell, G.J. (2013) 'mRNA Localization: An Orchestration of Assembly, Traffic and Synthesis', *Traffic*, 14(1), pp. 2–14. doi:10.1111/tra.12004.

Xu, Z. *et al.* (2021) 'Suppression of Experimental Autoimmune Encephalomyelitis by ILT3.Fc', *The Journal of Immunology*, 206(3), pp. 554–565. doi:10.4049/jimmunol.2000265.

Xue, J. *et al.* (2014) 'Transcriptome-Based Network Analysis Reveals a Spectrum Model of Human Macrophage Activation', *Immunity*, 40(2), pp. 274–288. doi:10.1016/j.immuni.2014.01.006.

Yamanaka, S. *et al.* (1997) 'A novel translational repressor mRNA is edited extensively in livers containing tumors caused by the transgene expression of the apoB mRNA-editing enzyme.', *Genes & Development*, 11(3), pp. 321–333. doi:10.1101/gad.11.3.321.

Yamasaki, S. *et al.* (2007) 'T-cell Intracellular Antigen-1 (TIA-1)-induced Translational Silencing Promotes the Decay of Selected mRNAs', *Journal of Biological Chemistry*, 282(41), pp. 30070–30077. doi:10.1074/jbc.M706273200.

Yan, M. *et al.* (2005) 'Coronin-1 Function Is Required for Phagosome Formation', *Molecular Biology of the Cell*, 16(7), pp. 3077–3087. doi:10.1091/mbc.e04-11-0989.

Yáñez, A. *et al.* (2017) 'Granulocyte-Monocyte Progenitors and Monocyte-Dendritic Cell Progenitors Independently Produce Functionally Distinct Monocytes', *Immunity*, 47(5), pp. 890-902.e4. doi:10.1016/j.immuni.2017.10.021.

Yang, C.-C. *et al.* (2017) 'ADAR1-mediated 3' UTR editing and expression control of antiapoptosis genes fine-tunes cellular apoptosis response', *Cell Death and Disease*, 8(5), pp. e2833–e2833. doi:10.1038/cddis.2017.12.

Yang, W. *et al.* (2006) 'Modulation of microRNA processing and expression through RNA editing by ADAR deaminases', *Nature structural & molecular biology*, 13(1), pp. 13–21. doi:10.1038/nsmb1041.

Yao, Z. and McLeod, R.S. (1994) 'Synthesis and secretion of hepatic apolipoprotein B-containing lipoproteins', *Biochimica et Biophysica Acta (BBA)/Lipids and Lipid Metabolism*, 1212(2), pp. 152–166. doi:10.1016/0005-2760(94)90249-6.

Yates, R.M., Hermetter, A. and Russell, D.G. (2005) 'The Kinetics of Phagosome Maturation as a Function of Phagosome/Lysosome Fusion and Acquisition of Hydrolytic Activity: Assays of Phagosome Maturation', *Traffic*, 6(5), pp. 413–420. doi:10.1111/j.1600-0854.2005.00284.x.

Yona, S. *et al.* (2006) 'Impaired phagocytic mechanism in annexin 1 null macrophages', *British Journal of Pharmacology*, 148(4), pp. 469–477. doi:10.1038/sj.bjp.0706730.

Yona, S. *et al.* (2013) 'Fate Mapping Reveals Origins and Dynamics of Monocytes and Tissue Macrophages under Homeostasis', *Immunity*. Edited by P.A. de Alarcón and E.J. Werner, 38(1), pp. 79–91. doi:10.1016/j.immuni.2012.12.001.

Yoneyama, M. *et al.* (2004) 'The RNA helicase RIG-I has an essential function in double-stranded RNA-induced innate antiviral responses', *Nature Immunology*, 5(7), pp. 730–737. doi:10.1038/ni1087.

Young, S.G. (1990) 'Recent progress in understanding apolipoprotein B.', *Circulation*, 82(5), pp. 1574–1594. doi:10.1161/01.CIR.82.5.1574.

Yu, G. *et al.* (2012) 'clusterProfiler: an R Package for Comparing Biological Themes Among Gene Clusters', *OMICS: A Journal of Integrative Biology*, 16(5), pp. 284–287. doi:10.1089/omi.2011.0118.

Yu, J. *et al.* (2009) 'Reticulon 4B (Nogo-B) is necessary for macrophage infiltration and tissue repair', *Proceedings of the National Academy of Sciences of the United States of America*, 106(41), pp. 17511–17516. doi:10.1073/pnas.0907359106.

Yue, Y., Liu, J. and He, C. (2015) 'RNA N6-methyladenosine methylation in post-transcriptional gene expression regulation', *Genes & Development*, 29(13), pp. 1343–1355. doi:10.1101/gad.262766.115.

Yunna, C. *et al.* (2020) 'Macrophage M1/M2 polarization', *European Journal of Pharmacology*, 877, p. 173090. doi:10.1016/j.ejphar.2020.173090.

Zawawi, K.H. *et al.* (2010) 'Moesin-induced signaling in response to lipopolysaccharide in macrophages', *Journal of Periodontal Research*, 45(5), pp. 589–601. doi:10.1111/j.1600-0765.2010.01271.x.

Zhang, B. *et al.* (2018) 'Arf1 regulates the ER –mitochondria encounter structure ( ERMES ) in a reactive oxygen species-dependent manner', *The FEBS Journal*, 285(11), pp. 2004–2018. doi:10.1111/febs.14445.

Zhang, Y. *et al.* (2014) 'An RNA-Sequencing Transcriptome and Splicing Database of Glia, Neurons, and Vascular Cells of the Cerebral Cortex', *Journal of Neuroscience*, 34(36), pp. 11929–11947. doi:10.1523/JNEUROSCI.1860-14.2014.

Zhang, Y. *et al.* (2017) 'Upregulation of PD-L1 by SPP1 mediates macrophage polarization and facilitates immune escape in lung adenocarcinoma', *Experimental Cell Research*, 359(2), pp. 449–457. doi:10.1016/j.yexcr.2017.08.028.

Zimmermann, P. *et al.* (2001) 'Characterization of syntenin, a syndecan-binding PDZ protein, as a component of cell adhesion sites and microfilaments', *Molecular Biology of the Cell*, 12(2), pp. 339–350. doi:10.1091/mbc.12.2.339.

# 8 Appendix

| position | adjusted_pval | |
|---|---|---|
| chr5_104440908 | 9.63E-05 | spp1 |
| chrX_9437096 | 0.000168 | cybb |
| chr5_104440840 | 0.000304 | spp1 |
| chr5_104440953 | 0.000355 | spp1 |
| chr2_122152902 | 0.001506 | b2m |
| chr14_75230678 | 0.001802 | lcp1 |
| chr5_104440853 | 0.00196 | spp1 |
| chrX_9436542 | 0.002807 | cybb |
| chr5_104440859 | 0.007245 | spp1 |
| chr7_16247630 | 0.009381 | C5ar |
| chrX_9435591 | 0.009381 | cybb |
| chrX_9437487 | 0.009381 | cybb |
| chr9_58651953 | 0.009381 | nptn |
| chr1_165774490 | 0.011747 | Creg1 |
| chrX_9437473 | 0.013169 | cybb |
| chr1_63179557 | 0.013169 | Eef1b2 |
| chrX_9437680 | 0.014015 | cybb |
| chrX_9437102 | 0.015436 | cybb |
| chrX_9437409 | 0.015436 | cybb |
| chr19_3949249 | 0.016415 | UNC93B1 |
| chr3_144596946 | 0.017823 | Selenof |
| chr2_122152740 | 0.020916 | b2m |
| chr17_57483462 | 0.024073 | Adgre1 |
| chr1_165774559 | 0.027587 | Creg1 |
| chr2_122152871 | 0.034401 | b2m |
| chr19_34493295 | 0.034401 | lipa |
| chr17_57483199 | 0.035252 | Adgre1 |
| chr14_73362471 | 0.036074 | Itm2b |
| chr10_117277360 | 0.037971 | lyz2 |
| chrX_9436496 | 0.039636 | cybb |
| chrX_9436580 | 0.039636 | cybb |
| chrX_9437668 | 0.039636 | cybb |
| chr19_12464694 | 0.039636 | Mpeg1 |
| chr11_29742625 | 0.039636 | Rtn4 |
| chr4_6395221 | 0.039636 | Sdcbp |
| chr14_63144668 | 0.039776 | Ctsb |
| chrX_9435570 | 0.041577 | cybb |
| chrX_9437630 | 0.041577 | cybb |
| chr19_20373571 | 0.042091 | Anxa1 |
| chr3_36449144 | 0.042091 | Anxa5 |
| chr11_59211597 | 0.042091 | Arf1 |
| chr2_122152763 | 0.042091 | b2m |

| | | |
|---|---|---|
| chrX_9436535 | 0.042091 | cybb |
| chrX_9436570 | 0.042091 | cybb |
| chrX_9436601 | 0.042091 | cybb |
| chrX_9437257 | 0.042091 | cybb |
| chrX_9437723 | 0.042091 | cybb |
| chr14_73362665 | 0.042091 | Itm2b |
| chr14_73362671 | 0.042091 | Itm2b |
| chr8_13174696 | 0.042091 | Lamp1 |
| chr19_34492587 | 0.042091 | Lipa |
| chr6_122317195 | 0.042091 | M6pr |
| chrX_96168043 | 0.042091 | Msn |
| chr11_29742725 | 0.042091 | Rtn4 |
| chr3_144596912 | 0.042091 | Selenof |
| chr15_3279914 | 0.042091 | Selenop |
| chr6_35509577 | 0.042495 | Mtpn |
| chr3_36449183 | 0.043131 | Anxa5 |
| chr19_12464639 | 0.043131 | Mpeg1 |
| chrX_9437635 | 0.043686 | cybb |
| chr14_63143075 | 0.044602 | Ctsb |
| chr19_9015769 | 0.044973 | Ahnak |
| chrX_9435719 | 0.044973 | cybb |
| chr6_125460633 | 0.048907 | Cd9 |
| chr17_57483451 | 0.049495 | Adgre1 |
| chr8_13174689 | 0.049495 | Lamp1 |
| chr7_111072211 | 0.049826 | Eif4g2 |

Table S 1 Transcripts with positional editing changes after stimulation in BMDMs.

Calculated with one way ANOVA $p < 0.05$

| position | adjusted_pval | gene |
|---|---|---|
| chr16_44087323 | 3.27E-07 | Atp6v1a |
| chr4_6395365 | 1.21E-06 | Sdcbp |
| chr2_126890834 | 1.21E-06 | Sppl2a |
| chrX_12616481 | 2.70E-06 | Atp6ap2 |
| chrX_96167976 | 2.70E-06 | Msn |
| chr3_144597438 | 2.70E-06 | Selenof |
| chr16_32632307 | 3.23E-06 | Tfrc |
| chr3_144597442 | 3.41E-06 | Selenof |
| chr2_151561326 | 4.79E-06 | Fkbp1a |
| chr3_65379869 | 1.19E-05 | Ssr3 |
| chr15_99408620 | 1.28E-05 | Tmbim6 |
| chr15_4154093 | 1.48E-05 | Oxct1 |
| chrX_109162174 | 1.99E-05 | Sh3bgrl |
| chrX_38421565 | 2.01E-05 | Lamp2 |
| chr12_54645900 | 2.01E-05 | Sptssa |

| | | |
|---|---|---|
| chr3_36449126 | 2.18E-05 | Anxa5 |
| chr4_6394955 | 2.18E-05 | Sdcbp |
| chr6_52546355 | 2.38E-05 | Hibadh |
| chr7_128697852 | 2.38E-05 | Mcmbp |
| chr7_99839094 | 2.38E-05 | Spcs2 |
| chr3_60628677 | 3.14E-05 | Mbnl1 |
| chr9_58652207 | 4.00E-05 | Nptn |
| chrX_74304364 | 5.60E-05 | Atp6ap1 |
| chr5_108122658 | 6.21E-05 | Tmed5 |
| chr6_86737465 | 6.57E-05 | Anxa4 |
| chrX_57232897 | 6.57E-05 | Arhgef6 |
| chrX_12616387 | 6.57E-05 | Atp6ap2 |
| chrX_109160420 | 6.57E-05 | Sh3bgrl |
| chr2_122152804 | 8.12E-05 | B2m |
| chrX_75786161 | 9.01E-05 | Pls3 |
| chrX_53021354 | 9.39E-05 | Hprt |
| chr1_160203055 | 0.000135 | Cacybp |
| chr15_38691904 | 0.000141 | Atp6v1c1 |
| chr9_88453092 | 0.000141 | Syncrip |
| chr2_73093495 | 0.000165 | Ola1 |
| chr4_107200739 | 0.000191 | Tmem59 |
| chr18_46587938 | 0.000193 | Tmed7 |
| chr2_151560843 | 0.000212 | Fkbp1a |
| chr3_95947171 | 0.00023 | Anp32e |
| chrX_75786156 | 0.00025 | Pls3 |
| chr13_48879731 | 0.000273 | Fam120a |
| chr11_20064345 | 0.000301 | Actr2 |
| chrX_12615988 | 0.000301 | Atp6ap2 |
| chrX_73686405 | 0.000301 | Bcap31 |
| chr14_75229549 | 0.000301 | Lcp1 |
| chr3_103067494 | 0.000301 | Nras |
| chr9_52086866 | 0.000301 | Rdx |
| chr3_8930700 | 0.000301 | Tpd52 |
| chr19_20373556 | 0.000308 | Anxa1 |
| chrX_142238684 | 0.000357 | Nxt2 |
| chr14_122158980 | 0.000357 | Tm9sf2 |
| chr1_71579139 | 0.000358 | Atic |
| chr6_86737574 | 0.000381 | Anxa4 |
| chr1_156429956 | 0.000381 | Soat1 |
| chr9_71845716 | 0.000498 | Tcf12 |
| chrX_53021282 | 0.000511 | Hprt |
| chr13_12440288 | 0.000551 | Lgals8 |
| chr7_114215802 | 0.00057 | Copb1 |
| chr5_124549772 | 0.00057 | Tmed2 |
| chr6_51589202 | 0.000705 | Snx10 |
| chrX_38420630 | 0.001453 | Lamp2 |

| | | |
|---|---|---|
| chrX_134606646 | 0.001514 | Hnrnph2 |
| chr9_56136180 | 0.001751 | Tspan3 |
| chr18_38464647 | 0.001837 | Ndfip1 |
| chr9_58652474 | 0.00197 | Nptn |
| chr2_122595412 | 0.002419 | Gatm |
| chr3_8930119 | 0.002636 | Tpd52 |
| chrX_73686399 | 0.002818 | Bcap31 |
| chr16_84954817 | 0.003405 | App |
| chr12_70467236 | 0.003405 | Tmx1 |
| chr2_109897906 | 0.003592 | Lin7c |
| chr1_182276405 | 0.003787 | Degs1 |
| chr6_17105467 | 0.004195 | Tes&Gm4876 |
| chr5_108122830 | 0.004287 | Tmed5 |
| chrX_38421335 | 0.005198 | Lamp2 |
| chr11_20062532 | 0.005275 | Actr2 |
| chr16_84954841 | 0.006751 | App |
| chr15_93285265 | 0.009409 | Yaf2 |
| chrX_38420739 | 0.017594 | Lamp2 |
| chr3_107664031 | 0.020015 | Ahcyl1 |
| chr16_84954868 | 0.022029 | App |
| chr3_108581894 | 0.030356 | Taf13 |
| chr1_162594878 | 0.038338 | Vamp4 |
| chr10_88743572 | 0.047671 | Arl1 |
| chr6_3600213 | 0.048282 | Vps50 |

Table S 2 Edited positions that change with LPS stimulation in RAW 264.7 cells.

Positions determined by one way ANOVA $p < 0.05$

| Gene | cluster |
|---|---|
| 9530068E07Rik | 1 |
| Acadsb | 1 |
| Adam10 | 1 |
| Adam9 | 1 |
| Adi1 | 1 |
| Ahcyl1 | 1 |
| Alg10b | 1 |
| Aplp2 | 1 |
| Arsb | 1 |
| Atp6v1a | 1 |
| Atp6v1g1 | 1 |
| Bc1 | 1 |
| Bcap29 | 1 |
| Cadm1 | 1 |
| Calm2 | 1 |
| Calu | 1 |
| Ccng1 | 1 |
| Ccni | 1 |
| Celf2 | 1 |
| Cltc | 1 |
| Coa5 | 1 |
| Colec12 | 1 |
| Csnk1a1 | 1 |
| Ctnna1 | 1 |
| Ctnnb1 | 1 |
| Dpp8 | 1 |
| Eif4g2 | 1 |
| Fam120a | 1 |
| Fkbp1a | 1 |
| Gatm | 1 |
| H3f3a | 1 |
| Hibadh | 1 |
| Hmgb1 | 1 |
| Hnrnpc | 1 |
| Hprt | 1 |
| Isoc1 | 1 |
| Itga4 | 1 |
| Kdm1b | 1 |
| Lamp1 | 1 |
| Lbr | 1 |
| Lcp1 | 1 |
| Lpl | 1 |
| Mcm4 | 1 |
| Memo1 | 1 |
| Ndfip1 | 1 |

| | |
|---|---|
| Nucks1 | 1 |
| Paics | 1 |
| Pclaf | 1 |
| Pign | 1 |
| Prkar1a | 1 |
| Prps1 | 1 |
| Prps2 | 1 |
| Ptbp3 | 1 |
| Rab18 | 1 |
| Rcn2 | 1 |
| Rhoa | 1 |
| Rtn3 | 1 |
| Septin11 | 1 |
| Serbp1 | 1 |
| Sfpq | 1 |
| Slc35a3 | 1 |
| Slc44a1 | 1 |
| Soat1 | 1 |
| Spcs3 | 1 |
| Spp1 | 1 |
| Ssr1 | 1 |
| Ssr3 | 1 |
| Sypl | 1 |
| Tcea1 | 1 |
| Tfrc | 1 |
| Tmed7 | 1 |
| Tmx3 | 1 |
| Tnpo1 | 1 |
| Tpd52 | 1 |
| Tram1 | 1 |
| Trip4 | 1 |
| Tspan3 | 1 |
| Twsg1 | 1 |
| Ugdh | 1 |
| Vbp1 | 1 |
| Xpr1 | 1 |
| Adk | 2 |
| Aldoc | 2 |
| Arl8b | 2 |
| Atl3 | 2 |
| Commd10 | 2 |
| Csgalnact2 | 2 |
| Edil3 | 2 |
| Fundc1 | 2 |
| Gls | 2 |
| Hmgn5 | 2 |

| | |
|---|---|
| Impad1 | 2 |
| Klhl5 | 2 |
| Magt1 | 2 |
| Mmgt1 | 2 |
| Naa50 | 2 |
| Nap1l1 | 2 |
| Nnt | 2 |
| Pcnp | 2 |
| Pdha1 | 2 |
| Prkacb | 2 |
| Rab10 | 2 |
| Rab10os | 2 |
| Sdha | 2 |
| Slc39a10 | 2 |
| Sms | 2 |
| Sppl2a | 2 |
| Syncrip | 2 |
| Tmem64 | 2 |
| Ube2e3 | 2 |
| Anp32e | 3 |
| Anxa4 | 3 |
| Anxa5 | 3 |
| App | 3 |
| Atp6ap2 | 3 |
| B2m | 3 |
| Bcap31 | 3 |
| Cd9 | 3 |
| Cmpk1 | 3 |
| Dek | 3 |
| Dynlt3 | 3 |
| Lamp2 | 3 |
| Lypla1 | 3 |
| Mbnl1 | 3 |
| Msn | 3 |
| Mtpn | 3 |
| Nptn | 3 |
| Nxt2 | 3 |
| Oxct1 | 3 |
| Pls3 | 3 |
| Rab7 | 3 |
| Rac1 | 3 |
| Rpe | 3 |
| Sdcbp | 3 |
| Selenof | 3 |
| Selenot | 3 |
| Septin2 | 3 |

| | |
|---|---|
| Serinc3 | 3 |
| Sh3bgrl | 3 |
| Sptssa | 3 |
| Tmed5 | 3 |
| Tmem123 | 3 |
| Tmem30a | 3 |
| Cybb | 4 |
| H2-D1 | 4 |
| H2-L | 4 |
| Ifi207 | 4 |
| Lilr4b | 4 |
| Ms4a6c | 4 |

Table S 3 Genes with differential number of editing sites after LPS stimulation.

Table shows gene name and cluster from Figure 11

| Annotation Cluster 1 | Enrichment Score: 1.916764112765253 | | | |
|---|---|---|---|---|
| Category | Term | PValue | Fold Enrichment | FDR |
| INTERPRO | IPR001680:WD40 repeat | 0.001362 | 4.16482 | 1.764891 |
| SMART | SM00320:WD40 | 0.001952 | 3.839597 | 1.910658 |
| INTERPRO | IPR017986:WD40-repeat-containing domain | 0.002927 | 3.68486 | 3.75652 |
| INTERPRO | IPR015943:WD40/YVTN repeat-like-containing domain | 0.004706 | 3.406279 | 5.976335 |
| UP_SEQ_FEATURE | repeat:WD 3 | 0.004896 | 3.799244 | 6.502403 |
| UP_SEQ_FEATURE | repeat:WD 2 | 0.005393 | 3.731702 | 7.140358 |
| UP_SEQ_FEATURE | repeat:WD 1 | 0.005393 | 3.731702 | 7.140358 |
| UP_KEYWORDS | WD repeat | 0.005833 | 3.687224 | 6.725006 |
| UP_SEQ_FEATURE | repeat:WD 4 | 0.046979 | 3.027523 | 48.27404 |
| UP_SEQ_FEATURE | repeat:WD 5 | 0.109707 | 2.719019 | 79.64804 |
| INTERPRO | IPR019775:WD40 repeat, conserved site | 0.148526 | 2.976658 | 87.75911 |
| UP_SEQ_FEATURE | repeat:WD 6 | 0.428369 | 2.044561 | 99.95295 |
| | | | | |
| Annotation Cluster 2 | Enrichment Score: 1.0942437272747987 | | | |
| Category | Term | PValue | Fold Enrichment | FDR |
| GOTERM_BP_DIRECT | GO:0051028~mRNA transport | 0.037035 | 5.396016 | 42.05663 |
| UP_KEYWORDS | mRNA transport | 0.037713 | 5.371512 | 36.7116 |
| KEGG_PATHWAY | mmu03013:RNA transport | 0.373388 | 2.263081 | 99.40694 |
| | | | | |
| Annotation Cluster 3 | Enrichment Score: 0.9363078417752105 | | | |
| Category | Term | PValue | Fold Enrichment | FDR |
| UP_KEYWORDS | Lysosome | 0.046835 | 3.035529 | 43.49332 |
| GOTERM_CC_DIRECT | GO:0005764~lysosome | 0.108129 | 2.361072 | 75.44487 |
| GOTERM_CC_DIRECT | GO:0005765~lysosomal membrane | 0.30659 | 2.04472 | 98.88121 |

Table S 4. Annotation Clusters for categorial pathway analysis ADAR1 editing.

Done with Database for Annotation, visualization and Intregrated Discovery (DAVID)(Dennis *et al.*, 2003)

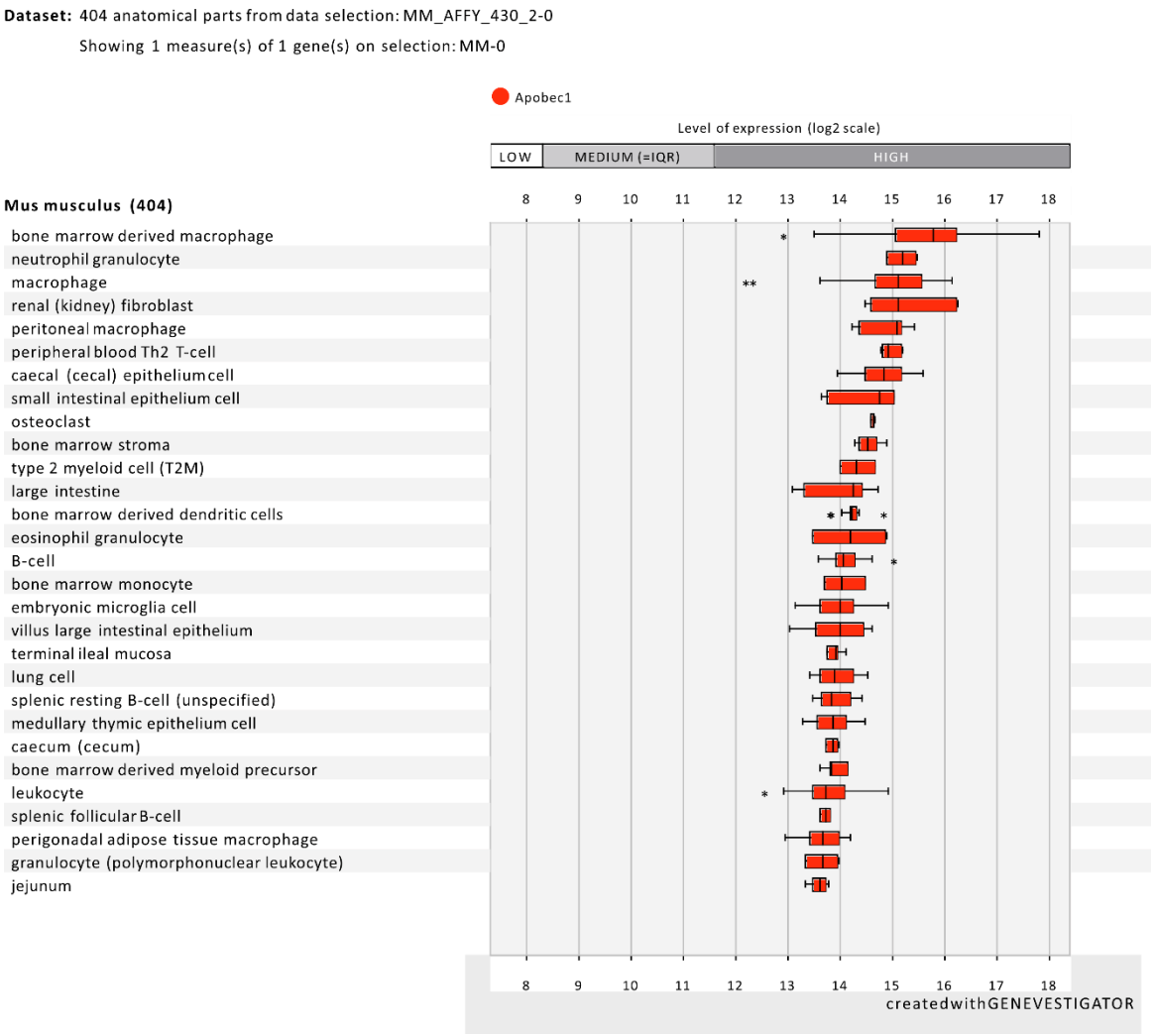


Figure S 1 Expression of APOBEC1 in different mouse tissues.

Figure shows only the topmost expressing cell types, 404 different tissues were included in the analysis.

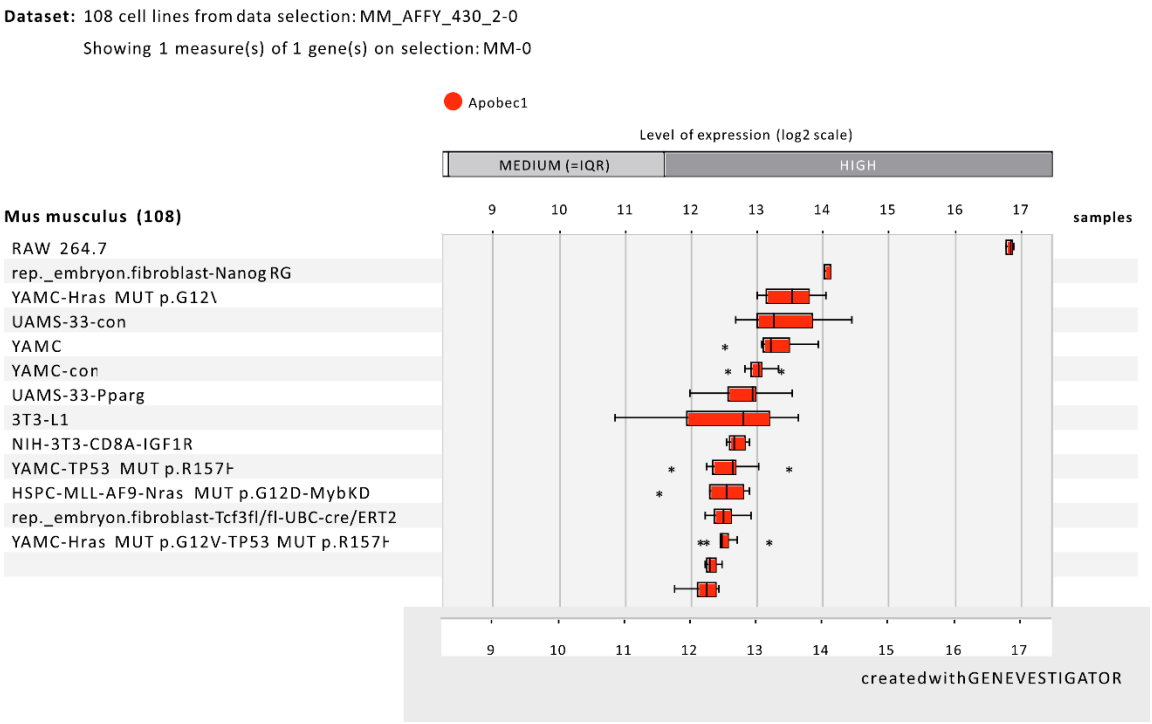


Figure S 2 Expression of APOBEC1 in different mouse cell line.

Figure shows only the top most expressing cell types, 108 different cell lines were included in the analysis

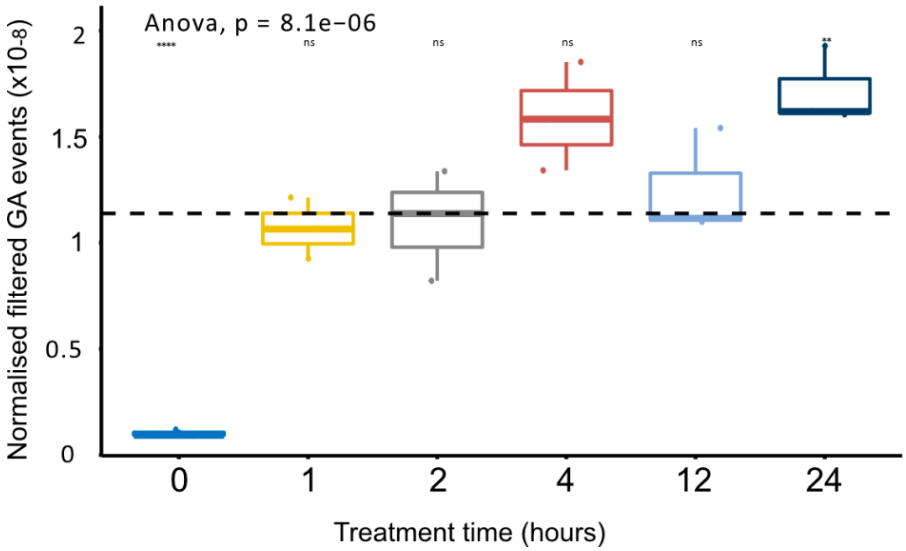


Figure S 3 G-to-A changes in RAW cell activation.

GA events were determined from REDItools tables from RAW 264.7 sequencing comparing WT and A1 KO. One way ANOVA shows an increase in GA levels after the first hour and levels remain without significant change between other time points. Dotted lean indicates mean normalised number of events.

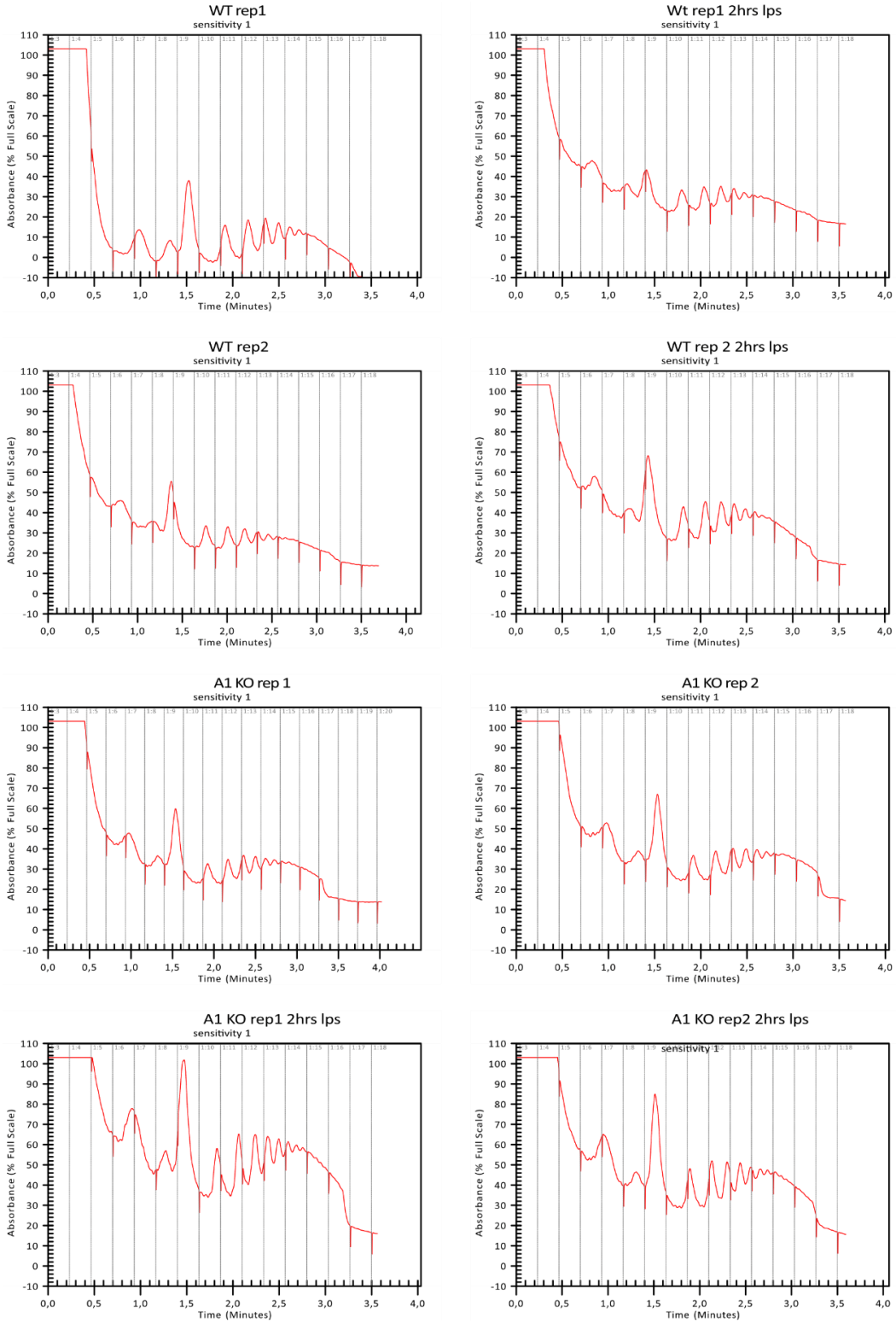


Figure S 4 Polysome profiles of WT and A1 KO RAW 264.7.

Cells were either stimulated for 2 hours with 100ng/ml LPS and 100U/ml IFN-γ. Samples are representative and are from one independent repetition

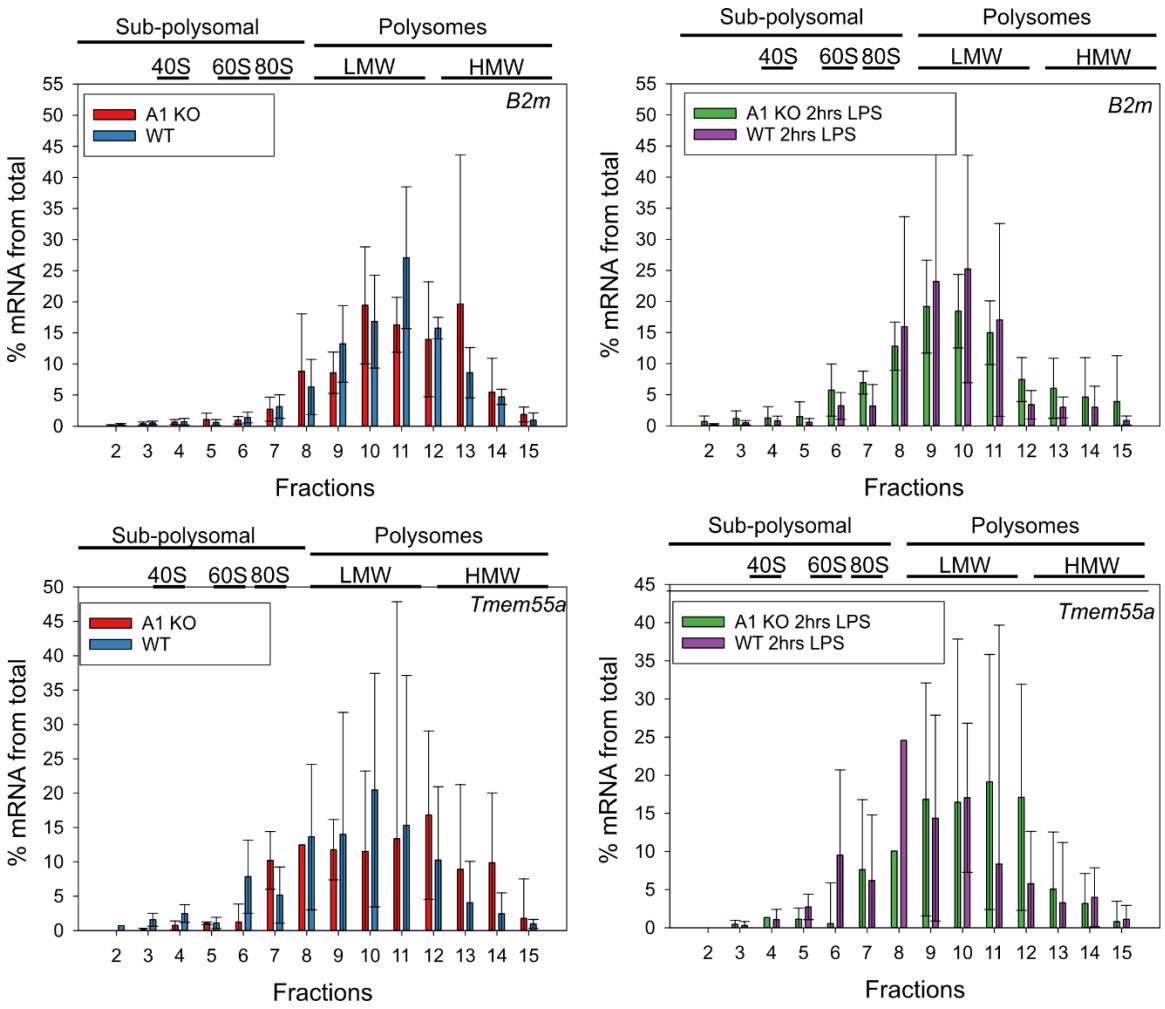


Figure S 5 Editing increases translational efficiency in a subset of targets.

mRNA distributions of B2m (top) and Tmem55a (bottom). determined by RT-qPCR from RNA extracted from polysome fractionations.Data shows percentage calculated from 5 replicates, RT-qPCR of each done in triplicates. Error bars show standard deviation.

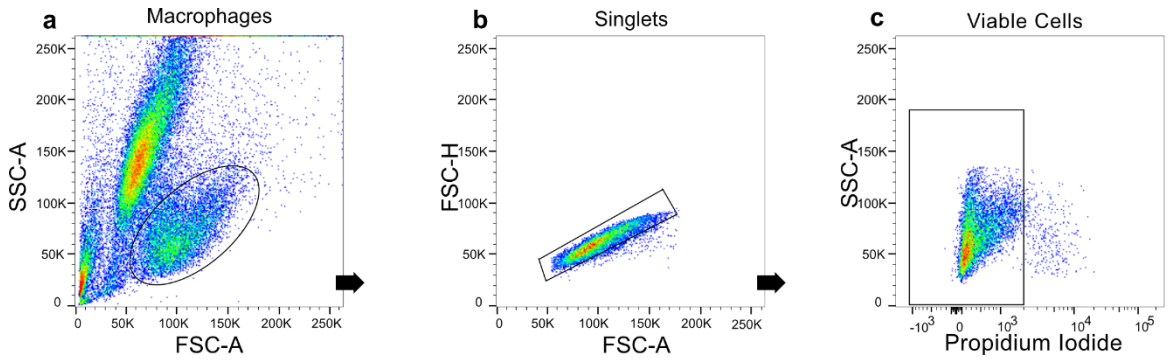


Figure S 6 Gating strategy of RAW 264.7 cells

Example of gating strategy for RAW cells for flow cytometry. a macrophage population identified; second larger population consists of dead cells. b singlet selections c. Viable cells are selected by low staining with propidium iodide or with live dead fixabe violet.

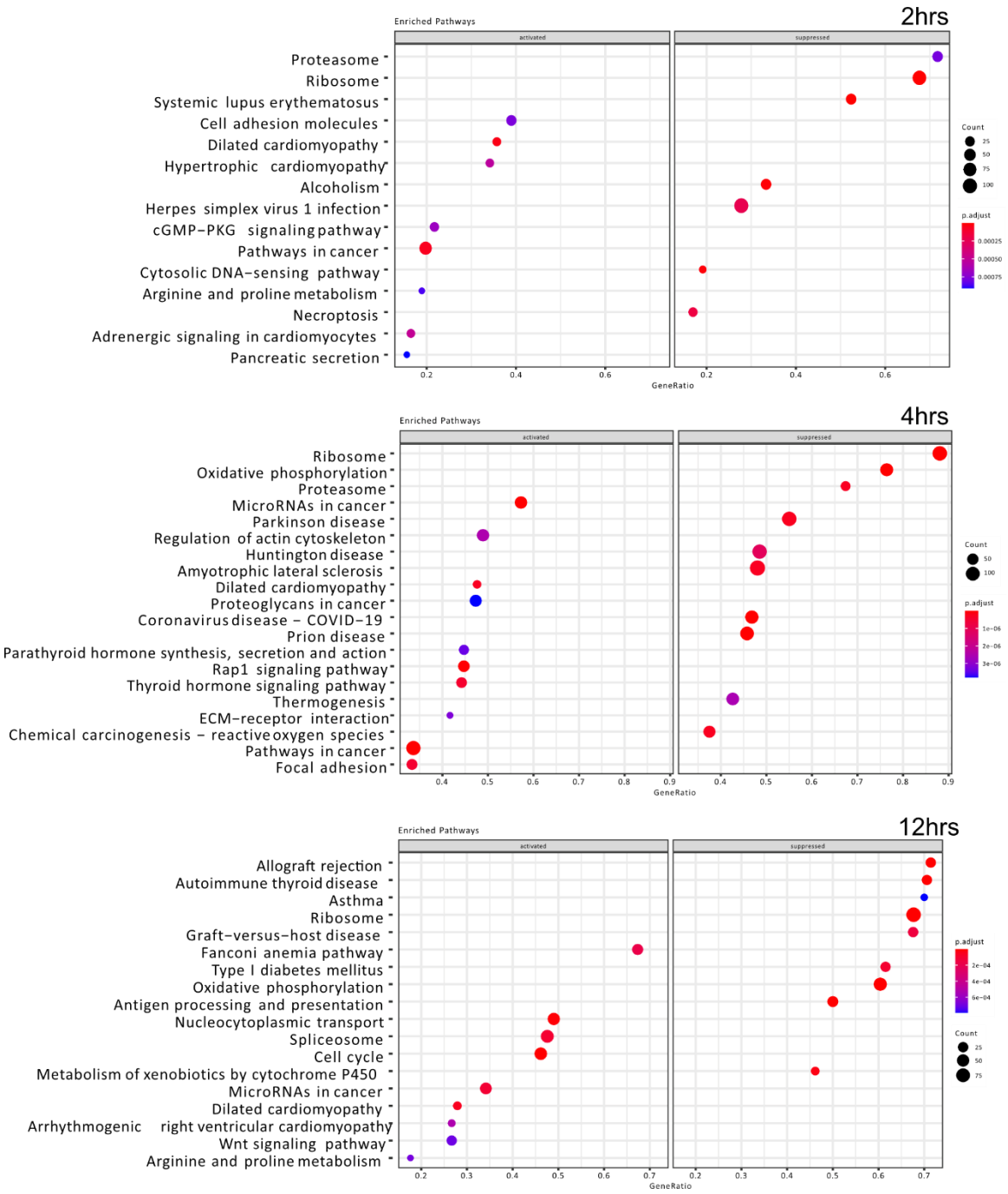


Figure S 7 A1 KO induced differential expression during stimulation

KEGG pathway Gene Set Enrichment analysis of WT vs A1 KO raw 264.7 cells after incubation with 100ng/ml LPS and 100U/ml IFN-γ. After 2,4 and 12 hours. P values corrected with Benjamini-Hochberg correction. FDR < 0.0001 FC > 3.

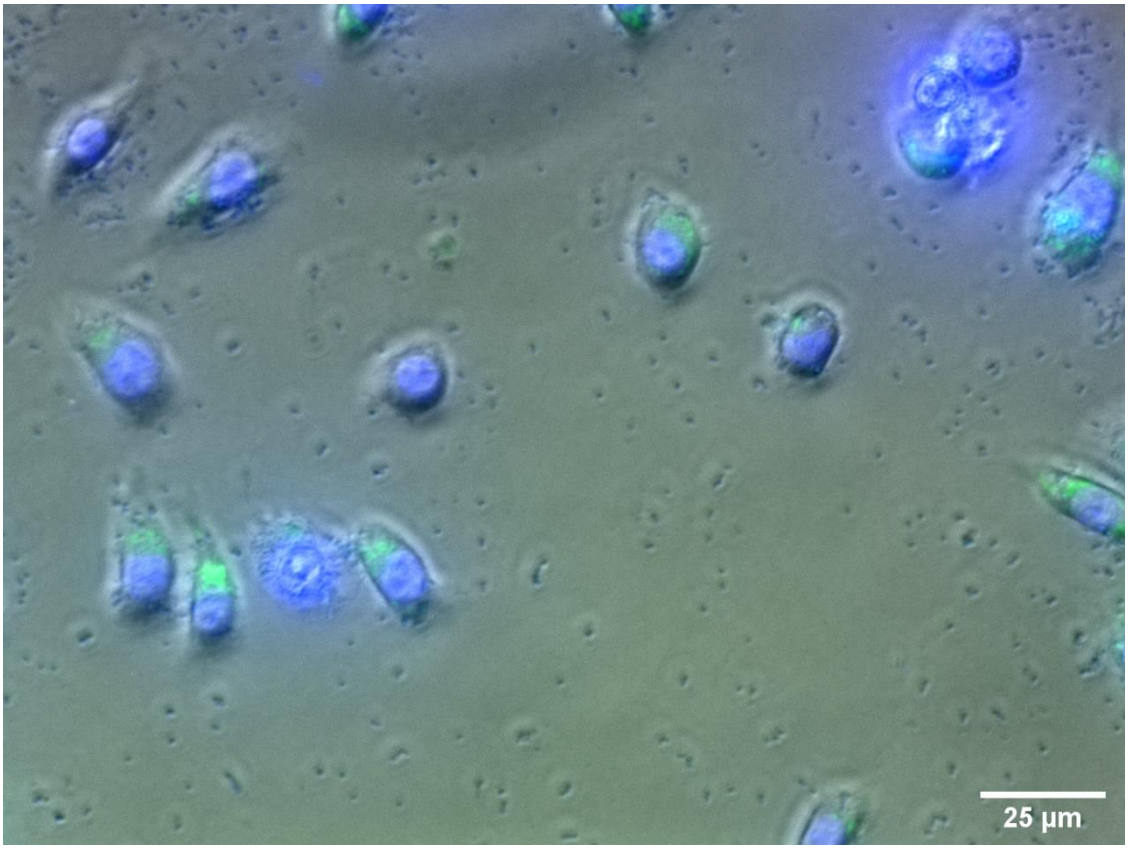


Figure S 8 A1 KO RAW 264.7 with E. coli pHrodo green.

Image overlay of phase contrast and fluorescence images taken with Zeiss cell observer during phagocytosis assay. Unengulfed bacteria left behind after washing of the well can be seen as small blue dots through the well.